STEM CELL MOBILISATION AND HOMING TO IMPROVE FRACTURE HEALING

Richard Lawrence Meeson

Submitted for the Degree of Doctor of Philosophy

University College London

July 2018

Institute of Orthopaedics and Musculoskeletal Science

University College London

Royal National Orthopaedic Hospital

Stanmore HA7 4LP

UK

DECLARATION

I, Richard Meeson, confirm that the work presented in this thesis is my own. Where information has been derived from other sources, I confirm that this has been indicated in the thesis.

ABSTRACT

Stem cell homing and migration is regulated through chemokine SDF-1 and its receptor CXCR4. *In vitro* studies in mice have demonstrated endogenous mobilisation of mesenchymal stem cells (MSCs) and endothelial progenitor cells (EPCs) by administering growth factors and AMD3100, which is an antagonist of CXCR4. The hypothesis of my study was that antagonism of the CXCR4-SDF1 axis would mobilise stem and progenitor cells into the circulation, and by increasing the available pool of cells in early fracture healing, improve bone formation.

Peripheral blood MSCs and EPCs were isolated from rats treated with VEGF and AMD3100. Non-mobilised controls did not yield any viable MSC CFUs, whereas mobilised were significantly higher at 2.9±1.8 CFUs/ml blood (p=0.029). The MSCs were CD29 and CD90 positive and CD34 negative, however unlike bone marrow MSCs, they had a mixed CD45 expression. These cells were only able to differentiate down osteogenic lines *in vitro*. Mobilised EPCs had the typical 'cobblestone' morphology, were CD45 and CD34 negative, with low to variable expression of endothelial markers CD31 and VEGFR2, and MSC marker CD29. These cells had variable *in vitro* tube forming ability and could differentiate down adipogenic and not osteogenic lines.

In order to evaluate the potential of endogenous mobilisation on fracture healing, a rat femoral osteotomy model stabilised with an external skeletal fixator was used. Several modifications were made to improve the reliability of the model and are reported in my thesis. The influence of gap size on interfragmentary strain and subsequent healing using this system was evaluated to identify the optimised situation to measure the effect of endogenous mobilisation. Mechanical analysis of the construct stiffness and the interfragmentary strain showed the gap size did not have an influence on the construct stiffness. However, increased gap size significantly reduced day 0 interfragmentary strain (p=0.013), with 1.0mm gap having significantly higher interfragmentary strain than the 2.0mm gap (p=0.029).

To evaluate the effect of interfragmentary strain on healing, a femoral osteotomy in 12-14 week old female Wistar rats was stabilised with an osteotomy gap of 1.0mm, 1.5mm and 2.0mm. After five weeks, the 1.0mm gap had the largest callus ($0.069um^3$) and bone volume per microCT slice ($0.035um^3$). As the gap size increased, the bone volume per slice decreased, however significance was not found (p=0.082). Histomorphometry also showed the bone formation deceased as the gap increased. There was an increase in cartilage formation associated with the decrease in bone in the 1.5mm gap, whereas the 2.0mm gap had an increase in fibrous tissue associated with a decrease in cartilage and bone, indicating

that the 2.0mm gap was tending towards fibrous non-union. The 1.5mm gap provided a suitable compromise to test endogenous mobilisation, and although the interfragmentary gap strain reduced as the gap enlarged, there was a reduction in osteotomy healing as the gap size increased.

VEGF (V), IGF-1 (I) or GCSF (G) combined with AMD3100, or AMD3100 alone (A) were subsequently investigated using the rodent fracture model with a 1.5mm gap. At 5 weeks, groups V, I and A had increased bone formation compared to control animals, however, group A had a significant increase in bone volume ($p=0.01$) and group I a significant increase in % bone within the callus ($p=0.035$). Group G on the other hand, showed a decrease in bone volume. Irrespective of whether there was an increased or decreased bone content, all treated groups had an increase in trabecular thickness, or more accurately, thicker segments of woven bone, compared with the controls. Histomorphometric analysis showed decreased cartilage tissue was associated with increased bone in groups with improved healing, and was associated with increased fibrous tissue in poorly performing groups.

Overall therefore, AMD3100 given alone significantly increased fracture healing over and above the control level. In conclusion, disruption of SDF1-CXCR4 axis can mobilise stem and progenitor cells, and can boost impaired fracture healing in a rat femoral osteotomy model.

IMPACT STATEMENT

Clinical translation

Around 10% of fractures seen by the NHS do not successfully heal, with a significant economic cost to the NHS and social cost to the individual. Fracture healing can be enhanced by administration of stem cells, however, typically they require processing or expanding in a laboratory prior to re-implantation. The question I asked in my thesis was whether it would be possible to mobilise stem cells endogenously within the body to enhance fracture healing? If successful, this methodology avoids the potential problems associated with cell isolation, culture and re-delivery to the patient. My study identified that endogenous mobilisation of stem and progenitor cells into the circulating blood steam can boost bone formation in a compromised healing scenario, akin to a non- or delayed-union. This is the first time this has been demonstrated and offers a non-invasive means to improve fracture healing. Notably, the most effective mobilising agent, AMD3100, is already licensed for another clinical purpose. Through presentation at international research meetings and proposed publications in high impact journals, this work will be disseminated internationally. The next step will be to develop a clinical trial, which if successful could have a positive economic impact on the NHS, as it would reduce the financial burden associated with revision fracture surgery.

Endogenous mobilisation is a low cost, low risk means to boost healing and could potentially be given as a prophylaxis to patients with fractures at risk of delayed healing or non-union. These patients may include those with fragility fractures, comminuted tibial fractures, or when treating established non-unions. This approach could have promise for other conditions that may benefit from stem cell treatment, such as liver cirrhosis patients, musculoskeletal disease including osteoarthritis, myocardial infarction, and neurological degeneration/damage. Veterinary clinical patients, who can also have problems of fracture union, may also benefit from this approach, as well as being informative as a 'one medicine' model.

Development of a robust research model & understanding of fundamental bone biology

Rodents are becoming the preferred model for the understanding of fracture healing and evaluation of regenerative strategies. I re-developed a highly adaptable and reliable femoral fixator model, which would be of interest to other researchers. Further, its biomechanics have been evaluated, and over a defined range day 0 interfragmentary strain theory does not accurately predict the course of healing. This should be considered by researchers working in the field of fracture mechanobiology and for groups using a critical size defect model in their

research. This work will be disseminated through international conference meetings and publications in international peer reviewed journals.

A non-invasive stem/progenitor cell isolation technique

My thesis also expanded on fundamental and applied stem cell biology, specifically aspects of stem and progenitor cell mobilisation. If optimised, this approach could have both national and international impact for researchers, as a simple and cost effective means to isolate adult stem cells that avoids the morbidity associated with bone marrow aspirate or adipose tissue extraction.

ACKNOWLEDGEMENTS

Although there are so many people to thank when undertaking a PhD, there really is one person without whom this would not have been possible. I owe a huge debt of gratitude to Professor Gordon Blunn. He very kindly took the time to support my fellowship application enabling me to undertake a PhD at this stage of my career, and has been an inspirational supervisor throughout. Having had the opportunity to work with such a rare individual has been a pleasure and an honor, and I shall endeavor to take everything he has taught me forward in the rest of my career.

I would also like to thank Prof Melanie Coathup for being a very supportive secondary supervisor throughout my studies and also to Dr. Mehran Moazen, who kindly stepped in to provide supervisory support when significant staffing changes occurred at IOMS. I would also like to thank Keith Raynor for his assistance when re-developing the fixator system, Mark Harrison for his various help along the way, and Jo Dlugozima and Graham Hagger at the RVC for their hard work and helpful approach.

It has been a pleasure to spend time with and get to know the other PhD students and post-docs at IOMS. In particular, I must thank Anita, who helped me to adjust from orthopaedic surgery to cell culture; not an easy task. I would also like to thank the MRC for funding my PhD studies as a clinical fellowship.

Finally, and most importantly I need to thank my family. Without the support of my Mum and Dad I would not be where I am today. To my wife, for her unwavering love and support through the ups and downs of life, and my two wonderful daughters who punctuated the start and finish of my PhD. I am truly grateful to have you all in my life.

CONTENTS

LIST OF FIGURES

4.4	Photograph showing the previous drill and pin guide apparatus. This apparatus allowed for the table-top to be moved intra-operatively using precision XY axis adjustment dials, allowing the hand driven chuck to be positioned correctly.	**136**
4.5	a) Photograph showing the revised miniaturised drill and guide-block, which sits directly on the craniolateral femoral surface. i) Shows the lateral surface with the concavity on the underside. ii) Shows the top surface with recesses to accept insert-sleeves and micro-ratchet recesses. iii) Shows medial surface. b) Photograph showing the titanium pin sleeve (i) and the drill sleeve (ii). The guide-block universally accepts either of the two sleeves (iii).	**136**
4.6	a) Photograph showing different aspects of the revised fixator. i) Shows the cranial surface of the fixator, which reveals the M2 stainless steel grub screws to secure the proximal and distal blocks. The distal screws can be loosened to allow sliding and distraction of the osteotomy. ii) Shows the lateral surface of the fixator; notably, the pin-holes are eccentric such that the bulk of the block can be positioned caudal to the pins, as most of the rubbing occurred on the cranial surface. iii) Shows the caudal surface of the fixator, which has the four M2 stainless steel grub screws that secure each individual pin. b) Photograph showing the various degrees of axial distraction available.	**137**
4.7	Photographs showing the original blunt trochar tipped pins (a, and c) and the revised sharp cutting trochar tipped pins (b and c).	**138**
4.8	a) Radiograph showing osteolysis and lucency around the proximal pins. b) Radiograph showing a distal femoral fragment with marked remodeling around the distal pin tracts. The upper pin tract has a sclerotic region with a surrounding lucent zone suggestive of a ring sequestrum.	**139**
4.9	a) (i) Photograph of the 3:2 proximal pin fixator next to the standard 2:2 fixator. (ii) Radiograph taken five weeks post surgery using the 3:2 fixator system with 1.25mm diameter pins. b) Photograph showing the 1.25mm sharp trochar pin (i) next to the 1.4mm sharp trochar pin (ii). c) Radiograph taken five weeks post-operatively showing no evidence of pin loosening with the 1.4mm fixator pins.	**142**

LIST OF TABLES

6.1	Radiographic assessment of degree of union from microCT scout images, shown as absolute numbers and percentage.	**182**
6.2	Quantitative morphometry indices evaluated from the microCT analysis of bone formation within the central 60% volume of the osteotomies. All values are the mean±SD.	**190**
6.3	Mean±SD tissue area measured (square pixels), showing histomorphometric characteristics of the tissue in between the two innermost fixator pin tract holes at x1 magnification.	**192**
6.4	Histomorphometric percentage area of tissue formed within the original osteotomy gap as evaluated at x2.5 magnification. All data expressed as mean±SD.	**195**

ABBREVIATIONS

2D – two dimensional

3D – three dimensional

acLDL – acetylated low density lipoprotein

ALP – alkaline phosphatase

AO - arbeitgemeninschaft fur osteosynthsesfragen

APC - allophycocyanin

BM – bone marrow

BMP – bone morphogenic protein

BS – bone surface

BSA – Bovine Serum Albumin

BV – Bone Volume

BV/TV – percentage bone volume

Ca – cartilage

CACs – circulating angiogenic cell

Cbfa1- core-binding factor subunit alpha-1

CBG – cancellous bone graft

CD – cluster of differentiation

CFU – colony forming unit

CFU-F – colony forming unit - fibroblastic

CoB – cortical bone

COL 1- collagen type I

CXCR4 - C-X-C chemokine receptor type 4

DiI - 1,1'-Dioctadecyl-3,3,3',3-tetramethylindocarbocyanine perchlorate

DMEM- Dulbecco's Modified Eagle Medium

DXA – dual-energy x-ray absorptiometry

ECFC - endothelial colony forming cells

ECM – extracellular matrix

EDTA - ethylenediaminetetraacetic acid

eEPCs – early endothelial progenitor cell

EGM-2 MV – endothelial growth media 2 microvascular

EOCs – early outgrowth cells

EPC – endothelial progenitor cell

FCS – fetal calf serum

FGF - fibroblast growth factors

FITC - fluorescein

flk – fetal liver kinase

GABA - gamma-aminobutyric acid

GAG - glycosaminoglycans

GCSF – granulocyte colony stimulating factor

GDF – growth differentiation factor

GF – growth factor

GFP – green fluorescent protein

GPI - glycophosphatidylinositol

H and E - hematoxylin and eosin

HIF1 - hypoxia-inducible factor

HIV – human immunodeficiency virus

HLA-DR – human leukocyte antigen – antigen d related

HSS – high speed steel

HUVEC – human umbilical vein endothelial cells

IFS – interfragmentary strain

IGF1 - insulin-like growth factor 1

IgG – immunoglobulin G

IL - interleukin

IOMS – Institute of Orthopaedics and Musculoskeletal Science

ip – intra peritoneal

IU – international units

KDR - kinase domain region

LDL – low density lipoprotein

Lin- lineage (positive marker expression)

M-CSF – macrophage colony stimulating factor

MAPK - mitogen-activated protein kinase

MC – medullary cavity

MMP - matrix metalloproteinase

MNC – mononuclear cell

MSC – mesenchymal stem cell

NHS – National Health Service

NICE – National Institute for Health and Care Excellence

NIH – National Institutes of Health

NSAIDs – non-steroidal anti-inflammatory drug

Oct – octamer –binding transcription factor

OPG - osteoprotegerin

P - passage

P/S – penicillin streptomycin

PBEPC – peripheral blood (mobilised) endothelial progenitor cell

PBMSC – peripheral blood (mobilised) mesenchymal stem cell

PBS – phosphate buffered saline

PCL- poly-ε-caprolactone

PDGF - platelet derived growth factor

PE – Phycoerythrin

PECAM - platelet endothelial cell adhesion molecule

PEEK – polyether ether ketone

PGA - polyglycolic acid

PI3kinase - phosphatidylinositol-4,5-bisphosphate 3-kinase

PLA - polylactic acid

PLGA - poly(lactic-co-glycolic acid)

PMN - polymorphonuclear leukocytes

PPARɣ - peroxisome proliferator-activated receptors

PRP – platelet rich plasma

PTH – parathyroid hormone

RANKL - receptor activator of nuclear factor kappa B ligand

RBC – red blood cell

RCF – relative centrifugal field

rhBMP – recombinant human bone morphogenic protein

ROI – region of interest

RPM – revolutions per minute

Runx – runt-related transcription factor

SCID – Severe combined immunodeficiency

SD – standard deviation

SDF1 - stromal cell-derived factor 1

SEM – standard error of mean

Sox – Sry related HMG box

Tb.N – trabecular number

Tb.Sp – trabecular spacing

Tb.Th - trabecular thickness

TCP - tricalcium phosphate

TGFb - transforming growth factor beta

Thy – thymocyte differentiation antigen

TNF – tumour necrosis factor

TS – tissue surface area

UCL – University College London

VCAM-1 - vascular cell adhesion molecule 1

VEGF - vascular endothelial growth factor

WB – woven bone

Wnt - Wingless-related integration site

CHAPTER 1: Literature Review & Introduction

1.1 Background

The NHS sees around 850,000 fractures each year with a non-union rate of 10%. Treatment can be difficult and usually requires surgery with a cost of up to £80,000 per patient, not to mention the associated morbidity (Mills & Simpson 2013). Stem and progenitor cells clearly have an important role in fracture healing and have been the focus of intense research to avoid and treat union problems. Currently however, stem cell therapy requires isolation of cells from the body, selection and expansion *ex vivo* and then a further operative procedure to deliver them back to the body. Even minimally manipulated bone marrow aspirate carries donor site morbidity and potential complications. An alternative method to improve fracture healing may be to boost the physiological migration of stem cells to the fracture site through a process known as 'mobilisation'. The main purpose of this work was to investigate the potential to mobilise stem and progenitor cells by manipulating the SDF1-CXCR4 chemokine receptor interaction, to augment fracture healing. The aim of my PhD was to investigate the hypothesis that antagonism of the CXCR4-SDF1 axis could mobilise stem and progenitor cells into the circulation of rats and by increasing pool of cells available after fracture, improve healing.

My introduction gives an overview of the structure and function of bone, the mechanisms of fracture healing and the factors that influence it. I follow with failure of fracture healing and approaches to management, with an emphasis on stem cell therapy. Finally, I will describe the migration and mobilisation of stem/progenitor cells.

1.2 Bone

1.2.1 Role of the skeleton in the body

The functions of the skeleton are directly attributable to the structure and function of bone, which is a dynamic and biologically active tissue. Bone as a 'hard tissue' is able to provide protection to more delicate organs, such as the brain or the heart, but also provides mechanical leverage permitting movement. As a quintessential composite material, the combination of apatite mineral with a collagen matrix allows bone to have tensile strength equivalent to cast iron and yet be three times lighter and ten times more flexible (Buckwalter et al. 1996). Bone as a significantly mineralised tissue has further roles in ion homeostasis and acid base balance. As a home to the marrow, it is the source of many progenitor and stem cells, allowing continuous recapitulation of other tissues and the fostering of healing (Rodan 1992).

1.2.2 Anatomic structure of bone

Bones are morphologically grouped as long bones or flat bones. Long bones consist of three distinct regions, the largest of which is the compact diaphysis which transitions to an intermediate metaphyseal region and terminates in the epiphysis, each with a distinct gross and histological appearance (Figure 1.1). Grossly, on a macroscopic level, a longitudinal section of a long bone has location dependent, macroscopic architectural arrangements of bone structure. Generally, in the adult skeleton there are two predominating morphological varieties of bone: a hard dense form of bone known as cortical/compact bone, and a sponge-like arrangement of bone known as trabecular/cancellous bone (Figure 1.1). These two forms of bone have the same matrix and mineral content, however cortical bone is more dense, with 10% porosity, compared with cancellous bone having a 50-90% porosity (Buckwalter et al. 1996). Cortical bone forms the diaphysis of long bones, with an internal 'medullary canal' which contains fat and stem cell niches. The cortical bone continues from the diaphysis as an outer shell over the metaphyseal and epiphyseal regions, which are comprised of cancellous bone. In skeletally immature animals, a cartilaginous plate known as a 'growth plate' or physis physically separates these two regions. In the skeletally mature adult, the physis is absent and the cancellous bone of the epiphysis is connected to the cancellous bone of the diaphysis by a fine line of compact bone called the 'physeal scar'.

Flat bones are structured as a sandwich of two layers of compact bone separated by intervening cancellous bone, and include the majority of bones in the skull, sternum, scapula and pelvis. Overall, the skeleton is considered 80% cortical and 20% cancellous by mass (Buckwalter et al. 1996).

1.2.3 Microscopic structure of bone

Cortical and cancellous bone are built from two microscopic building blocks; flat lamellae which consist of organised parallel layers of collagen and mineral, or woven bone in which the collagen and deposited mineral are haphazardly organised. Woven bone is associated with the immature skeleton and is also seen in the adult when bone is being formed rapidly, such as in response to injury. Lamellae in cortical bone are arranged as circular osteons with a central canal containing a vascular supply, whereas lamellae in cancellous bone are arranged in rods or plates called trabeculae, without any such canal. Martin and Burr (1989) described four organisations of microscopic cortical bone structure:

1. *Woven cortical bone*; has a disorganised arrangement that lacks a clear structural unit, underlying the rapidity of its deposition. It has disorganised type I collagen and can become highly mineralised. Being the only type of bone that can form *de novo*,

it is found in the embryonic skeleton and in fracture healing; in both scenarios it is subsequently remodelled into an organised bone structure. It is also found in entheses, skull sutures, ear ossicles and in the growth plate. Otherwise, it is rarely seen over the age of five years in humans, unless new bone formation occurs (Buckwalter et al. 1996).

2. *Plexiform cortical bone*; is a rapidly deposited mechanically strong arrangement of bone, typified by fast growing large animals such as sheep and cows, and rarely seen in humans. In this type of bone, vascular plexii are seen between lamellar and non-lamellar bone (Martin & Burr 1989). The parallel and perpendicular deposition gives a pattern akin to a brick wall. Plexiform bone is stiffer than other types, however this structure is more prone to crack propagation.
3. *Primary osteonal cortical bone*; has lamellae arranged concentrically surrounding a blood vessel, creating an osteon (Figure 1.1). They are formed from cartilage mineralisation (endochondral ossification) and have smaller vascular channels than the more common secondary osteonal bone.
4. *Secondary osteonal cortical bone*; develops from remodelling of existing bone. Osteoclasts within a tunnel known as a 'cutting cone' resorb bone at the leading edge and osteoblasts replace it at the trailing edge. A central canal develops due to incomplete filling by the osteoblasts known as a 'Haversian canal', which contain blood vessels, lymphatics and sometimes nerves. Secondary osteons or Haversian systems are larger than primary osteons. These systems are connected together by perpendicular Volkmann's canals. The remodelling processes involved in this type of bone provides some of its characteristic features such as cement lines, which are non-collagenous lines where bone resorption ended and bone formation began; and interstitial lamella, which are remnants of remodelled osteons, not seen in primary osteonal bone (Hillier & Bell 2007).

1.2.4 Species considerations

When considering animal models for orthopaedic research, and indeed 'one medicine' collaborations between human and veterinary researchers, it is essential to understand species similarities and differences. Human bone has circumferential lamellae at the endosteal and periosteal surfaces sandwiching Haversian bone in the middle. Both 'complete' and 'active' remodelling Haversian systems will be seen. The cortical bone of the rat on the other hand, is almost exclusively comprised of primary osteonal bone, with a scattering of Haversian systems at the endosteal surface. The cat and the dog both exhibit dense Haversian bone however, and the young dog shows evidence of prior osteonal banding and plexiform bone. For large animals, the pig has primary plexiform with some Haversian bone,

whereas the goat and sheep demonstrate plexiform with a scattering of Haversian bone. Finally, the horse exhibits dense Haversian bone with remnants of primary and plexiform bone (Hillier & Bell 2007). In terms of composition, density and bone quality, there is also significant interspecies variation, and the rat has been shown to be the least and the dog most like human bone (Aerssens et al. 1998). However, when contemplating animal models for research, these differences are important, but are not the only considerations.

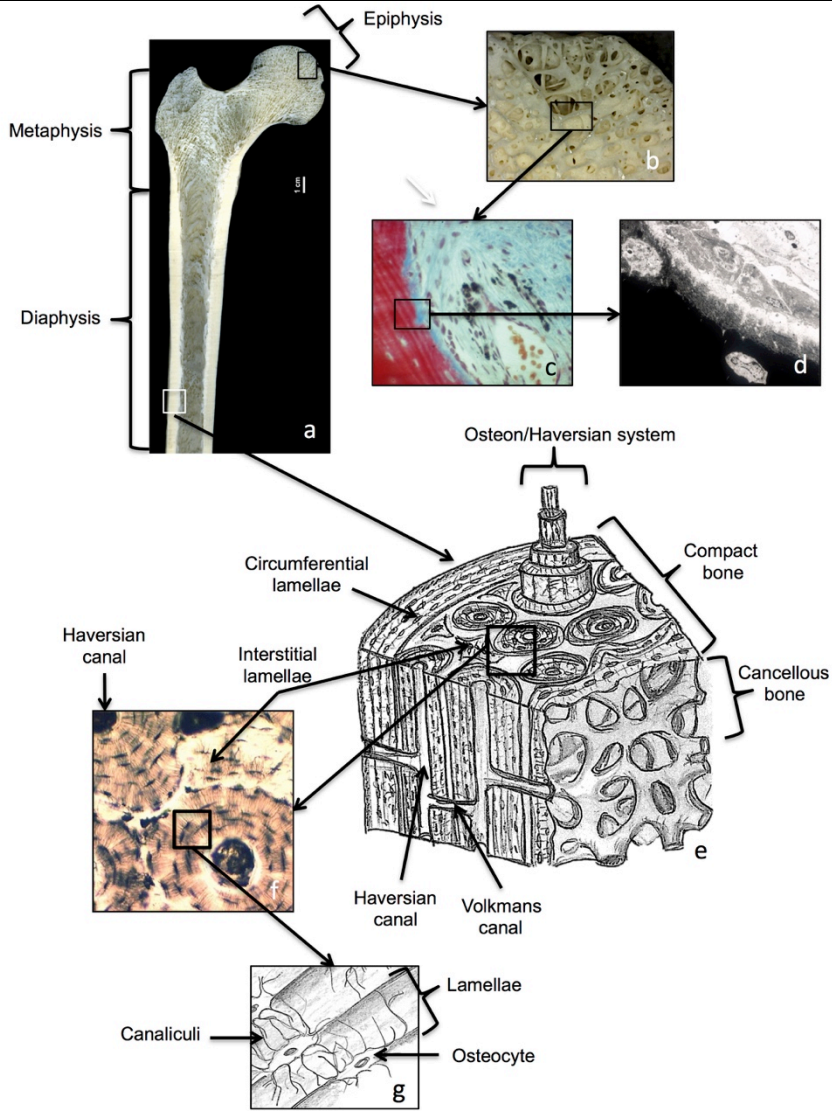

Figure 1.1: Bone from macroscopic to microscopic a) Photograph of a sagittal transection of a preserved bone showing cortical/compact and cancellous bone structure. b) Higher magnification image of the cancellous region showing the rod and plate structure of trabecular bone. c) Histograph stained with Martius Scarlet Blue, showing collagen in red and bone in blue separated by osteoid. d) Scanning electron microscope image of osteoblasts and osteoclasts within bone. e) Diagram showing the levels of cortical bone structural arrangement. f) Ground histology section showing the concentric arrangement of lamellae making up Haversian systems (RVC library image). g) Diagram showing the arrangement of lamellae and osteocytes.

1.2.5 Cells in bone

Bone is a highly vascularised tissue composed of a calcified extracellular matrix 'osteoid', associated with several differentiated cell types derived from mesenchymal and haematopoietic stem cell lines (Buckwalter et al. 1996). Bone marrow derived mesenchymal stem cells are considered by some to be the true 'skeletal stem cell' due to their *in vivo* ability to form all the component tissues of bone (bone, cartilage and fat) in transplantation models, without the need for exogenous growth factor cues (Owen & Friedenstein 1988; Bianco et al. 2013)

Osteoblasts are derived from mesenchymal stem cells from the bone marrow, bone canals, endosteum and periosteum. These cuboidal cells form layers and deposit non-mineralised extracellular bone matrix 'osteoid' from their basal surface, which subsequently becomes mineralised (Rodan 1992; Buckwalter et al. 1996). As osteoid is deposited, some osteoblasts become trapped within the matrix and subsequently become osteocytes (Figure 1.1 & 1.2a) Osteocytes are proposed to communicate through cytoplasmic extensions, within canaliculi, and have a role in mineral ion homeostasis and detection of mechanical stimuli (Klein-Nulend et al. 2012). Osteoblasts express parathyroid hormone receptors and have an important role in signaling to osteoclasts. Osteoclasts are derived from haematopoietic stem cells and are likely closely related to the monocyte/macrophage lineage. Osteoclasts are large multinucleate cells (Figure 1.2b) that have tartrate resistant acid phosphatase and calcitonin receptors (Rodan 1992). They have a complex folded basal cytoplasmic surface (referred to as the ruffled boarder) from which the mineral component of bone is resorbed. Initially, they bind to the surface of the bone and create a sealed space, and then through endosomal membrane coalescence, the brush border develops and efficiently pumps protons into an extracellular sealed region. This creates an acidic pH4 environment which dissolves the calcium and phosphate ions, and together with matrix metalloproteinases able to operate a low pH (Cathepsin K), the organic matrix is also resorbed (Buckwalter et al. 1996). The resultant resorption pit under the central potion of the osteoclasts is known as a Howship's lacunae.

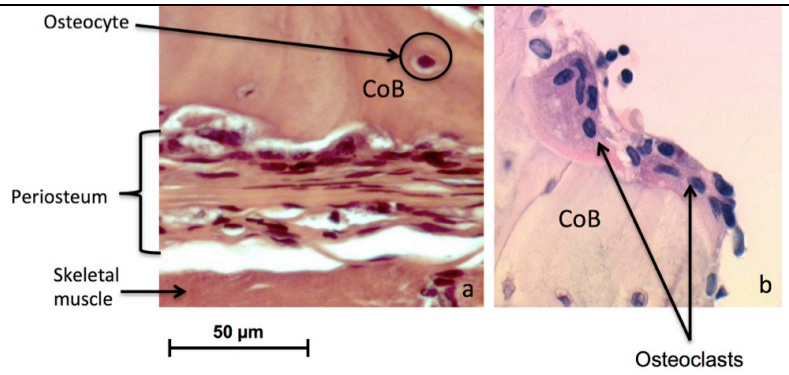

Figure 1.2: a) Histology slide, H and E, from a rat femoral diaphysis, sagittal slice. b) Histology slide, H and E, from a rabbit femoral diaphysis transverse section (RVC library image). CoB = Cortical bone.

1.2.6 Composition of bone

Cells constitute less than 10% of bone and the remainder is bone matrix; a composite material consisting of 65% inorganic, 20% organic and 10% water by wet weight. The organic component gives bone its form and is a dense fibrous tissue, not dissimilar to tendons, ligaments and joint capsule. Collagen makes up 90% of the organic matrix, with the majority being type I with its large diameter fibrils giving excellent resistance to tensile forces, in addition to small amounts of collagen V and XII. The remaining 10% of the organic matrix that is not collagen consists of glycoproteins and bone-specific proteoglycans, such as growth factors including BMPs, TGFb, IGF1 (Buckwalter et al. 1996).

Without the inorganic component, bone could not perform many of its key functions. The mineral phase of bone is not pure hydroxyapatite ($Ca_{10}[PO_4]_6[OH]_2$) crystals, but contains carbonate groups and hence bone crystals should be considered apatite. Around 99% of body calcium, 85% of phosphorus, and 40-60% magnesium and sodium are in phase with bone mineral (Buckwalter et al. 1996). Alone, this material would be highly brittle and prone to shattering but in composite with the organic osteoid, it forms a lightweight mechanically strong material.

1.3 Fracture healing

1.3.1 Bone healing – a remarkable process

Bone can heal without scar formation. Post-natal bone healing recapitulates ontological events from embryogenesis and hence bone is able to truly regenerate itself (Einhorn & Gerstenfeld 2014). Fracture healing involves an anabolic phase of *de novo* recruitment and differentiation of stem/progenitors to form skeletal and vascular tissues (Figure 1.3). A

prolonged catabolic state follows, whereby primary bone is remodelled into secondary bone (Einhorn & Gerstenfeld 2014). The majority of fracture healing is considered 'indirect healing' (also termed 'secondary bone healing' or 'callus healing') whereas under certain surgically engineered situations, bone can be tricked into remodelling, and will directly fuse across a fracture line in a process known as 'direct' or primary bone healing.

1.3.2 Indirect bone healing

Indirect bone healing is the most common form, and is the body's natural means to re-unite fractured bone. Conservatively managed fractures and those given relative stability with surgical stabilisation permitting some micromotion, such as intramedullary nails, external fixators, or non-compressed internal fixation, heal through indirect union (McKibbin 1978; Marsell & Einhorn 2011). A bridge of tissue forms rapidly, called a 'fracture callus', to restore mechanical stability and reduce fracture movement. Indirect bone healing has been described as a sequence of distinct phases (McKibbin 1978), but it should be remembered that these processes will not be entirely linear nor simultaneous in any one fracture (Figure 1.3).

Inflammatory phase

Tissue damage associated with trauma will trigger a necessary inflammatory response and the clotting cascade. The resulting coagulated haematoma of fibrin and platelets fills potential space between the fracture ends, providing a scaffold for fracture callus and a source of pro-inflammatory cytokines (Gerstenfeld et al. 2003). Invading inflammatory cells attracted to the haematoma, create a suitable cytokine milieu to drive fracture healing. Factors such as Fibroblast Growth Factor (FGF), Transforming Growth Factor (TGFβ), and Vascular Endothelial Growth Factor (VEGF), increase in concentration (Simpson et al. 2006), and IL-1, -6 and TNFα are thought to be the main inciting cytokines signalling the move from inflammation towards repair and revascularisation (Marsell & Einhorn 2011). These factors are produced by macrophages, mesenchymal stem cells and other inflammatory cells, with peak levels seen at 24 hours (AI-Aql et al. 2008). The initial acute inflammatory response peaks at 24 hours and is usually abating by seven days, although key individual inflammatory mediators continue to have influence throughout fracture healing (Cho et al. 2002).

Critical to *de novo* tissue formation is the recruitment and differentiation of stem and progenitor cells to the site of the fracture. New blood vessel formation requires local sprouting in addition to recruitment of circulating and bone marrow resident endothelial progenitor cells (EPCs) (Alev et al. 2011). Mesenchymal stem cell (MSC) recruitment has

been shown to occur as soon as 24 hours after fracture (Dimitriou et al. 2005), and a range of sources are proposed including bone marrow, periosteum, peripheral blood and nearby soft-tissues (Kumagai et al. 2008; Knight & Hankenson 2013). Bone marrow and periosteal MSCs certainly contribute, as bone marrow removal or periosteal stripping delays fracture healing (Ozaki et al. 2000). Elegant chimeric labelling studies have shown that GFP bone marrow cells become incorporated into the fracture, particularly in the central callus region populated by osteoblasts (Taguchi et al. 2005). Transgenic lineage studies have shown a role for bone marrow MSCs differentiating into osteoblasts and osteocytes, and a contribution of periosteal cells to the fracture callus (Colnot 2009). Periosteal cells can differentiate down chondrogenic and osteogenic pathways, in contrast to the osteogenic limited marrow cells (Colnot 2009), indicating a role of periosteal stem cells in cartilage formation during bone healing. Although only recently an area of focus (Kuznetsov et al. 2001; Zvaifler et al. 2000), there has been an awareness of peripheral blood circulating skeletal progenitors since the nineteenth century, when they were first described by Paget (Chesney & Bucala 1997). Clinical evidence from fracture patients corroborates a potential role of circulating skeletal/mesenchymal stem cells (Alm et al. 2010) and EPCs (Ma et al. 2012) in fracture healing. Experimental parabiotic mouse studies also support physiological mobilisation of progenitors via the circulation to a fracture site (Kumagai et al. 2008). These cells have been identified circulating in small numbers of around 1 per 10^{6-8} blood mononuclear cells in mice, rabbits, guinea pigs and humans (Khosla & Eghbali-Fatourechi 2006).

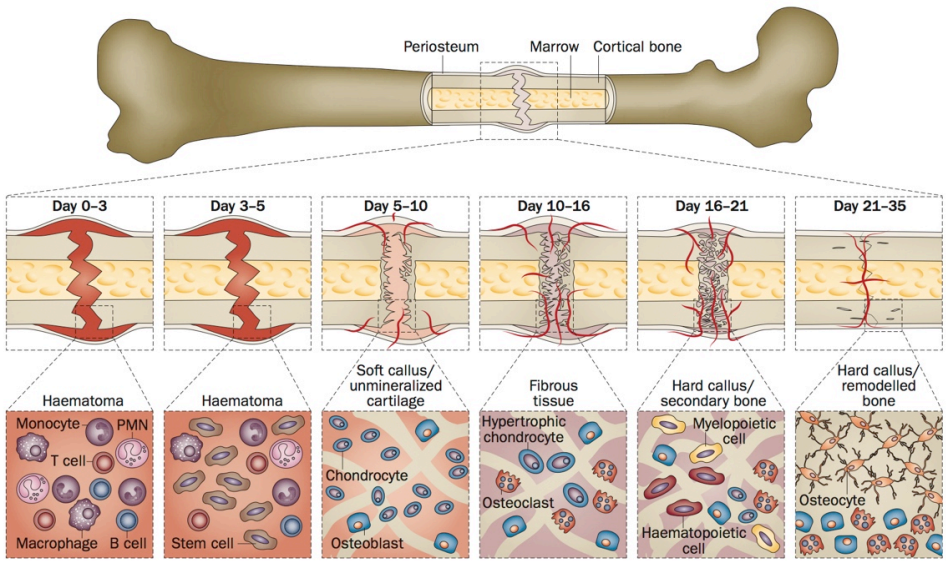

Figure 1.3: Diagram of the phases of Indirect fracture healing; from inflammatory through to endochondral bone formation and remodeling. The images denote the cells recruited and present at the different stages. The time scales shown are based upon a mouse femoral fracture model stabilised with intramedullary pin. (PMN = polymorphonuclear leukocyte). Image from Einhorn & Gerstenfeld (2014).

Once recruited, stem and progenitor cell differentiation will be driven by the mechanical environment and signalling from growth factors and other molecules. BMP2, 6 and 9 have all been shown to drive MSCs down an osteoblastic lineage (Cheng et al. 2003). The mechanical environment at the fracture site also influences the differentiation of recruited stem cells, with experiments showing chondrocyte (Angele et al. 2003) and osteoblast (Mauney et al. 2004) differentiation being influenced by the amount of mechanical strain they are exposed to. Undifferentiated stem cells demonstrate sensitivity to their local matrix mechanical environment and stiffer environments drive osteogenic differentiation whilst softer environments favour neuro or myogenic pathways. Mechanical influence subsequently dominates over growth factor driven differentiation after several weeks of exposure to a particular mechanical environment (Engler et al. 2006).

Indirect fracture healing has two mechanisms of bone formation

After the initial trauma, indirect bone healing develops through two anatomically associated processes (Figure 1.4); intramembranous and endochondral ossification, with the endochondral pathway tending to dominate in indirect healing, whereas, only intra-membranous ossification is seen in direct fracture healing.

Intramembranous ossification forms bone along periosteal and endosteal surfaces associated with the fracture, and can develop along the bone diaphysis. In this situation, bone matrix is produced by periosteal derived osteoprogenitors depositing bone directly onto a scaffold of fibrous tissue. Seen as early as three days after trauma, a variably wide cuff of hard callus tissue forms to bridge the cortical fracture ends. In the areas between and aside, fracture haematoma becomes reorganised as fibrovascular granulation tissue, rich in collagen fibres and matrix. In *endochondral ossification* the granulation tissue becomes progressively replaced by fibrous tissue, fibrocartilage and hyaline cartilage. Endochondral ossification occurs in between the fracture ends, outside of the periosteum and within the granulation tissue that has formed (Brighton & Hunt 1991).

Endochondral ossification is the predominant pre-natal bone forming pathway. It remains present until skeletal maturity, facilitating physeal growth of the long bones, and involves cellular proliferation, differentiation, matrix synthesis and increased cellular volume (Breur et al. 1991). A sequential replacement of tissue belies endochondral ossification, with an initial formation of soft cartilaginous callus that is replaced by hard bony callus. Its recapitulation of embryonic bone formation is corroborated by the int/wingless signal transduction pathway (Wnt pathway) being critical in both embryology, fracture healing and oncogenesis. This pathway is intimately involved in regulation of the differentiation of

MSCs down osteoblastic lineages and regulates osteoblast driven bone formation (Chen & Alman 2009).

For cartilage formation in fracture healing, MSCs differentiate to chondrocytes that proliferate and hypertrophy in regions adjacent to the woven bone of the hard callus. The hypertrophic chondrocytes deposit a cartilage matrix (type II collagen with aggrecan) to form a soft-callus, which starts to provide some mechanical stability. Animal studies have shown maximal levels of procollagen type II and soft callus formation around 7-9 days after fracture (Dimitriou et al. 2005). Whilst the soft callus forms, intramembranous ossification lays down bone without a cartilage intermediate from the periosteal and endosteal surfaces of the fracture, creating a hard callus. Both processes depend upon MSC recruitment and differentiation (Marsell & Einhorn 2011), in addition to the TGFβ superfamily of growth factors. TGFβ2, -β3 and GDF5 drive chondrogenic differentiation and are crucial to endochondral ossification, whereas BMP5 and 6 drive intramembranous ossification (Cho et al. 2002; Marsell & Einhorn 2009).

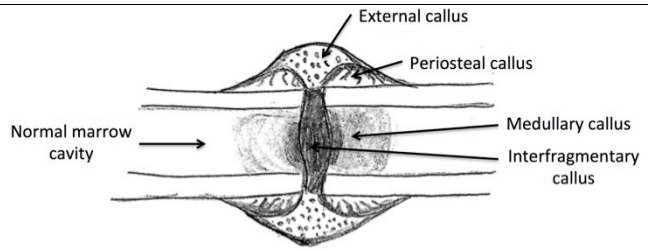

Figure 1.4: Diagram adapted from Brighton & Hunt (1991), showing the regionalised associations of intramembranous ossification (periosteal callus) and endochondral ossification (external and interfragmentary callus) in indirect fracture healing.

Over time, the soft callus cartilage matrix starts to calcify. Calcification is driven by relative hypoxia inducing the chondrocytes to accumulate calcium granules within their mitochondria. These get transported into the extracellular matrix where the calcium can precipitate with phosphate to form mineral deposits, creating a nidus for apatite formation (Ketenjian & Arsenis 1975). The changes in the soft callus are regulated by a range of growth factors and signalling molecules including receptor activator of nuclear factor kappa B ligand (RANKL), osteoprotegerin (OPG) and macrophage stimulating factor (M-CSF). These factors stimulate woven bone formation by signalling to osteoblasts and osteoclasts. Additionally, TNFα has roles in inducing chondrocyte apoptosis and osteogenic MSC differentiation (Gerstenfeld et al. 2003; Barnes et al. 1999).

In order to remodel and form bone, the cartilage in the fracture requires vascularisation to facilitate migration of osteoblasts and to provide the increased oxygen tension they require.

This process requires the coordination of new blood vessel formation and a sequence of chondrocyte apoptosis, matrix degradation and angiogenesis (AI-Aql et al. 2008). Vascularisation is controlled by at least two signalling pathways; the angiopoietin and VEGF pathways. Angiopoietins peak early in healing and hence are thought to have a role in budding of adjacent blood vessels from the periosteum (Keramaris et al. 2008). Both osteoblasts and chondrocytes expressed VEGF, a key mediator of *de novo* vascular network formation (vascularisation) and induction of existing vessels to bud new ones (angiogenesis), through signalling to MSCs and EPCs (Kanczler & Oreffo 2008). Experimental studies have shown the critical role VEGF plays in fracture healing, as blocking VEGF with soluble receptors decreases angiogenesis, bone formation and callus mineralisation, whereas exogenous VEGF enhances vascularisation, ossification and callus formation in mouse femoral and rabbit radial defects (Street et al. 2002). VEGF can act indirectly through its receptors on endothelial cells to influence the development of a new vascular network, allowing bone orientated stem and progenitors to migrate into the fracture callus and differentiate into osteoblasts (Stegen et al. 2015). VEGF can also stimulate endothelial cells to produce cytokines that promote differentiation of progenitors down an osteoblastic lineage (Bouletreau et al. 2002).

Osteoblasts subesquently invade the calcified and vascularised cartilage and synthesise osteoid onto calcified cartilage septa. Apatite crystals form giving 'mixed spicules' which are woven bone with calcified cartilage cores, akin to embryonic bone formation (Buckwalter et al. 1996).

Remodelling phase

The hard callus creating a bridge between the fracture ends provides temporary restoration of mechanical stability, but is not the same as normal bone. The final phase in bone healing involves a second process of resorption and bone formation, this time, replacing the woven bone in hard callus with lamellar bone organised as osteons, to develop a cortex and re-cannulise the medullary canal (Gerstenfeld et al. 2003). During remodelling, callus including calcified cartilage is resorbed by osteoclasts (chondroclasts), and osteoblasts simultaneously deposit lamellar bone. Although it starts within four weeks of trauma, the process can take months to years to be fully complete. Remodelling is associated with a reduction in the expression of the TGFβ family of growth factors, whereas IL1 and TNFα predominate, although BMP2 also has a role (Marsell & Einhorn 2009; AI-Aql et al. 2008; Mountziaris & Mikos 2008).

Physiochemical processes may also influence remodelling. In the 1960s it was identified that the application of strain to compact bone created an electrical potential difference. The

convex surface became a cathode and activated osteoclasts to reduce the profile of the bone, whereas the concave surface became an anode, activating osteoblasts to infill the defect. This piezoelectric effect was generated by collagen in a crystalline matrix, and it was postulated that this might be the means by which cells detect and remodel bone according to the stresses applied. This theory has since lost its popularity as other mechanisms, such as fluid shear stress gained traction (Ahn & Grodzinsky 2009).

1.3.3 Direct Fracture healing

Discovered by chance and as a by-product of the evolution of rigid internal fixation for fracture repair, direct fracture healing is actually a perturbation of bone remodelling. First noted by Lane as 'per primum intentionem' and Robert Danis as 'soudure autogen', or internal welding, this type of fracture healing occurs without any callus formation. Rigid plate and screw fixation with fracture compression is necessary to create the correct biomechanical environment (Rahn et al. 1971; Perren 1979). Mechanically, direct union requires the relative displacement of fracture ends versus initial fracture gap width, known as the interfragmentary strain (IFS) (Perren 1979), to be under 2%, and the gap between the fracture ends also needs to be very small. Direct fracture healing is classified as either 'contact' or 'gap healing'. Where the fracture ends are in contact (gap <0.01mm) and the interfragmentary strain (IFS) is <2%, 'contact healing' occurs (Shapiro 1988), whereby cutting cones form at the osteons closest to the fracture and cross the fracture site at 50-100um/day, being trailed by osteoblasts forming osteonal bone directly. However, in any visibly compressed fracture, there will be regions where there is no microscopic bone contact; 'gap healing' will occur if there is a gap <800um-1mm, in which there is intramembranous bone formation and formation of lamellar bone, deposited perpendicular to the axis of the bone. This is subsequently remodelled to axial osteonal bone, restoring integrity (Marsell & Einhorn 2011). Direct fracture healing is a slow process and takes months to develop full mechanical competency (McKibbin 1978).

Comment: Most fracture healing will take place as indirect healing and hence I will identify a model system that reflects indirect bone healing. As the recruitment and differentiation of stem and progenitor cells are essential for this process, I believe they could be a potential point of manipulation to improve fracture healing.

1.3.4 Role of the mechanical environment in fracture healing

Although the overall shape of a bone is genetically programmed, bone is constantly subjected to direct and indirect loads. Wolff in 1892, observed that trabeculae in the proximal femur are aligned along the direction of stresses, leading to "Wolff's Law of Bone

Remodelling", stating the form and structure of bone is reflected by the loads it is subjected to (Wolff, 1892). Wolff's law is clearly in action when considering the reduction of bone mass associated with bed rest (Krølner & Toft 1983), spaceflight (Stupakov et al. 1984), and implant stress protection (Lanyon et al. 1981; Baggott et al. 1981), or in contrast, the increase in bone mass seen in tennis player's dominant racket arm (Jones et al. 1977) or when bone is subject to increasing strain and loading frequency (Lanyon 1984). Fracture healing is not exempt, and the influence of mechanical stability on fracture healing has been extensively investigated (Betts & Müller 2014). The role of the mechanical environment is notably evident when looking at callus formation, particularly using an external fixator system to alter the supporting mechanical environment (rigidity of fixation) to influence interfragmentary motion (Goodship & Kenwright 1985; Claes et al. 1997; Klein et al. 2003; Schell et al. 2005). However, as healing progresses, the tissues developing within the gap may influence the interfragmentary motion and strain, making studies difficult to compare and variable in outcome. It was Pauwels in the 1960s that first linked the mechanical environment to the development of fracture healing tissues, suggesting hydrostatic pressures drive stem cells down chondroblastic lines, and shear strains result in osteo and fibroblastic lineages (Betts & Müller 2014).

Interfragmentary strain & other theories

Consideration of interfragmentary motion and its relationship to the gap size has been extensively described by Stefan Perren, and is postulated to dictate whether bone heals by direct or indirect means, and the course of that healing. Perren's interfragmentary strain (IFS) theory is based upon the supposition that if tissues were strained beyond their ultimate strain tolerance, they could not form within the gap (Perren 1979). Perren went on to describe the strain range in context of healing fracture; an IFS greater than 10% would lead to non-union, as it would only permit fibrous tissue, whereas between 2-10% cartilage could form and endochondral ossification would follow. When strains were under 2%, bone can be laid down immediately, and with a suitably small gap, direct bone formation would occur. It was also suggested that over time, as tissues develop within and around the fracture gap, they would modulate and reduce the IFS, permitting sequentially more vulnerable tissues to be deposited until bone formation occurred. Perren's theory mathematically predicts that a bigger fracture gap would have lower IFS and hence improved healing, however the opposite is seen in experimental studies, with smaller gaps healing better than larger ones (Claes et al. 1997; Harrison et al. 2003).

Carter et al. proposed that the course of healing was not only related to the magnitude of IFS, but the differing roles of hydrostatic pressure and octahedral shear stress, and that good

vascularisation was critical to outcome (Carter et al. 1988). Their finite element model also accounted for eccentric callus formation with asymmetric cartilage deposition associated with the tension and compression surfaces of a stabilised fracture. They suggested that the fracture drives an osteogenic stimulus and when there is low cyclic stress with good vascularisation, bone forms directly. High hydrostatic compressive stress drives fibrocartilage and high tensile or shear stress drive fibrous tissue formation. When fibrocartilage does form, shear stresses then result in bone formation (Carter et al. 1998). They agree with Perren, in as much as too much mechanical stimulation will prevent healing, and very low levels will permit direct bone formation. Neither have however, accurately depicted what happens between the extremes and current experimental and finite models do not fully explain clinical and experimental findings. Inherently, the nature of the fracture and the method of stabilisation (rigidity of fixation), will influence the mechanical environment experienced at the fracture site, and in turn dictate the balance and course of healing.

Comment: The effects of the biological environment such as the supply of stem cells to the fracture will affect healing, however, the combined effects of biology together with the mechanical environment is not that well understood. In order to establish the effects of a biological intervention on fracture healing in a model system, I need to take account of the mechanical environment. I will seek a highly standardised mechanical environment in order to evaluate my hypotheses.

1.4 Problems with fracture healing: delayed & non-unions

Bone healing is a protracted process, but a fracture can be considered 'healed' when there is sufficient mechanical union to restore function. Clinically, this union is usually monitored through sequential radiography, looking to see mineralised callus uniting the fracture ends. 'Non-unions' are a failure of the fracture ends to unite and 'delayed-unions' are those that do not progress as expected. Fixed time lines are not useful due to the diversity of individuals, anatomic locations and fracture configuration. However, non-unions have been variably defined as; fractures over nine months in duration without any signs of progression for three months; a failure to unite within 6-8 months; or when fracture union has not developed after twice the typically expected time for union (Harwood et al. 2010). Experimental studies have looked towards a consensus definition and based on the somewhat arbitrary ratio of eight weeks for human long bone fractures to heal, and a non-union definition of six months, a three-fold time span was suggested. A rat non-union is hence defined as incomplete healing by 15 weeks, assuming five weeks for normal healing duration, and the same ratio gives a non-union definition of 12 weeks in mice (Garcia et al. 2013). Delayed-union is more

straightforward, being defined as "a fracture in which healing has not occurred in the expected time and the outcome remains uncertain" (Harwood et al. 2010).

Non-unions are reported in up to 10% of human clinical fractures, with a treatment cost reaching £79,000. However, this does not account for the associated morbidity and productivity impact (Mills & Simpson 2013). Upper limb fractures are 60% more likely to result in non-union, with the highest level of non-unions found in young men suffering high-energy fractures and elderly women suffering osteoporotic 'fragility' fractures.

1.4.1 Types & causes of impaired fracture healing

Weber and Cech (1976) radiographically classified non-unions into hypertrophic and atrophic forms. The hypertrophic or 'hypervascular' forms are thought to have suitable vascularisation and hence biology, but unsuitable mechanics, leading to prolific non-unifying callus formation. These have been subcategorised by the relative size of callus and are often described as an 'elephant's foot', 'horses hoof', or as oligotrophic. The avascular types have been thought to lack suitable vascularisation and are biologically as well as mechanically compromised. Recent evidence suggests however, that the vascularity of atrophic non-unions is not relatively reduced (Reed et al. 2002).

Atrophic non-union has characteristically sparse callus formation, closure or capping of the medullary canal by sclerotic bone and fibrous tissue in the intervening gap between fracture ends. If sufficient motion remains at the site of atrophic non-union formation, a pseudoarthrosis may form with cartilage deposition and a fluid interface lined with a synovial type membrane reminiscent of an articular joint (Heppenstall et al. 1987; Loboa et al. 2001). Due to the lack of clarity in defining the pseudoarthrosis, Mills et al. suggested defining the pseudoarthrosis as a 'mobile' atrophic non-union, in contrast to the more common 'stiff' atrophic non-union (Mills & Simpson 2012).

Alluded from the description of fracture healing, different factors influence its progression. Giannoudis et al. coined the 'diamond concept' of fracture healing, which has four corners including: osteogenic cells, osteconductive scaffolds, growth factors and the mechanical environment (Giannoudis et al. 2007). It is proposed that failure in any single factor will compromise fracture healing. To that end, a lack of adequate vascularisation will prevent the recruitment of stem and progenitor cells necessary for *de novo* tissue formation and growth factor production. Open fractures and high energy fractures have increased risk of non-union development, likely in part due to their compromised extraosseus and intraosseus blood supplies, typified by tibial fractures increased non-union rates appropriated to their inherently vulnerable vascular supply (Rhinelander 1974). Surgical or traumatic removal of

the blood clot will also deprive the fracture of the initial growth factor rich haematoma (Harwood et al. 2010). As discussed above, the mechanical environment will also directly affect the progression of fracture healing, with either excessive motion from inadequate fixation or insufficient loading both compromising healing. Excessively stiff fixation with large gaps will also be unable to heal. Where there is a large gap as a result of comminution, poor surgical reduction, or surgical/traumatic removal of bone, there will be loss of the osteoconductive scaffold (Nilsson et al. 1993; Harwood et al. 2010).

The reported risk factors for non-unions will have influence on differing aspects of the diamond concept. Gender itself is not a risk factor, although young men and older women are over-represented due the types of fractures they sustain; men with high energy traumatic fractures, older women with osteoporotic associated fractures (Mills & Simpson 2013). The young, as growing individuals, have their bone forming machinery already in play and see an accelerated pattern of healing attributed to a thicker periosteum and larger subperiosteal haematomas (Lindaman 2001). Increasing age however, does suppress the speed and ability of bone to heal itself. Clinical and experimental studies suggest that mesenchymal stem cells and endothelial progenitors are reduced in number and the responsiveness of fracture healing reduces with increasing age; typified by delayed periosteal reaction, reduced tissue formation and slowed endochondral ossification (Gruber et al. 2006). Other comorbidities such as diabetes mellitus, thyroid disorders, and malnutrition can also impair healing. Experimentally, diabetes mellitus reduces growth factor production (IGF1, VEGF, TGFβ), cellular proliferation, collagen synthesis and osteoblast activity. Prescribed medications including NSAIDs and steroids, in addition to smoking and alcoholism can all impair the biological aspects of fracture healing (Gaston & Simpson 2007).

1.4.2 Model systems of impaired fracture healing

Experimentally, non-union can be created through several techniques including mechanical instability, damaging the vascular supply with periosteal stripping/removal local soft-tissues, reaming the intramedullary cavity, applying distraction and introducing material to prevent bridging (Mills & Simpson 2012). The most common method is to establish a critical sized defect, which is defined as the "minimum amount of bone loss that will not heal by bone formation in an animals lifetime" (Schmitz & Hollinger 1986). 'Key's hypothesis' proposes that a gap in the bone of 1.5x the diaphyseal diameter would lead to non-union (Key 1934). The actual size varies in terms of the phylogenetic scale of the animal, the position of the defect within the bone and how the periosteum and soft-tissues are managed. Typically, a critical size defect ranges from 1.5x to 3x the diameter of the bone (Garcia et al. 2013). These models are the mainstay of investigation into non-union, however, they are usually

created with a background of ‘effective biology’ whereas many non-unions develop in subcritical sized defects, with some other aspect, often biological, being compromised. Despite these drawbacks, critical sized defects can be standardised and are relatively simple to achieve, providing a consistent test scenario for experimentation. Many of these models will provide mechanical stability by plate and screws or more commonly an external fixator frame or an intramedullary pin.

When choosing the test species, it is important to consider the feasibility of the procedure, husbandry, costs, and similarity to human bone structure and physiology. Historically, large animal models have been popular, typically sheep and goats. As noted, their bone formation differs with a predominant primary bone structure (plexiform), however their weight and size permits direct use of human implants and tools. Pigs are a closer match to human in terms of bone structure and healing, however they are more problematic to handle and their hind limb long bones are relatively short (Newman et al. 1995). The use of rodent models has significantly increased to nearly 50% of all fracture studies over the last two decades, associated with availability of rodent molecular tools, their low cost and easy husbandry. Rats have primary lamellar bone, with cancellous remodeling, although their cortical remodeling is less than in humans (Garcia et al. 2013). Currently, the rat is used for around one third of all *in vivo* fracture studies (Mills & Simpson 2012). The size of a critical sized defect in rats varies between studies and reflects in part the differing mechanics of their chosen stabilisation, or lack of, and whether periosteal stripping is performed. Typically, researchers have used very large defects of around 3-8mm or moderate defects <3mm. It is currently recommended to induce an atrophic non-union through either a critical sized defect or by periosteal stripping/endosteal damage of a non-critical gap, due to their differing aetiopathogeneses (Garcia et al. 2013). Previous work using a relatively rigid rodent external fixator developed at the Institute of Orthopaedics, UCL, showed consistent union with a 0.5mm gap and non-union with a 3mm gap by five weeks (Harrison et al. 2003). Arguably, the aforementioned study and many others studies do not give sufficient time to determine the development of a non-union as analogous to the human clinical scenario, and hence these models may be considered delayed-union models. That said, when a characteristic atrophic non-union is visible at five weeks, this end stage remodeled fracture is unlikely develop a union, even with more time.

Comment: Based on the considerations above, I will use a rodent model with a standardised critical sized defect, stabilised with an external fixator as the test model system.

1.5 Treatments to improve fracture healing

1.5.1 Biophysical modulation

Electromagnetic fields and electrical currents have been used in fracture healing modulation, in particular for non-union treatment since the 1800s (Brighton et al. 1981; Mollon et al. 2008). Experimental studies have shown electromagnetic stimulation affects growth factor production, collagen turnover and cytokine synthesis (Mollon et al. 2008). The electrical potential from current application affects oxygen concentrations, enhancing osteoblast activity; induces pH changes affecting the activity balance between osteoblasts and osteoclasts; and increases hydrogen peroxide concentrations, which drives release of VEGF from macrophages. Indirect application using pulsed electromagnetic fields, appears to mediate its effect on cellular activity by increasing cytosolic calcium concentrations and subsequent signalling pathways mediated through calmodulin (Schemitsch & Kuzyk 2009). A meta-analysis on clinical efficacy however, was unable to show conclusive evidence of a positive effect on delayed or non-unions, however the studies were highly variable in design and execution (Mollon et al. 2008).

Low-intensity pulsed ultrasound has been used in a range of clinical scenarios to boost fracture healing. Ultrasonic sound waves create pressure effects on tissues, transmitted by molecular vibrations and collisions. They are thought to mediate their effects through subsequent thermal changes and non-thermal micro-mechanical strains, mediated through piezoelectric effects and changes in calcium ion concentrations (Martinez de Albornoz et al. 2011). Downstream osteoinductive effects include increased gene expression (VEGF, osteocalcin, alkaline phosphatase, COL I, fibronectin), blood flow and improved healing, however a clinical meta-analysis was unable to identify significant impact conclusively (Busse et al. 2009), although NICE guidelines support its use (Nandra et al. 2015).

1.5.2 Bone graft

Bone autograft, and in particular cancellous bone grafts (CBG), have been the ‘go to’ stimulant for fracture healing for many years and generally considered the ‘gold standard’ graft material. CBG remains the only graft material with osteogenic (provision of donor site stem cells or stimulation of resident cells to form bone), osteoinductive (provision of growth factors to stimulate recipient site stem cell differentiation) and osteoconductive (provision of a framework for tissue deposition and cellular migration) properties. In fulfilling the above categories, it has a proven track record in stimulating and aiding fracture healing with non-union healing rates of up to 87-100%. The most common source of CBG in humans is the iliac crest, and in dogs the proximal humerus. The issues are that it is limited in volume and

requires a separate harvesting procedure with associated morbidity (Sen & Miclau 2007). Cortical bone can also be of benefit, but is less cellular than CBG and its replacement with new bone through creeping substitution is significantly slower. However, it does provide good mechanical support.

1.5.3 Demineralised bone matrix (DBM)

Allograft bone, with its mineral content removed through acid extraction, leaves only the osteoinductive proteins of bone including collagen, non-collagenous proteins and growth factors that drive endochondral ossification (Khan et al. 2005). First described by Urist, his landmark studies demonstrated that bone demineralised with HCL, can form cartilage and bone when implanted in extra-skeletal tissues (Urist 1965). Subsequently, it became clear that Bone Morphogenic Proteins (BMPs) were underlying this effect (Innes & Myint 2010). DBM is now produced by different companies and is generally widely available. The donor and the production methodology influence its performance, with some products performing better than others. It may be less effective than a CBG (Sen & Miclau 2007), but does avoid donor morbidity and is available in large volumes 'off the shelf'.

1.5.4 Growth factors, cytokines & signalling peptides

Of the growth factors or soluble factors used to augment bone healing, Bone Morphogenic Proteins (BMPs) are the best known. They are members of the TGFβ superfamily, of which BMP2 and BMP7 are most used. Two randomised controlled trials using rhBMP7 in tibial non-unions have shown a benefit. The first compared rhBMP7 with autograft and had comparable results by two years; the second compared surgical management alone or with rhBMP7 and showed significant benefit of rhBMP7 (Simpson et al. 2006).

FGF2 (Fibroblast Growth Factor 2) and PDGF (Platelet Derived Growth Factor) have also been evaluated in randomised controlled trials of fracture healing and arthrodesis respectfully. FGF2 increased radiographic union, and PDGF combined with b-tricalcium phosphate had equivalent outcomes to autograft (Einhorn & Gerstenfeld 2014).

Parathyroid hormone (PTH) modulates calcium homeostasis, typically increasing blood calcium ion levels by osteoclast mediated bone resorption. PTH can variably have a catabolic or anabolic influence on bone depending on its dose, frequency and duration. In a femoral rat fracture model, daily pulsed PTH during healing enhanced the stiffness and bone/cartilage volume in the callus, although there were no changes in osteoclast density. Similar outcomes were seen in treated post-menopausal women with radial fractures and pelvic fractures (Einhorn & Gerstenfeld 2014). Teriparatide, a man made recombinant

analogue of PTH is currently used clinically in osteoporosis as an anabolic treatment (Saag et al. 2007).

The Wnt signalling pathway has roles in bone formation and fracture healing, by signalling osteoblasts to form bone. Sclerostin, which was identified from studies on sclerosing bone dysplasias, and the subsequent anti-sclerostin antibody therapy (romosozumab) which blocks the inhibitor of Wnt, have shown increased metaphyseal bone formation and tibial defect healing in rats (Einhorn & Gerstenfeld 2014).

1.5.5 Platelet rich plasma (PRP)

The fracture haematoma has an important role in stemming blood loss, but also provides a growth factor rich environment aiding and abetting early cell migration and differentiation. Platelets and fibrin make up the haematoma and activated platelets degranulate their alpha granules releasing growth factors such as TGFβ, PDGF, VEGF and IGF (Dimitriou et al. 2005; Alsousou et al. 2009). PRP is an autologous product isolated from plasma where the platelets have been concentrated to about five times the normal level; 1,407,640 platelets per mL is considered a working definition. Three different production techniques are available including cell separators, selective filtration (plateletpheresis) and gravitation sequestration (centrifugation protocols) (Alsousou et al. 2009). Currently, the evidence for their efficacy is limited and the NIH and a Cochrane review failed to find sufficient evidence to support their usage (Nandra et al. 2015). Animal studies whereby PRP has been combined with PDGF, or polycaprolactone-tricalcium phosphate scaffolds have shown improved mechanical strength, vascular invasion and bone union in bone defects (Nandra et al. 2015).

1.5.6 Gene therapy

Gene therapy is most commonly associated with restoring the function of a defective gene, however, it is also a means to augment key signals during fracture healing. Critical to this type of therapy is the delivery of the desired genetic signal. Typically, this is achieved through viral vectors *in vivo,* either directly to the site of interest or by making use of viral tropisms. Alternatively, cells such as stem cells are extracted and transfected with a viral vector to enhance certain characteristics, such as homing or retention and deliver them back to the fracture site to enhance healing (Ho et al. 2014). BMP2 has been most extensively researched for gene therapy to enhance fracture healing experimentally using recombinant adenovirus, retro or lentiviruses in segmental defects and spinal fusions (Evans 2012). Concerns over the risks associated with viral vectors and the difficulties of *in vitro* cell transfection are hampering translation.

1.5.7 Scaffolds/tissue engineering

Osteoconductive scaffolds, either inert, biologically osteoinductive, or cell-seeded, are under investigation for treatment of non-union and bone defects. Critically, when implanting foreign materials, they need to be biocompatible and have the correct porosity, appropriate mechanical performance, ideally be osteoinductive and biodegradable to allow replacement with regenerated bone.

Scaffolds consisting of natural biological materials such as collagen, fibrin, hyaluronan and chondroitin sulphate, mimic bone ECM, and hence provide excellent cellular support, however they are usually mechanically limited and complex to manufacture. Collagen type I is a key component of all musculoskeletal tissues and beneficially has osteoinductive properties. It has been manufactured into membranes, sponges and gels, and enhances chondrogenic differentiation of MSCs (Nöth et al. 2010). Structured tissues are also of interest, such as demineralised cortical bone (Guo et al. 1991) and de-cellularised cartilage, which has shown promise as a means to bypass earlier indirect bone healing steps and start with endochondral ossification immediately (Vas et al. 2018) .

The ideal scaffold pore size should approximate trabecular bone morphology, with the average pores size in humans being 223um. Most scaffolds fall into the range of 200-400um, with a high level of interconnected porosity, ideally around 90%, to allow cell adhesion and bone ingrowth, with exchange of nutrients and waste products throughout the scaffold structure (Wu et al. 2017). Natural inorganic materials are usually coral based, mainly comprised of calcium carbonate or phosphate, with high porosity and osteoconductivity, but poor mechanical strength and osteoinductivity. Treating the coral structure with a hydrothermal process leads to transformation of the calcium carbonate into hydroxyapatite. Microwave treated squid bone has improved characteristics over coral and has some promotive properties for osteogenic differentiation (Wu et al. 2017). A series of studies has shown that calcium phosphate derived scaffolds can be osteoinductive (Amini et al. 2012).

Synthetic scaffolds are usually based on metal or inorganic materials such as glass, calcium based structures, or ceramics. Metals used for scaffolds include stainless steel, cobalt chrome and most commonly titanium. They are straightforward to manufacture and have superior mechanical strength, yet their modulus is significantly stiffer than bone, potentially leading to stress shielding. They may also release metal ions under certain circumstances and have no biologically inductive properties (Wu et al. 2018).

Non-metal biological scaffold materials such as hydroxyapatite and tri-calcium phosphate, are treated to high temperatures and termed bioceramics. These have been extensively

researched and can osseointegrate with osteoinductive and osteoconductive properties. However, they are brittle and their biodegradation unpredictable (Wu et al. 2017). Synthetic poly(α-hydroxy esters) scaffolds are bio-absorbable and include polyglycolic acid (PGA), polylactic acid (PLA), poly(lactic-co-glycolic acid) (PLGA), and poly-ε-caprolactone (PCL). They are broken down by hydrolysis, and through chemical modification can have their rate of degradation altered. Although easy to manufacture, they carry no significant mechanical support, have no osteoinductive properties, and rapid breakdown release of their monomers can induce macrophage driven inflammation (Nöth et al. 2010).

Current limitations of scaffolds may be overcome by combining differing scaffold types to provide synergy with the organic and inorganic scaffold properties. A further evolution is the development of 'intelligent scaffolds' that have signalling molecules/growth factors intentionally attached, or indeed be used to seed stem cells prior to application (Shrivats et al. 2014).

1.5.8 Stem & progenitor cell therapy

In the late 1800s, there was an awareness of a need for a source of cells 'stem cells' to allow certain tissues, such as blood, skin, bone, to renew continuously over a lifetime. Stem cells are undifferentiated cells that can self-renew by cellular division, and depending on from where and when they are isolated, are variably able to differentiate terminally down a variety of cell lineages. Totipotent stem cells can form an entire organism from a single cell and this ability is restricted to the stem cells of the embryo 'embryonic stem cells', prior to the eight cell morula stage (Wobus & Boheler 2005). Pluripotent stem cells can form all the embryonic germ layers tissues (endo-, meso-, ectoderm) and finally multipotent stem cells are further lineage restricted. Stem cells are considered as either embryonic or adult, with adult being defined as those found in the postnatal animal. Finally, there is a category of artificial adult stem cell, created in the laboratory from an adult terminally differentiated cells; the induced pluripotent stem cell (Fortier 2005).

Embryonic stem cells

Embryonic stem cells were first isolated over 30 years ago and are closely associated with the *in vitro* fertilisation revolution. The excitement associated with stem cell therapy is directly attributed to these cells, due to their self-renewal, pluripotency and prolonged culture sustainability (up to two years) (Fortier 2005), making them a universal tissue healing donor (Amini et al. 2012). Adult stem cells generally have a more limited lifespan, associated with their shorter telomere length and reduced telomerase activity (Rubin 2002).

Osteogenic differentiation of embryonic stem cells has been successfully performed and single cell suspensions supplemented with b-glycerolphosphate, ascorbate and dexamethasone to induce differentiation, is effective and simple. Combining them with 3D scaffolds appears to potentiate their osteogenic differentiation, with increased expression of ALP and osteocalcin when compared with 2D culture (Tian et al. 2009). BMP 3D scaffolds of PLGA and hydroxyapatite have regenerated bone *in vivo*, and embryonic stem cell derived osteoblasts will form bone when implanted in the soft-tissues of donor mice (Kim et al. 2008). They have also been differentiated down a chondrogenic pathway prior to transplantation, mimicking endochondral ossification and used to treat critical sized defects in rats (Jukes et al. 2008). Embryonic stem cells remain a source of ethical debate in human research as they are derived from fertilised embryos, specifically the inner cell mass of the blastocyst, and autogenous therapy in adults is not possible by their nature.

Perinatal derived stem cells

These stem cells are sourced from the tissues associated with the neonate, including the umbilicus, placenta and Wharton's jelly. They are considered an intermediate between embryonic and adult stem cells. Beneficially, they can be isolated from tissues usually discarded after birth. Amniotic fluid derived stem cells, amniotic membrane isolated and chorion derived stem cells have all been described (Si 2015). Ectopic bone formation has been demonstrated with chorionic derived stem cells combined with hydroxyapatite/tri-calcium phosphate implanted into SCID mice (Kusuma et al. 2015).

Due to their ease of isolation, umbilical cord blood and the connective tissue between the umbilical arteries and vein, known as Wharton's jelly, are also of interest. The blood in the umbilicus is unusually rich in pluripotent stem cells and have healed critical sized defects when combined with a collagen/TCP scaffold in nude rats (Jäger et al. 2007).

Adult stem cells

In the tissues of the post-natal animal, there are adult stem cells, also known as somatic stem cells, which are responsible for the maintenance, repair and replacement of body tissues; from the rapid turnover of blood cells and intestinal linings, to the slow turnover of brain tissue. Bone marrow is a relatively straightforward tissue to isolate cells from and hence adult stem cell research began there in the 1950s. Adult stem cells are generally considered lineage restricted relating to their source tissue, typically being multipotent. The best characterised adult stem cell is the haematopoietic stem cell, from the seminal work of Till and McCulloch (Till & McCulloch 1961; Becker et al. 1963).

1.5.8.1.1 Haematopoietic stem cells

The 'atomic era' drove significant research into the irradiation of tissues and several important observations were noted. Firstly, mice could be spared the effects of lethal irradiation by protecting either their femur or spleen with lead shielding, and later, Lorenz et al. demonstrated that intravenous infusion of bone marrow after irradiation would also spare them (Little & Storb 2002). Eventually, it became clear that haematopoietic stem cells residing within the bone marrow were able to reconstitute lifelong multilineage haematopoiesis in transplanted hosts (*in vivo*). Bone marrow transplantation remains a key feature in the treatment of haematological malignancies to this day (Little & Storb 2002).

1.5.8.1.2 Bone marrow derived mesenchymal stem cells

At the same time as bone marrow was being researched for its potential to recapitulate the blood system, researchers were becoming aware if its osteogenic potential (Tavassoli & Crosby 1968). However, it was the Russian Alexander Friedenstein, who identified the responsible osteogenic sub population of bone marrow stromal cells (Friedenstein et al. 1968). In further work, Friedenstein identified them as fibroblastic-like cells, isolated by their adherence to tissue culture plastic and ability to form colonies (CFU-F). These bone marrow stromal cells, or skeletal stem cells, or mesenchymal stem cells (MSCs), a term coined by Caplan in the 1990s (Caplan 1991), have unique properties that are used to describe MSCs, namely, tissue culture plastic adherence, self-renewal, and tri-lineage differentiation (bone, cartilage and fat). Notably, when bone marrow stromal cells are transplanted *in vivo*, they can develop into a fully fledged 'bone organ' without the need for exogenous growth factors to cue bone formation (Owen & Friedenstein 1988; Bianco et al. 2013). Within the bone marrow, they are a rare population equating for approximately 1 in every 10,000 nucleated bone marrow cells (Friedenstein et al. 1970; Owen & Friedenstein 1988; Pittenger et al. 1999).

Bone marrow MSCs are found on the surface of sinusoidal blood vessels within the bone marrow, below the endothelium, where they form on the perivascular stromal strata of bone marrow. It is here that osteogenic committed cells are found and invade the bone during development. In postnatal bone marrow, MSCs have a supportive role for haematopoietic stem cells. They also provide a source of osteoblasts and adipocytes during growth and remodeling, and chondrocytes during fracture healing. The transcriptome of these cells includes osteogenic genes such as Runx2 (Bianco et al. 2013).

Bone marrow aspirates have clearly demonstrated a beneficial effect on fracture healing in numerous animal studies (Hadjiargyrou et al. 2014). Clinically, Hernigou used concentrated

bone marrow aspirates to treat tibial non-unions and was able to correlate efficacy to a critical number of colony forming units, i.e. the number of MSCs (Hernigou et al. 2005). This has been developed experimentally with improved healing of critical sized defects using culture expanded bone marrow MSCs (Kadiyala et al. 1997; Bruder et al. 1998). Despite numerous pre-clinical studies, clinical evidence in humans is not currently available, although they have been used in veterinary clinical patients (Smith et al. 2014; Kriston-Pál et al. 2017). What remains clear from *in vivo* transplantation assays, is that bone marrow MSC are a *bona fide* skeletal stem cell capable of regenerating an entire bone organ (Bianco et al. 2013).

1.5.8.1.3 Other tissue derived mesenchymal stem cells

Bone marrow MSCs have been the most extensively researched, however, the same *in vitro* criteria of plastic adherence, tri-lineage differentiation and self-renewal has been shown by cells isolated from a range of adult connective tissues (da Silva Meirelles et al. 2006). Despite this, identification of an *in vivo* MSC niche has been problematic, although evidence emerged that pericytes, which are mural branched cells on the abluminal side of small blood vessels, share some markers with MSCs including CD44, CD73, CD90, CD105 and CD146 (Shi & Gronothos 2003). These cells could demonstrate *in vitro* characteristics of MSCs (Augello 2010), however, whether or not they represent a true niche remains unclear.

Criteria for identification of MSCs has varied between studies due to a lack of consensus and the variability of MSCs relating to their method of isolation, species of isolation, passage number and culture conditions. In 2006, a position statement was made for the minimal criteria for defining multipotent human mesenchymal stromal cells. The International Society for Cellular Therapy position statement identified the following criteria: *1) tissue-culture plastic adherence, 2) expression of CD105, CD73, CD90 and lack of CD45, CD34, CD14 or CD11b, CD79a or CD19, HLA-DR and 3) capacity to differentiate down osteoblastic, adipogenic and chondrocytic lineages* under *in vitro* differentiating conditions (Dominici et al. 2006). This *in vitro* criteria does not require *in vivo* transplantation evidence as demonstrated by haematopoietic stem cells or bone marrow derived mesenchymal stem cells.

1.5.8.1.3.1 Adipose mesenchymal stem cells

First discovered by Zuk et al. from processed lipoaspirate (Zuk et al. 2001), there is interest in adipose derived stem cells due to their ease of availability and the relatively greater yield of stem cells compared with an equal volume of bone marrow aspirate (Knight & Hankenson 2013). Although they can be *in vitro* tri-differentiated, rat adipose MSCs have reduced

osteogenic capacity compared with bone marrow MSCs, as demonstrated by lower ALP and osteocalcin expression, and negligible *in vivo* bone formation (Hayashi et al. 2008). Their apparent efficacy in some rodent and canine studies on fracture healing (Barba et al. 2013) may be indirect by recruitment of 'tissue resident' stem cells through paracrine signalling, and the possible benefit of their immunomodulatory effects (Knight & Hankenson 2013). It remains unclear and of debate as to whether administered stem cells contribute directly to repair tissues, or whether they have a role in orchestration through trophic and/or immunomodulatory effects, probably through recruitment and signalling to tissue resident and host migrating stem cells (Fortier 2005).

1.5.8.1.3.2 Periosteal progenitor cells/mesenchymal stem cells

As discussed in the fracture healing section, the periosteum is a source of progenitors for fracture healing (Colnot 2009; Hadjiargyrou et al. 2014) and damage to their niche leads to non-union (Nicholls et al. 2013). Tracking studies have identified that these cells develop into cartilage and bone producing cells in the callus (Colnot 2009) and have shown *in vitro* tri-lineage differentiation (Wang et al. 2010). When transplanted in a carrier scaffold, these cells were tracked forming new bone. Although seemingly important in fracture healing, they are not a viable source for therapy because they are difficult to obtain. Clinically, it is rare to see non-union in the skeletally immature individuals, possibly attributed to their thick periosteum and likely increased niche of periosteal stem cells.

1.5.8.1.4 Induced pluripotent stem cells

These cells have been artificially manipulated through altered gene expression to have pluripotency. They were first developed in 2006 by retroviral delivery of four transcription factors into fibroblasts; Oct4, Sox2, Klf4 and myc (Takahashi & Yamanaka 2006), and since then, human terminally differentiated cells have also been de-differentiated back to pluripotency (Takahashi et al. 2007). Although these cells appear to have *in vitro* equivalence to embryonic stem cells, the epigenetic imprint of the native transformed cell may remain and influence their *in vivo* function. They also raise a therapeutic concern due to the presence of oncogenes to drive their 'stemness', with reports of teratoma formation (Takahashi et al. 2007). Induced pluripotent stem cells have been differentiated down an osteoblastic lineage and have successfully formed new bone when implanted in SCID mice, however to avoid teratoma formation, irradiation of the cells was required prior to transplantation (Hayashi et al. 2012). The potential risk of oncogenesis and concerns over viral transfection are currently limiting their application.

Endothelial progenitor cells & CD34+ cells

Endothelial progenitor cells (EPCs) were first described by Asahara et al. in 1997. They were isolated from peripheral blood mononuclear cells selected for CD34 expression and then grown on fibronectin in the presence of certain growth factors. They expressed endothelial cell markers VEGFR2 and CD31, and could form microvascular tube-like networks (Asahara et al. 1997). EPCs isolated from the blood have been shown to form chimeric vessels in the host when injected into ischaemic models, suggesting a key role in neovasculogenesis through differentiating into mature endothelial cells (Patel et al. 2016). They have been the focus of intense research in cardiovascular disease, as a potential therapy for myocardial infarcts and peripheral vascular disorders (Chong et al. 2016; Ward et al. 2007). There is a proposed influence on fracture healing as vascularisation is essential for bone formation (Keramaris et al. 2008; Hankenson et al 2011; Rhinelander 1968). In experimental models, cultured transplanted EPCs have improved healing possibly through promoting neovascularization (Li et al. 2011). However since Asahara et al., various isolation techniques and definitions of EPCs have been described leading to some confusion in the field.

CD34+ expressing cells include EPCs and haematopoietic stem cells, and have been isolated from the peripheral blood and bone marrow of humans. In a series of rodent studies, human CD34+ cells have been transplanted into immunocompromised rats and shown improved fracture healing. It is thought that these cells improve fracture healing through both differentiation into osteoblasts (Chen et al. 1997) and endothelial cells and by releasing VEGF (Kuroda et al. 2014). The composition of CD34+ cell populations is mixed and hence the proportion and cell type from that population that actually contributes remains unclear.

Circulating skeletal stem cells

Although only recently an area of focus (Kuznetsov et al. 2001; Zvaifler et al. 2000), there has been an awareness of peripheral blood circulating skeletal progenitors since the nineteenth century, when they were first described by Paget (Chesney & Bucala 1997). Zvaifler et al. were the first to isolate MSCs from blood conclusively, by expanding them on glass in DMEM + 20% FCS, and could induce osteogenic differentiation (Zvaifler et al. 2000). Others have found isolating these cells controversial and difficult, with positive and negative results in the literature (Kassis et al. 2006; Kamal et al. 2014). Clinical evidence from fracture patients supports a role of circulating skeletal/mesenchymal stem cells (Alm et al. 2010) and EPCs (Ma et al. 2012) in fracture healing. Experimental parabiotic mouse studies also support the mobilisation of progenitors to fracture sites (Kumagai et al. 2008). Currently these cells are thought to circulate in small numbers of around 1 per $10^{6\text{-}8}$ blood

mononuclear cells in mice, rabbits, guinea pigs and humans (Khosla & Eghbali-Fatourechi 2006).

1.6 Migration & homing of stem cells: SDF1-CXCR4 axis

1.6.1 SDF1-CXCR4 structure & expression

In development, homeostasis and inflammation, cells need to navigate successfully through the body to complete their tasks. Chemokines are small, mostly secreted proteins of 8–14 kDa, and function to recruit and activate cells. Based upon the position of two cysteine residues, they are categorised into four groups: CXC, CC, C, and CX3C. Cells have G-protein-coupled seven-transmembrane receptors, which bind their respective chemokine, driving cell migration or chemotaxis, usually along a concentration gradient of the chemokine. Their main functions are in immune cell activation and recruitment, however, a key function in stem cell migration and homing has been identified, not to mention their role in pathologies such as autoimmunity, inflammatory disease, HIV and cancer (Lewellis & Knaut 2012). The chemokine stromal cell derived factor 1 (SDF1), also known as CXCL12, binding to its classical receptor CXCR4 and alternative receptor CXCR7, has numerous roles in guiding cells in development and adulthood. The CXCR4 receptor is thought to have primary responsibility for migration whereas CXCR7 plays a role in cell adhesion (Puchert & Engele 2014; Chen et al. 2015). Activation of the receptors initiates several signalling cascades including MAPK, phospholipase C and PI3kinase pathways, to drive cellular migration and adhesion molecule expression (Janssens et al. 2017).

1.6.2 SDF1-CXCR4 physiology

SDF1 was initially identified as a soluble agent that activated B-lymphocytes, and its importance in primordial germ cell migration was demonstrated with SDF1 or CXCR4 knockouts being lethal. SDF1 also has a role in cortical brain development, with the expression of CXCR4 on Cajal-Retzius and GABAergic interneurons being essential for correct spatial arrangements (Lewellis & Knaut 2012). SDF1 has two splice variants; α and β, with α being the ubiquitous form. SDF1 is rapidly cleared from the circulation due to the active form being unstable and through its binding to charged GAGs on endothelial cells, which shield the active form from proteolytic cleavage. This binding facilitates haptotactic gradients in diapedesis, facilitating cell migration into tissues (Netelenbos et al. 2003; Teixidó et al. 2018).

In addition to migration, this chemokine-receptor pair is essential for temporospatial maintenance of cells in locations within the body. Extensive work on haematopoietic stem

cells identified the endosteal surface of bone as their homing site (Wilson & Trumpp 2006). More precisely, haematopoietic stem cells are found within perivascular regions, in association with reticular cells that express SDF1 (Sugiyama et al. 2006). SDF1 is therefore essential for maintaining haematopoietic stem cells in their 'niche' as notation for a "defined spatial structure in which stem cells are housed and maintained by self-renewal in the absence of differentiation" (Wilson & Trumpp 2006) (Figure 1.5a).

Beyond maintaining the bone marrow stem cell niche, SDF1-CXCR4 functions in the migration and homing of stem cells from the circulation to the bone marrow (Peled 1999). Under resting physiological conditions, stem cells will migrate from one location and home to another within the body. This phenomenon is best researched in haematopoietic stem cells, which have been shown to leave the bone marrow niche, enter the circulation, extravasate into different tissues and then return to the bone marrow, with circadian rhythms influencing this process (Wright et al. 2001; de Lucas et al. 2017). Bone marrow engraftment of human haematopoietic stem cells transplanted into SCID mice demonstrated the importance of SDF1-CXCR4 to this process, with monoclonal CXCR4 blocking antibodies preventing migration and engraftment (Peled 1999). An underlying driver of SDF1 expression pattern in the bone marrow is thought to be the reduced oxygen tension at endosteal surfaces (Eliasson & Jönsson 2010). Similar migratory patterns have also been identified after intravenous transplantation of MSCs; initially they locate to the lungs and liver, possibly due to microvascular entrapment, however by three days in the presence of a fracture, they subsequently home to the fracture (Granero-Moltó et al. 2017). Again only MSCs expressing CXCR4 were capable of this migration, with CXCR4 null cells remaining in the lungs.

1.6.3 SDF1-CXCR4 in repair & fracture healing

SDF1 is constitutively expressed in a range of adult tissues including brain, spleen, stomach, intestines, thymus and lymphatics (Nagasawa et al. 1994). After damage, SDF1 expression is increased in the heart (Askari et al. 2003), kidney (Tögel et al. 2005), skin (Toksoy et al. 2007), and brain (Imitola et al. 2004), with an associated migration of CXCR4 expressing cells, including stem cells to the damaged regions. This is also true of fracture healing, which needs to recruit a range of cells including inflammatory cells, endothelial cells and stem cells in order to heal without a scar (Marsell & Einhorn 2011; Einhorn & Gerstenfeld 2014; Tawonsawatruk et al. 2012). Experimentally, distraction osteogenesis, stress fractures and segmental defects have all demonstrated local increases in SDF1 (Lee et al. 2010; Kidd et al. 2010; Toupadakis et al. 2012). SDF1 is increased in hypertrophic and immature cartilage near cortical bone in fractures, and the co-localisation of hydroxyprobe (identifies hypoxic cells) (Toupadakis et al. 2012) suggests a mechanism mediated by vascular damage leading to hypoxia, which in turn increases SDF1 expression via HIF1**α** (Hirota & Semenza 2006;

Ceradini et al. 2004). When a fracture occurs therefore, it is postulated that a chemotactic gradient develops, with high levels of SDF1 at the fracture site, and subsequently increased levels in the blood steam, facilitating stem cell migration (Yellowley 2013) (Figure 1.5b). Corroborating this theory, the vast majority of cells in the fracture including chondrocytes, osteoblasts, osteoclasts and MSCs, express CXCR4 (Toupadakis et al. 2012).

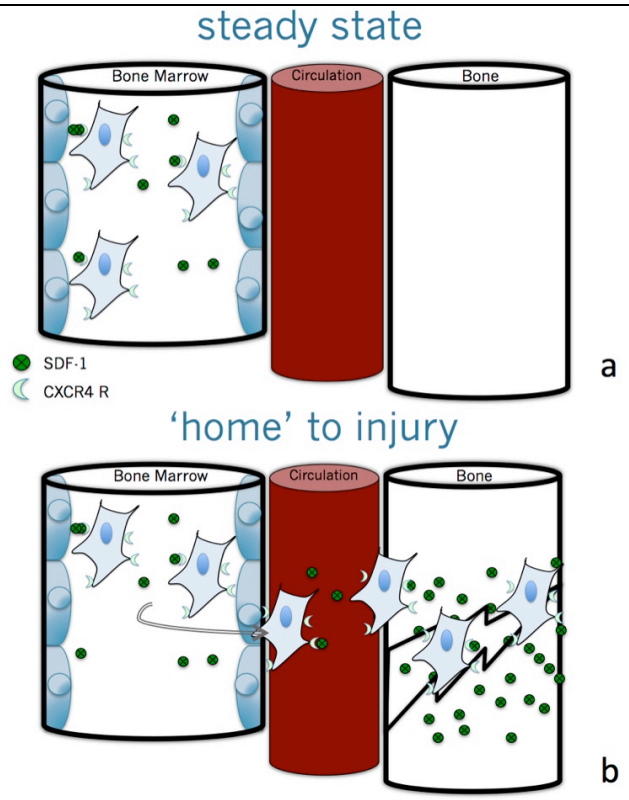

Figure 1.5: a) Diagram showing stem cells bound by their CXCR4 receptors to the bone marrow niche which expresses SDF1. b) Diagram illustrating stem cells migrating along an SDF1 concentration gradient, from the bone marrow niche into the peripheral circulating and then homing to a fracture expressing high levels of SDF1.

Otsuru et al. demonstrated the essential role of CXCR4 for systemically delivered GFP labelled osteoblast progenitors to migrate to the sites of fracture (Otsuru et al. 2008). Other elegant parabiotic GFP studies have shown stem cells from the labelled donor will travel via the circulation and home to a fracture site of the conjoined partner, and these cells expressed ALP at similar levels to other cells in the fracture callus (Kumagai et al. 2008). Notably, there is a low level of donor cells relocating to the uninjured bone marrow after four to seven weeks, however when a fracture is introduced, there is significantly higher homing within two weeks, but this homing is more evident between 7-14 days than 0-7 days. A role for SDF1 and CXCR4 with EPC migration in fracture healing is also supported from experimental studies, where CXCR4 conditional knock-out sourced EPCs had reduced

migration and colony forming ability *in vitro*, and reduced fracture healing *in vivo* (Kawakami et al. 2015).

For migration and subsequent homing to occur, stem cells need to be able to undergo diapedesis with its associated stages, much like a neutrophil or other white blood cell (Nitzsche et al. 2017). MSCs do have some of the same adhesion molecules such as selectins and integrins (Sohni & Verfaillie 2013), and MSCs, like haematopoietic stem cells, can bind to endothelial cells from the umbilicus with TNFα potentiating this effect (Rüster et al. 2006). MSCs therefore, also have the required tools to home and migrate.

Comment: The published literatures shows the interaction of SDF-1 and CXCR4 is essential in stem cell niche maintenance and for migration to a site of injury to facilitate healing. Therefore, if I intervene with the SDF1-CXCR4 axis, I may be able to utilise endogenous stem cell therapy for fracture healing, potentially through MSC and EPC mobilisation.

1.7 Stem cell mobilisation

An intentional forced egress of cells, termed 'mobilisation', has been in clinical use for some time with haematopoietic stem cells. These cells are mobilised from the bone marrow for bone marrow transplantation to treat a range of blood related malignancies (Broxmeyer et al. 2005; Liles et al. 2003; Martin et al. 2006; Bendall & Bradstock 2014). GCSF was the first growth factor used to mobilise haematopoietic stem cells from the bone marrow and into the peripheral circulation for stem cell transplantation (Bendall & Bradstock 2014). The mechanism of stem cell mobilisation by GCSF involves increased production of CD34+ cells within the bone marrow, proteolytic cleavage of VCAM-1 (Lapidot & Petit 2002), and SDF1 (Lévesque et al. 2003), such that the adherence of stem cells to their niche is reduced allowing their mobilisation into the peripheral circulation.

1.7.1 AMD3100 in haematopoietic stem cell mobilisation

AMD3100, (1,1-[1,4-Phenylenebis(methylene)] bis-1,4,8,11-tetraazacyclotetradecane octahydrochloride), is a symmetric bicyclam derivative and was initially found as a functional contaminant when screening commercially available cyclams for HIV treatment. AMD3100 affects the CXCR4 receptor, which was shown to be the route of entry for HIV into T cells. AMD3100, as a non-peptide antagonist, is now thought to cause conformational constraint upon the CXCR4 receptor (Gerlach et al. 2001), preventing SDF1 binding. During phase I clinical trials, it caused further unexpected results with a leukocytosis in treated patients. Later work confirmed mobilisation of a population of CD34+ haematopoietic stem cells into the peripheral circulation by highly selective, high affinity

competitive blockade of the CXCR4 receptor (Rosenkilde et al. 2004; De Clercq 2009), displacing them from the bone marrow niche. Currently, it is used as Mozibil™, to mobilise rapidly high numbers of haematopoietic stem cells from the bone marrow into the peripheral circulation for transplantation in haematological cancers, sometimes in synergistic combination with GCSF (Lévesque et al. 2003; Hendrix et al. 2000; Calandra et al. 2008) (Figure 1.6a).

1.7.2 AMD3100 in non-haematopoietic stem cell mobilisation

Although haematopoietic stem cells have been successfully mobilised, work on MSC and other progenitors is limited. These cells do not seem to be as migratory as hematopoietic stem cells, potentially due to their larger size and increased niche adherence (Lévesque et al. 2007). Pitchford's seminal work on different mobilisation protocols in mice, demonstrated that AMD3100 combined with VEGF rather than GCSF, preferentially mobilises a population of MSCs and EPCs, rather than haematopoietic stem cells (Pitchford et al. 2009).

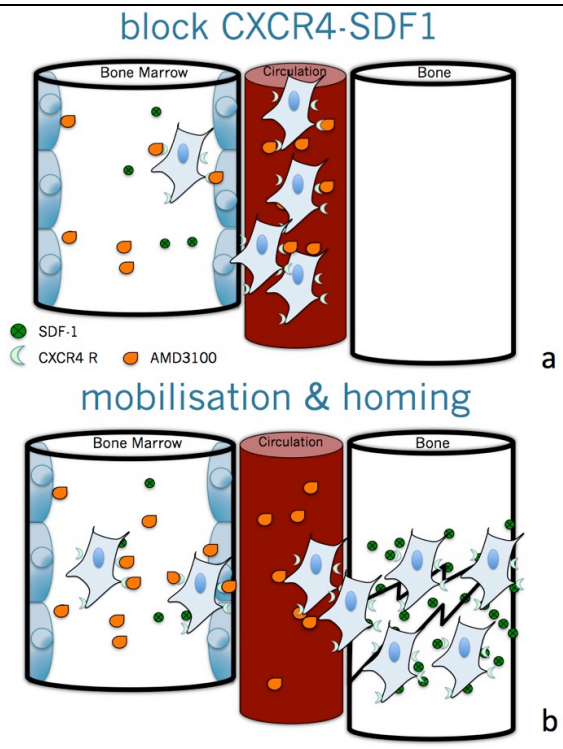

Figure 1.6: a) Diagram showing the postulated effect of mobilising MSCs from their niche, by the binding of AMD3100 to the CXCR4 receptor leading to displacement into the circulation. b) Diagram showing the proposed beneficial mechanism of mobilising MSCs from the niche in the presence of a fracture with high expression of SDF1 to increase the numbers of MSCs available to home to the fracture.

Only a few groups have started to investigate mobilisation of stem cells to augment bone healing. If it is possible to increase the pool of circulating stem and progenitors cells by using mobilising agents, this could increase the number of cells available to home to the fracture site, and potentially enhance healing (Figure 1.6b). To date, critical sized calvarial defects have shown enhanced healing with 15 daily injections of AMD3100 in mice (Wang et al. 2011), and McNulty showed significant improvement in intramedullary trabecular bone re-formation with a single dose of AMD3100 (McNulty et al. 2012). For evaluation in diaphyseal long bone fracture healing, there are two publications in mice. Kumar et al. mobilised MSCs using IGF1 with AMD3100 in a tibial segmental defect that was externally coapted. On DXA scan, they showed a significant increase in bone mineral density and an increase in bone mineral content, however their paper did not give detailed assessment of fracture healing (Kumar & Ponnazhagan 2012). Yellowley's group used AMD3100 alone once daily for three days after creating an Einhorn style mouse femoral fracture stabilised with a single intramedullary pin. They showed a significantly larger fracture callus at 21 days which became significantly smaller by 84 days, suggesting accelerated remodelling (Toupadakis et al. 2013). Kumar's study did not provide much detail on the fracture healing, and both Kumar and Toupadaki's studies were subject to a highly variable mechanical fracture healing environment and used models expected to heal. Notably, it has also been shown that prolonged treatment with AMD3100 over the course of fracture healing has an inhibitory effect, reducing the mineralised and cartilaginous callus volume, down regulating genes associated with endochondral ossification, probably by blocking homing to the fracture itself (Toupadakis et al. 2012).

Comment: There is a role of SDF1 and CXCR4 in fracture healing, and evidence for selective stem cell population mobilisation, potentially enhancing fracture healing. I intended to evaluate this proposition using a mechanically standardised model, without guaranteed healing, to determine whether endogenous stem cell mobilisation, in particular MSC mobilisation may improve compromised fracture healing. I shall evaluate AMD3100 with growth factors that have been used to mobilise stem and progenitor cells for boosting fracture healing.

1.8 Research gap & context of thesis

It is currently unknown whether the combination of VEGF and AMD3100 will mobilise MSCs and EPCs in a rat model. Further, evaluation of endogenous mobilisation has not been performed in a mechanically standardised fracture model, which has impaired healing, more akin to the translational clinical situation. A direct comparison between differing

combinations of growth factors and AMD3100 to boost fracture healing is also not currently available.

The research questions were:

1. Is it possible to mobilise MSCs and EPCs in rats by administering AMD3100 combined with VEGF?
2. What is the ideal critical sized defect, stabilised with a micro external fixator, to evaluate endogenous mobilisation?
3. What is the most effective combination of growth factor with AMD3100 to improve fracture healing?

1.9 Thesis aims & hypothesis

The aims were:

1. To establish whether it is possible to increase the circulating numbers of MSCs and EPCs, as measured by CFU count, through mobilisation in a rat model, and to compare them to bone marrow stromal cells and adult endothelial cells.
2. To improve the ease and consistency of application, and to reduce complications such as pin tract loosening, with the micro femoral fixator system used at IOMS.
3. Using the updated rat femoral fixator system, to determine the preferred osteotomy gap to evaluate endogenous mobilisation to improve fracture healing, in addition to establishing the effect on interfragmentary strain and construct stiffness.
4. Using the improved fixator and the preferred mechanical environment, to evaluate different mobilisation strategies on impaired fracture healing *in vivo*.

The main hypothesis of my thesis was: ***Antagonism of the CXCR4-SDF1 axis can mobilise stem and progenitor cells into the circulation of rats and by increasing the available pool of cells early in fracture healing, improve fracture healing.***

1.10 Potential benefits

Should this methodology of endogenous mobilisation show potential, this may be an appropriate prophylactic adjunct to give to 'at risk' fractures, such as fragility fractures, tibial fractures, open high energy comminuted fractures, or those with comorbidities for impaired healing. Endogenous mobilisation may provide an additional biological stimulus when operatively treating established non-unions.

CHAPTER 2: Isolation & Characterisation of Mesenchymal Stem Cells & Endothelial Cells

2.1 INTRODUCTION

The potential of bone marrow to generate a bone ossicle dates back to classical transplantation experiments of Goujon in the nineteenth century, where bone marrow from rabbits and chickens formed ectopic bone with marrow, in muscle recipient beds (Bianco et al. 2008). Alexander Friedenstein went on to identify a fibroblastic type cell with plastic adherence, within bone marrow stromal cells (Friedenstein et al. 1968). Following Friedenstein's seminal work, different methods have been used to isolate MSCs from bone marrow, including isolation by plastic adherence (Friedenstein et al. 1970), gradient density separation (Pittenger et al. 1999) and sorting combined with selection through cell surface markers (Gothard et al. 2014). Due to the ease of obtaining cells, and the small volumes of tissue available in rodent models, direct plating of bone marrow for plastic adherence is commonly used, however, this technique results in a population of cells that are not a pure stromal culture, although this may actually be beneficial with improved growth of CFU-Fs (Mareschi et al. 2012).

2.1.1 Characterising mesenchymal stem cells

Once a culture is obtained, it is necessary to confirm 'stemness' or multipotency by differentiation down at least two lineages *in vitro* (Pittenger et al. 1999). *In vitro* differentiation of MSCs by incubation with insulin, 1-methyl-3-isobutylxanthine, indomethacin and dexamethasone will drive adipogenic differentiation and lipid vacuole development (Pittenger et al. 1999; Augello et al. 2010). Alternatively, when supplemented with dexamethasone, ascorbate and β-glycerolphosphate, MSCs become cuboidal and produce calcium deposits as osteoblasts (Friedman et al. 2006). Finally, if centrifuged to create a pelleted micromass and cultured without serum but with TGFβ supplementation, the cells form a proteoglycan rich matrix, consistent with cartilage production (Pittenger et al. 1999; Augello et al. 2010). Their *in vitro* ability to differentiate is classically used in conjunction with their CFU-F forming self-renewal as confirmation of cell type. Importantly, in the contradictory and complex field of mesenchymal stem cell biology, when bone marrow stromal cells are transplanted *in vivo* they can develop into a fully fledged 'bone organ', without the need for exogenous growth factors to cue bone formation (Owen & Friedenstein 1988; Bianco et al. 2013). Although there is evidence that MSCs can be sourced from a range of adult tissues based upon *in vitro* criteria (da Silva Meirelles et al. 2006), the *in vivo* evidence is lacking. There is a consideration that bone marrow MSCs are currently the most appropriate target for managing bone tissue related healing (Bianco et al. 2013) and hence is the stem cell source of choice to improve fracture healing.

Cell surface markers are a further method to characterise cells. Again, this is complex as there is no defining unitary cell surface marker for MSCs, and many of the markers used to identify MSCs are expressed on a range of other cells types. Ultimately, a panel of absent and present markers are employed, however, species antibody cross-reactivity, variable expression levels and lack of cell type-specific expression creates difficulties (Boxall et al. 2012). Although there is an international consensus statement for a set of markers which should or should not be expressed on human MSCs (Dominici et al. 2006), many research publications have used different markers, or differing combinations. This is further complicated by the effect of *in vitro* culture on marker expression and inherent species differences (Boxall & Jones 2012; Spencer et al. 2011). Although there are numerous monoclonal antibodies available for the human and mouse, there are significantly fewer for the rat, however the rat is a better model for bone research due to its increased size over the mouse. Based on previous work in the rat, the working definition of MSCs used in this thesis included low expression of both CD45 (leukocyte marker) and CD34 (haematopoietic stem cell marker) and high expression of CD29 and CD90 (Boxall et al. 2012; Davies et al. 2015; Spencer et al. 2011; FafianLabora 2015).

CD34 was first identified on haematopoietic stem cells and is used for cell isolation and enrichment in bone marrow transplantation. CD34 is a transmembrane phosphoglycoprotein, however its function has not been fully elucidated, although a role in cell adhesion, differentiation and proliferation is suggested (Lin et al 2013). Usually considered a marker of haematopoietic stem cells, it is also seen in some endothelial progenitors, embryonic fibroblasts, potentially some isolates of MSCs, dendritic cells and epithelial progenitors (Sidney et al. 2014; Lin et al. 2012). Notably, it is positively expressed in adipose derived MSCs, although *in vitro* culture does reduce this (Lin et al 2013).

CD45, a receptor-like protein tyrosine phosphatase cell surface marker, is expressed on all haematopoietic cells (other than red blood cells), platelets and plasma cells, and hence considered a pan-leukocyte marker, with a role in signal transduction. Nearly all literature sites absence of CD45 as a criterion for MSC identification and there is only one report of CD45 expression on MSCs (Yeh et al. 2006). Currently, the prevailing literature identifies the co-absence of CD34 and CD45 as characteristics of MSCs in culture (Boxall et al. 2012; Dominici et al. 2006).

CD90 (Thy-1), originally discovered as a thymocyte antigen, is a glycophosphatidylinositol (GPI) coupled receptor, thought to mediate cell to cell interactions (Lin et al 2013). It may have a role in MSC differentiation (Moraes et al. 2016), and molecular targeting to reduce expression of CD90 in MSCs resulted in increased adipogenic and osteogenic differentiation.

CD90 is universally expressed on MSCs isolated from any source, however it is not exclusive to MSCs (Boxall et al. 2012).

CD29, also known as integrin beta-1, is a transmembrane protein with a role in cell to extra-cellular matrix adhesion. Again, it is expressed on a range of cells types including MSCs in a range of species (Boxall et al. 2012) and is frequently used in combination with CD90 in panels to identify MSCs (Boxall et al. 2012; Davies et al. 2015).

Currently, the international Society for Cellular Therapy have established three criteria for identification of human MSCs: 1) tissue-culture plastic adherence, 2) expression of CD105, CD73, CD90 and lack of CD45, CD34, CD14 or CD11b, CD79a or CD19, HLA-DR, and 3) capacity to differentiate down osteoblastic, adipogenic and chondrocytic lineages under *in vitro* differentiating conditions (Dominici et al. 2006). The cells in this chapter were evaluated for plastic adherence, *in vitro* tri-differentiation and cell surface marker expression. Of the four CD markers in my panel, CD90 (Thy-1), CD45 and CD34 are all cited as key markers in the position statement.

2.1.2 Characterising endothelial progenitor cells

Endothelial progenitor cells (EPCs) were also of interest as the mobilisation strategies used in chapters 3 and 6 mobilise EPCs as well as MSCs into the peripheral circulation (Pitchford et al. 2009). Further, there is also a role for vascularisation during bone formation and fracture healing (Keramaris et al. 2008; Hankenson et al 2011; Rhinelander 1968) and blocking angiogenesis has been shown to drive atrophic non-union development experimentally (Hausman et al. 2001). Clinical data also supports their role in fracture healing, with EPCs being significantly increased in the peripheral blood after fracture (Ma et al. 2012). Additionally, models of distraction osteogenesis and fracture healing have shown increases in circulating EPCs, peaking at day three, but remaining high throughout healing (Lee et al. 2010). Culture expanded and locally transplanted EPCs have also increased bone healing and avoided non-union development in a rat femoral defect model. The subsequent microCT analysis showed a significant increase in bone volume, trabecular number, trabecular thickness and spacing (Li et al. 2011). However, it is unclear how EPCs improve fracture healing (Atesok et al. 2010). The previous paradigm of blood vessel formation was that new blood vessels form from proliferation and migration of the local undamaged endothelium, known as ‘sprouting’. However, in the 1960s, it was noted that Dacron patches would become covered in endothelium (Stump et al. 1963) and the source was circulating CD34+ bone marrow cells (Shi et al. 1998), now referred to as EPCs. More recent studies have shown that EPCs can differentiate into endothelial cells and contribute to

neovascularisation (Ward et al. 2007).

Peripherally circulating bone marrow derived EPCs were first described by Asahara et al., after culturing CD34+ cells on fibronectin in the presence of certain growth factors. After seven days in culture they showed endothelial characteristics, including amongst others, expression of endothelial markers VEGFR2 and CD31, and the ability to form tube-like structures (Asahara et al. 1997). CD31 is also known as platelet endothelial cell adhesion molecule (PECAM-1) and is expressed on several cell types but reliably seen on endothelial cells (DeLisser et al. 1994). VEGFR2 is a receptor tyrosine kinase, (also known as KDR (kinase domain region) and Flk-1), that has a key role in proliferation, migration and survival of endothelial cells (Ferrara et al. 2003).

Since Asahara et al., some groups have corroborated and others have shown different marker expression and described different types of EPCs, leading to confusion in this field (Mund & Case 2011; Patel et al. 2016; Minami et al. 2015). The confusion is further confounded by the presence of two distinct cell morphologies seen in culture. The "early-outgrowth EPCs" with a spindle shaped morphology (Hur et al. 2004), have been most extensively studied and are from monocytic lineages, poorly proliferate and often die during prolonged culture (Ward et al. 2007). The "late-outgrowth EPCs" are usually seen after two weeks of culture and colonies of cells typically show a cobblestone morphology (Hur et al. 2004), resembling differentiated endothelial cells. Current thinking is that the two EPCs types may have complimentary roles, with early EPCs expressing inflammatory cytokines and paracrine angiogenic factors, whereas late EPCs express proliferation and angiogenesis genes driving tubulogenesis (Cheng et al. 2013). This difference may also influence their effect on fracture healing, as when transplanted, early-outgrowth EPCs improved segmental fracture healing more than late EPCs. The early-outgrowth EPCs appear to have trophic effects with higher VEGF expression (Giles et al. 2017); perhaps having similarity to the functional paracrine properties of MSCs. In a similar vein, *in vitro* plasticity of human MSCs towards an endothelial gene expression profile and morphology, has been shown experimentally (Janeczek Portalska et al. 2012).

2.2 Plan for chapter 2

In this chapter I planned to isolate and evaluate rat bone marrow MSCs, to form a baseline comparison for assessment of endogenously mobilised blood MSCs in chapter 3. In order to develop the methodology and assess the EPCs isolated in chapter 3, I chose to work with human umbilical vein endothelial cells (HUVECs) as a gold standard for endothelial cells. Owing to the confusion in definitions for EPCs, and the possible isolation of late or early-

outgrowth cell populations, I sought a clearly defined population with known characteristics including VEGFR2 and CD31 expression, microvascular network formation and a clear monolayer polygonal cell morphology, "cobblestones", distinct from fibroblasts (Jaffe et al. 1973). Additionally, HUVECs are readily available at relatively low cost and are frequently the cell of choice to compare endothelial progenitors against (Bou Khzam et al 2015; Asahara et al. 1997; Shi et al. 1998; Bompais et al. 2004). I therefore planned to evaluate the expression of my monoclonal antibodies for CD31 and VEGR2, and also functionally test *in vitro* tube formation using extracellular matrix synthesised by Engelbreth-Holm-Swarm tumour cells, often referred to as Matrigel or Geltrex on HUVECs (ThermoFisher, UK) (Faulkner et al. 2014; DeCicco-Skinner et al. 2014).

Hypotheses:

- **Bone marrow derived MSCs isolated by tissue culture plastic adherence from rat femoral bone marrow form CFU-Fs, and can be expanded and differentiated into osteoblasts, adipocytes and chondrocytes *in vitro,* and have high expression of CD90 & CD29, and low expression of CD45 & CD34.**
- **Adult endothelial cells (HUVECs) have a cobblestone cell morphology, are able to form tubule-like arrangements *in vitro* when plated on Geltrex (ThermoFisher, UK), and would positively express endothelial cell markers CD31 & VEGFR2.**

The aims and objectives of this chapter were:

1. To isolate bone marrow MSCs and expand in 2-dimensional cell culture.
2. To identify bone marrow MSCs by their cell surface marker expression and cell culture characteristics.
3. To differentiate bone marrow MSCs into osteoblasts, adipocytes and chondrocytes.
4. To expand Human Umbilical Vein Endothelial Cells (HUVEC) in 2-dimensional cell culture.
5. To confirm Endothelial cell identity by their cell surface marker expression, cell culture characteristics and *in vitro* tube formation assay.

2.3 MATERIALS & METHODS

2.3.1 Bone marrow MSC isolation & characterisation

Healthy, ex-breeder female wistar rats were the donors (n=3). All procedures were carried out according to the Home Office Animals Scientific Procedures Act of 1986. The rats were euthanised via cervical dislocation. The skin over the femur was clipped and aseptically prepped with 4% chlorhexidine solution (Hibiscrub, UK). The limb was draped with a sterile fenestrated drape and under aseptic conditions, a lateral skin incision from dorsal to the greater trochanter to the proximal tibia was made to expose the musculature of the femur, and the femur was dissected out. Femora were placed in a sterile universal container with Dulbecco's Modified Eagle Medium low Glucose (DMEM) (Sigma-Aldrich UK) with 1% Pen-strep (Invitrogen, UK) for transport. Under a tissue culture hood, the femora were washed in 70% isopropyl alcohol and then sterile PBS. All soft tissues were removed and both ends of the bone were resected using a no.10 scalpel blade to expose the medullary canal. The medullary canal was flushed with 5mls of stem cell culture media (DMEM 4500 mg/L glucose, Sigma-Aldrich, UK) with 20% fetal calf serum (FCS) and 1% penicillin/streptomycin) using a 21g needle and syringe, into a 25cm^2 polystyrene cell culture flask (Corning, USA). The cells were cultured in a humidified incubator at 37°C, 95% air and 5% CO_2. The media was changed after 5-7 days to remove non-adherent cells and every 3-4 days thereafter. Within 7-10 days, colonies became apparent. Once they had reached 70-80% confluence, they were "passaged" or expanded, typically around 10-14 days post seeding using 1% Trypsin-EDTA (Sigma-Aldrich, UK), applied to cover the surface of the flask. The flask was incubated at 37°C for five minutes, during which time the cells lost their adhesion to the cell surface, rounded and lifted off. The trypsin was neutralised by the addition of at least the same volume of media. Passage 3 (P3) cells were used in subsequent studies. The cell suspension was pelleted by centrifugation at 2000rpm for five minutes. The supernatant was discarded and the cells were re-suspended in media and plated in 75cm^2 cell culture flasks (Corning, USA).

A cell viability count was performed using a 0.4% Trypan Blue solution (Sigma-Aldrich, UK); a small quantity of the cell suspension was removed and then added in a 1:1 ratio with Trypan Blue. A haemocytometer was used to count the number of viable cells. Trypan Blue has a negatively charged azo chromophore which binds to damaged cell membranes only. Therefore, unstained bright cells are live, and dark blue stained cells are considered dead.

Cell surface marker analysis of rat bone marrow MSCs

After trypsinisation and washing in PBS, P3 cells were suspended in 200ul 4% formalin for 15minutes at room temperature. Cells were then centrifuged at 2000rpm for five minutes to pellet the cells and remove the formalin. They were then washed twice with flow cytometry buffer (PBS + 0.5% Bovine serum antigen (BSA) (Sigma-Aldrich, UK)). The cells were then aliquoted into micro-Eppendorf tubes for staining (30,000 per group) with the appropriate antibodies at the recommended concentration for one hour, in the absence of light, at room temperature. After one hour, the cells were pelleted and then washed twice in blocking buffer (PBS+0.5% BSA) and kept at around 4^0C by placing on wet-ice. Analysis was performed using a flow cytometer (Cytoflex, Beckman Coulter, UK) with Cytexpert (Beckman Coulter, UK) software. Debris was removed from analysis via gating on a forward - side scatter plot. Doublets were subsequently gated out and colour compensation was applied.

Two negative markers for MSCs were used based on published literature for rat MSCs:

- CD34 (Anti-CD34 antibody [ICO-115] Phycoerythrin, IgG1 K, abcam ab187284)
- CD45 (Anti-Rat CD45 APC, IgG1 K, eBioscience 17-0461)

Two positive markers for MSCs were used based on published literature for rat MSCs:

- CD90 (Anti-Mouse/Rat CD90.1 (Thy-1.1) APC, Mouse IgG2a K, eBioscience, 17-0900)
- CD29 (Anti-Mouse/Rat CD29 (Integrin beta 1) FITC, Armenian Hamster IgG, eBioscience, 11-0291)

Isotype controls for each CD marker as follows:

- For CD34: Mouse IgG1 K Isotype Control PE (eBioscience 12-4714)
- For CD45: Mouse IgG1 K Isotype Control APC (eBioscience 17-4714)
- For CD90: Mouse IgG2a K Isotype Control APC (eBioscience 17-4724)
- For CD29: Armenian Hamster IgG Isotype Control FITC (eBioscience 11-4888)

MSC tri-differentiation

Plastic adherent cells with fibroblastic morphology were isolated and expanded by serial passage. Tri-differentiation capacity (osteogenic, adipogenic and chondrogenic potential) was determined from P3 cells (n=3). Cells were freed using trypsin-EDTA (Sigma-Aldrich, UK) and then counted by Trypan blue staining (Sigma-Aldrich, UK) and then subdivided to achieve appropriate cell suspension densities for subsequent experiments.

2.3.1.1.1 Osteogenic differentiation

Osteogenic media consisted of standard media with 100nM dexamethasone (Sigma-Aldrich, UK), 50μg/ml L-ascorbic acid 2-phosphate (Sigma-Aldrich, UK) and 10mM Glycerol-2-phosphate disodium salt hydrate, (Sigma-Aldrich, UK). For osteogenic differentiation, 30,000 P3 cells (n=3) were seeded into a sterile 48 well plate in triplicate and initially cultured in standard media for 48 hours, which allowed the cells to adhere and form a confluent monolayer. After this period, the media was changed for osteogenic media and subsequently changed every 3-4 days for 21 days. For controls, 30,000 P3 cells were seeded into a sterile 48 well plate, in triplicate, with standard media throughout. Cells were grown at 37°C, 95% air and 5% CO_2.

To identify calcium phosphate deposits positively from differentiated osteoblasts, Alizarin red stain was applied. The stain is an anthraquinone derivate and binds positively charged ions such as magnesium, strontium and calcium, staining them red. The osteogenic media was carefully aspirated to avoid disturbing calcium phosphate deposits and the wells were washed in 150μl of PBS. 150μl of 10% formalin was added to each well and then left at room temperature for 30 minutes. The formalin was then carefully aspirated and the wells washed again in 150μl of PBS. Prepared Alizarin red stain (0.2 Molar, pH 4.32, Sigma-Aldrich, UK) was added to each well to cover the surface of the base of the well and then left at room temperature for 30 minutes, in the dark. The stain was then carefully removed and the wells were washed three times in PBS until the solution became clear. A small amount of PBS was added to cover the base of the well prior to visualisation using light microscopy.

2.3.1.1.2 Adipogenic differentiation

Adipogenic media consisted of standard media with 0.1mM dexamethasone (Sigma-Aldrich, UK), 0.45 mM 3-Isobutyl-1-methylxanthine (Sigma-Aldrich, UK), 10mg/ml Insulin (1.7mmol/L) (Sigma-Aldrich, UK), and 50mM Indomethacin (Sigma-Aldrich, UK). For adipogenic differentiation, 30,000 P3 cells were seeded into a sterile 48 well plate in triplicate. After 48hours of culturing in standard media, the cells were confirmed to have adhered and the media was changed for adipogenic media and subsequently changed every 3-4 days for 21 days. For negative controls, 30,000 P3 cells in triplicate were fed with standard media throughout. Cells were grown at 37°C, 95% air and 5% CO_2. The Oil red O stain was used to confirm adipogenic differentiation by staining intracellular lipid droplets. Oil red O is a lysochrome diazo dye that binds to neutral triglycerides and lipids, staining them red. A 0.5% (w/v) Oil Red O stock solution was prepared in isopropyl alcohol and incubated at room temperature for one hour and then filtered through a 0.22μm filter to

remove precipitates. After 21 days of culture, cells were washed with PBS and fixed in 4% formalin for five minutes, then washed with PBS. Adipogenic media was aspirated and the wells were carefully washed in PBS. Wells were then fixed using 4% paraformaldehyde for three minutes at room temperature, which was then carefully removed and washed with PBS. A 60% isopropanol solution was then added to cover the bottom of the wells and incubated for 15 minutes, and then aspirated. Working Oil Red O solution was added to ensure the base of each well was covered, and then left for 15 minutes at room temperature. After removal, the wells were washed twice with PBS and then covered in a small volume of PBS to identify staining at x40 using a light microscope.

2.3.1.1.3 Chondrogenic differentiation

Chondrogenic media consisted of 100ml StemPro® Osteocyte/Chondrocyte Differentiation Basal Medium StemPro® (Gibco, UK), + 10ml serum free, transforming growth factor-β3 supplemented (StemPro® Chondrogenesis Differentiation Kit, Gibco, UK), Chondrogenesis Supplement. For chondrogenic differentiation, 1,000,000 P3 cells were suspended in a sterile universal container, in triplicate. The cells were pelleted by centrifugation at 2000rpm for five minutes. After 48 hours of culture in standard media, the media was changed for chondrogenic media: serum free, supplemented with transforming growth factor-β3, and subsequently changed every 3-4 days for 21 days. For negative controls, 1,000,000 P3 cells were pelleted as described and fed with standard media, in triplicate, and changed every 3-4 days. Cells were grown at 37°C, 95% air and 5% CO_2. After 21 days, cells were stained with Alcian Blue, a polyvalent basic dye that binds to acidic polysaccharides such as glycosaminoglycans in cartilage, staining them blue. Cell spheroids were washed in PBS and fixed with 10% formalin for 60 minutes at room temperature, before being washed with distilled water. Alcian blue solution (Sigma-Aldrich, UK) was added and then the spheroids were incubated for 24 hours at room temperature. The stain was removed and then a de-staining solution (30mls Ethanol (pure: 98-100%), + 20mls Acetic Acid) was added and removed twice. Spheroids were then viewed for blue staining indicating cartilage matrix deposition.

2.3.2 Endothelial cell characterisation

HUVECs from a single donor (500,000 cryopreserved Promocell C-12200, Promocell, UK) passage 5, cell line *1915,* were evaluated. Cells were grown in a 75cm^2 polystyrene cell culture flask and cultured in a humidified incubator at 37°C, 95% air and 5% CO_2. Endothelial growth media was made from EBM-2 Basal Medium 500 ml (Lonza, UK) combined with EGM-2 MV BulletKit (CC-3202, Lonza, UK), containing 5% fetal bovine

serum, human VEGF-1, human fibroblast growth factor-2, human epidermal growth factor, insulin-like growth factor-1, ascorbic acid, amphotericin and gentamycin. The media was changed after one day and then every 3-4 days. Once they had reached 70-80% confluence, they were subject to tubule assays and flow cytometric analysis.

Cell surface marker analysis of HUVECs.

P5 cells were passaged using Trypsin-EDTA as previously described. For each analysis 100,000 P5 cells were suspended in 100μl 4% formalin for 15 minutes at room temperature. Cells were then centrifuged at 2000 rpm for five minutes to remove the formalin. They were then washed twice with flow cytometry buffer (PBS + 0.5% BSA). The cells were aliquoted into micro-Eppendorf tubes for staining with the appropriate antibodies for one hour, in the absence of light at room temperature. After one hour, the cells were pelleted and then washed twice in blocking buffer (PBS + 0.5% BSA). All work was carried out on ice. Flow cytometry analysis was performed as described for the MSCs. Cells were evaluated for EPC markers:

- Anti-VEGFR-2 (KDR/EIC) (Fitc) (abcam ab184903)
- CD31 (TLD-3A12) (Fitc) (abcam ab33858)

Cells were also evaluated for lack of CD34 expression indicative of haematopoietic progenitors, and CD90 indicative of mesenchymal stem cells:

- CD34 (Anti-CD34 antibody [ICO-115] Phycoerythrin, IgG1 K, abcam ab187284)
- CD90 (Anti-Mouse/Rat CD90.1 APC, Mouse IgG2a K, eBioscience, 17-0900)

Controls included unstained cells, and isotype controls for each CD marker as follows:

- For CD34: Mouse IgG1 K Isotype Control PE (eBioscience 17-4714)
- For CD90: Mouse IgG2a K Isotype Control APC (eBioscience 17-4724)
- For VEGFR2: Mouse IgG1 (ICIG1) (Fitc) (abcam ab91356)
- For CD31: Mouse IgG1 (ICIG1) (Fitc) (abcam ab91356)

Functional 3D tube forming assay

When the HUVECs were confluent, the media was removed and cells were serum deprived by replacing with low serum media: EBM-2 Basal Medium 500 ml (Lonza, UK) + 1% FCS and incubated in a humidified incubator at 37°C, 95% air and 5% CO_2 for two hours. A 96 well plate was pre-cooled to 5°C and then all work was performed on ice. Per well, 2μl of 5°C Geltrex™ 'LDEV-Free Reduced Growth Factor Basement Membrane Matrix' (ThermoFisher Scientific, UK) was placed in the centre of each well and then carefully

spread across the entire base of each well using a sterile applicator (Faulkner et al. 2014). Control and inducted wells were performed in triplicate. The plate was then incubated at 37°C for 45 minutes to polymerise the Geltex. After two hours of serum deprivation, cells were trypsinised as previously described and then re-suspended in serum-deprived media and counted. Cells were re-suspended to achieve 5,000 cells per well, in 100µl of either full media (containing associated growth factors) or low serum media. Phase-contrast images were acquired using a Leica DMIRB (Leica, Germany) inverted microscope (×10 magnification).

2.4 RESULTS

2.4.1 Isolation & culture of rat bone marrow MSCs

By seven days of primary culture, fibroblastic-spindle shaped cells were adherent to the surface of the plastic culture flask and fibroblastic colony-forming units (CFU-F) were seen (Figure 2.1a). Each colony had originated from a single precursor mesenchymal stem cell. The cells had a clear flat fibroblastic morphology at later passages (Figure 2.1b and c).

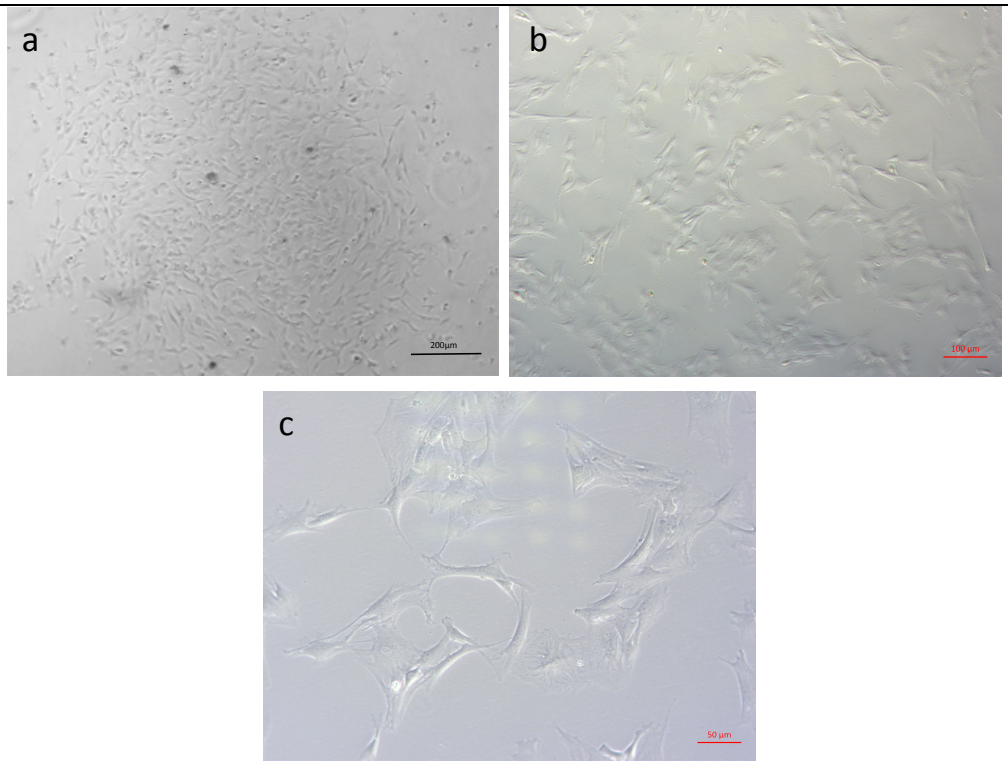

Figure 2.1: Light microscopy images of bone marrow MSCs at various stages. a) Passage 0 MSCs colony (day 10, x4 magnification). b) Passage 3 MSC (day 10, x5 magnification). c) Passage 3 MSCs (day 10, x10 magnification). Cells were flat and spindle shaped, characteristic of a CFU-F.

Cell surface marker analysis of rat bone marrow MSCs

A scatter plot of forward scatter versus side scatter showed a distribution of similar sized cells indicative of a cultured mono-population with a region of dead cells and debris relating to the processes involved in preparation for flow cytometry (Figure 2.2a). A dot plot of forward scatter area versus forward scatter height showed minimal variation indicative of a largely single cell pollution, however, it was gated to eliminate any possible doublets (Figure 2.2b). This cell population showed a lack of positive shift of increased fluorescence when compared with isotype fluorochrome control background levels, indicative of low/negative expression of known negative MSC markers CD34 and CD45 (Figure 2.3). Concomitantly, these cells showed a right shift indicating increased fluorochrome intensity compared with the isotype control level for mesenchymal stem cell markers CD90 and CD29 (Figure 2.4).

Cells isolated from all three rat donors showed similar cell surface expression patterns, being predominantly CD34 negative (99.8%), CD45 negative (94.3%), CD29 positive (98.4%), and CD90 positive (98.9%). (Table 2.1).

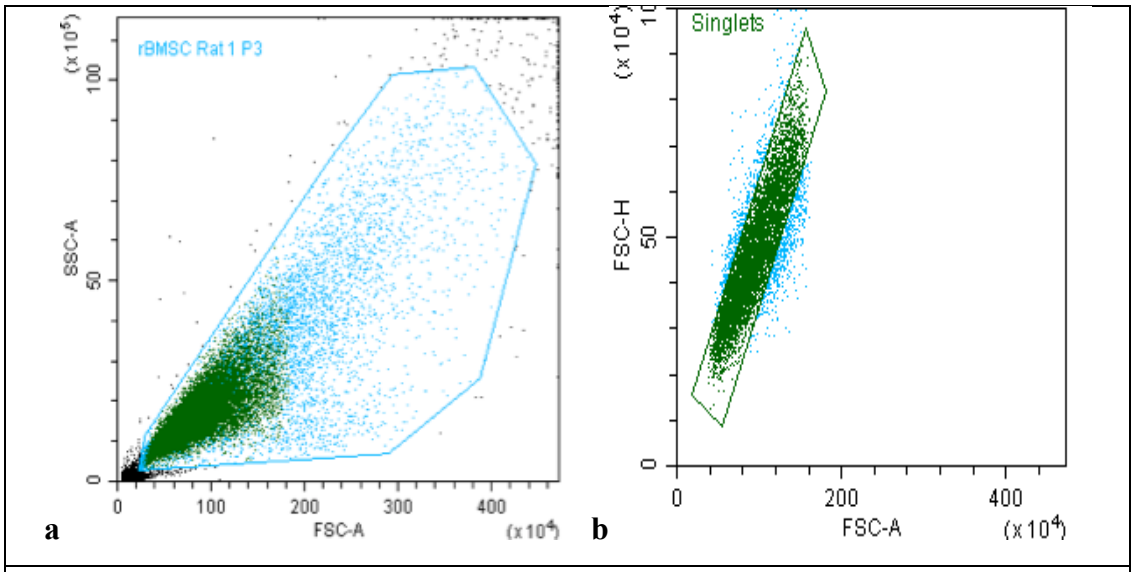

Figure 2.2: a) Flow cytometry dot plot for bone marrow MSCs, showing forward scatter vs side scatter for all events read. The gated region excluded dead cells and debris in the lower left corner. b) The gated region of live cells from the previous plot was assessed for clumping of cells. A close population was selected for all further analyses. (SSC-A = side scatter area, FSC-A = forward scatter area, FSC-H = forward scatter height.)

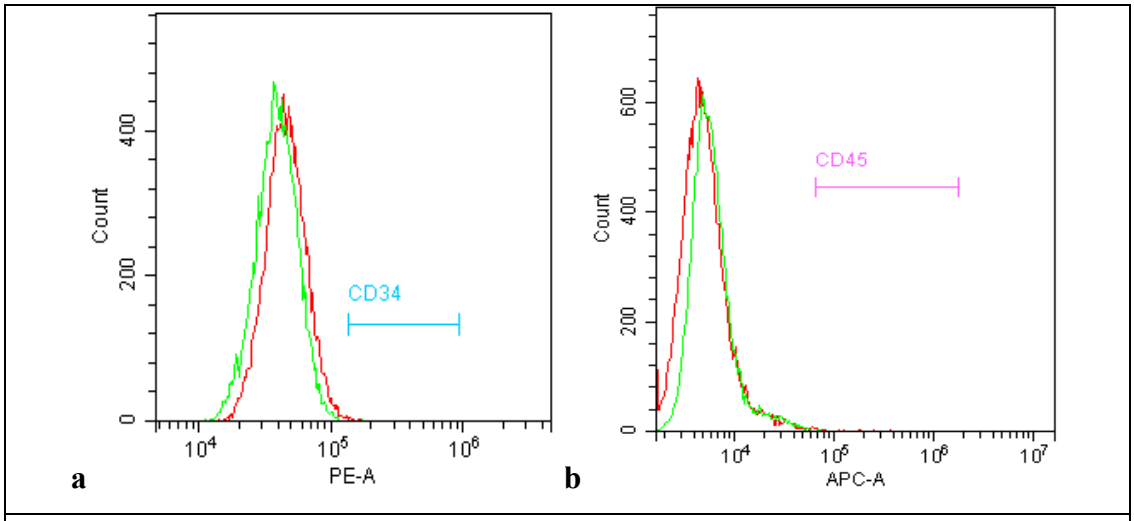

Figure 2.3: Flow cytometry histogram fluorescence counts for bone marrow MSCs. a) The red plot shows cells stained with PE conjugated isotype control and the green plot shows cells stained with PE conjugated CD34 antibody. b) The red plot shows cells stained with APC isotype control and the green plot shows cells stained with APC conjugated CD45 antibody. (PE-A = Phycoerythrin, APC-A = Allophycocyanin). In both plots, there is no right shift in fluorescence, indicating no staining above background, and therefore no expression of CD34 or CD45 markers on the MSCs.

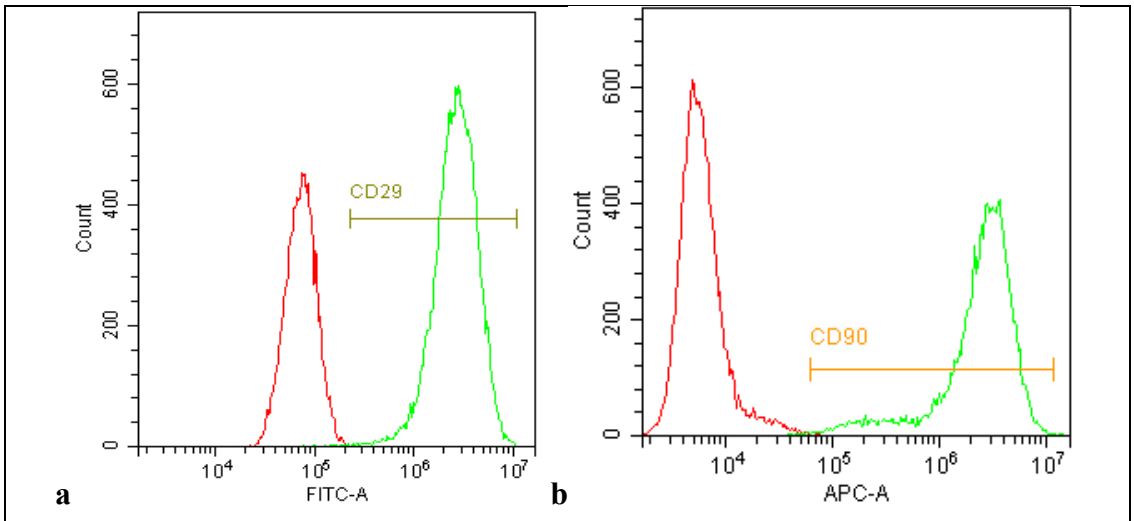

Figure 2.4: Flow cytometry histogram fluorescence counts for bone marrow MSCs. Figure a) The red plot shows cells stained with FITC conjugated isotype control and the green plot shows cells stained with FITC conjugated CD29 antibody. b) The red plot shows cells stained with APC conjugated isotype control and the green plot shows cells stained with APC conjugated CD90 antibody. (FITC-A = Fluorescein isothiocyanate, APC-A = Allophycocyanin). In both plots, the right shift in fluorescence indicates positive expression of CD29 and CD90 markers on the MSCs.

Rat	% CD45+	% CD34+	% CD29+	% CD90+
1	0.30	0.11	99.74	99.50
2	6.42	0.24	96.86	97.74
3	10.29	0.22	98.54	99.59
Mean±SD	5.7±5.0	0.2±0.1	98.4±1.4	98.9±1.0

Table 2.1: Individual and mean±SD flow cytometry expression levels (%) of the markers evaluated for bone marrow MSCs.

Osteogenic differentiation of rat bone marrow MSCs

Cells formed a monolayer on the base of the well within three days. The cell morphology became less spindaloid and more cuboidal and multiple small granules became apparent. Staining for Alizarin red after 21 days clearly demonstrated red granules indicative of calcium deposits, consistent with osteoblast differentiation and activity (Figure 2.5).

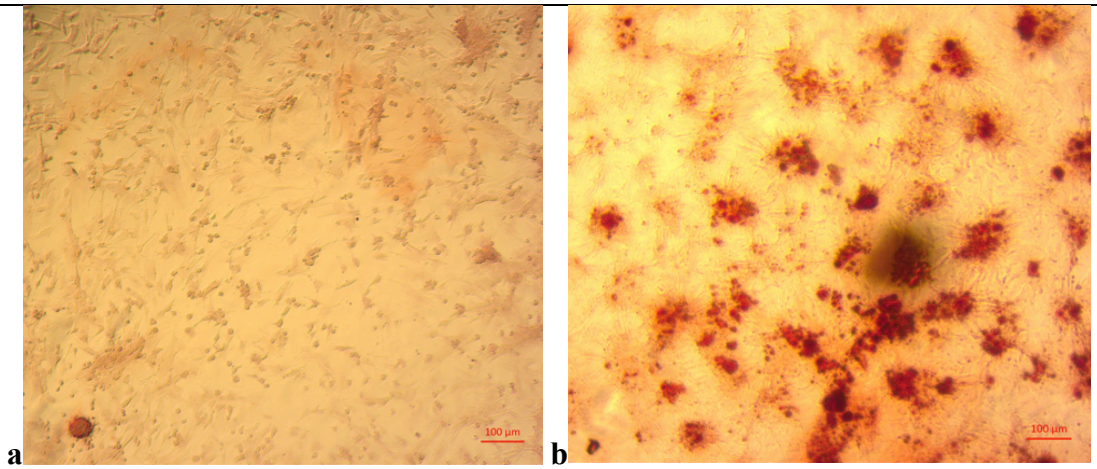

Figure 2.5: Light microscopy images of osteogenic differentiation at x4 magnification after 21 days culture. a) Control sample post Alizarin red staining where confluent MSCs have been treated with standard media. b) Positive Alizarin red staining of calcium deposits indicative of osteogenic differentiation.

Adipogenic differentiation of rat bone marrow MSCs

Cells formed a monolayer on the base of the well within three-five days. After 21 days of incubation with adipogenic media, a change in morphology was evident with cells appearing less spindle shaped, being shorter with longer extensions. Positive Oil Red O staining was evident by red dots indicating the presence of lipid and therefore adipogenesis (Figure 2.6).

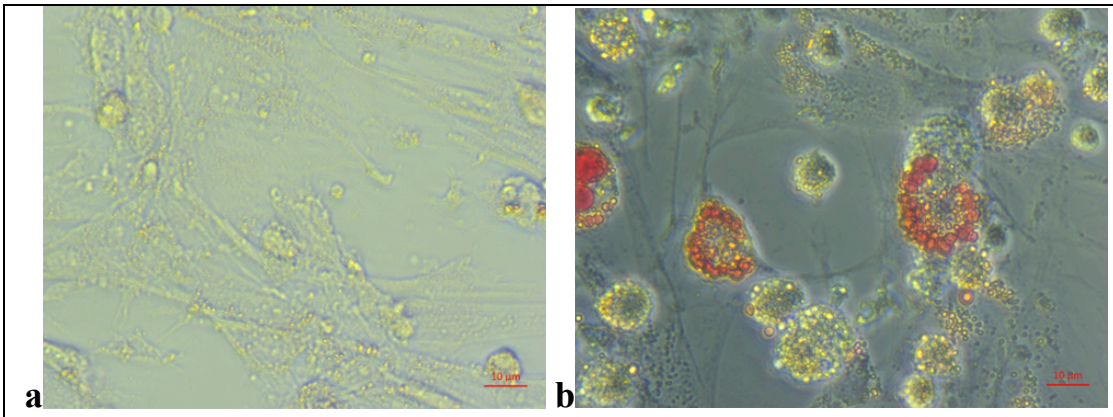

Figure 2.6: Light microscopy images of adipogenic differentiation, at x40 magnification after 21 days culture. a) Control sample post Oil Red O staining where confluent MSCs have been treated with standard media. b) Test samples with accumulations of red staining lipid droplets indicative of adipogenic differentiation.

Chondrogenic differentiation of rat bone marrow MSCs

Under gross observation, the chondrogenic supplemented pellets appeared to increase in size marginally when compared to the control samples. Staining with Alcian Blue at 21 days showed blue staining indicative of glycosaminoglycan synthesis, consistent with chondrogenic differentiation (Figure 2.7).

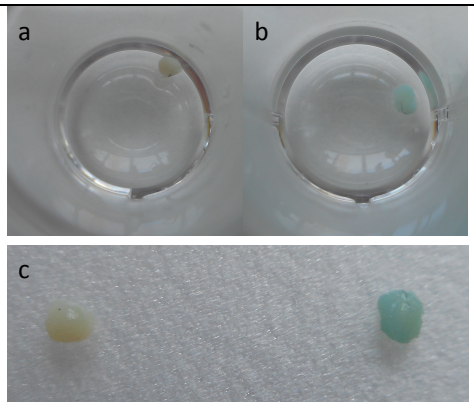

Figure 2.7. Photographs of the pelleted MSCs after 21 days culture. a) Control media pellet without any blue staining. b) Pellet cultured in chondrogenic media, with positive Alcian Blue staining indicating chondrocyte differentiation. c) Shows the two pellets at increased zoom (control sample on the left, test sample on the right).

2.4.2 HUVEC cell culture

HUVECs were grown to confluence and exhibited cobblestone morphology, distinct from that of the MSCs (Figures 2.8 & 2.9).

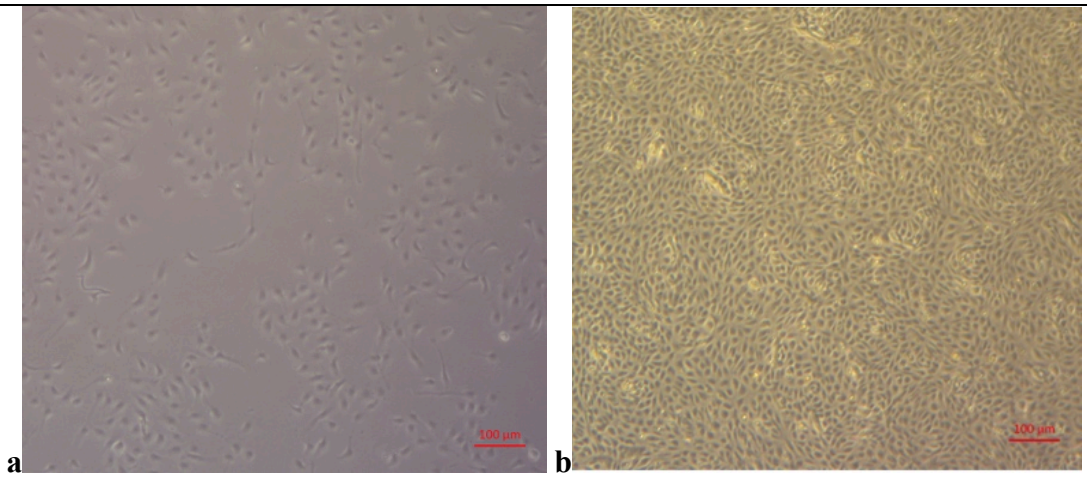

Figure 2.8: Light microscopy images of HUVECs in culture x4 magnification. a) At two days. b) Full confluence by seven days.

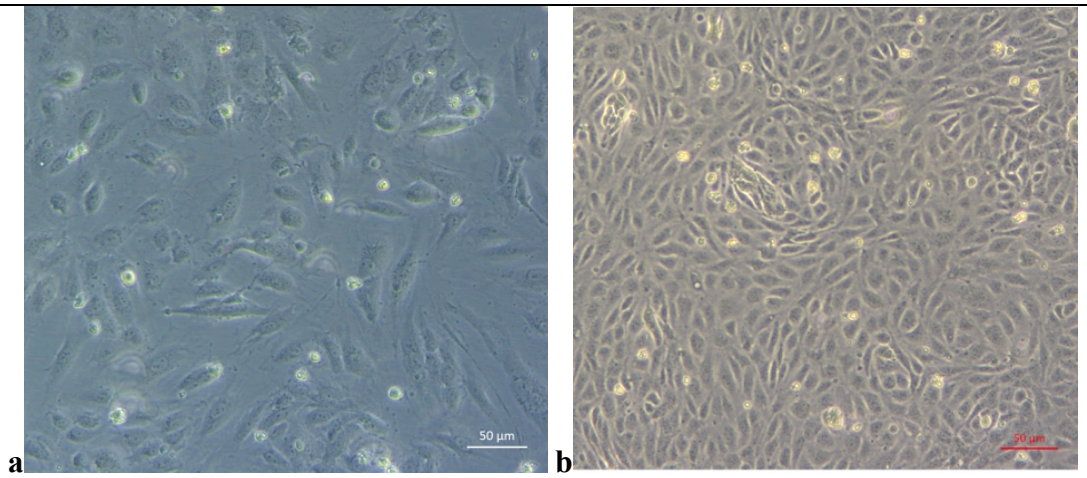

Figure 2.9: Light microscopy images of confluent HUVECs in culture. a) At three days. b) After seven days at x10 magnification. Clear cobblestone morphology quite distinct from the planar elongated MSCs was seen.

HUVEC cell surface marker analysis

A scatter plot of forward scatter versus side scatter showed a distribution of similar sized cells indicative of a cultured mono-population with a region of dead cells and debris relating

to the processes involved in preparation for flow cytometry. HUVECs showed positive expression of endothelial markers CD31 and VEGFR2 (Figure 2.10) and lacked expression of stem/progenitor markers CD90 and CD34 (Figure 2.11).

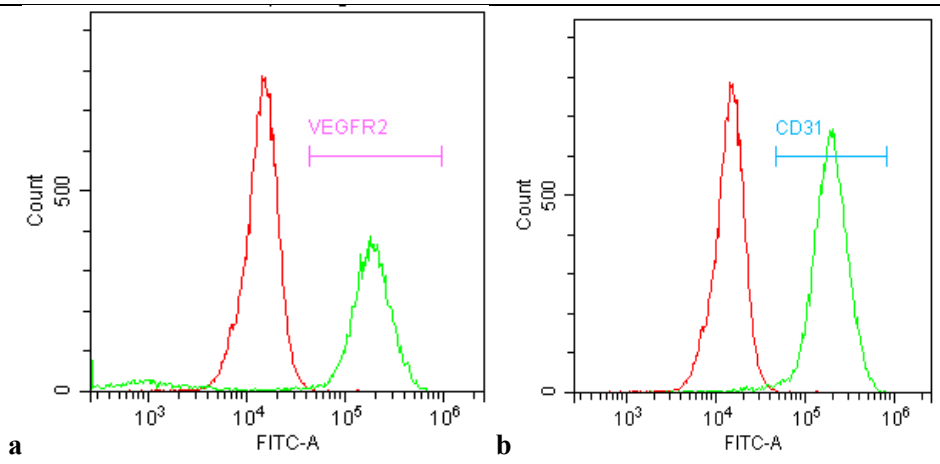

Figure 2.10: Flow cytometry histogram fluorescence counts for HUVECs. a) The red plot shows cells stained with FITC conjugated isotype control and the green plot shows cells stained with FITC conjugated VEGFR2 antibody. b) The red plot shows cells stained with FITC conjugated isotype control and the green plot shows cells stained with FITC conjugated CD31 antibody. In both plots, the right shift in fluorescence of the test population from the control indicates positive expression of VEGFR2 and CD31 on the HUVECs.

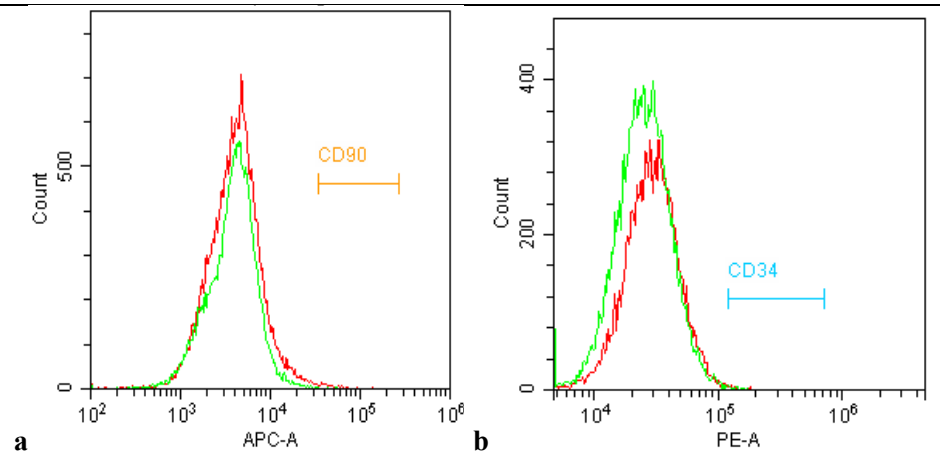

Figure 2.11: Flow cytometry histogram fluorescence counts for HUVECs. a) The red plot shows cells stained with APC conjugated isotype control. The green plot shows cells stained with APC conjugated CD90 antibody. b) The red plot shows cells stained with PE conjugated isotype control. The green plot shows cells stained with PE conjugated CD34 antibody. In both plots there is no right shift in expression for the test group indicating no staining above background and therefore no expression of CD90 or CD34 markers on the HUVECs.

HUVEC in vitro tube formation assay

HUVECs plated on a Geltrex matrix and treated with full growth medium were able to form a clear 'vascular' network by 16 hours (Figure 2.12).

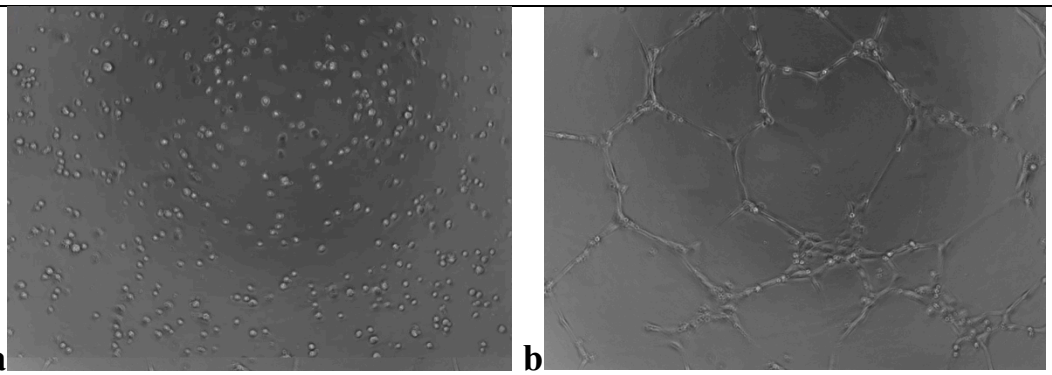

Figure 2.12: Light microscopy images at x10 magnification of HUVECs plated on Geltrex matrix. a) The arrangement and morphology of cells at 0 hours. b) 16 hours post plating, cells had elongated, aligned and formed a network.

2.5 DISCUSSION

The aim of this chapter was to characterise rat bone marrow MSCs and HUVECs as a benchmark for assessment of the cells I would mobilise in chapter 3. Bone marrow MSCs were chosen as the circulating pool of stem cells that I am interested in mobilising and are thought to be mainly from the bone marrow (Pitchford et al. 2009; Otsuru et al. 2008). Direct plating of rat bone marrow successfully resulted in the formation of CFU-Fs, with a clearly fibroblastic spindaloid morphology visible by five days, consistent with the work by Friedenstein et al. (1970). These cells were successfully passaged to P3 for all subsequent experiments, with an unchanged morphology indicative of replication as undifferentiated cells (Pittenger et al. 1999). It is acknowledged that selection by plastic adherence, although common, does make it impossible to obtain a pure stromal culture, however, it may be the best way to maximise initial yields of CFUs (Mareschi et al. 2012).

In vitro tri-differentiation, an agreed characteristic of MSCs (Dominici et al. 2006; Pittenger et al. 1999) was demonstrated with the rat bone marrow MSCs I isolated. The methods I used to confirm stem potency were functional *in vitro* assays. These tests assess for the production of matrix, presumed to be from lineage differentiated osteoblasts and chondrocytes and for the production of intracellular lipid droplets, a characteristic of adipocytes (Pittenger et al. 1999). When subjected to osteogenic or adipogenic stimulation *in vitro* for 21 days, all samples isolated by plastic adherence formed a calcium based matrix,

confirmed by Alizarin Red staining, and produced lipid droplets characterised by Oil Red O staining respectively. Chondrocytic differentiation was also shown with pellet culture by staining with Alcian Blue. Chondrocyte pellet culture required a very large number of cells, at 1x10^6 per pellet, and when controls and replicates are used this test requires 6x10^6 cells per individual evaluated. It is likely therefore, that if insufficient mobilised cells are cultured in Chapter 3, only bi-differentiation down the osteoblastic and adipogenic pathways will be evaluated. Although not performed here, a further functional assay of osteoblastic differentiation would be to measure alkaline phosphatase production (Oreffo et al. 1998).

In addition to classical functional assays to identify MSCs, I evaluated cell surface markers, as outlined in the International Society for Cellular Therapy position statement (Dominici et al. 2006). CD29 and CD90, although not exclusively expressed on MSCs, are considered mesenchymal stem cell markers, and these two markers are expressed across species and are widely used (Davies et al. 2015). The selection of four cell surface markers, notably the presence of CD29 and CD90, and absence of haematopoietic CD34 and leukocytic CD45, has been used for identification of rat MSCs in other studies (Fafián-Labora et al. 2015; Fu et al. 2012; Dezawa et al. 2004). In the absence of a single unifying stem cell marker, increasing the numbers of markers used increases the certainty of identity. There are several drawbacks however. One is the increased cost and the other is the ability to combine markers for simultaneous measures per cell, which is limited by the mechanics of the flow cytometry; the number of lasers and filters, and the available antibody fluorochromes. Often therefore, more cells are required for a larger panel of markers, and different combinations will have to be run on different batches of cells. This means there may be no definitive confirmation that the markers assessed between samples from the same population are truly co-expressed. Finally, the availability of rat cross-reactive marker antibodies is more limited than for human and mouse.

The aforementioned functional assays and cell surface marker analyses are well established, if not without some controversy, and form the mainstay of any mesenchymal stem cell research. Over recent years however, some have investigated molecular assessments such as characteristic transcription factors to identify and understand the different aspects of MSCs and their differentiation. An alternative assessment of MSCs for their ‘stemness’ would be to look for markers of pluripotency in mRNA transcripts including Rex1, Oct4, Sox2 and Nanog (Fafián-Labora et al. 2015). Post *in vitro* differentiation, transcriptomic analysis is also possible for identification of lineages and associated hierarchies (Kubo et al. 2009). For osteoblast differentiation, runt-related transcriptome factor 2 (Runx2), also known as Cbfa1, is a key transcription factor of osteoblast differentiation of MSCs (Ducy et al. 1997; Frith & Genever 2008). Runx2 knock-out mice have a purely cartilaginous skeleton and lack

osteoblasts. A similar cartilaginous skeleton has been seen with another key regulator knock-out, osterix (Giuliani et al. 2013). Current thinking is that Runx2 drives MSCs down an osteochondral lineage, and downstream, osterix directs to osteoblastic exclusivity (Frith & Genever 2008). For chondrogenic differentiation, SOX9, and its down stream pair of transcription factors SOX5 and 6, promote early differentiation of chondroblasts into chondrocytes (Ikeda et al. 2004), with knock-out studies leading to chondrodysplasias (Akiyama et al. 2002). For adipogenesis, peroxisome proliferator activated receptor (PPAR), which is a nuclear hormone receptor, is thought to play a critical role in adipogenesis (Frith & Genever 2008), with the absence of PPAR preventing adipogenic differentiation (Rosen et al. 2002). A further 'level' of analysis would be to look at epigenetic modulation (Eslaminejad et al 2013; Im & Shin 2015). These molecular means were not additionally pursued here due to associated costs and time limitations, and their limited benefit when considering the objective of this thesis.

An important consideration of all the assays described, other than perhaps a transcriptomic analysis, is that it is not possible to know whether individual cells from one 'population' are truly MSCs in terms of tri-, bi- or uni-differentiation potential. Even Pittenger's seminal MSC paper noted that all isolated cells could form bone, however, not all could tri- or bi-differentiate, and the heterogeneity of cultured MSCs is now well established (Augello et al 2010). Invariably, only a serial dilution approach or colony picking could allow evaluation of clonal populations. Although this is an interesting area of stem cell biology, it is not directly relevant to the research question addressed by this thesis, as inevitably an endogenously mobilised population will be heterogeneous. Perhaps a clonal population might be undesirable? It has been shown that homogeneity by selection for CD29 and CD90 expression can lead to reduced ability for osteogenic and adipogenic differentiation compared with the unsorted mixture (Davies et al. 2015). In this situation, there may have been inadvertent selection of a population that suppresses or has reduced bone-forming ability. Heterogeneity, which is my expectation from the endogenous mobilisation, may provide the necessary variety and diversity of cells, including those that promote bone tissue formation. It is possible that the inter-relationship and paracrine signalling between a heterogenous group may be more important than having a mono-population of stem cells for bone healing and hence heterogeneity should not be viewed as necessarily bad.

As a baseline for characterisation of EPCs, I chose HUVECs, which are well characterised and straightforward to obtain (Jaffe et al. 1973). The vast majority of *in vitro* angiogenesis assays have used HUVECs (Staton et al. 2009) however, it is known that there is heterogeneity in endothelial cells, affected by their location and hence associated organ function, as well as the vessel size and whether from an artery or vein (Staton et al. 2009).

Despite this, the optimum choice for a comparison to an EPC is unknown and hence HUVECs are a suitable starting point, not to mention the numerous studies evaluating EPCs against HUVECs (Bou Khzam et al 2015; Asahara et al. 1997; Shi et al. 1998; Bompais et al. 2004). As expected, the HUVECs I cultured formed a monolayer of large polygonal cobblestones (Jaffe et al. 1973). These cells had clear expression of endothelial and EPC markers CD31 (Asahara et al. 1997) and VEGFR2 (Peichev et al. 2000). CD31, also known as platelet endothelial cell adhesion molecule (PECAM-1) is expressed on several cell types but reliably seen on endothelial cells (DeLisser et al. 1994), and VEGFR2 has a key role on proliferation, migration and survival of endothelial cells (Ferrara et al. 2003). Asahara's landmark paper identified EPCs from blood within a haematopoietic CD34+ population with expression of VEGR2 (Asahara et al. 1997). CD133 (another haematopoietic stem marker) has also been used to isolate EPC cells and hence many studies relied on co-expression (Bongiovanni et al. 2014). These markers are thought to be associated with juvenile EPCs, within the bone marrow, and as they move into the peripheral circulation, CD133 and CD34 decrease and CD31, VE-Cadherin and Von Willebrand factor are expressed (Hristov et al. 2003). Rather than choosing early stem markers which will include precursors of lineage determined EPCs, I looked at later markers seen in both differentiated endothelial cells and EPCs. From *in vitro* cell culture, the early outgrowth spindaloid EPC has been shown to express only low levels of CD34 and CD133, moderate CD31, and high CD45. The late outgrowth cobblestone EPC however, have low CD45, moderate CD34 and high CD31 and VEGFR2 (Cheng et al. 2013). In that particular study they compared the EPCs to HUVECs that had high CD31 and VEGR2, and low CD133, CD34 and CD45 expression. By including markers that are differentially seen with bone marrow EPCs compared to circulating, and early-outgrowth culture compared with late-outgrowth cultured EPCs, I hope to be able to identify these cells in chapter 3. Alternative or additional cell surface marker analysis could have been performed with Von Willebrand or VE-Cadherin (Hristov et al. 2003), but again, there are cost considerations and more importantly there could be an issue of having insufficient cells for multiple analyses.

The functional assay performed for the EPCs was *in vitro* 2D microvascular tubulogenesis, where cells are encouraged to form capillary-like tubes. 3D tube formation is possible, but is complex and time consuming and hence most groups only use 2D assays (Staton et al. 2009). Often known as a Matrigel or Geltrex assay, it involves plating the cells on a growth factor enriched extracellular matrix synthesised by Engelbreth-Holm-Swarm tumour cells and is the classical functional *in vitro* assay of endothelial cells and their progenitors (Faulkner et al. 2014; DeCicco-Skinner et al. 2014). The assay involved plating endothelial cells on the top surface of a gel matrix, and in my study, I used the modified thin layer angiogenesis assay which is more sparing on the Geltrex volumes required (Faulkner et al. 2014). The components of the matrix signal the endothelial cells to elongate and form links leading to

structures akin to blood vessels and is considered to recapitulate the differentiation stage of angiogenesis (Staton et al. 2009). Although this is the benchmark test of function, there is debate, as some have shown true lumen formation others have not (Connolly et al. 2002; Bikfalvi et al. 1991). It is also the case that other cell types have been able to form similar networks, including glioblastoma cells, prostate carcinoma and primary human fibroblasts (Donovan et al. 2001). The test can be interpreted in a binary manner for simple characterisation, however it is possible to determine specific characteristics such as tube length, number, area and branch points for studies investigating cell function or pharmacological agents (Staton et al. 2009). In my study, HUVECs were able to form microvascular networks by 16 hours post plating and this provided a good benchmark for Chapter 3. A further potential functional assay is uptake of low-density lipoprotein through scavenger pathways (Voyta et al. 1984). Asahara initially showed the cells they isolated as EPCs would uptake DiI-labeled acetylated LDL (Asahara et al. 1997), and this has been shown elsewhere, however other cell types including macrophages and pericytes are also capable of LDL uptake (Whitman et al. 2000; Voyta et al. 1984). Due to the lack of specificity and the potential for myeloid cell contamination in populations isolated from peripheral blood (Chong et al. 2016), I chose not to use this test for evaluating EPCs.

In conclusion, I have established baseline characteristics and shown efficacy of methodology in chapter 2 for characterisation of endogenously mobilised stem and progenitor cells in chapter 3.

CHAPTER 3: Endogenous Mobilisation of Peripheral Blood Mesenchymal Stem Cells & Endothelial Progenitor Cells

3.1 INTRODUCTION

In order for bone to heal successfully, there is a need to recruit a range of cells including inflammatory cells, endothelial cells and stem cells, from different tissue sources including muscle, bone marrow, adipose tissue or periosteum (Marsell & Einhorn 2011; Einhorn & Gerstenfeld 2014; Tawonsawatruk et al. 2012). At rest, there are low basal levels of peripherally circulating skeletal progenitors, approximately 1 per $10^{6\text{-}8}$ blood mononuclear cells (Kuznetsov et al. 2001; Zvaifler et al. 2000; He et al. 2006), and the levels of MSCs, (Alm et al. 2010) and EPCs (Ma et al. 2012) increase post bone fracture, with progenitor cells migrating from the bone marrow to a fracture site (Kumagai et al. 2008). Bone marrow is a well described niche for a range of stem and progenitor cells, including haematopoietic stem cells, EPCs and MSCs (Wilson & Trumpp 2006), and the chemokine axis of SDF1-CXCR4 has a major role in the retention of haematopoietic stem cells within the bone marrow (Lévesque et al. 2003). Beyond niche maintenance, SDF1-CXCR4 has a global role in migration of stem cells from the circulation to the bone marrow (Peled 1999) as shown by CXCR4 blocking antibodies preventing bone marrow engraftment of human haematopoietic stem cells transplanted into SCID mice. The SDF1-CXCR4 axis also plays a role in fracture healing where local increases in SDF1 expression have been measured in distraction osteogenesis, stress fractures and segmental defects (Lee et al. 2010; Kidd et al. 2010; Toupadakis et al. 2012). Vascular damage causes hypoxia and increases SDF1 expression via HIF1**α** (Hirota & Semenza 2006; Ceradini et al. 2004) creating a chemotactic gradient, with high levels of SDF1 at the fracture site and subsequently increased levels in the blood facilitating stem cell migration (Yellowley 2013).

Mobilisation of haematopoietic stem cells is a mainstay of clinical bone marrow transplantation to treat a range of blood related malignancies (Broxmeyer et al. 2005; Liles et al. 2003; Martin et al. 2006; Bendall & Bradstock 2014). GCSF was the first growth factor used to mobilise haematopoietic stem cells from the bone marrow into the peripheral circulation for transplantation (Bendall & Bradstock 2014). AMD3100, a highly selective, high affinity competitive antagonist of the CXCR4 receptor (Rosenkilde et al. 2004; DeClerq 2006) commercially known as Mozibil^{TM}, rapidly mobilises high numbers of haematopoietic stem cells by blocking their interaction with SDF1 in the marrow niche, and is used for transplantation in haematological cancers (Wan 2013; Lévesque et al. 2003; Hendrix et al. 2000; Calandra et al. 2008). In experimental rodent models, AMD3100 has been shown to have a 'bell-shaped' type dose response, with peak dosage effects of 5mg/kg and peak elution at one hour post administration (Broxmeyer et al. 2005).

Although haematopoietic stem cells have been successfully mobilised, work on MSCs and other progenitors is limited and these cells do not seem to be as migratory as hematopoietic stem cells, potentially due to their larger size and increased niche adherence (Lévesque et al. 2007). However, MSCs share some of the adhesion molecules such as selectins and integrins (Sohni & Verfaillie 2013) required to undergo diapedesis, and can bind endothelial cells (Rüster et al. 2006). Pitchford's seminal work on different mobilisation protocols in mice, demonstrated that AMD3100 combined with VEGF rather than GCSF, preferentially mobilises a population of MSCs and EPCs (Pitchford et al. 2009), rather than haematopoietic stem cells. Using this protocol and based on the number of CFUs enumerated, they were able to increase blood-circulating MSCs from one MSC/ml in non-mobilised controls to 15 MSCs/ml. Likewise, EPCs increased from six to 230 CFUs/ml. They also showed that although AMD3100 alone increased MSCs and EPCs above resting levels (3 MSCs/ml and 40 EPCs/ml), the combination of VEGF with AMD3100 was synergistic. This mobilising protocol is of interest as MSCs (Mansilla et al. 2006; Y. Wang et al. 2006; Kumagai et al. 2008; Alm et al. 2010; Khosla & Eghbali-Fatourechi 2006; McNulty et al. 2012; Wang et al. 2011) and EPCs (Kawakami et al. 2015; Lee et al. 2010) have both been shown to influence fracture healing.

In chapter 6 I planned to evaluate the effect of endogenous stem cell mobilisation on fracture healing, using a mechanically controlled rat fracture model. To date, no studies have shown this in rats. I therefore needed to demonstrate proof of concept that VEGF and AMD3100 could mobilise MSCs and EPCs in rats, by comparing the peripheral blood mobilised cells with the bone marrow isolated MSCs and HUVECs as characterised in chapter 2.

3.1.1 Question & plan for chapter 3

Question: Could the number of MSCs and EPCs be increased within the peripheral circulation by the administration of VEGF and AMD3100 in a rat model?

Hypothesis:

- **The number of MSC CFU-Fs and EPC CFUs isolated from peripheral blood would be significantly higher after mobilisation using AMD3100 and VEGF (VEGF-AMD).**

The aims and objectives of this chapter were:

1. To select a methodology to prepare peripheral blood optimally for cell culture.
    - To compare red blood cell lysis and density gradient separation techniques for the numbers of mononuclear cells and CFUs isolated.
2. To isolate MSCs and EPCs from rat peripheral blood with and without mobilisation using VEGF with AMD3100.
3. To expand peripheral blood MSCs (PBMSC)s and peripheral blood EPCs (PBEPC)s in 2-dimensional cell culture and characterise them by cell morphology, surface marker expression and cell culture characteristics:
    - MSCs were characterised by their adherence to tissue culture plastic, formation of CFU-Fs, differentiation into osteoblasts and adipocytes *in vitro* and their high expression of CD90 and CD29, and low expression of CD45 and CD34.
    - EPCs were characterised by their ability to form early (spindaloid) and/or late CFUs (cobblestone), their expression of CD31 and/or VEGFR2, with a low expression of CD90 and CD45. Their ability to form microvascular type networks on basement membrane extract (Geltrex) was also assessed.

3.2 MATERIALS & METHODS

3.2.1 Assessment of techniques for isolation of mononuclear cells & CFUs

Female Wistar rats, 12-14 weeks old (n=3) had their blood collected by terminal cardiac sample, without any administration of mobilising protocols. Rats were anaesthetised using isoflurane and placed in dorsal recumbency. The ventral midline was shaved from mid abdomen to mid-sternum. The skin was prepped with 4% chlorhexidine solution (Hibiscrub) and 70% isopropyl-alcohol. Wearing sterile gloves, the xiphoid process was palpated at the caudal sternum. A 1 inch 21 gauge needle attached to a 10 mL syringe and pre-primed with sterile heparin sodium 1,000 I.U./ml (Wockhardt, UK), was inserted midline, dorsal to the xiphoid and directed toward the heart. Once through the skin, gentle negative pressure was applied. After removing the blood, pentobarbitone was injected intra-cardiac followed by cervical dislocation for euthanasia. The blood was transferred to a sterile heparinised container (BD Vaccutainer 9 ml Lithium – Heparin, BD, UK) for transport. All procedures were performed at the Royal Veterinary College, under project and personal licenses approved by the Home Office.

For each rat, the blood was thoroughly mixed and then divided equally between a red blood cell lysis procedure and a density separation protocol to isolate MNCs. *Previous pilot work had shown that culturing unprocessed whole blood did not produce viable cultures. I also*

determined that endothelial progenitor cells could be grown from non-mobilised peripheral blood, whereas MSCs could not. For that reason, the assessment of isolation efficacy was performed by mononuclear cell counts (MNC) and PBEPC CFU counts.

Density gradient separation method

For density gradient separation, whole blood was diluted 1:1 with PBS and carefully layered upon ficoll (Ficoll-PaqueTM PLUS, GE Healthcare life sciences, UK), and centrifuged at 400g (RCF) for 30-40 minutes, without brake. The buffy layer was identified and carefully aspirated and washed with 6mls of PBS, and then centrifuged at 60-100g for 10 minutes. The supernatant was removed and the cell pellet was re-suspended in EPC culture media (as described in chapter 2 (2.3.2) for HUVEC culture. A cell viability count was performed using a 0.4% Trypan Blue solution (Sigma-Aldrich, UK), using a haemocytometer under a phase-contrast microscope.

Red blood cell lysis method

For Red blood cell (RBC) lysis, 10mls of lysis solution (Red Blood Cell lysing Buffer Hybri-Max solution Sigma-Aldrich, UK), at room temperature, was added per 1ml of blood and mixed in a 50ml Falcon tube (Corning, USA). After five minutes, 35mls of PBS was added to neutralise the lysis solution and then centrifuged at 400g for five minutes. The supernatant was aspirated and the cells were re-suspended in EPC culture media. A cell viability count was performed using a 0.4% Trypan Blue solution (Sigma-Aldrich, UK), using a haemocytometer under a phase-contrast microscope.

Fibronectin flask preparation & cell culture

To determine the number of PBEPC CFUs, fibronectin coated flasks were prepared. Bovine fibronectin (F1141 Sigma-Aldrich, UK) was dissolved in sterile PBS to achieve a 10ug/ml solution. Each 25cm^2 polystyrene cell culture flask (Corning, USA) was then coated with 3mls of working fibronectin solution and each 75cm^2 flask was coated with 10mls of fibronectin working solution to achieve 1.25ug/cm^2, and then incubated at 37°C overnight. After incubation, excess fibronectin was aspirated and the flask washed once with PBS, prior to storage at 4°C in a sealed sterile container for up to four weeks.

After the MNC count, cell suspensions were plated onto the fibronectin coated T25 flasks. The culture media used for EPC isolation and expansion was the EGM-2 MV (Lonza CC-3202) media, as described in chapter 2 (2.3.2). The cells were cultured in a humidified incubator at 37°C, 95% air and 5% CO_2. The media was changed after 5-7 days to remove non-adherent cells and then every 3-4 days thereafter. Colonies were counted at x4

magnification under a phase-contrast light microscope, using a custom-made acetate grid placed below the flask (Figure 3.1). Final CFU count was performed at 20±2 days.

3.2.2 Endogenous mobilisation with VEGF and AMD3100

Growth factor & pharmaceutical preparation

Rat Vascular Endothelial Growth Factor 165 (VEGF) (PeproTech, USA, 400-31) was prepared by dissolving the lyophilized product in sterile water to make a 0.1mg/ml stock solution. A working solution was prepared by adding 1ml of stock solution to 4mls of sterile PBS + 0.1% BSA (Sigma-Aldrich, UK) to achieve a 100ug/ml injection solution which was then aliquoted and stored at -20°C until needed. AMD3100 (octahydrochloride hydrate, Sigma-Aldrich, UK A5602) stock solution was prepared by dissolving 5mg lyophilized product in 0.5mls sterile water, and then added to 4.5mls PBS to produce a 1mg/ml injection solution, which was then aliquoted and stored at -20°C until needed.

Experimental protocol

For the mobilisation study, the VEGF-AMD group (n=8) and PBS treated controls (n=6) were healthy, ex-breeder female Wistar rats (380-600g). Rats were pre-treated with VEGF (Peprotech, USA), at 100ug/kg, once daily i.p. for four days, at a volume of 0.5mls/100g. On day 5, rats received a single 5mg/kg dose of a CXCR4 receptor antagonist (AMD3100 Sigma A5602) at a volume of 0.5mls/100g. One hour post administration, rats were anaesthetised for terminal cardiac venipuncture as previously described. Figure 3.2 outlines the timing of the mobilisation protocol. Controls were treated with PBS i.p. at the same volume dose and time intervals.

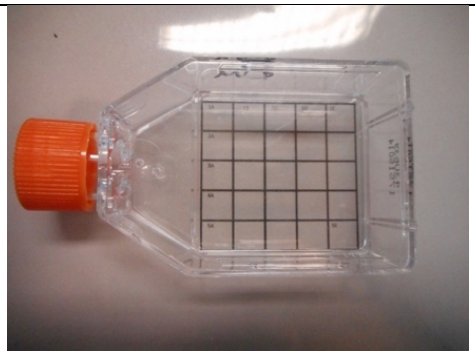

Figure 3.1: Photograph showing a T25 cell culture flask with the acetate grid in position to facilitate colony counting.

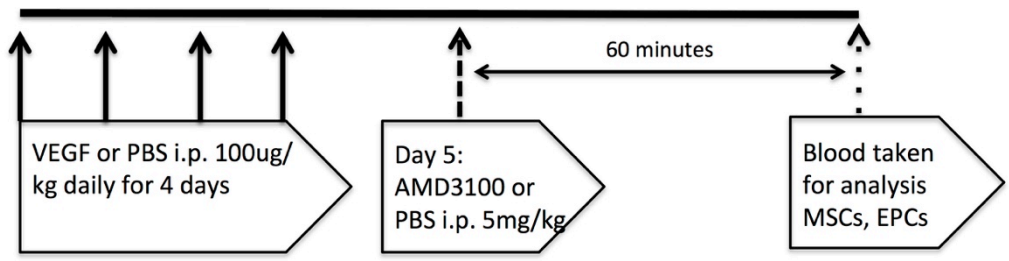

Figure 3.2: Diagram depicting the temporal sequence of events for endogenous mobilisation of stem cells into the peripheral circulation.

Preparation of blood for assessment of VEGF AMD3100 mobilisation

The blood was fully mixed and then split between EPC culture and MSC culture. All blood was processed with the RBC lysis protocol, as described above (3.2.1.2). The MNCs were re-suspended in MSC media (DMEM, 20% fetal calf serum, 1% Penicillin Streptomycin), or EPC media (EGM2 MV) and carefully plated into 25cm^2 polystyrene cell culture flasks for MSC culture, or fibronectin coated T25 flasks for EPC culture, and then cultured as described in chapter 2.

The media was changed after five to seven days to remove non-adherent cells and thereafter every 3-4 days. Colonies were counted at x4 magnification placed under a phase-contrast light microscope using a custom-made acetate grid overlay (Figure 3.2). Final CFU count was performed at 20±2 days. After P0 CFUs were counted, cells were passaged when they were 70-80% confluent.

Cell surface marker analysis of cultured PBMSCs & PBEPCs

P3 cells were prepared in the same manner as described in chapter 2 (2.3.1.1 & 2.3.2.1). In this instance, the same set of surface markers were evaluated for PBMSCs and PBEPCS, with 30,000 cells per group:

- CD34 (Anti-CD34 antibody [ICO-115] Phycoerythrin, IgG1 K, abcam ab187284)
- CD45 (Anti-Rat CD45 APC, IgG1 K, eBioscience 17-0461)
- CD90 (Anti-Mouse/Rat CD90.1 (Thy-1.1) APC, Mouse IgG2a K, eBioscience, 17-0900)
- CD29 (Anti-Mouse/Rat CD29 (Integrin beta 1) FITC, Armenian Hamster IgG, eBioscience, 11-0291)
- Anti-VEGFR-2 (KDR/EIC) (Fitc) (abcam ab184903)
- CD31 (TLD-3A12) (Fitc) (abcam ab33858)

Isotype controls for each CD marker as follows:

- For CD34: Mouse IgG1 K Isotype Control PE (eBioscience 12-4714)
- For CD45: Mouse IgG1 K Isotype Control APC (eBioscience 17-4714)
- For CD90: Mouse IgG2a K Isotype Control APC (eBioscience 17-4724)
- For CD29: Armenian Hamster IgG Isotype Control FITC (eBioscience 11-4888)
- For VEGFR2: Mouse IgG1 (ICIG1) (Fitc) (abcam ab91356)
- For CD31: Mouse IgG1 (ICIG1) (Fitc) (abcam ab91356)

Differentiation potential of PBMSCs & PBEPCs

As previously described in chapter 2 for bone marrow MSCs, plastic adherent fibroblastic morphology cells were isolated by serial passage. Due to the lower yield and slower growth seen with the peripheral blood mobilised cells, only osteogenic and adipogenic differentiation was assessed.

3.2.2.1.1 Osteogenic differentiation & Alizarin Red staining

Osteogenic differentiation of 30,000 P3 cells per well (48 well plate), in triplicate, was performed and then stained for calcium deposits exactly as described in chapter 2 (2.3.1.2).

3.2.2.1.2 Adipogenic differentiation & Oil Red O staining

Adipogenic differentiation of 30,000 P3 cells per well (48 well plate), in triplicate, was performed and then stained for lipid exactly as described in chapter 2 (2.3.2.2).

Functional 3D tube forming assay of PBEPCs

P3 PBEPCs cells were subjected to *in vitro* tube forming assay as described for HUVECs in chapter 2 (2.4.2.2).

3.2.3 Statistical analysis

Due to the relatively small group sizes ($n<9$), a non-parametric Mann-Whitney U (MWU) test was used. Significance was set a $p<0.05$ and tests were analysed with SPSS version 24 (IBM, Chicago, USA).

3.3 RESULTS

3.3.1 Assessment of cell isolation techniques

The mean±SD number of mononuclear cells isolated after RBC lysis was 2.0±0.8x10^6 cells/ml (n=3) and Ficoll was 0.6±0.4x10^6 cell/ml (n=3), (Figure 3.3a). Analysis using the Mann Whitney-U test showed no significant difference in the number of MNCs/ml isolated by each technique. In terms of CFUs formed, RBC lysis yielded 2.8±3.4 CFU/ml blood, whereas the Ficoll did not produce any CFUs after 20±2 days culture (Figure 3.3b). The PBEPC CFUs that did form were comprised of cobblestone cells; some forming circumscribed luminal type configurations (Figure 3.4). Again there was no significant difference between the numbers of CFUs/ml isolated between these techniques, however a type II error owing to the small sample size should be considered. On balance, the RBC lysis technique was used despite the increased yields not being statistically significant, as it was also quicker and simpler to perform and in line with Pitchford's protocol (Pitchford et al. 2009). The full results are outlined in table 3.1

.

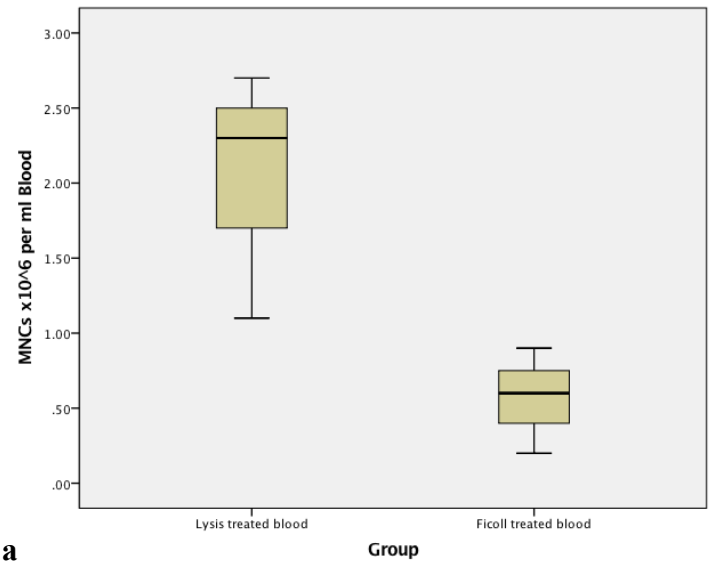

a

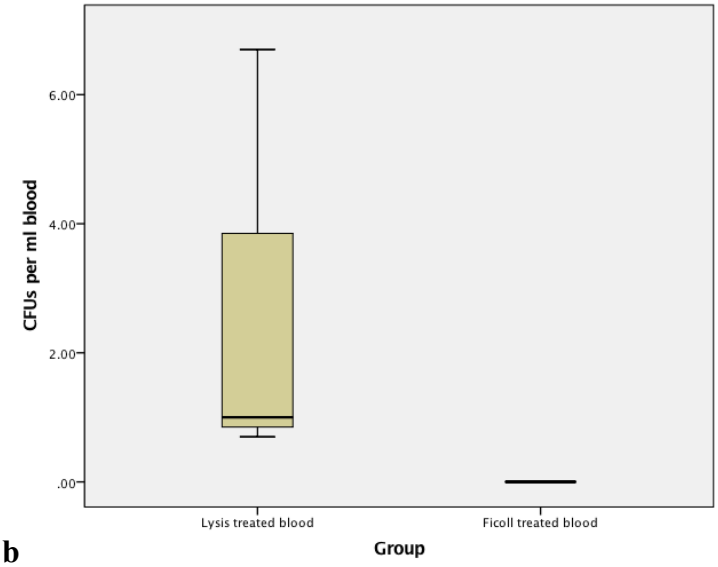

b

Figure 3.3: a) Boxplot comparing the number of mononuclear cells (MNCs) per ml blood after isolation using a RBC lysis protocol or a ficoll protocol. b) Boxplot comparing the number of EPC colonies per ml blood after a RBC lysis protocol or a ficoll protocol. The cells were isolated from the peripheral blood without any prior mobilisation.

	Lysis treated blood		Ficoll treated blood	
Rat	MNCs x10^6 /ml	CFU/ml	MNCs x10^6 /ml	CFU/ml
R21	2.7	6.7	0.9	0.0
R22	1.1	1.0	0.6	0.0
R23	2.3	0.7	0.2	0.0
Mean±SD	**2.0±0.8**	**2.8±3.4**	**0.6±0.4**	**0.0±0.0**

Table 3.1: The effect of isolation technique for isolating mononuclear cells (MNCs) per ml blood isolated and the number EPC colonies per ml blood, in non-mobilised rats. Results are mean±SD.

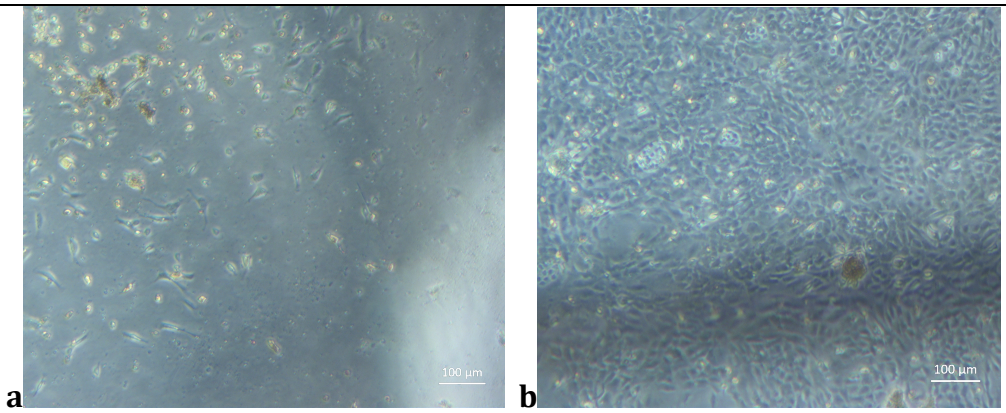

Figure 3.4: Light microscope images of adherent PBEPCs at x4 magnification. a) Early EPC colony forming at day 9. b) Large confluent colony also at day 12.

3.3.2 Endogenous mobilisation of PBMSCs.

There were no adverse reactions seen in the PBS treated control group (n=6) or the VEGF-AMD group (n=8). The mean±SD MNC count for controls (n=5) was 2.0±0.7x10^6 cells/ml and mobilised (n=6) was 2.8±1.3x10^g cells/ml (Figure 3.5a) There was no significant difference between groups. Due to some remaining red blood cell contamination after the RBC lysis protocol, it was not possible to identify any adhesion of cells to the surface of the tissue culture plastic until after the first media change at five to seven days. The control blood culture showed adherence of a round MNC-type cell by day seven. There were a few elongated cells but the typical MSC type morphology was absent in 5/6 of the controls. Initially attached cells continued to detach over the culture period of 20±2 days. Cells isolated from one rat did produce a single CFU-F, however, these cells proliferated poorly up to day 14 and subsequently began to detach.

The VEGF-AMD group formed CFU-Fs in 6/8 individual cultures. Initially, round mononuclear cells were present with some immature elongating cells (Figure 3.6a). Over time, the cells began to take on a similar morphology to those obtained by bone marrow isolation; spindle or fibroblastic-shaped cells, with a centrifugal arrangement of cells to form a colony (Figure 3.6b, 3.7a, 3.7b). Notably however, they took longer to form clear CFUs, typically around 14-18 days, when compared with bone marrow isolated cells. The mean CFU-F/ml for controls was zero, and for VEGF-AMD was significantly higher at 2.9±1.8 CFU-F/ml (p=0.029) (Figure 3.5b).

Present in all cultures, but to varying extents, were small round adherent mononuclear cells that did not form CFUs or demonstrate cell division (Figure 3.6a). Over time, in the control cultures, large multi-nucleate cells were seen and again no clear cell division was observed (Figure 3.8). Cultures from the VEGF-AMD group were passaged to P3 for further analysis.

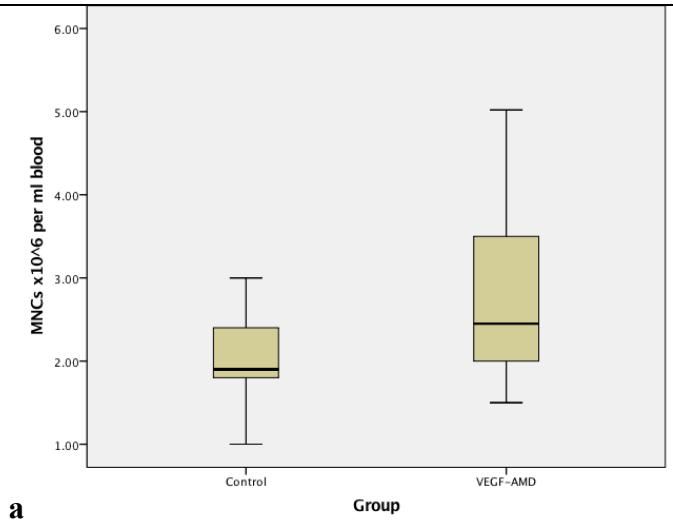

a

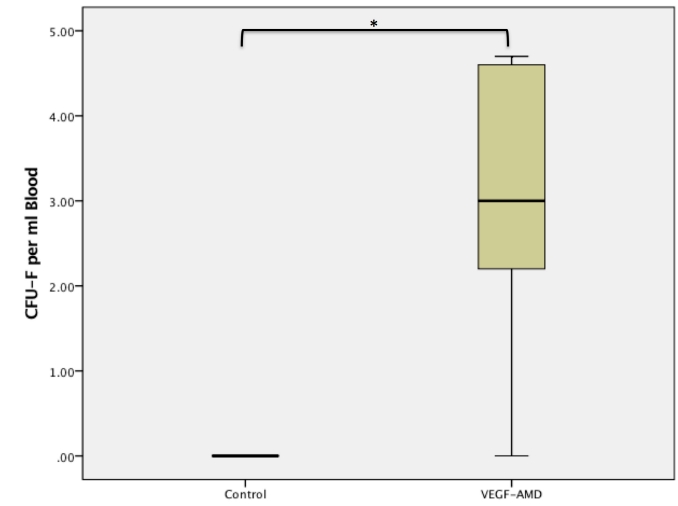

b

Figure 3.5: a) Boxplot showing the number of MNC x10^6 per ml of blood taken after RBC lysis protocol prior to plating. b) Boxplot showing a significant (* p=0.029) increase in CFU-Fs per ml of blood in the VEGF-AMD group.

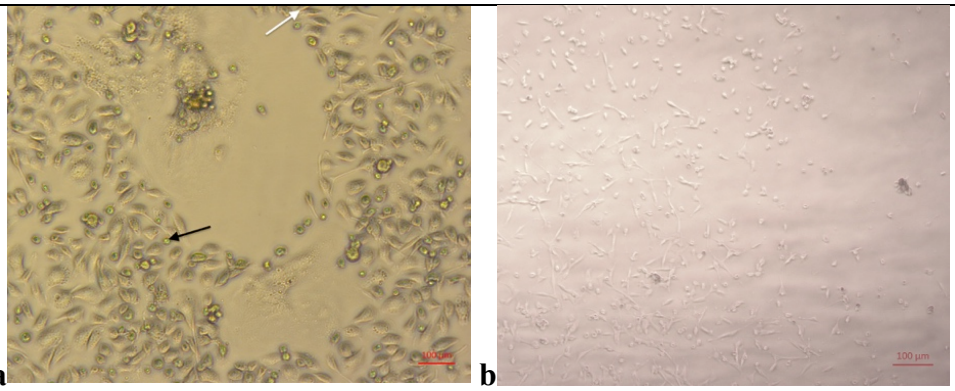

a b

Figure 3.6: Light microscope images of P0 PBMSCs from the VEGF-AMD group, at x4 magnification. a) Adhered round mononuclear cells (black arrow) and early elongating cells, presumed MSCs (white arrow) at seven days. b) Early CFU-F forming at 14 days.

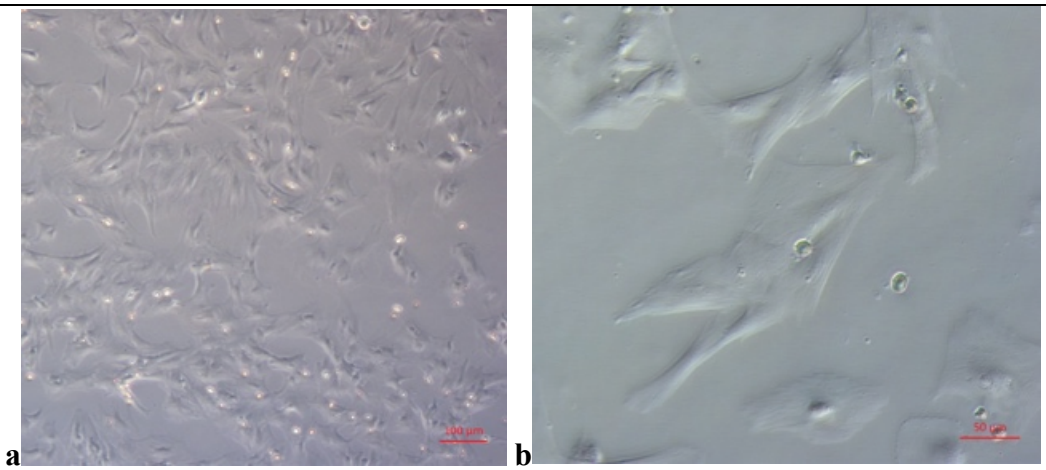

Figure 3.7: Light microscope images of P3 PBMSCs at 12 days from the VEGF-AMD group. a) Spindaloid fibroblastic cells, at x4 magnification. b) At x10 magnification, cells had a flat, spindle shaped morphology, similar to the bone marrow MSCs.

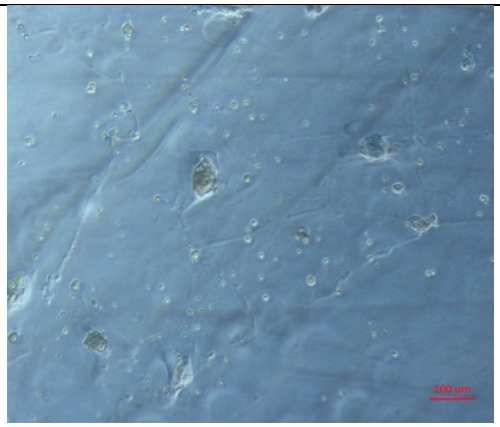

Figure 3.8: Light microscope images of P0 PBMSC culture from the control group (x4 magnification, 21 days). The cells had detached and there was no evidence of CFU-Fs or any other cell population. Some cellular debris remained.

Cell surface marker analysis of cultured PBMSCs

Flow cytometry analysis was performed on P3 cells (n=3). In common with the bone marrow MSCs in chapter 2, the plastic adherent CFU-F cells were CD34 negative, however CD45 which is typically negative in MSCs, was positive on some cells with both CD45+ and CD45- cells present (Figures 3.9 and 3.10), varying from 9 to 60% positive within any population. MSC markers CD90 and CD29 were highly expressed at 78% and 64% respectively (Figure 3.11). There were negligible to minimal expression of endothelial markers CD31 and VEGFR2 (Figure 3.12). See table 3.2 for full results.

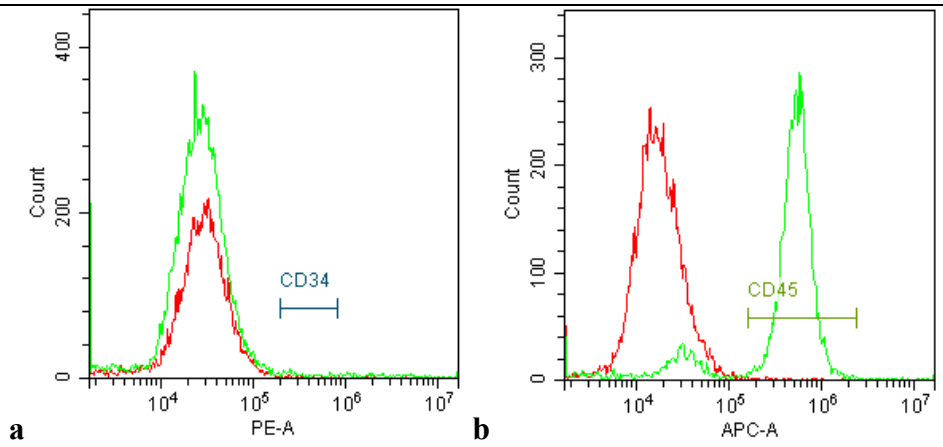

Figure 3.9: Flow cytometry histogram fluorescence counts for VEGF-AMD PBMSC CD34 and CD45 expression. a) Red plot shows cells stained with PE conjugated isotype control. Green plot shows cells stained with PE conjugated CD34 antibody. b) Red plot shows cells stained with APC isotype control. Green plot shows cells stained with APC conjugated CD45 antibody. In plot a, there is no right shift in expression, indicating no staining above background and therefore no expression of CD34 in PBMSCs. In plot b however, there is a clear right shift in fluorescence indicating CD45 expression in PBMSCs. Additionally, a small peak in the same region as the red control histogram was seen indicating a smaller second CD45- population.

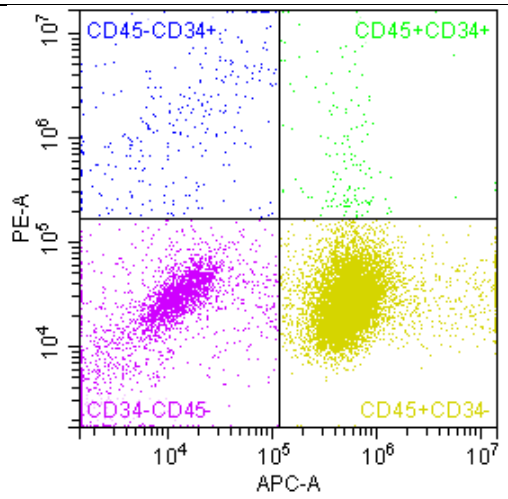

Figure 3.10: Flow cytometry scatterplot for VEGF-AMD PBMSCs showing CD34 PE and CD45 APC expression, with two dominating populations: the largest is a CD45+CD34- population, in addition to a significant CD34-CD45- population, and a scattering of CD45-CD34+ cells and CD45+CD34+ cells.

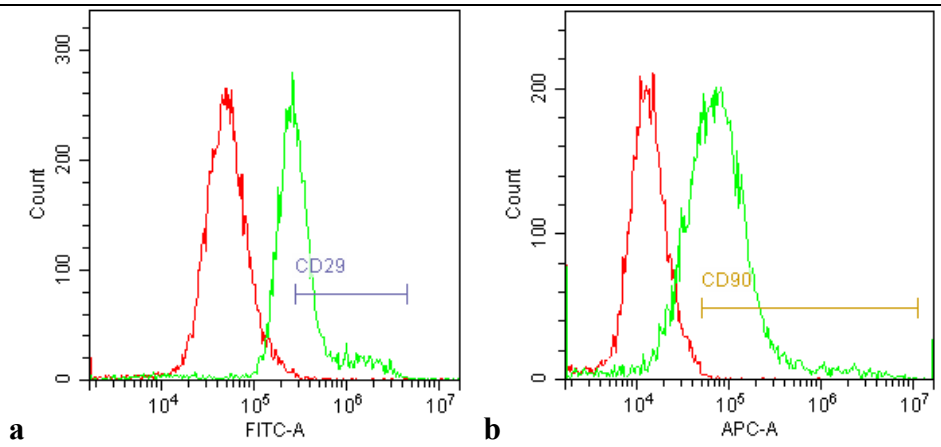

Figure 3.11: Flow cytometry histogram fluorescence counts for VEGF-AMD PBMSC CD29 and CD90 expression. a) Red plot shows cells stained with FITC conjugated isotype control. Green plot shows cells stained with FITC conjugated CD29 antibody. b) Red plot shows cells stained with APC conjugated isotype control. Green plot shows cells stained with APC conjugated CD90 antibody. In both plots, the right shift in fluorescence indicates positive expression of CD29 and CD90 markers on the PBMSCs.

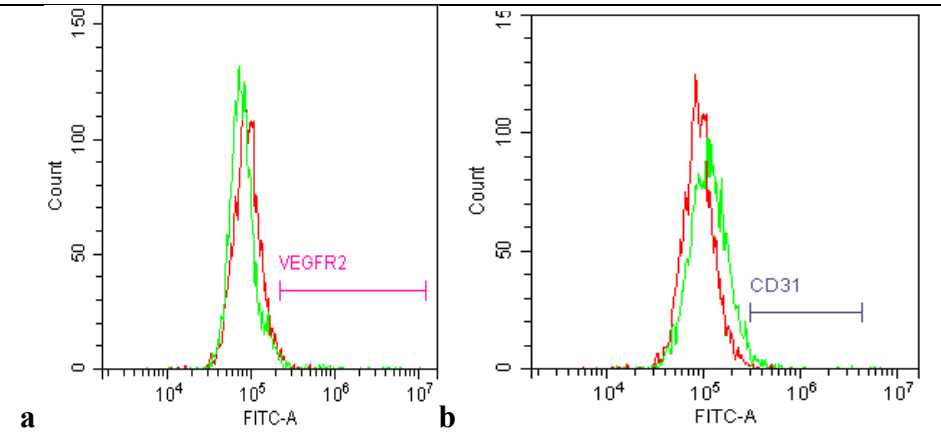

Figure 3.12: Flow cytometry histogram fluorescence counts for VEGF-AMD PBMSC VEGFR2 and CD31 expression. a) Red plot shows cells stained with FITC conjugated isotype control. Green plot shows cells stained with FITC conjugated VEGFR2 antibody. b) Red plot shows cells stained with FITC conjugated isotype control. Green plot shows cells stained with FITC conjugated CD31 antibody. In both plots there is no right shift in fluorescence, indicating no expression of VEGFR2 or CD31 in PBMSCs.

Rat	CD45+	CD34+	CD29+	CD90+	VEGFR2+	CD31+	CD34- CD45-	CD34+ CD45-	CD45+ CD34-	CD45+ CD34+
R3A	60.9	3.0	76.2	77.8	2.1	0.7	37.0	2.6	59.3	1.0
R2B	35.4	1.8	60.7	83.9	2.3	1.8	61.3	2.2	36.1	0.4
R2C	8.6	1.8	55.2	70.7	0.9	0.9	87.0	2.3	10.6	0.2
Mean ± SD	**35.0±26.2**	**2.2±0.7**	**64.0±10.9**	**77.5±6.6**	**1.8±0.8**	**1.1±0.6**	**61.8±25.0**	**2.4±0.2**	**35.3±24.2**	**0.5±0.4**

Table 3.2: Individual and mean±SD flow cytometry percentage expression levels (%) of the markers evaluated for PBMSCs from VEGF-AMD treated group.

Osteogenic differentiation of PBMSCs

VEGF-AMD mobilised PBMSCs formed a monolayer along the base of the well within seven days. During supplementation with osteogenic media the cell morphology became less spindaloid and more cuboidal and multiple small granules became apparent. Staining for Alizarin red after 21 days demonstrated red stained calcium deposits in all samples, consistent with osteoblast activity (n=5). (Figure 3.13a).

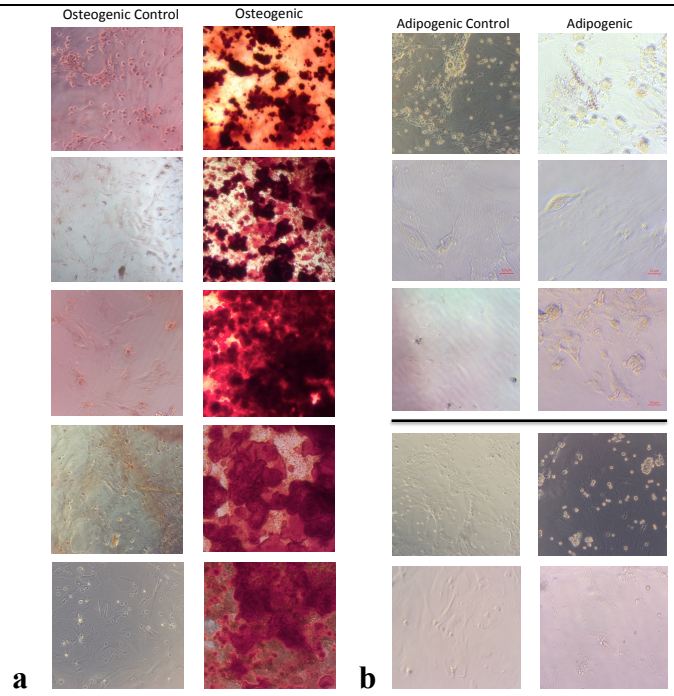

Figure 3.13: a) Light microscopy images of osteogenic differentiation (x10 magnification), after 21 days of osteogenic supplementation of VEGF-AMD PBMSCs (n=5). Wells were stained with Alizarin red and there were no stained mineral deposits in the control wells and significant staining in the supplemented group. b) Light microscopy images of adipogenic differentiation (x40 magnification above the horizontal dividing line, x10 below), post staining with Oil Red O of VEGF-AMD PBMSCs (n=5). There were no visible stained lipid droplets in the control group, and only 1/5 showed any signs of adipogenesis, which was less evident than seen with the bone marrow MSCs from chapter 2. The panels from top to bottom represent cultures from different individual rats.

Adipogenic differentiation of PBMSCs

VEGF-AMD PBMSCs formed a monolayer along the base of the well within seven days. After 21 days of incubation with adipogenic media a change in morphology was evident, with cells appearing less spindle shaped, being shorter with longer extensions. Positive Oil Red O staining was not seen in 4/5 samples and therefore these cells did not appear to have adipogenic lineage potential (n=5) (Figure 3.13b).

3.3.3 Endogenous mobilisation of PBEPCs.

The mean±SD mononuclear cell count post RBC lysis was significantly higher for VEGF-AMD with 2.9±0.9x10^6 cells/ml compared to controls with 1.8±0.5x10^6 cells/ml (*p*=0.035) (Figure 3.14a).

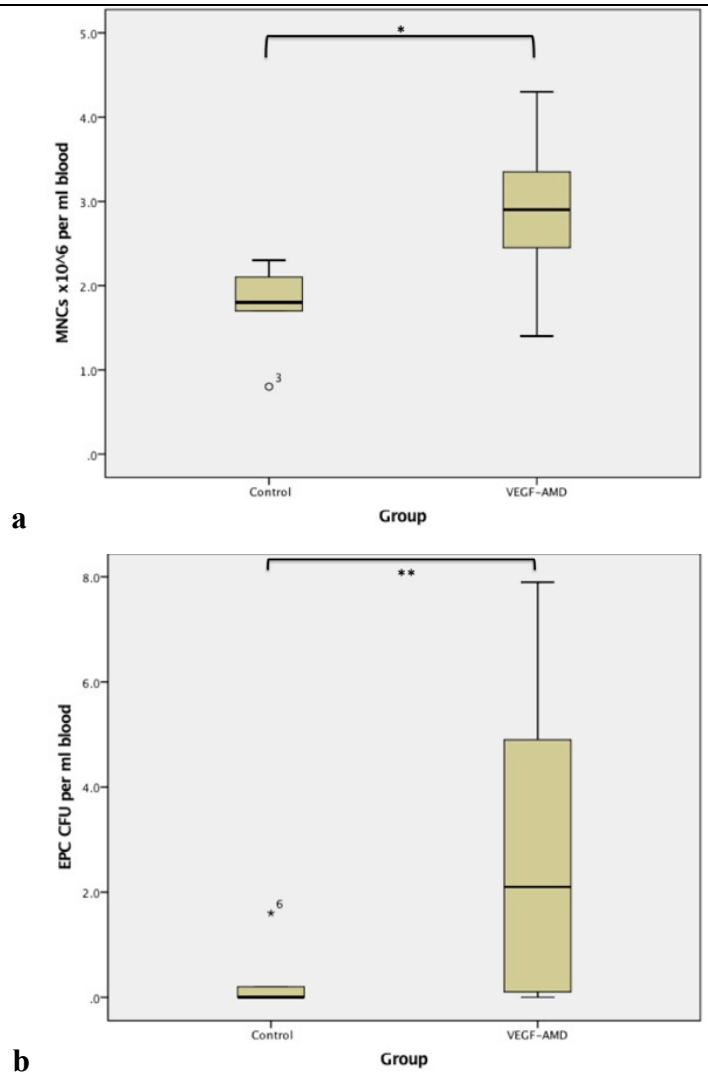

Figure 3.14: a) Boxplot showing the number of MNC x10^6 per ml of blood taken after red blood cell lysis protocol (* p=0.035). b) Boxplot showing a significant (** p=0.036) increase in EPC CFUs per ml of blood in the VEGF-AMD group.

At 20±2 days, the EPC CFU count for the VEGF-AMD group was significantly increased at 2.9±3.3 CFUs/ml compared with 0.3±0.6 CFUs/ml blood for controls (p=0.036) (Figure 3.14b).

Two distinct EPC cell morphologies were seen. An 'early-outgrowth' spindle type morphology (Figure 3.15a) was seen within the first 10 days. Latterly, I saw more classical 'late-outgrowth' type morphology, characterised by a cobblestone appearance, not visible until at least 10 days, and most notably after 14 days of culture (Figure 3.15b). The cells grew slowly, sometimes taking up to 30 days to achieve confluence and their morphology was more varied than seen in the PBMSC cultures (Figures 3.16, 3.17, 3.18). In a few samples there were occasional islands of rare colonies that were tightly packed and circumscribed with elongated ovoid cells. These cells were distinct from the spindaloid cells, and were not seen in all cultures and did not proliferate significantly (Figure 3.19).

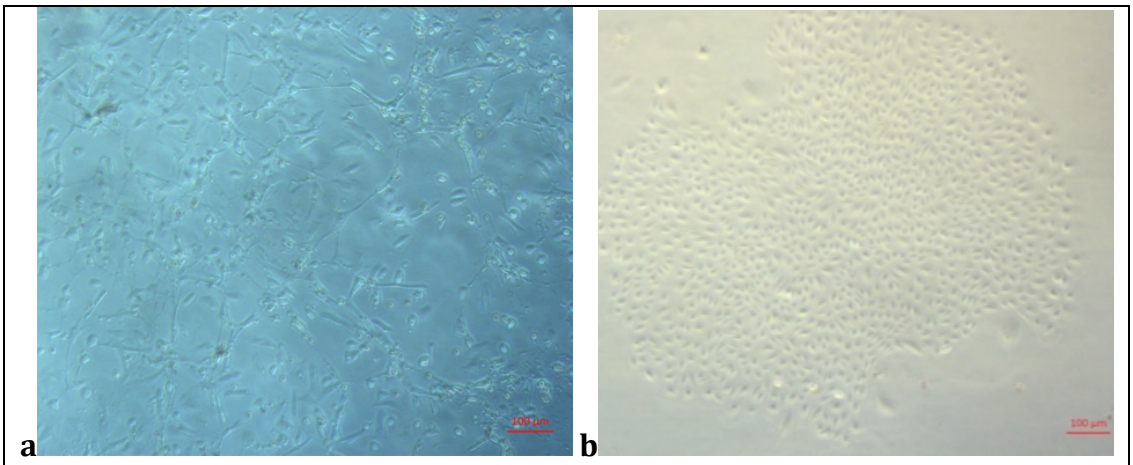

Figure 3.15: Light microscopy images showing P0 VEGF-AMD PBEPC CFUs on fibronectin coated flasks in the presence of endothelial media, at x4 magnification. a) An early outgrowth style colony showing mostly spindle shaped cells at day 7. b) Late outgrowth style colony showing cobblestone shaped cells at day 15.

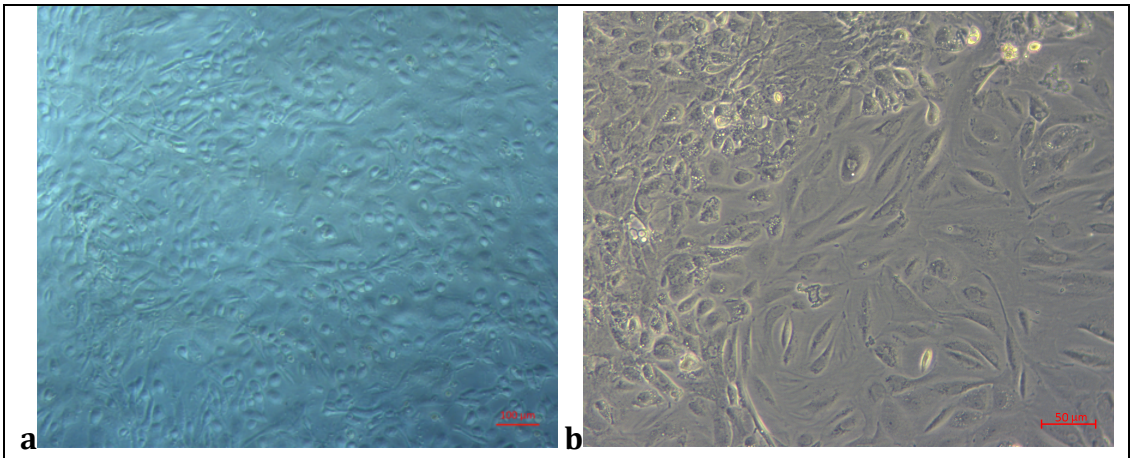

Figure 3.16: Light microscopy images showing P0 VEGF-AMD PBEPC CFUs at day 18, with classical cobblestone cells and some elongated cobblestone cells. a) At x4 magnification. b) At x10 magnification.

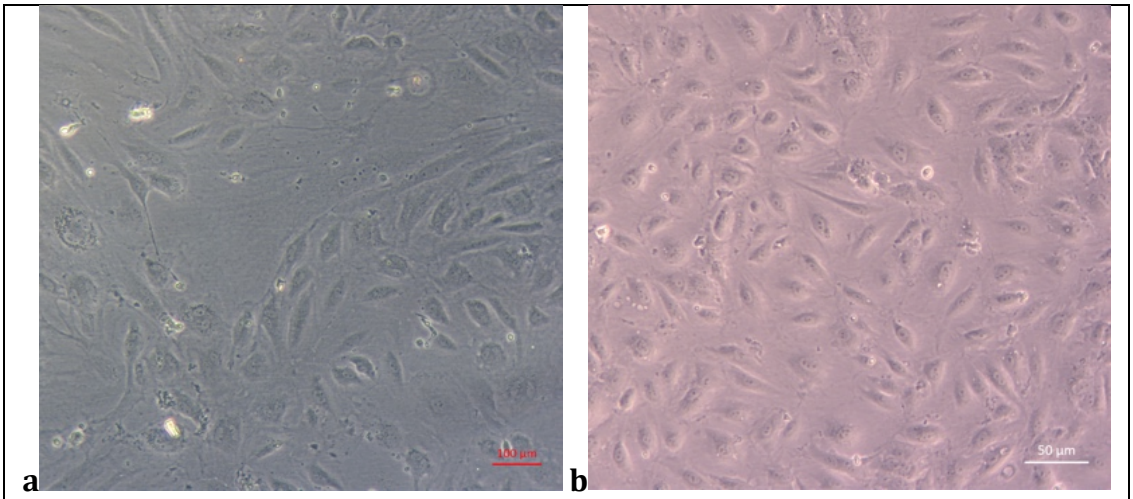

Figure 3.17: Light microscopy images taken at x10 magnification. a) P3 VEGF-AMD PBEPCs at day 30. b) HUVECs P5 at day 7. These two cultures had a similar cell morphology and were unlike the fibroblastic MSCs.

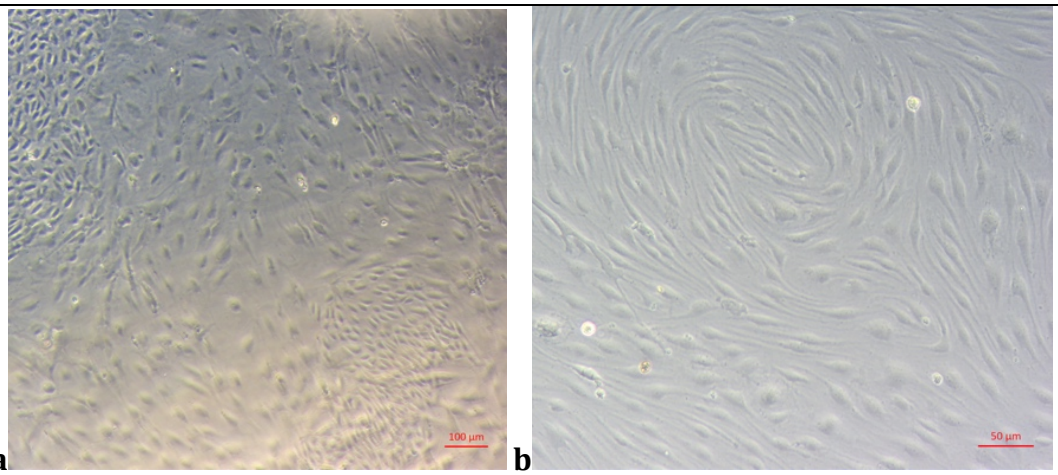

Figure 3.18: Light microscopy images of VEGF-AMD PBEPCs in culture. a) Dense P3 PBEPC colonies with cobblestone appearance, with some elongated EPCs between, shown at x4 magnification. b) P2 cells at day 19, at x10 magnification, displaying a swirling pattern. These cells were more elongated than other seen.

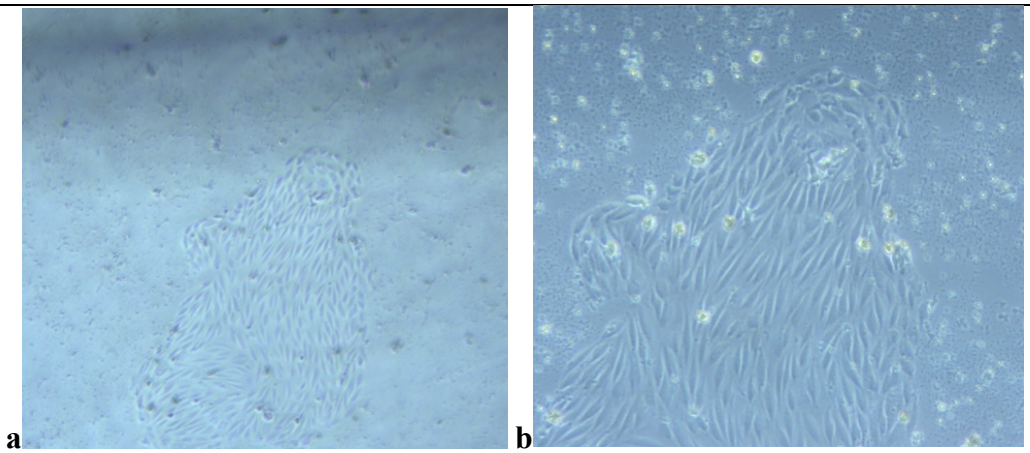

Figure 3.19: Light microscopy images of P0 VEGF-AMD PBEPC culture showing an isolated, circumscribed, rare colony morphology, seen in some cultures with a morphology distinct from the typical early- or late-outgrowth cells, day 10. a) At x4 magnification. b) At x10 magnification.

Cell surface marker analysis of cultured PBEPCs

P3 VEGF-AMD PBEPCs cells showed a monopopulation in terms of size and complexity. All analysed populations (n=4) were uniformly CD34- CD45- (Figure 3.20a-c). All expressed CD29 to varying levels (Figure 3.20d). One population had no EPC markers and very high CD29 and CD90 expression, rather like an MSC expression profile (Figure 3.21). Two populations had CD31 expression, one relatively low with high CD29 and low CD90 expression, the other had very high CD31 and CD29, and low CD90 (Figure 3.22). Only one population had some VEGFR2 expression with low CD29, CD90, and CD31. Based on the

morphology and cell surface marker analysis, these cells were quite different to the PBMSCs, however they didn't uniformly express classical EPC markers. See table 3.3 for all marker expression profiles.

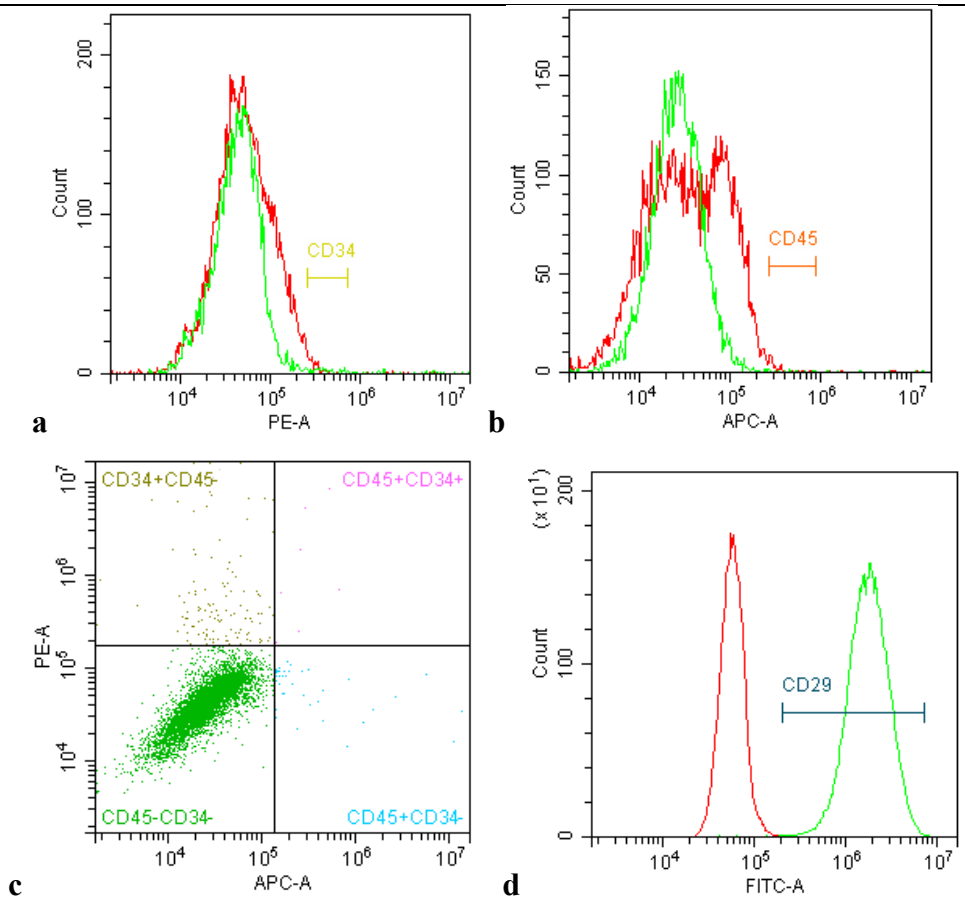

Figure 3.20: Flow cytometry fluorescence histograms and scatterplots for VEGF-AMD PBEPCs. a) Red plot shows cells stained with PE conjugated isotype control. Green plot shows cells stained with PE conjugated CD34 antibody. b) Red plot shows cells stained with APC conjugated isotype control. Green plot shows cells stained with APC conjugated CD45 antibody. c) Fluorescence scatterplot of CD34 PE vs CD45 APC fluorescence for PBEPCs. d) Red plot shows cells stained with FITC conjugated isotype control. Green plot shows cells stained with FITC conjugated CD29 antibody. In plots a and b, there is no right shift in fluorescence, indicating no expression of CD34 and CD45 in PBEPCs. In plot c, the vast majority of cells represent a CD34-CD45- population, with a scattering of CD34+CD45- cells. In plot d there is a clear right shift in fluorescence indicating high expression of CD29.

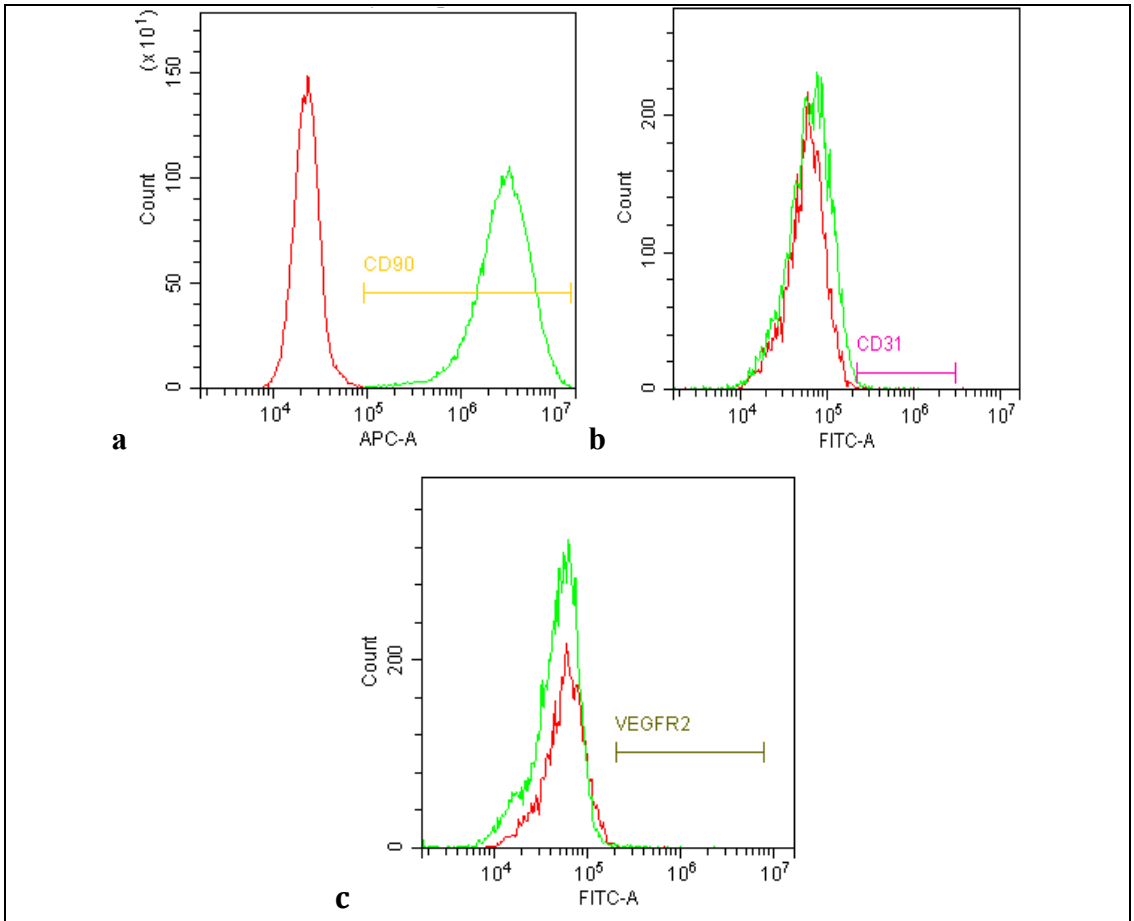

Figure 3.21: Flow cytometry fluorescence histograms for VEGF-AMD PBEPCs. a) Red plot shows cells stained with APC conjugated isotype control. Green plot shows cells stained with APC conjugated CD90 antibody. b) Red plot shows cells stained with FITC conjugated isotype control. Green plot shows cells stained with FITC conjugated CD31 antibody. c) Red plot shows cells stained with FITC conjugated isotype control. Green plot shows cells stained with FITC conjugated VEGF2 antibody. In plot a, there is a right shift in fluorescence, indicating expression of CD90. In plots b and c, there is no right shift in fluorescence, indicating no expression of endoethelial markers CD31 and VEGFR2 (n=2).

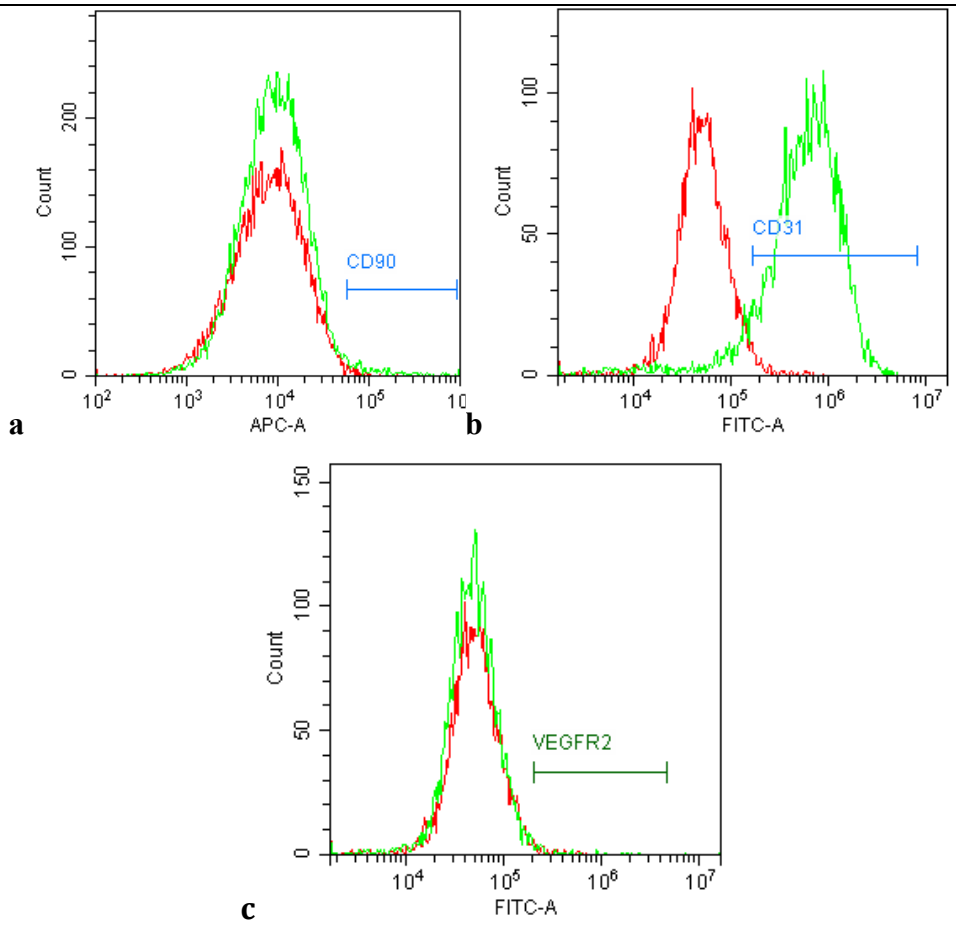

Figure 3.22: Flow cytometry fluorescence histograms for VEGF-AMD PBEPCs. a) Red plot shows cells stained with APC conjugated isotype control. Green plot shows cells stained with APC conjugated CD90 antibody. b) Red plot shows cells stained with FITC conjugated isotype control. Green plot shows cells stained with FITC conjugated CD31 antibody. c) Red plot shows cells stained with FITC conjugated isotype control. Green plot shows cells stained with FITC conjugated VEGF2 antibody. In plots a and c there is a no right shift in fluorescence, indicating no expression of CD90 or endothelial marker VEGR2. In plot b there is a right shift in fluorescence, indicating expression of endoethelial marker CD31 (n=2).

Rat	CD45+	CD34+	CD29+	CD90+	VEGFR2+	CD31+	CD34- CD45-	CD34+ CD45-	CD45+ CD34-	CD45+ CD34+	Tube formation
R3A	0.4	1.7	85.9	95.0	0.8	1.4	95.9	3.1	0.8	0.2	+
R1B	9.4	6.8	4.3	7.3	8.5	2.5	82.2	7.2	8.9	1.7	±
R2B	0.6	0.7	64.8	0.8	1.1	90.3	97.8	0.8	1.3	0.7	-
R3B	1.3	2.1	77.6	1.0	0.6	7.7	90.9	3.9	4.0	1.1	+
Mean±SD	**2.9±4.3**	**2.8±2.7**	**58.2±36.9**	**26.0±46.1**	**2.8±3.8**	**25.5±43.3**	**91.7±7.0**	**3.8±2.6**	**3.8±3.7**	**0.9±0.6**	

Table 3.3: Individual and mean±SD flow cytometry percentage expression levels (%) of the markers evaluated for VEGF-AMD PBEPCs. For assessment of *in vitro* microtubule formation, ++ is equivalent to HUVECs, + indicates at least two luminal structures, ± indicates some cellular connections and – indicates no evidence of change above control.

Osteogenic differentiation of PBEPCs

P3 PBEPCs formed a monolayer along the base of the well within seven days. Staining for Alizarin Red after 21 days of osteogenic supplementation did not demonstrate red granules indicative of calcium deposits and therefore the PBEPCs do not appear to have formed osteoblasts at the time point investigated (Figure 3.23a).

Adipogenic differentiation of PBEPCs

P3 PBEPCs formed a monolayer along the base of the well within seven days. After 21 days of incubation with adipogenic media a change in morphology was evident, with cells appearing less spindle shaped, being shorter with longer extensions. Positive Oil Red O staining was evident by red dots indicating the presence of lipid (Figure 3.23b) and therefore adipogenesis in all samples tested (n=3). One sample formed lipid granules in the control media.

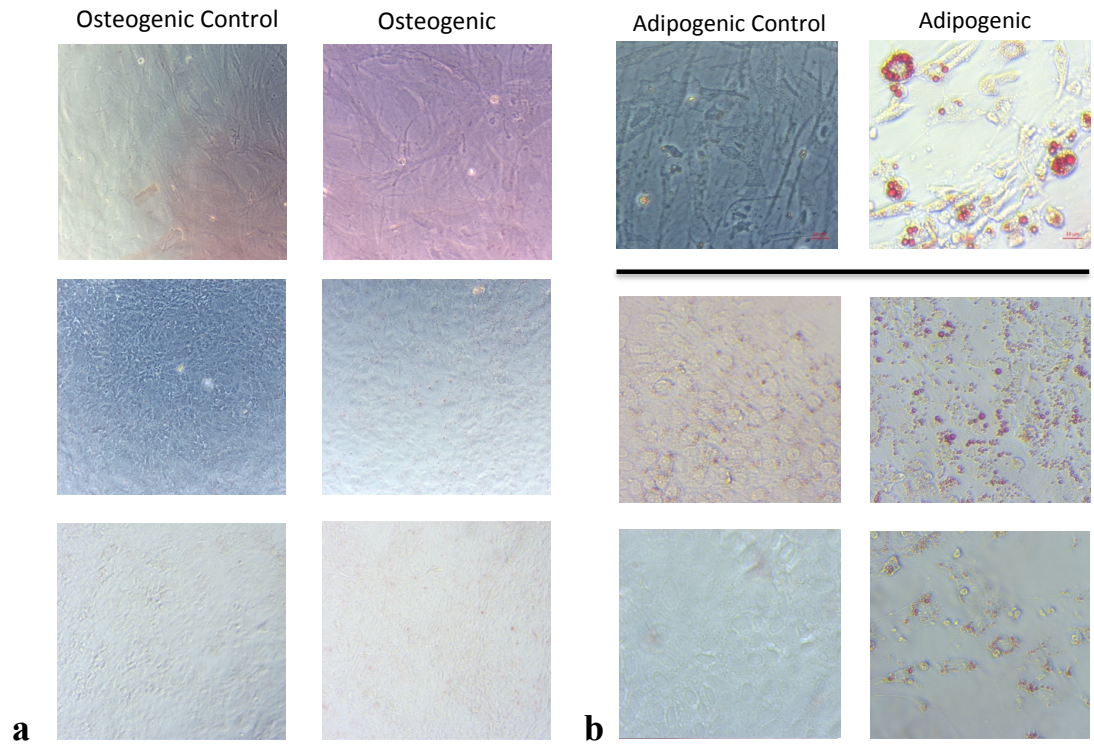

Figure 3.23: a) Light microscopy images showing the results of osteogenic media supplementation (x10 magnification), on VEGF-AMD PBEPCs after 21 days of supplementation. There was no visible red staining post Alizarin Red, indicating no calcium deposition and therefore no osteoblastic differentiation. b) Light microscopy images showing the results of adipogenic media supplementation on VEGF-AMD PBEPCs (x40 magnification above the horizontal dividing line, x10 below). Post being fixed and stained with Oil Red O, multiple red lipid droplets were evident in the supplemented media compared with the standard media. In the middle panel, the control group also shows some positive staining indicative of lipid deposition without adipogenic stimulation. The panels from top to bottom represent cultures from different individual rats.

Functional 3D tube forming assay

VEGF-AMD PBEPCs plated on Geltrex and treated with full growth medium (n=4) formed fewer connections and appeared less organised than seen with HUVECs. Two samples partly formed capillary-like structures, however, the remainder did not look especially different from the control group (Figure 3.24 and table 3.3).

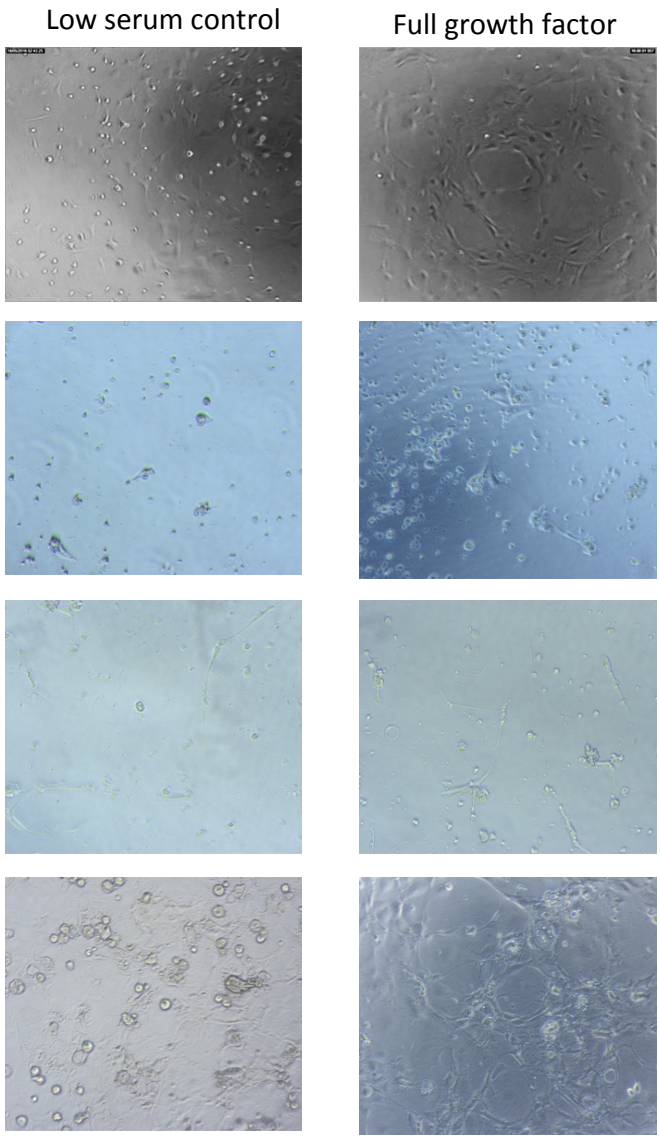

Figure 3.24: PBEPCs plated on Geltrex, treated with growth factor depleted media (low serum) or full growth factor enriched media, at 18±2 hours post plating (x40 magnification). In the top and bottom panels, there is evidence of a capillary like network forming, with cellular connections and luminal type spaces emerging. However, the middle two panels do not show such advanced structural arrangements. Results are summarised in table 3.3. The panels from top to bottom represent cultures from different individual rats.

3.3.4 Qualitative observations: PBEPC-like cells in a PBMSC culture system

A P0 PBMSC VEGF-AMD mobilised culture was passaged when confluent after colony counting. The P1 PBMSC culture however, did not thrive and only a few CFU-F colonies formed and subsequently detached, and those cells that remained appeared senescent (Figure 3.25a). In spite of this, the culture was continued and after 16 days, several small 'late-outgrowth' style EPC-like CFUs began to form (Figure 3.25b-d). By day 21 multiple CFUs were present and several very large and tight colonies developed by day 30 culture (Figure 3.25e & f).

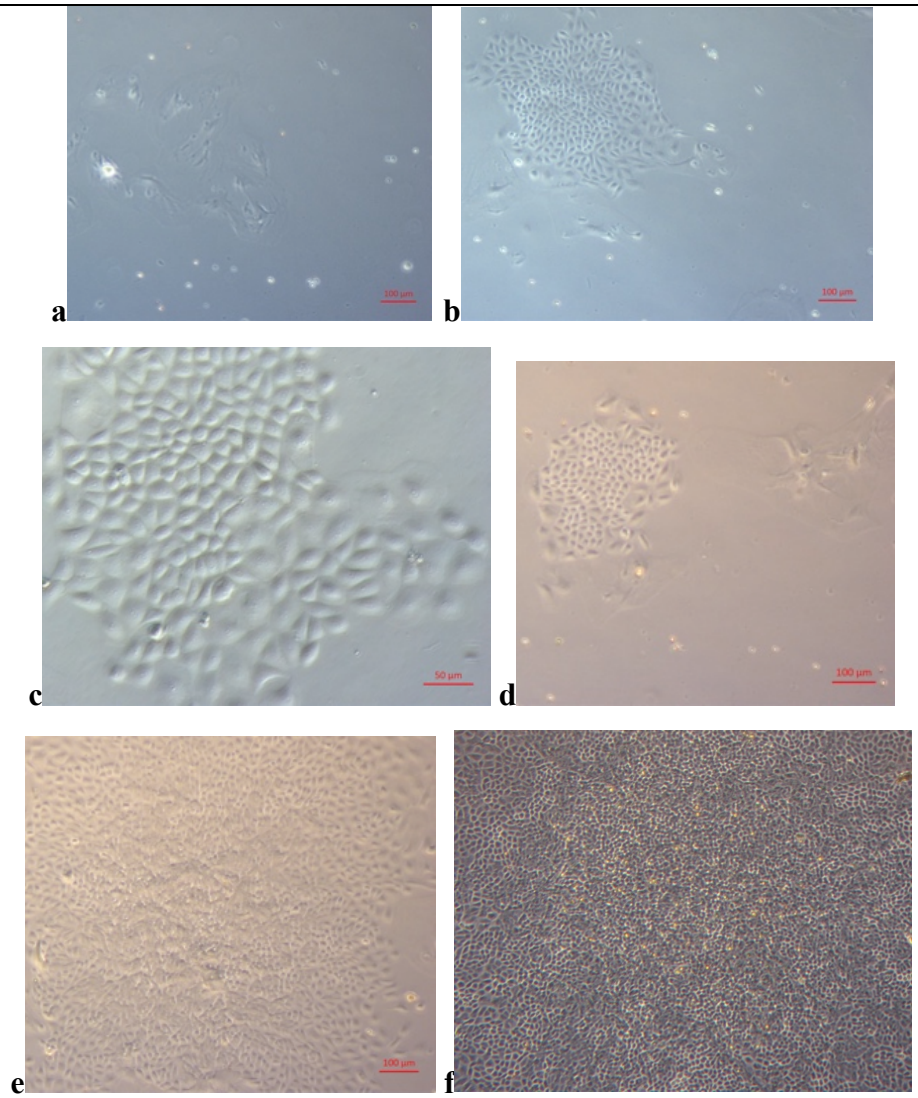

Figure 3.25: Light microscopy images of P1 VEGF-AMD PBMSC culture that failed to establish after passage, and multiple 'late-outgrowth' style PBEPC CFUs developed after 16 days. a) Senescent cells at day 16 after passage. b) Late outgrowth style PBEPC colony that appeared, shown at x4 magnification. c) Further late outgrowth PBEPC colonies developed over the following five days, (at x10 magnification) and figures d) and e) at x4 magnification. f) By day 30, several very large, dense, tightly packed colonies were present (x4 magnification).

These cells were passaged to P2 and subsequently tested for bi-differentiation, tube formation (in triplicate) and cell surface marker characteristics. Despite their EPC style morphology, these cells were more like the PBMSCs, having CD29 expression with a mixed CD45 expression without CD34 (Figure 3.26a & b), however they had low CD90 (Figure 3.26c), no CD31 and some expression of VEGFR2 (Figures 3.26d &e), more similar to PBEPCs. In terms of bi-differentiation they mirrored the PBMSCs being able to only differentiate down an osteoblastic lineage (Figure 3.27 a & b). Interestingly, they could form microvascular networks when plated in Geltrex (Figure 3.27 c).

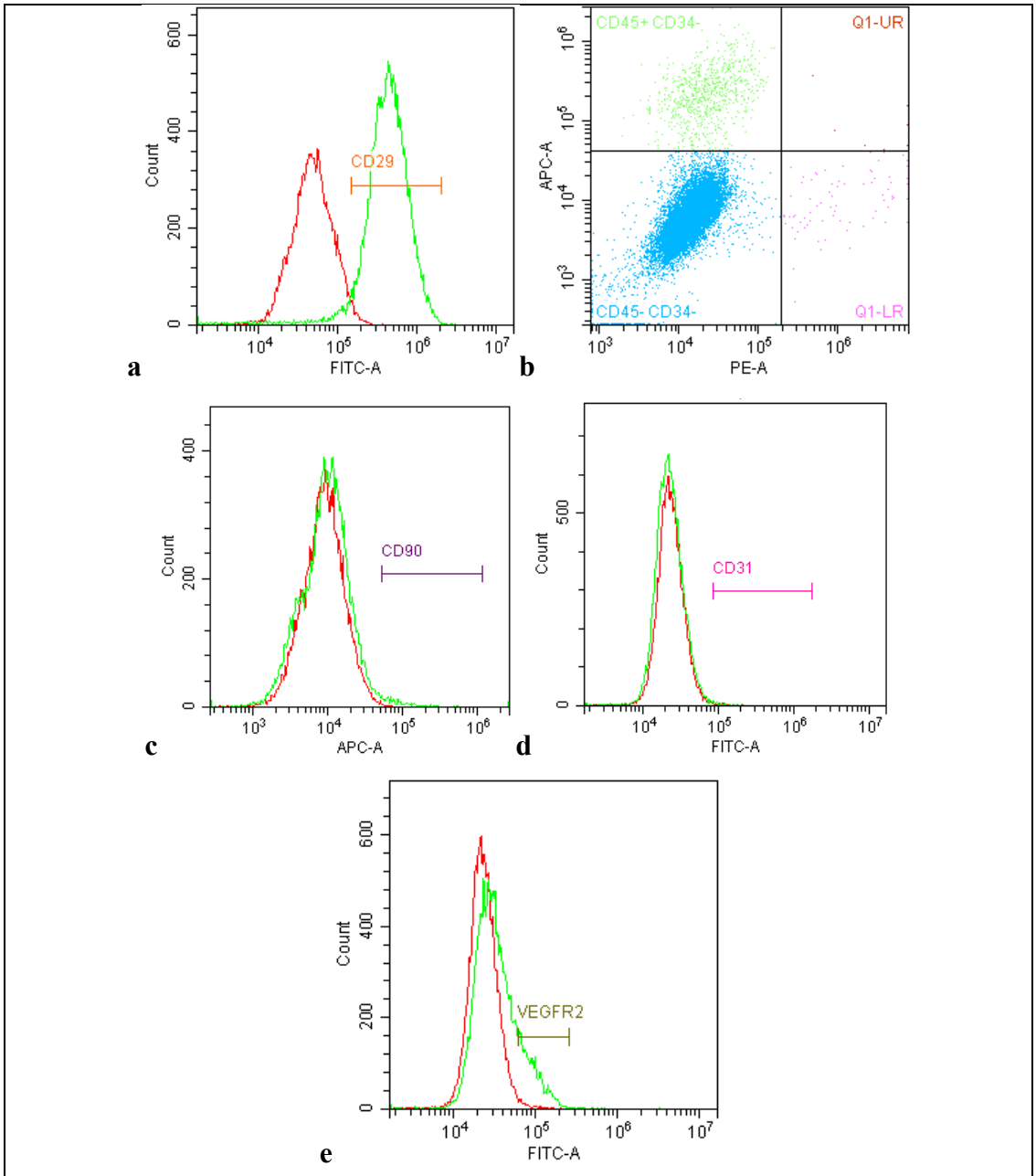

Figure 3.26: Flow cytometry fluorescence histograms and scatterplots for P2 PBMSC late outgrowth EPC like cells. a) Red plot shows cells stained with FITC conjugated isotype control. Green plot shows cells stained with FITC conjugated CD29 antibody. b) Fluorescent scatterplot showing PE conjugated CD34 against APC conjugated CD45 showing a predominantly CD34- CD45- negative population with a smaller secondary population of CD34- CD45+ cells. c) Red plot shows cells stained with APC conjugated isotype control. Green plot shows cells stained with APC conjugated CD90 antibody. d) Red plot shows cells stained with FITC conjugated isotype control. Green plot shows cells stained with FITC conjugated CD31 antibody. e) Red plot shows cells stained with FITC conjugated isotype control. Green plot shows cells stained with FITC conjugated VEGFR2 antibody.

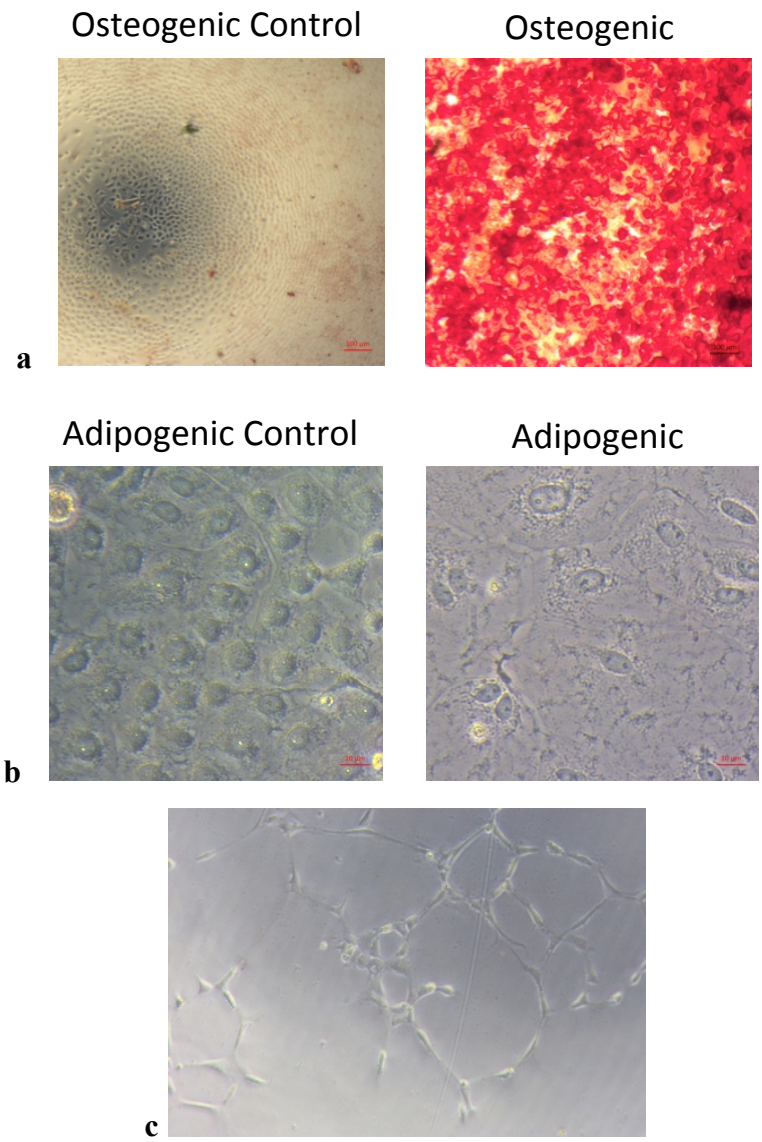

Figure 3.27: Light microscopy images post differentiation and plating on Geltrex of P2 VEGF-AMD PBEPC-like cells, that developed in a PBMSC failed culture. a) The results of osteogenic media supplementation (x4 magnification), after 21 days of supplementation. There was significant staining in the supplemented culture indicative of calcium deposition from osteoblast differentiation. b) The results of adipogenic media supplementation (x40 magnification). Post being fixed and stained with Oil Red O, no red droplets indicative of lipid deposition was seen, indicating no adipogenic lineage differentiation. c) Microvascular type network formation at 20 hours after plating on Geltrex when supplemented with full growth factor EPC media (x40 magnification).

3.4 DISCUSSION

3.4.1 Mobilisation

In this chapter I was able to support my hypothesis and showed a significant increase in peripheral blood circulating PBMSCs and PBEPCs post VEGF with AMD3100 administration. However, the actual yields were surprising low. Conceptually, a single CFU is produced from a single stem/progenitor (Friedenstein et al. 1974; Bianco et al. 2013) and in my model system this equated to an average yield of three stem/progenitor cells per ml of blood. When considering the total volumes available were around 6-8mls, cell evaluation became more challenging than predicted. To that end, *in vitro* identification with expansion was necessary and allowed a wider platform of evaluation, although cell expansion was also slow. In terms of methodology, my work was comparable to Pitchford's work in mice (Pitchford et al. 2009). The cells isolated in this chapter were evaluated functionally and on surface marker expression from third passage samples. A human or large animal study would have allowed significantly greater blood volumes and potentially serial sampling, facilitating a longitudinal view of mobilisation, potentially on non-cultured cells. These studies however, are significantly more costly, particularly in terms of the amount of growth factors required. One further issue with primary cytometric analysis would be the large number of leukocytes mobilised making stem progenitor cell identification difficult (Pitchford et al. 2010), and there are significantly fewer monoclonal antibodies available for species such as sheep.

Pitchford's work in mice showed greater MSC mobilisation of 15 MSCs/ml blood. Likewise, EPCs increased from six EPCs/ml to 230 CFUs/ml, whereas I only achieved around 3cells/ml for PBMSCs and PBEPCs. They also showed that although AMD3100 alone increased MSCs and EPCs above resting levels (3 MSCs/ml and 40 EPCs/ml), the combination of VEGF with AMD3100 was the most effective (Pitchford et al. 2009). The relatively poor results in my study could be an artefact of *in vitro* culture and the processing performed to remove red blood cells prior to culture, or related to species or age differences in the donors. A further theory is the known requirement for bone marrow CFU-Fs to have at least four growth factors present for sufficient growth and perhaps there was insufficient paracrine stimulation with my PBMSCs due to the low initial seeding density (He et al. 2006) The problems of isolating stem cells from the peripheral circulation is not new however. Other groups had to modify their techniques, such as using fibrin microbeads that bind matrix-dependent cells to concentrate the proportion of MSCs within MNCs to improve subsequent plating density and yields (Kassis et al. 2006).

A further issue is the single time point of sampling, which essentially provides only a 'snap-shot' of the circulating pool of cells at the predicted peak elution time of one hour post administration of AMD3100 (Broxmeyer et al. 2005). When evaluating the potential of endogenous mobilisation for fracture healing *in vivo*, it must be considered that the single time point measurement may be misleading. The duration and character of the profile of cell elution into the circulatory system is probably more important and so the true kinetics of the mobilisation I induced is unknown. It is also clear that mobilised cells home back to the bone marrow, or indeed other tissues such as liver, spleen, or lungs and therefore mobilisation has to be considered as a highly dynamic and complicated process, which begets the inadequacies of a single 'snap-shot' evaluation (Pitchford et al. 2010; Wilson & Trumpp 2006).

It is assumed that the mobilised cells are of bone marrow origin, however with systemic administration of the mobilising agents, they may also be from other niches, particularly when considering the conservation of SDF1-CXCR4 axis beyond the bone marrow niche (Lee et al. 2010; Kidd et al. 2010; Toupadakis et al. 2012). To confirm a bone marrow based source of the mobilised cells, the options would be to either perform bone marrow ablation with recapitulation using labelled cells, or to isolate a vascular compartmental, such as Pitchford performed in later studies, with isolation of the femoral artery and vein (Pitchford et al. 2009). The bone marrow recapitulation is complicated and high risk, and the isolated femoral component actually only informs of all possible niches within the hind limb, and not exclusively the bone marrow compartment. As the exact location of the mobilised cells was not my primary focus, this was not pursued further.

3.4.2 PBMSCs

For my control samples, I could not isolate any PBMSCs. Others have had more success using young animals however (Kamal et al. 2014). The influence of age on the function of donor MSCs has been looked at with neonatal (0 days), infant (seven days), young (14 days), pre-pubertal (35-38 days), pubertal (45 days) and adult (two months) rats (Fafián-Labora et al. 2015). In contrast, my study used ex-breeders that are at least adult through to geriatric; with increasing age, there was no change in surface marker expression, (CD34, CD45 negative, and 75% CD90 and 30% CD29 positive). However, there were age related changes in differentiation, proliferation and cell metabolism (Fafián-Labora et al. 2015). Although there are contradictions in the literature, likely relating to issues of species, gender, and consideration of what constitutes 'old', the consensus is that older rats have fewer CFUs, fewer MSCs in the bone marrow (Sethe et al. 2006), and indeed humans also show reduced CFUs with ageing (Kuznetsov et al. 2001). This could create an issue with endogenous

mobilisation strategies, as those individuals with compromised healing may simply have a smaller reservoir to mobilise. A recent study also showed an age relationship with CXCR4 dependent migration (Sanghani-Kerai et al. 2017) and hence the effect of antagonism of the CXCR4-SDF1 axis may also reduce with age. Should my mobilised cells have grown more reliably, the growth kinetics could have been evaluated with population doubling assays (Tawonsawatruk et al. 2012) and compared with bone marrow cells to determine if the differences were due to age, the individual, an inherent difference between PBMSCs and bone marrow MSCs, or the low seeding density.

As noted, the VEGF-AMD mobilised PBMSCs proved more difficult to culture than the bone marrow MSCs. They established colonies later and grew more slowly, resulting in prolonged periods of culture of up to 30 days per passage. Although passage is frequently talked about in terms of cell function, the passage number is a derivative of doublings or the number of times the cell has replicated itself. Studies looking at PBMSCs have shown the cells become flatter and bigger, and growth stops with increased numbers of apoptotic cells as passage increases (Fu et al. 2015). Therefore, if the seeding density is low, as was the case in my study, the number of replications required to get to the point of passage will be greater, and hence cells will be 'replicatively older' than their passage number may imply. Obtaining P3 cultures in my study was challenging whereas Fu et al. managed to achieve up to 25 passages (Fu et al. 2015), however they used rabbits, which would provide a significantly bigger volume of blood and hence higher numbers of seeding stem cells. A recurring theme in the literature is the relative difficulty in expanding peripheral blood cells as effectively as bone marrow derived cells (Kamal et al. 2014). Most studies looking at peripheral blood circulating stem cells and mobilisation in animal models have used immature animals (Fu et al. 2015; Pitchford et al. 2010; Toupadakis et al. 2013; Kamal et al. 2014), and therefore there may be merit in evaluating the role of age in mobilisation potential. In terms of clinical translation however, it is likely to be an older population that is more at risk of non-union, perhaps in part for this reason of impaired and reduced numbers of stem cells.

The traditional view is that a single MSC would be able to produce cells that were capable of differentiation into osteoblasts, chondrocytes and adipocytes. The PBMSCs mobilised and cultured were unable to undergo adipogenic differentiation, but were effective at osteoblastic differentiation with effusive calcium precipitates. Even classical bone marrow stem cell work has shown different clonal populations frequently do not have full tri-differentiation, whilst interestingly the osteogenic lineage is always present (Pittenger et al. 1999). Other studies have suggested a hierarchy of sequential lineage loss with the potential for osteogenic differentiation remaining (Muraglia et al. 2000). They showed that only 1/3 of clones were capable of tri-differentiation and the majority were osteo or chondro orientated.

In my study, due to the paucity of cells and the long duration of culture required, there were insufficient cells for pellet culture and chondrogenic differentiation, and therefore it remains unclear if the PBMSCs were osteo-chondro bi-potent or osteo uni-potent. Liu et al. (2018), used Cobalt Chloride with AMD3100 to mobilise MSCs and their cells also had osteo and chondro potential and reduced adipogenic potential. In any case, it is not unreasonable to suggest that the PBMSCs with osteogenic potential that I mobilised could contribute to fracture healing in a positive manner. It is also conceivable that mobilised cells may also provide trophic/paracrine support to tissue resident cells after homing, which may stimulate fracture healing.

In terms of cell surface marker expression, the PBMSCs were the same as the bone marrow MSCs expect for the presence of two CD45 populations; CD45- and CD45+ groups. CD45 is a key leukocyte marker and MSCs are universally considered to be CD45- (Boxall et al. 2012; Dominici et al. 2006). However, in patients with haematological malignancies, CD45+ MSCs have been cultured, and hence under certain circumstances the CD45 rule may be broken (Yeh et al. 2006). For my study, it was impossible to tell if these cells were simply contaminants or represented a true CD45+ MSC population. Studies in rabbits (Fu et al. 2014) and a comprehensive comparison of rat bone marrow to blood MSCs showed no difference in CD marker expression, morphology or tri-lineage potential, although growth and differentiation potential are reduced in peripheral blood isolated MSCs (Fu et al. 2012). Their study used GCSF with AMD3100 and Ficoll isolation, and perhaps the use of a different growth factor affected the cell types identified. Interestingly, they had no CD45 expression in their cells and they noted a slower growth rate than bone marrow derived MSCs. A human study that compared bone marrow MSCs to circulating MSCs after burn injuries also showed that circulating cells were identical to bone marrow MSCS in terms of surface markers (Mansilla et al. 2006).

In summary, an MSC like cell was mobilised following VEGF-AMD administration with strong osteogenic potential and hence I hypothesise that these circulating cells could have a positive influence on fracture healing.

3.4.3 PBEPCs

Broadly speaking, I saw two morphologically distinct cells types in the EPC culture system. The initial fibroblastic style population was overtaken by a cobblestone style of cell, although there were several iterations of this squarer cell type. The first description of EPCs by Asahara et al. identified a spindle shaped cell grown on fibronectin in enhanced media from CD34+ MNCs. These cells expressed VEGFR2, formed microvascular networks, and took up acLDL, and appeared to support collateral blood vessel formation in an ischaemia

model (Asahara et al. 1997). CD34 is a haematopoietic stem cell marker and hence EPCs were thought to share a common lineage. Subsequently, early outgrowth phenotype cells were frequently isolated by sorting for haematopoietic markers CD34 or CD133 with expression of endothelial VEGFR2 (Bongiovanni et al. 2014). Later studies showed these cells could only differentiate down haematopoietic lineages and did not produce endothelial cells. These cells were hence not considered to be the true endothelial progenitor, but a trophoblastic or supportive cell in vasculogenesis (Case et al. 2007). Other researchers also identified spindle shaped cells that developed early in culture with similar features to above, and called them 'early-outgrowth' EPCs. These have been suggested to be from a CD34 fraction and potentially have a monocytic origin due to CD14 expression (Medina et al. 2010), although that may be from contamination or a result of culture conditions (Chong et al. 2016). It has now been widely reported that these cells are trophic and not direct contributors to blood vessel formation (Cheng et al. 2013; Minami et al. 2015; Rehman et al. 2003). In my study, after prolonged culture and passage, there were few if any of these cells present based on cell morphology. The current nomenclature for these cells includes early outgrowth cells (EOCs) (Minami et al. 2015), circulating angiogenic cells (CACs), or early EPCs (eEPCs) (Chong et al. 2016).

The population I have evaluated here were the 'late-outgrowth' EPCs, also known as non-haematopoietic EPCs or endothelial colony forming cells (ECFCs) (Chong et al. 2016). These are more frequently grown on a collagen substrate in endothelial enriched media (Ormiston et al. 2015), but have also been grown on other substrates such as fibronectin (Pitchford et al. 2009). These cells have the characteristic cobblestone morphology, emerge later in culture and are not thought to have a haematopoietic origin or lineage (Chong et al. 2016). Late-outgrowth cells express lower VEGFR2 than early outgrowth cells, high CD31 and form microvascular tubular structures and proliferate well (Bou Khzam et al 2015). They have also been shown to have endothelial ultrastructures on electron microscopy imaging, such as adheren junctions, and a gene expression more similar to dermal microvascular endothelium than monocytes (Medina et al. 2010). The chronology of the emergence of these cells also appears to affect their ability to drive neovascularisation with the latest ones providing the best re-vascularisation in ischaemic models (Minami et al. 2015). Interestingly, in some studies late EPCs show higher CD31 and VEGFR2 expression than early (Cheng et al. 2013).

The cell surface marker expression of my 'late outgrowth' EPCs was negative for CD34 which is characteristic of "an early out growth EPC" and fits with cultures being ostensibly cobblestone. There was no CD45 expression as expected. One culture had low expression of VEGFR2, and cells from two cultures were positive for CD31, which is a late-outgrowth

EPC marker. These CD31+ cells did not co-express VEGFR2. Surprisingly, one culture fitted my criteria for MSCs. A clear relationship between the microvascular network formation and CD marker expression was not evident, with networks forming on Geltrex clearly in two, and moderately in one out of four cultures tested. This may indicate a fundamental inability of these cells to perform this activity and fits with the marker expression not being as convincing as some studies, or potentially indicates the need for further optimisation of this *in vitro* test for blood mobilised cells.

EPCs are not expected to have any differentiation potential. Unusually and unrelated to CD marker expression or tube formation potential, all cultures were able to move down an adipogenic lineage. This begs the question of whether the PBEPCs were actually MSCs with the 'adipogenic switch' turned on, favouring adipogenesis only (Moerman et al. 2004).

3.4.4 Relationship between PBEPCs & PBMSCs?

The PBMSC culture that failed to establish but subsequently developed cobblestone cells in prolonged culture is particularly interesting. These cells were morphologically identical to the 'late-outgrowth' cobblestone PBEPCs that I grew, and could form a clear microvascular network and had some VEGFR2 expression. Despite this, they had the PBMSC osteogenic lineage exclusivity rather than the PBEPC adipogenic exclusivity. This prompts two thoughts. Firstly, are EPCs routinely present in MSC cultures, but are simply outcompeted by the rapid growth of MSCs. Clearly the cobblestone morphology is not dependent upon fibronectin coating or an endothelial enriched growth media and hence their morphology is not dictated by those factors. Secondly, are the PBEPCs I mobilised truly EPCs or MSCs, or a precursor to both? As a precursor is expected to be less lineage limited, the results seen may be due to the different culture conditions influencing lineage exclusivity. Certainly, one isolate of PBEPCs was CD34- CD45- CD90+ CD29+, fulfilling my criteria for MSCs in chapter 2 and yet the cell morphology was completely different to the fibroblastic MSC.

The relationship between MSCs and EPCs is not well understood, however, human bone marrow MSCs have been differentiated to 'endothelial like' cells by adding VEGF to the media which induced VEGFR2 and Von Willebrand expression, although no CD31. These cells could form microvascular networks, although cell morphology remained typically fibroblastic, unlike my PBEPCs. They also showed that standard bone marrow MSCs in the presence of VEGF were also able to form microvascular networks, albeit less well than the growth factor conditioned MSCs (Oswald et al. 2004). *In vitro* expanded MSCs that have been conditioned by culture in EGM-2, which is growth factor enriched media, (similar to my EPC media), could form tubes on Matrigel and expressed CD31 and VEGFR2 at higher levels than MSCs did, but lower than EPCs. They also showed no difference in CD90

expression. However, the transformed MSCs did not look like cobblestones and they also demonstrated a relative increase in CD34, which I did not see. Interestingly, they noted depressed adipogenic tendencies (Liu et al. 2007), compared with my lineage tendency. What this suggests is the plasticity and influence of culture environment on cells needs to be considered in these studies. If my PBMSCs and PBEPCs had been more numerous, a cross culture study to determine the influence on morphology and function would be a viable next step for assessing these two cell populations. However, it would not explain the cobblestone morphology cell establishment in the MSC culture system. Substrate differences may have also played as a role, as fibronectin has increased the ability of MSCs to form Matrigel microvascular networks compared with cells cultured on gelatin (Muscari et al. 2010). In any case, if VEGF-AMD mobilises 'late-outgrowth' EPCs and MSCs together, this combination may well have benefits in fracture healing.

Could I have mobilised a common precursor? Despite MSCs having been the subject of research for over 40 years and EPCs for 20 years, their developmental origins remain unclear. MSCs, haematopoietic stem cells and EPCs are derived from the middle of three embryonic primary germ layers in the embryo, the mesoderm, with MSCs also having a neural crest source in addition to the lateral plate mesoderm (Sheng 2015). Work using embryonic stem cells has shown two mesenchyme derived sub lineages; the haemangioblast and a mesenchymoangioblast lineage which lead to MSCs and EPCs (Vodyanik et al. 2010; Slukvin & Vodyanik 2011). The haemangioblast is thought to be a source of haematopoietic stem cells and endothelial precursors and again work on embryonic stem cells supports this theory (Huber et al. 2004). Therefore, an inter-related origin of these cells and hence a common precursors or possible plasticity between them may be possible. This could potentially explain some of the mixed *in vitro* findings, the relative roles of 'early-outgrowth' and 'late-outgrowth' EPCs (Cheng et al. 2013), a potential role for MSCs alone (Kumar et al. 2010) and in combination with EPCs for angiogenesis (Aguirre et al. 2010) and perhaps the relationship of MSCs and pericytes (Cano et al. 2017) with their vascular intimacy (da Silva Meirelles et al. 2006).

3.4.5 Conclusion

The very act of *in vitro* cell culture changes the cells, including their cell surface characteristics (Bara et al. 2014), and although the cells mobilised were not exactly as expected, VEGF-AMD treatment clearly increased the available stem/progenitor pool in rats, even when using this 'snap shot' *in vitro* assessment. Critically, there was an increase in circulating osteoprogenitor cells that may show promise for fracture healing. As atrophic non-unions in rats have some residual cells that can differentiate within the non-union and

bone marrow has increased MSCs when a non-union fracture develops (Tawonsawatruk et al. 2014), it seems appropriate to evaluate whether this protocol can boost fracture healing in an *in vivo* rat model of delayed/non-union. Having established proof of concept for mobilisation, and due to the difficultly in precisely determining the number and type of cells that are mobilised by *in vitro* investigation, it is entirely appropriate to investigate the potential effects of mobilisation in a fracture healing model system. In order to make this as informative as possible, this model needs to have consistent biomechanics to ensure any outcome differences are likely attributable to the effect of mobilisation. To that end, chapter 4 and 5 were focused on the development of the fixator model and evaluation of its biomechanics.

Pitchford et al. (2009) indicated that VEGF with AMD3100 was the most potent combination for mobilising MSCs and EPCs in a mouse model, however, I acknowledge that other growth factors may also have potency for mobilising stem cells. In this chapter, I chose to investigate the effect of VEGF with AMD3100 on stem and progenitor mobilisation from Wistar female as they are the chosen species and breed for the fracture model, and secondly, Pitchford's work indicated that VEGF with AMD3100 would mobilise MSCs and EPCs, both considered important in fracture healing. I could have gone on to investigate the mobilisation of MSCs and EPCs using other growth factors such as GCSF or IGF1, in the same manner as in this chapter, however as the number of stem cells were relatively low and as there was difficulty in characterising these cells, I considered it prudent to proceed to a translationally informative *in vivo* rat fracture model. This remained the only way to evaluate the potential for endogenous mobilisation to boost healing accurately, as it allowed for the full kinetic profile of mobilisation of unaltered cell combinations that may boost fracture healing.

CHAPTER 4: Redevelopment of a micro external fixator

4.1 INTRODUCTION

4.1.1 Models of fracture healing

In order to determine whether endogenous mobilisation could influence fracture healing, a standardised, repeatable and reliable fracture model system was required. Ideally, any model should mirror the clinical scenario in terms of location, fixation and pathology as closely as possible. However, no model can completely reflect a clinical scenario and the ability for the model to be highly consistent and reproducible is also critical to discriminate between treatments, and may be paramount depending on the questions being asked. Other factors also require consideration, such as cost, technical expertise, size and the intended questions to be asked. Reflecting these varied needs, there are several options for modelling fracture healing. Historically, large animal models were more popular for fracture healing, but the use of rodent models has significantly increased to nearly 50% of all fracture studies. This increase has in part been associated with the advent of the gene/molecular age and the availability of those tools in rodents, particularly the mouse (Garcia et al. 2013). The rat however, is a good model as they have straightforward husbandry, are readily available, not overly expensive and not so small that they prohibit an accurate, repeatable surgical procedure. In terms of bone physiology, rats have lamellar bone with cancellous remodeling, although their cortical remodelling is less than in humans. Currently, the rat is used for around one third of all *in vivo* fracture studies (Mills & Simpson 2012).

To model a fracture, a discontinuity in the bone is needed. This can be induced by application of external forces giving a realistic degree of associated soft-tissue trauma, but can result in variable fracture patterns, complicating the interpretation of results. Alternatively, a reproducible but arguably artificial 'surgical fracture' can be created by osteotomy or ostectomy. Typically, a method of stabilisation will follow. Stabilisation is usually designed with either direct bone union or indirect bone union in mind, as discussed in chapter 1. Clinically, indirect bone healing is seen in most fractures, including conservatively managed fractures, those stabilised by intramedullary nails or external fixators and when internal fixation is applied without compression and accurate reduction (Marsell & Einhorn 2011). Hence, indirect bone healing is the main mode of fracture healing evaluated in rodent research (Garcia et al. 2013) and several stabilisation options are available. A common method referred to as the 'Einhorn technique' (Bonnarens & Einhorn 1984) uses a guillotine weight to fracture the bone and stability is then provided by an intramedullary pin. This system is known to give reproducible stiffness, but there is variation in interfragmentary and torsional stability inherent to the nature of the stabilising device. Fixation with an internal plate and screws is an option, but the close apposition of the plate

to the bone creates difficulty with the analysis of the healing zone and the internal implants are more difficult to remove. Hence plate and screw studies are far less commonly undertaken and direct bone union in rats using close approximation and compression plating has only been studied once (Savaridas et al. 2012). Both internal fixation with a plate and screws, and intramedullary pins can interfere with fracture healing assessment, and hence the external fixator is a popular choice, as the implants are at a distance from the fracture site and can be easily removed (Mills & Simpson 2012). Additionally, mechanical modulation of the fracture through changes in stiffness of the construct or by the size of the fracture gap can be easily accommodated using external fixation (Goodship & Kenwright 1985). The main issue with external fixation is the relatively high level of pin tract complications, which are universally regarded as common and have been reported in up to 100% of clinical cases (Kazmers et al. 2016). A recent Cochrane review however, was unable to identify management regimes to reduce this (Lethaby et al. 1996).

4.1.2 A brief history of external (skeletal) fixation

External fixators or 'external skeletal fixators' as they are referred to in veterinary medicine, have a variety of indications including open and closed fracture repair, joint immobilisation and angular limb corrections. Principally, an external method to stabilise bone fragments dates back to around 400 BC with Hippocrates treating tibial fractures using leather rings with cherry wood rods (Hippocrates 1939). French surgeon Malgaigne devised the first true external fixator with transcutaneous implants in 1840. Colloquially known as the Malgaigne patellar clamp, this device with skin puncturing hooks was used to treat transverse patellar fractures by grasping the upper and lower poles of the patella and then compressing them together with an external screw mechanism (Malgaigne 1847). However, it was British surgeon Mr. Keetley who first described an external fixation device with percutaneous iron pins deliberately implanted within the bone. The first readily available external fixator, the 'Parkhill clamp', subsequently appeared in 1897. It was devised by an American surgeon and consisted of four screws, with two placed either side of the fracture, interconnected with external winged metal plates. Parkhill would apply this with an adjunctive posterior plaster-of-Paris splint and published a case series of nine individuals with 8/9 going on to bone union (Parkhill 1897). At the time, Belgian surgeon Lambotte had heard of the Parkhill bone clamp but could not access a copy of Parkhill's paper. He went on to develop his own device, which was designed to be the sole fixation for the fracture, and had parallel placed pins with adjustable clamps (Lambotte 1913). Some years later, Roger Anderson, an American military surgeon developed a fixator that consisted of connecting rods and single or double clamps, to create a modular system of fixation, known as the Anderson splint.

In veterinary medicine, US veterinarian Otto Strader pioneered external skeletal fixators in 1934. Dr. Strader began to treat long bone fractures in animals, and one of his animal patients was seen by surgeons working at the Bellevue Hospital, New York, leading to a collaboration and design modifications for humans. In the 1940s, Emerson Ehmer worked with the Kirschner company to develop the Kirschner-Ehmer splint, a veterinary modification of the Anderson splint for humans in 1947 (Pettit 1992). Versions of this system remained in widespread veterinary usage until the late '90s when other more adaptable and mechanically robust systems were developed.

In human orthopaedics, the popularity of external fixation declined in the mid 20th Century due to poor results caused by errors of application and the rise of the AO principles associated with stable internal fixation. However, unbeknown and inaccessible to the West during the Cold War, Gavriil Ilizarov from the Soviet Union began to develop a circular fixation system, initially from recycled bicycle parts. He went on to pioneer circular frames to treat non-union fractures in humans in the 1950s, which used small diameter crossing pins/wires that were fixed to external metal rings. After working with this system, it became apparent that by applying traction to the frame it was also possible to grow or lengthen bone through 'distraction osteogenesis' (Ilizarov 1990; Hernigou 2016). These techniques are now widely used to correct complex limb deformities, complex fractures, and to regain bone length, all over the world, often using extremely sophisticated computer-planning systems.

4.1.3 Fixator classification

Fixators are typically classified as linear, circular, hybrid or free form. Linear fixators consist of pins, bars (rods) and clamps (Figure 4.1). Different frame configurations can be created, which affect the strength/stiffness of the frame:

- Type Ia = unilateral, uniplanar, half-pins; Type Ib = unilateral, biplanar, half-pins.
- Type II = bilateral, biplanar, full-pins; Type IIb 'Modified Type II' = bilateral, biplanar, full and half-pins.
- Type III = bilateral, biplanar, full and half-pins.

Circular or ring fixators use supporting rings, connective rods, bolts and tensioned transfixation wires. Hybrid fixators are fixators that combine elements of linear and circular, and free-form/acrylic/epoxy putty fixators are related to linear fixators, however the bars and clamps are replaced by epoxy putty, or by acrylic that is poured into a malleable tubular mould.

4.1.4 Construction of the modern external fixator

The modern linear external fixator has three components making up the fixator montage or construct (Figure 4.1):

1. Transcutaneous bone implants – smooth Kirschner wires or threaded pins that pass through the skin and fix the bone fragments in place. Pins are termed *'half-pins'* if they penetrate only one skin surface and *'full-pins'* if they exit the other side. Pins are usually placed bi-cortically.

2. Connecting bars 'rods' – are rigid external structures (bars, circles, or set acrylic) that connect and immobilised the fixation pins.

3. Linkage device – a method of linking the pins to the connecting bar (clamps).

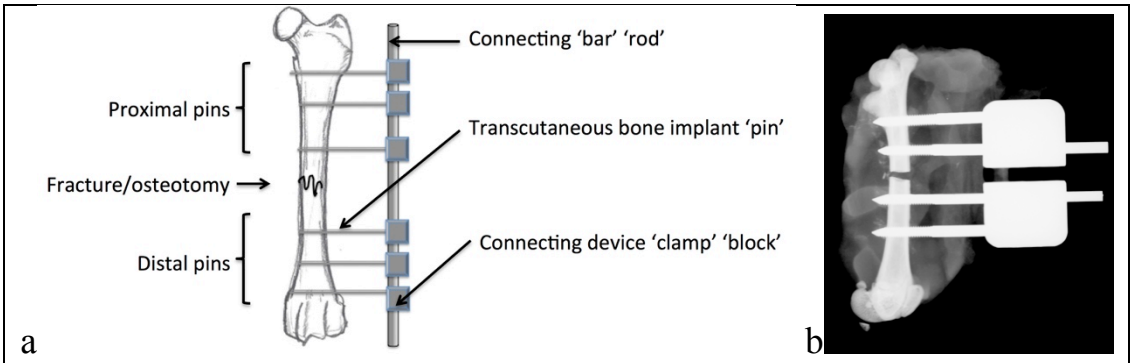

Figure 4.1: a) Schematic showing the basic components of a linear type 1a external skeletal fixator placed on a stylised canine femur. b) Radiograph showing the revised Stanmore micro-Fixator at day 0 on a rat femur.

4.2 REDESIGN OF THE STANMORE RODENT MICRO-FIXATOR SYSTEM

A miniaturised skeletal fixator from the Institute of Orthopaedics and Musculoskeletal science, UCL, Stanmore, has been used in several prior studies (Harrison et al. 2003; Ho et al. 2014; Smitham et al. 2014). It is a unilateral uniplanar (Type Ia) external fixator with two pins proximal and two pins distal to a surgically created osteotomy. It had a double connecting bar with two connecting blocks which can slide axially along the bar, allowing alteration of the osteotomy gap size. In early studies, the blocks were made of anodized aluminum with stainless steel bars and bar bushings. In later iterations the blocks were manufactured from titanium, with titanium bars and eventually carbon fiber bars to improve radiographic imaging and to reduce the weight of the fixator (Figure 4.2).

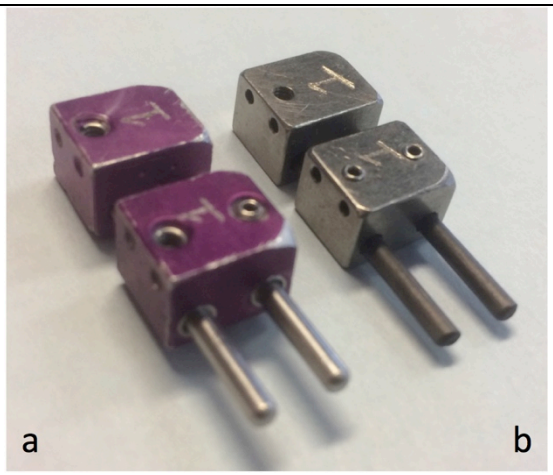

Figure 4.2: a) Photograph showing the first generation fixator; aluminum block and stainless steel bars b) The evolved version of the original fixator, with square titanium blocks and carbon fiber bars.

Despite its success, several issues were noted with the fixator and delivery system that warranted improvement:

1) Loosening of the pin to bone interface, sometimes within days, sometimes within weeks (Figure 4.3).
2) Fixator block interference with hindlimb soft-tissues.
3) The jig system was cumbersome and did not provide tactile instrument feedback during surgery. Additionally, the apparatus could not be sterilised increasing the risk of infection (Figure 4.4).

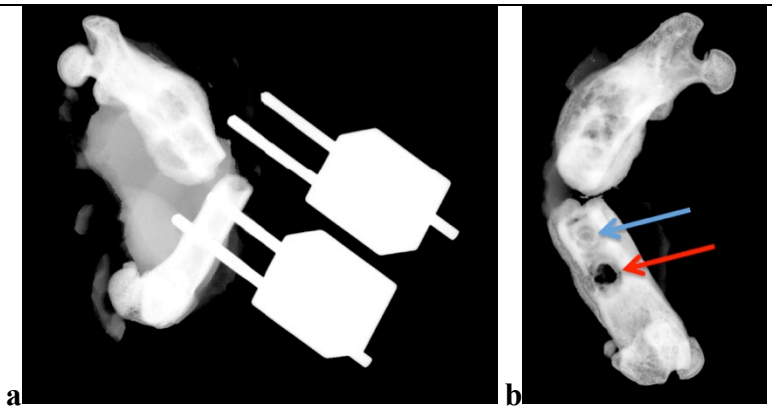

Figure 4.3: a) Radiograph showing failure of the fixator at three weeks, with complete pin extraction from the bone proximally. b) Radiograph at three weeks, showing the bone without the fixator. The red arrow shows a large osteolytic hole where the pin tract was. Blue arrow suggests the formation of a ring-sequestrum around the other pin tract.

4.2.1 New jig system to produce a highly repeatable pin location

Rather than using the table-top drilling and pin driving apparatus (Figure 4.4), a miniaturised guide-block was designed (Figure 4.5) to ensure consistent and standardised pin placement. The block had a concavity to allow it to sit on the craniolateral surface of the femur and was manufactured from Polyether ether ketone (PEEK) for durability, machinability and heat resistance allowing autoclave sterilisation. It also had indentations to facilitate the application of a precision micro-ratchet forceps (Kyon, Switzerland) to stabilise the guide on the bone. The guide-block could universally accept either a drilling insert-sleeve designed specifically for the drill bit size intended, or pin insert-sleeve, again designed to accept the fixator pin specifically (see Figure 4.5b). The insert-sleeves were manufactured from titanium and heat treated to change their colour, which aided in their identification; the drill sleeve was 'silver' and had a conical top, whereas the pin sleeve was 'gold' and had a flat top (Figure 4.5b).

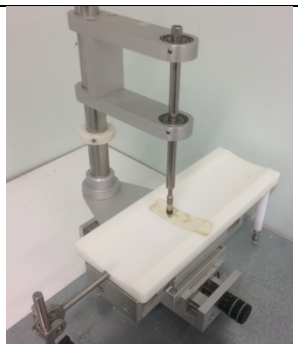

Figure 4.4: Photograph showing the previous drill and pin guide apparatus. This apparatus allowed for the table-top to be moved intra-operatively using precision XY axis adjustment dials, allowing the hand driven chuck to be positioned correctly.

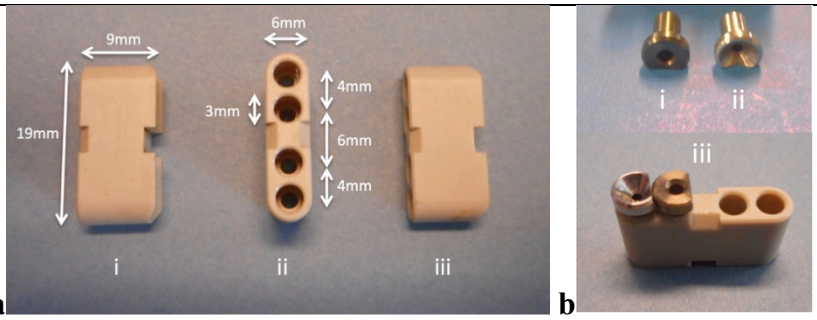

Figure 4.5: a) Photograph showing the revised miniaturised drill and guide-block, which sits directly on the craniolateral femoral surface. i) Shows the lateral surface with the concavity on the underside. ii) Shows the top surface with recesses to accept insert-sleeves and micro-ratchet recesses. iii) Shows medial surface. b) Photograph showing the titanium pin sleeve (i) and the drill sleeve (ii). The guide-block universally accepts either of the two sleeves (iii).

4.2.2 Block redesign

Titanium remained the preferred material for the blocks due to its reduced X-ray artifact generation in 3D imaging, its lightweight nature and wear resistance properties. To make the fixators truly modular, the connecting bars in the proximal block were no longer chemically bonded in place, but secured with M2 stainless steel grub screws. To reduce skin rubbing, the edges of the blocks were chamfered (Figure 4.6a). As before, these fixators are designed to allow axial displacement of the fragments such that any desired fracture gap size can be created within the range of the bar length (Figure 4.6b). The bars remained as 2mm diameter carbon-fiber-epoxy resin matrix (Goodfellow, UK).

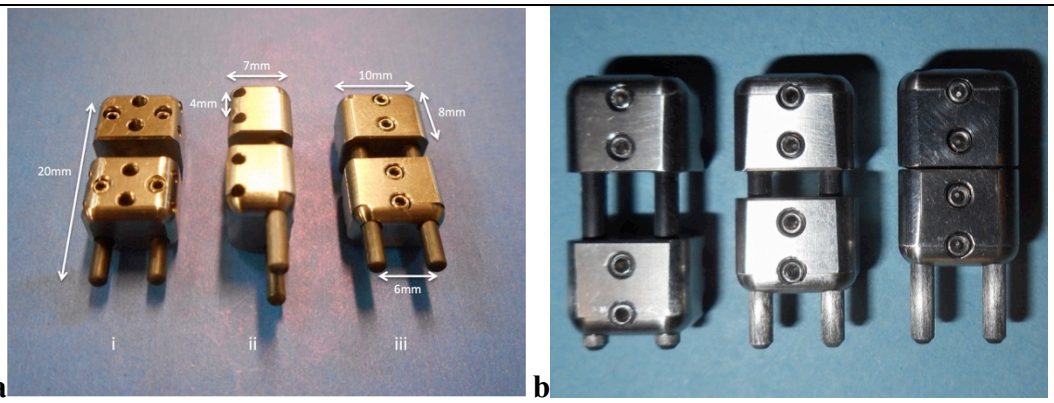

Figure 4.6: a) Photograph showing different aspects of the revised fixator. i) Shows the cranial surface of the fixator, which reveals the M2 stainless steel grub screws to secure the proximal and distal blocks. The distal screws can be loosened to allow sliding and distraction of the osteotomy. ii) Shows the lateral surface of the fixator; notably, the pin-holes are eccentric such that the bulk of the block can be positioned caudal to the pins, as most of the rubbing occurred on the cranial surface. iii) Shows the caudal surface of the fixator, which has the four M2 stainless steel grub screws that secure each individual pin. b) Photograph showing the various degrees of axial distraction available.

4.2.3 Pin redesign

The pin-bone interface is considered the mechanical 'weak link' in an external fixation construct (Lewis et al. 2001; Briggs & Chao 1982) and its stability is influenced by the pin design and methodology of its placement. Initially, a 1mm hole was predrilled into the bone using a high-speed dental burr (Hand Engine No.5, Royal, UK) to facilitate pin placement. Early pin loosening and concerns over initial pin stability during surgery inevitably related to the mechanical adequacy of initial pin placement. The original pins were 1.2mm diameter stainless steel, end threaded with a domed 'blunt trochar' leading edge (Figure 4.7a & c). These pins were difficult to place in the bone leading to noticeable hand wobble when driven with hand chucks. Hand wobble has been shown to create a conical deformation and hence

reduce the 'goodness' of fit of the pin in the cis (near) cortex (Bible & Mir 2015). Studies looking at screw insertion into pre-drilled holes have shown that a sharp trochar tipped screw required similar insertion torque to a pre-tapped hole. The blunt tipped screw was considered thread forming and caused more bone damage than the sharp trochar tipped screw, which was considered 'self-tapping' (Kuhn et al. 1995). Therefore, in order to improve pin placement, a self-tapping/cutting ability was sought. New pins were made by end-threading trochar tipped 316LVM stainless steel Kirschner wires, of 1.25mm diameter, with a three-point 45^0 trochar (Veterinary Instrumentation, UK) (Figure 4.7b & d). Trochar tip pins should improve stability, as they have been shown to have a higher initial pull-out resistance in canine metatarsals, when inserted at slow speeds, compared with other designs (Namba et al. 1987).

Pins inserted into a hole that is smaller than the pin itself generate a circumferential compressive interaction between the pin and bone, which increases pin stability, known as 'radial preload' (Biliouris et al. 1989). Canine experimental studies have shown however, that if the hole is excessively reduced, there is an increase in bone micro-fracture. A pilot hole that approximates but does not exceed the core diameter of a threaded pin is thought to provide the best compromise between increase initial pin stability and microstructural damage that may subsequently lead to necrosis and loosening (Clary & Roe 1996). Similar microstructural damage has also been shown in human samples with misfits greater than 0.4mm (Biliouris et al. 1989). A 1.2mm die produced a core diameter of 0.955mm, and therefore the pre-drill was reduced from 1.0mm to 0.9mm for the 1.25mm trochar tipped pins, with the aim of creating a tighter fit and increased radial pre-load, without undue microstructural damage. No early pin loosening was seen after these changes were implemented and immediate surgical pin stability in cadavers and *in vivo* was excellent (n=8). However, late pin loosening from around three weeks was still seen in 50% of individuals.

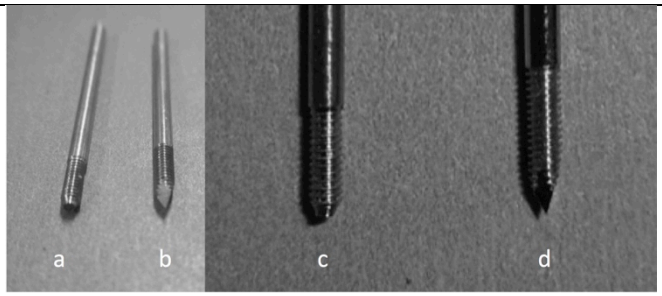

Figure 4.7: Photographs showing the original blunt trochar tipped pins (a, and c), and the revised sharp cutting trochar tipped pins (b and c).

4.2.4 Pin placement changes

Ongoing 'late' pin loosening was still being seen at around three weeks post-operatively (Figure 4.8a). Most commonly, but not exclusively, this was seen at the most proximal pin. Notably, on two occasions there appeared to be a radiographically pathognomonic ring sequestrum associated with some pin tracts (Figure 4.8b). Typically these have a "characteristic radiographic finding of a band of sclerotic bone adjacent to the pin tract, which is surrounded by an irregular radiolucent zone of bone destruction" (Nguyen et al. 1986). In human bone, thermal necrosis leads to a wide sclerotic zone of dead bone with a narrow lucent halo, suggested to be associated with increased osteoclastic activity, whereas the infected necrotic sclerotic zone is smaller and the lucent region consists of granulation tissue (Nguyen et al. 1986).

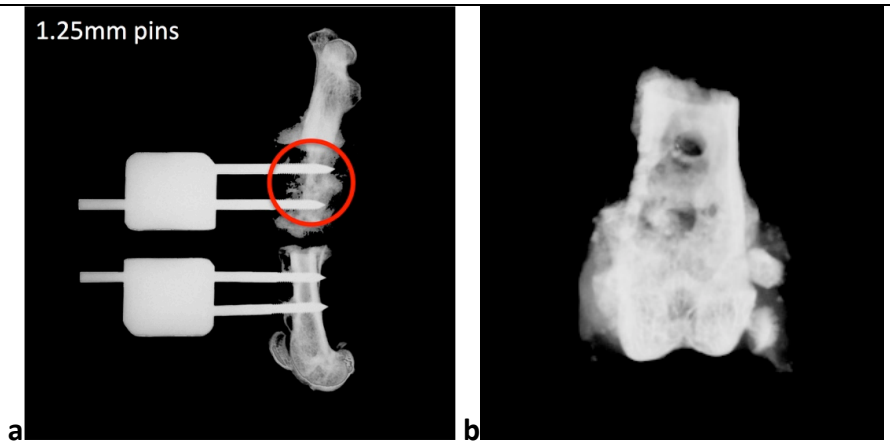

Figure 4.8: a) Radiograph showing osteolysis and lucency around the proximal pins. b) Radiograph showing a distal femoral fragment with marked remodeling around the distal pin tracts. The upper pin tract has a sclerotic region with a surrounding lucent zone suggestive of a ring sequestrum.

Although infection is also required, a relationship between thermal necrosis and the aetiology of this type of radiographic phenomena is widely reported (Augustin et al. 2007; Matthews et al. 1984). A broadly accepted risk factor for pin loosening and infection is thermal necrosis of bone and heat damage to soft-tissues (Matthews et al. 1984). Rabbit studies have shown that a temperature exposure of 70°C will cause immediate necrosis (Berman et al. 1984) and 47°C for greater than one minute will also lead to cortical bone necrosis (Eriksson et al. 1984). In human bone studies, predrilling prior to pin placement significantly reduced the temperature elevation (Matthews et al. 1984). Pre-drilling was already part of this procedure, however saline irrigation was not. Experiments with pig femurs have shown that applying 25°C external water cooling was more important in reducing drilling temperatures than drill bit size, speed, feed rates or bit design (Augustin et

al. 2007). The heat distribution associated with drilling has been investigated in *ex-vivo* bovine mandibles using embedded thermo-resistors. The greatest amount of heat was found at the superficial and not the deep region of the drilled hole, hence external coolant rather than a cannulated internal coolant to the drill tip is appropriate (Sener et al. 2009). From this point onwards, sterile saline was used to irrigate pins and drill bits whilst in use.

The pre-drilled hole for the fixator pin was initially performed using a high-speed dental burr (Hand Engine No.5, Royal, UK), which reaches speeds of 20,000rpm. The thermal effects of drill speed in the published literature is quite mixed (Pandey & Panda 2013). Work from the 1950s showed increased temperature when speeds increased from 125 to 2000rpm (Thompson 1958). A more recent study showed that sequentially increasing drill speed from 188 to 1820rpm with a consistent drill bit diameter increased the bone temperature from 31 to 55°C (Augustin et al. 2007). However, a cadaveric porcine mandible study showed high-speed drilling at 2500 rpm caused a significantly smaller increase in temperature than at 1667 or 1225rpm. This is not necessarily a simple contradiction in the literature, as they note the overall time the drill was in contact with the bone was less when the higher speeds were used, suggesting an additional influence of duration of drilling (Sharawy et al. 2002). Similar findings were seen in a rabbit tibial model that used concurrent coolant during osteotomy preparation, with thermocouple readings showing an inverse relationship of temperature and speed when 2,000, 30,000 and 400,000 rpm were compared (Iyer et al. 1997).

A confounding factor in evaluating drill speed data is the interaction of the driving or feeding force applied to the drill bit, such that it can cut effectively and not simply rotate on the bone creating excessive friction and heat. In an *ex vivo* study with different loads applied to a drill press, it was clear that increased drill driving load, significantly decreased the bone temperature as read by thermocouples, and importantly, it was below 50°C (Bachus et al. 2000). Others have shown a 10 fold increase in drill speed did not increase the temperature measured in the bone, however an increase in force applied to the drill did decrease the temperatures measured (Matthews & Hirsch 1972). On balance therefore, I changed from the dental burr to a spiral push drill (Rolson, UK). These drills do not rotate as quickly as a burr and require the application of axial load to rotate the drill bit, which was not as intuitive with the high-speed dental burr. Although not directly measurable, it is likely there was an improvement in the driving force applied and hopefully an improved cutting efficiency and reduced heat generation. To ensure good cutting efficiency the drill bits were regularly replaced with new ones.

As noted, high pin insertion speeds have been shown to generate more heat (Thompson 1958) and current recommendations are that they should be driven with power at low,

<150rpm speeds (Egger 1992; Lewis et al. 2001). In my model, pins were advanced by hand in a small chuck (162A Pin Vice, 0-0.040, Starrett, USA), as a low speed high torque driver at the micro scale was not available.

Pin site care to reduce pin tract infection and loosening is a debated topic in human and veterinary clinical fixator management. Antiseptic cleaning, specialised dressings and prophylactic antibiotics have all been suggested to reduce pin tract infections and associated loosening (Kazmers et al. 2016). However, a relatively recent Cochrane review of all available evidence was unable to give a clear indication of what pin care measures should be taken (Lethaby et al. 1996). Many of these ideas were not feasible in relation to this study due to the risks and welfare impact by regular handing and cleaning of the fixator pin tract sites, particularly when the evidence base is not strong.

A final option would have been to adopt a pin coating such as hydroxyapatite to improve the pin-bone interface (Magyar et al. 1997; Saithna 2010). However, this would have been cost-prohibitive and technically problematic with such small pin threads and was not pursued. Additionally, although the specimens were decalcified for histology, it could have introduced problems with histology processing when pin removal was required.

4.2.5 Pin size & number

As interfacial strains greater than 2% are thought to induce osteoclastic, chondrogenic and fibrous tissue formation, and hence pin loosening, a reduction in strain should be beneficial (Palmer et al. 1992). Further mitigation of late pin loosening was therefore sought via two alternative techniques. Firstly, the number of pins in the proximal segment was increased to increase the construct stiffness (Bouvy et al. 1993) and reduce the load at each individual pin-bone interface (Moss & Tejwani 2007). Two pins per fragment is the minimum to prevent rotational instability and beyond four per segment, there are no further changes in frame stiffness (Palmer et al. 1992). Unfortunately, there was limited space available on the rat femur for pin placement and instrument access and therefore a 2:3 configuration was adopted, with three proximal pins (Figure 4.9a). Although no pin loosening was seen (n=3), the additional pin made the fixator placement more challenging.

The alternative method investigated was to increase the pin diameter. The fixator construct in these osteotomies is not load sharing initially and therefore all limb loads will be transferred between the pins and the bone at their interfaces. A parametric analysis based on finite element models was able to show that these loads could be reduced by ensuring full pin insertion, decreased pin working length and by increasing the resistance of the pin to bending (Huiskes et al. 1985). I could not reduce the pin working length due to issues of

soft-tissue interference and therefore increasing the pin diameter was chosen. The resistance to bending of a cylindrical structure is dictated by the following equation; $3\pi d^4 E/64L^3$, where d is the pin diameter and L is the pin working length (distance from the edge of the bone to the fixator block) and E is the modulus of elasticity (Huiskes 1986). To that end, a small increase in pin diameter will give a large increase in bending resistance (to the forth power), which should reduce the loads and strains at the pin-bone interface. A threaded 1.4mm trochar tipped 316LVM stainless steel Kirschner wires, with a 3 point 45 degree trochar (Veterinary Instrumentation, UK), was chosen (Figure 4.9b), and the pre-drill hole was increased to 1.0mm. The core diameter from cutting a thread into this size pin was 1.155mm, ensuring radial preload generation. The 1.4mm diameter pin was also deemed around the maximum size appropriate relative to the size of the femur, as it was approximate 30% of the bone diameter. The use of hand tools and placement of trochar tipped threaded 1.4mm pins resulting in no radiographic or clinical evidence of pin loosening throughout the study period of five weeks (n=6) (Figure 4.9 c)

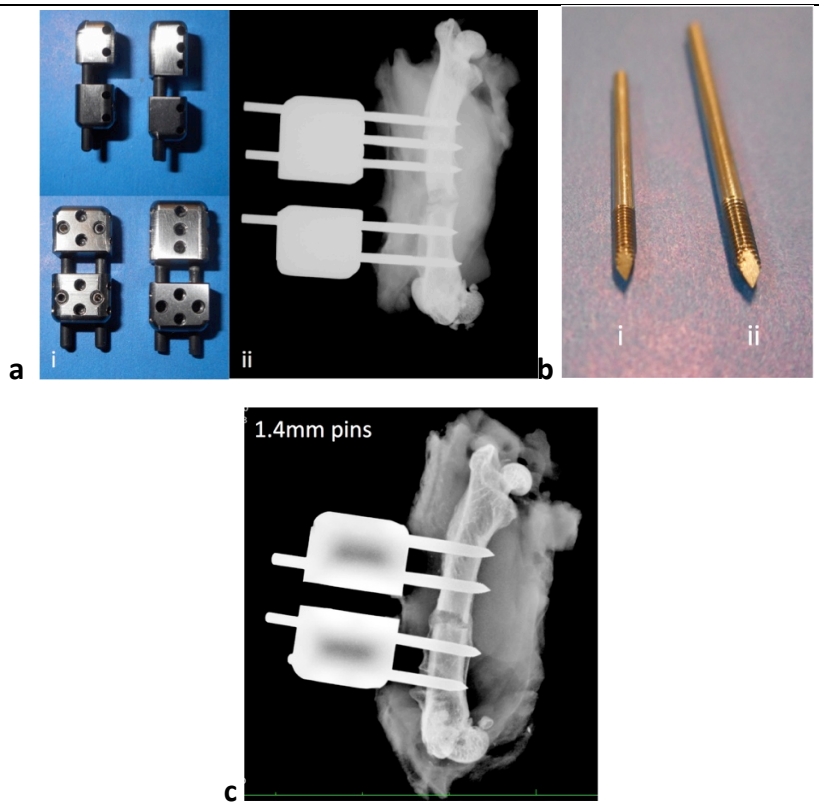

Figure 4.9: a) (i) Photograph of the 3:2 proximal pin fixator next to the standard 2:2 fixator. (ii) Radiograph taken five weeks post surgery using the 3:2 fixator system with 1.25mm diameter pins. b) Photograph showing the 1.25mm sharp trochar pin (i) next to the 1.4mm sharp trochar pin (ii). c) Radiograph taken five weeks post-operatively showing no evidence of pin loosening with the 1.4mm fixator pins.

4.2.6 Surgical summary

All procedures on live animals were performed under general anesthesia using aseptic techniques, in accordance with U.K. Government Home Office regulations. The procedure is summarised in figure 4.10. Briefly, the left hindlimb was disinfected and draped. A lateral femoral approach was made, with a 2cm skin incision followed by incising the external fascia along the cranial edge of the biceps femoris. The biceps femoris was bluntly separated from the tensor fascia lata along their adjacent planes and then elevated along the craniolateral aspect of the femur using a freer elevator. The distal extreme of the greater trochanter was used as a landmark for consistent positioning of the jig-guide over the craniolateral femur, which was then held in place using a precision micro-ratchet forceps (Kyon, Switzerland). The most proximal hole was loaded with a drill insert-sleeve. A 1.0mm HSS drill bit, was loaded into a spiral push drill (Rolson, UK) and used to drill both cortices whilst sterile saline coolant was applied. A 0.8mm temporary stabilising pin was then inserted (Figure 4.11a), and the distal hole was drilled, followed by the placement of a short (23mm) 1.4mm pin, using the pin insert-sleeve in the guide jig with a miniature hand chuck (162A Pin Vice, 0-0.040, Starrett, USA). Pins were placed bi-cortically, ensuring that the entire trochar tip had passed the trans cortical edge. This was checked using a small curved edge Mosquito haemostat and is of importance as bicortical pin placement significantly improves pin holding power (Oliphant et al. 2013). The remaining pins were placed as described, such that there was a short pin (23mm) next to a long pin (28mm) in the proximal pair and the distal pair, to facilitate the instrumentation. The cranial femoral skin was retracted caudally over the pins and a small pin tract was made using a no. 11 scalpel blade to allow the pin to pass through the skin. A custom precision fork-shaped spacer (Figure 4.11c) was placed to ensure a fixed distance between the cis cortex and connecting blocks of 9mm.

The fixator was then attached and the pin locking grub screws tightened. A mid-diaphyseal femoral osteotomy with no periosteal stripping was made using a diamond tipped handsaw, whilst applying sterile saline coolant/lubricant. The distal fixator block had its grub screws loosened and then the block was slid distally to distract the osteotomy gap. A precision spacer of the desired osteotomy size (Figure 4.11b) was placed within the osteotomy and then the osteotomy was closed down onto it and the distal block grub screws re-tightened. The biceps femoris was closed over the osteotomy with a single horizontal mattress suture (1.5M PDS II, Ethicon, UK), and the skin was closed with intradermal continuous suture (1.5M Monocryl, Ethicon, UK). Activity was unrestricted post surgery. In chapter 5, 1.0mm, 1.5mm and 2.0mm gaps were evaluated for their healing.

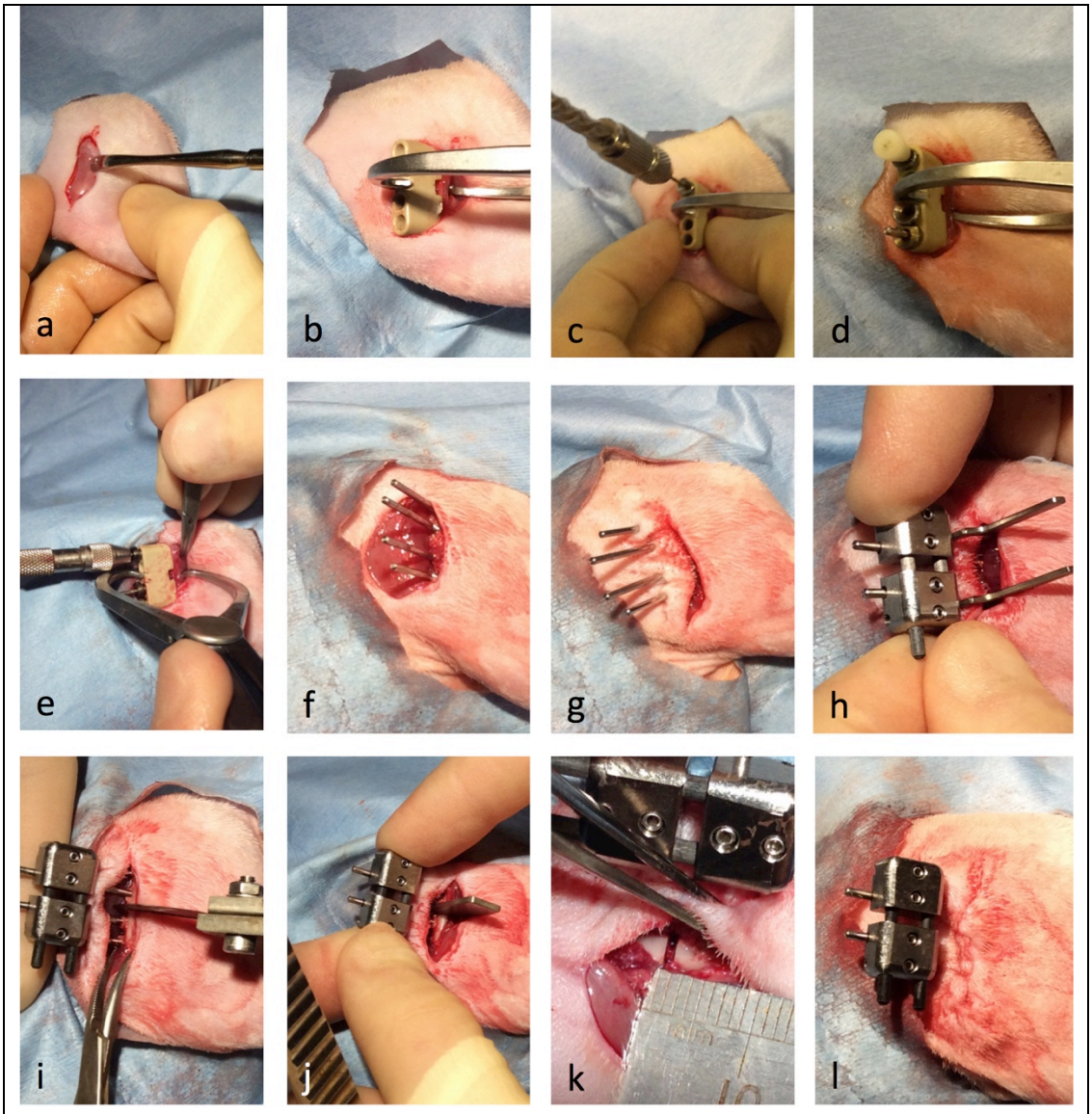

Figure 4.10: Photographs showing the temporal sequence of placement of the Stanmore micro fixator to achieve a 1mm osteotomy. a) Skin incision exposes boundary of the biceps femoris to tensor fascia lata. b) Placement of drill and pin guide jig, retained with micro-ratchet forceps. c) Proximal drill sleeve and drill bit, with spiral push drill. d) Proximal stabilising pin in place and distal fixator pin placed, with sleeves remaining. e) Checking the full trochar has penetrated the trans cortex. f) Four fixator pins placed – short pins proximal and distal, long pins centrally. g) Fixator pin tracts made and skin placed over pins. h) Fixator positioned along pins and spaced by precision spacer from bone. i) Cutting the mid-diaphyseal osteotomy with a diamond tipped handsaw. j) Setting the desired osteotomy distance using the precision titanium spacer. k) Checking the osteotomy size. l) Surgical incision closed with intradermal continuous suture.

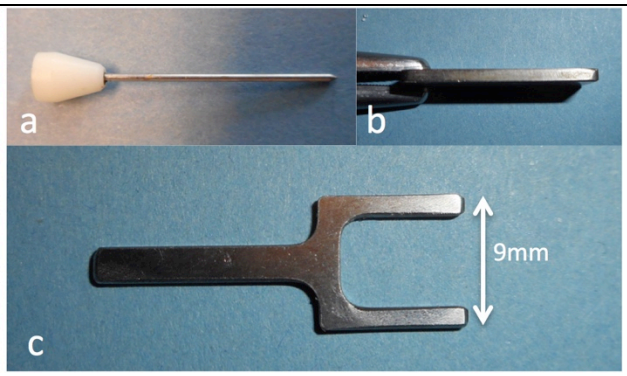

Figure 4.11: Photographs showing the new tools developed for the procedure. a) The temporary stabilising pin, placed after the first drill hole is made, to prevent jig-guide movement. b) The precision spacer temporarily placed within the osteotomy gap. c) The pin working length spacer, which accommodates the skin and sat between the inner aspect of the connecting block and the outer aspect of the bone.

4.2.7 PEEK scanning fixator blocks for microCT

After culling and formalin fixing, the femurs were microCT scanned. To reduce beam hardening artifact interference associated with the titanium connecting blocks, a PEEK scanning fixator was also designed (Figure 4.12). This could be placed between the bone and the titanium fixator prior to removal of the titanium fixator for scanning. This fixator also had a sliding mechanism such that it could accommodate the differing gaps between the proximal and distal pin pairs dictated by the size of the osteotomy created at surgery.

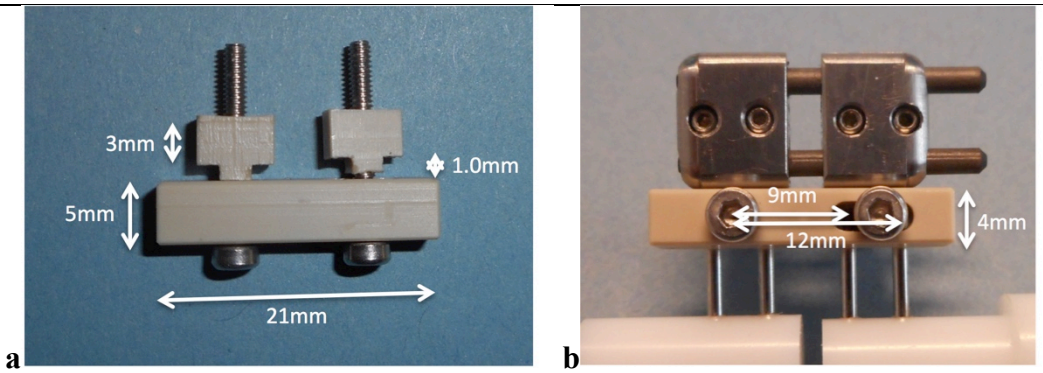

Figure 4.12: a) Photograph showing the cranial surface of the scanning fixator. The 'nut' component associated with the bolt threads can be rotated to pass in between the existing fixator pins, and then be rotated back to allow it to compress against the pins as the M2 stainless steel hex bolts are tightened. b) Photograph showing the scanning fixator in place below the titanium fixator. Note the ovoid hole on the right hand side, which accommodated for the differing gap sizes between the proximal and distal pin pair.

4.3 CONCLUSION

The revised jig system improved asepsis and allowed for a rapid and reliable surgical procedure. The 9mm pin working length and chamfered block edges significantly reduced soft-tissue interference. The reduced pre-drill size relative to pin size and utilisation of a cutting trochar tip improved initial pin stability. Using a spiral twist drill, applying irrigation and the increased pin diameter reduced late pin loosening attributed to osteolysis. Due to ethical consideration and 3Rs, it was not appropriate to evaluate these differences individually as the aim was to reduce pin loosening, rather than determine which change was most influential. The PEEK scanning fixators successfully reduced the microCT beam-hardening artifact.

Overall, the revisions made here improved the fixator system, increased its repeatability and reduced complications. In chapter 5 the redesigned fixator was used to determine the preferred gap size to impair healing for subsequent evaluation of endogenous mobilisation of stem and progenitor cells in chapter 6.

CHAPTER 5: Evaluation of Gap Size & Tissue Formation

5.1 INTRODUCTION: Goldilocks scenario

The influence of mechanical stability on fracture healing has been extensively investigated (Betts & Müller 2014). Numerous animal models have altered fracture rigidity to study the mechanisms underlying fracture healing, be it intramembranous ossification, endochondral ossification, or extreme nonunion models (Garcia et al. 2013; Mills & Simpson 2012). Previous work using the prototype Stanmore micro fixator has shown guaranteed union by five weeks with a 0.5mm osteotomy gap and non-union with a 3.0mm osteotomy (Harrison et al. 2003). This model demonstrated the influence of a critical sized defect, which is defined as the "minimum amount of bone loss that will not heal by new bone formation over an animal's lifetime" (Schmitz & Hollinger 1986). Key's hypothesis proposed that a segment 1.5x the diaphyseal diameter would lead to non-union (Key 1934). Toombs evaluated this in cats and determined that 1.5x was an overestimation (Toombs et al. 1985), although there may be species differences in healing capacity. The recommended defect size is unknown for rodents (Mills & Simpson 2012), however, the rats used in Harrison's study had an estimated diaphyseal diameter of 3-4mm and a 3mm gap resulted non-union (Harrison et al. 2003), implying the critical size may be smaller in rats than proposed by Key.

To evaluate endogenous mobilisation strategies effectively in later chapters, I was looking for a compromised healing environment; one not so compromised that it would be impossible to show an effect of intervention, but likewise not so competent at healing that any improvement would be lost; my so called 'Goldilocks scenario'. It is expected that this would be approximately 1.5mm, as 0.5mm and 3mm gave the extremes of union and non-union, however, this needed to be proven. In this chapter, I aimed to evaluate the biomechanical effect of osteotomy gap size between those two extremes and to map this against the associated interfragmentary strain (IFS). Perren's theory of IFS predicts that if IFS falls to levels where cartilage can form (<10%) then soft callus will develop, and if <2%, bone can form and hence 'hard callus' should follow. If however, the IFS was not initially or subsequently low enough, fracture union would fail (Perren 1979; Perren 2004). Perren's theory would also predict that for a given interfragmentary movement, the bigger the gap the better the predicted healing due to reduced IFS.

Question: Could the biomechanical environment between union and non-union be manipulated to identify a compromised healing environment to evaluate endogenous mobilisation strategies for fracture healing?

Hypothesis – *increasing gap size from 1.0 to 1.5mm to 2.0mm will decrease IFS, reduce construct stiffness and hence improve bone formation within the gap*.

5.2 MATERIALS & METHODS

5.2.1 Biomechanical assessment of interfragmentary strain & construct stiffness

The fixator was placed as per chapter 4 (4.2.6), on the femora of cadaveric 12-14 week old Wistar rats (n=4). Femora with the fixator still attached were then disarticulated at the hip and stifle and stripped of soft-tissue attachments. An orthogonal (lateral to medially orientated) 0.8mm bicortical hole was drilled between the two proximal and two distal fixator pins. A microminiature differential variable reluctance transducer (accuracy 0.001mm) (Lord MicroStrain, model 6101-0200) was then inserted and fixed in position using cyanoacrylate glue, to quantify fracture movement (Figure 5.1). Femurs were biomechanically tested using a materials testing machine (Zwick Roell 5T, UK). They were mounted in an axial loading jig with the femoral condyles centred over the lower mount and the upper mount was centred over the femoral head to simulate the physiological loading axis of the femur along its mechanical axis (Figure 5.1b). This design also effectively tested the entire construct of fixator and bone as a single unit, as it would be clinically.

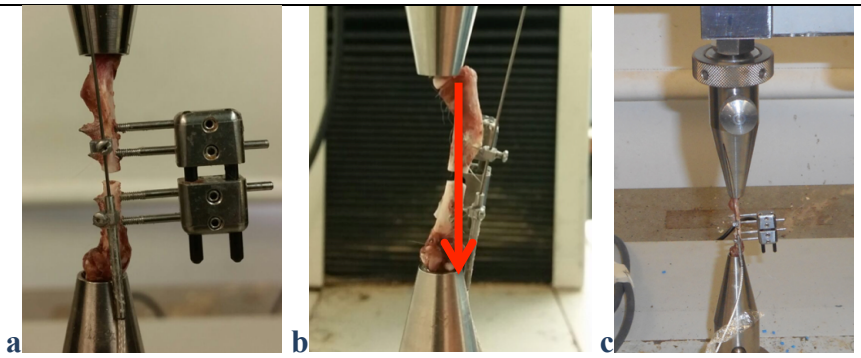

Figure 5.1: Photographs showing the set-up for the biomechanical analysis to determine the IFS and stiffness of the fixator construct. a) Lateral aspect of the femur with the fixator and microdisplacement sensor in place b) The load was applied from the femoral head to the femoral condyles to simulate physiological loading along the mechanical axis. In the orthogonal projection a LORD micro displacement sensor was attached to provide a highly accurate measure of displacement at the level of the osoteotmy. c) Zoomed out image of the test apparatus.

A calculated resting load for quadrupedal animals of 60% weight carriage to forelimbs and 40% to hindlimbs (Lee et al. 1999) gave 20% per hindlimb. A maximum weight of 300g was seen in the *in vivo* study and therefore peak-walking load was assumed to be 0.6N. A single cycle non-destructive test was performed, with a preconditioning load of 0.5N, followed with loading to a maximum of 10N in compression at 5mm/min, sampling rate of 50Hz. The first cycle was disregarded and then four repeats were performed per gap size, per sample. The microsensor millivoltage output was recorded and the difference pre and at peak load was determined. This was then converted into a displacement according to manufacturers calibration equation. Fixator–bone construct stiffness was determined from the load vs. displacement (deformation) graphs obtained from TestXpert software (Zwick, Roell, UK). A linear regression line (r^2) was calculated for the linear portion and r^2 >0.99 was considered appropriate for the linear elastic region. The gradient (m) was determined based on a y=mx+c equation and gave the stiffness (Figure 5.2).

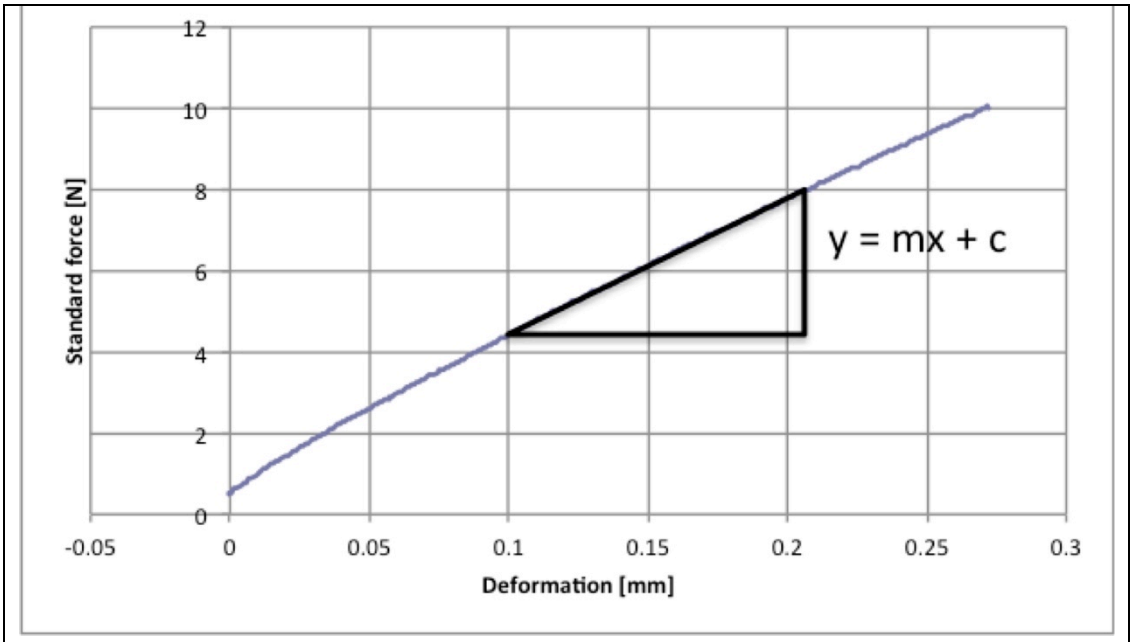

Figure 5.2: A typical load displacement (deformation) graph. The gradient of the linear portion of the curve provided the construct stiffness.

Three gap sizes were evaluated per specimen; 1.0mm, 1.5mm and 2.0mm. The distal fixator connecting block was loosened to allow insertion of the precision titanium spacer and then tightened again. The gap was then checked a second time prior to loading and again between each repeat by 'offering-up' the spacer to the gap. Care was taken to ensure the gap was even across the width of the osteotomy.

5.2.2 In vivo evaluation of osteotomy gap size on fracture healing

As previously described in chapter 4 (4.2.6), the modified Stanmore micro fixator was placed in 12-14 week-old female wistar rats (230-300g). Three groups were assessed: 1.0mm (n=5), 1.5mm (n=7), and 2.0mm gap (n=6). Activity was unrestricted post surgery.

MicroCT & radiography

After five weeks, the left femur including the fixator was retrieved from the sacrificed rats. A radiolucent PEEK fixator block was connected externally to the fixator pins after careful removal of the skin and surrounding soft-tissues. Without disturbing the fracture callus, the titanium block fixator was then removed to reduce beam-hardening artifact generated from the interaction of the X-ray beam and the metallic implant on the microCT scans. Samples were fixed in 10% buffered formaldehyde for up to three days. The formalin fixed samples were wrapped in cling film to prevent dehydration and mounted into a sample holder for microCT scanning. Samples were scanned using a Bruker Skyscan 1172 microtomograph machine (Bruker, Belgium), at 60KV, 167uA with a 0.5mm aluminum filter. A rotation step of 0.5 degrees, without frame averaging, and an image pixel size of 4.89um was used. A single capture image was taken with the image intensification 'scout' prior to scanning, for 2D radiographic assessment of the osteotomy union. Radiographic scouts were assessed for bone union in a randomised and blinded manner and then assigned to one of the three categories (Figure 5.3):

- *Non-union,* where there was no mineralised tissue bridging between the ends of the osteotomy
- *Partial-union,* where there was significant bone formation, however a radiolucent line remained between the proximal and distal segments
- *Union,* where no gap between bone ends was visible

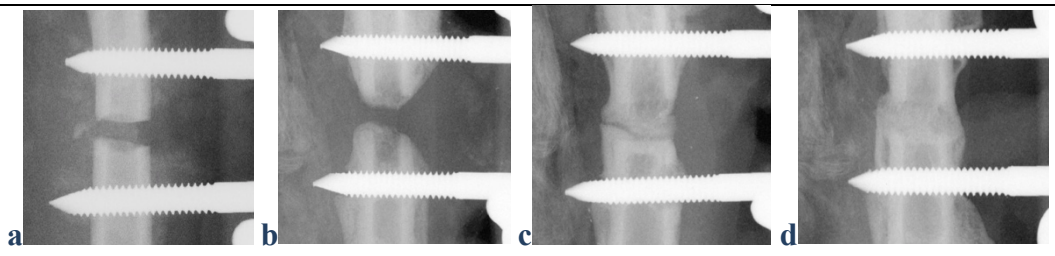

Figure 5.3: Plain radiographs showing a) 1mm osteotomy day 0. b) Non-union. c) Partial-union. d) Union. Images b-d were taken at five weeks post 2.0mm osteotomy.

MicroCT scans were reconstructed using NRecon (Bruker, Belgium) with smoothing = 2, ring artifact reduction = 12% and beam hardening artifact reduction = 41%. Analysis was performed using CTAn (Bruker, Belgium). Using the measuring tool, the centre point of the osteotomy was determined and the transverse slice at that point was selected as the reference slice. If the alignment of the osteotomy or the orientation of the osteotomy relative to the transverse slice section on the microCT were not identical, then analysis of the full width of the osteotomy could be misleading due to potential inclusion of cortical bone edges from the original osteotomy. To avoid this and to allow comparison between different gap sizes the central 60% of the osteotomy gap (Table 5.1), i.e. only new bone formation within the osteotomy was analysed (Figure 5.4 gives representative examples). This percentage was reached after trial and error. Due to the differing gap sizes between the groups and in order to determine a uniform measure of tissue healing, a comparison index was calculated by dividing the overall output parameters by the number of slices analysed.

Gap Size (mm)	Number of Slices (slice thickness 5um)	60% Osteotomy Gap Distance (mm)	60% Osteotomy Gap Slice Number
1.0	200	0.6	120
1.5	300	0.9	180
2.0	400	1.2	240

Table 5.1: The number of slices analysed and the effective osteotomy gap proportion analysed by microCT, to give a proportional analysis for direct comparison between groups.

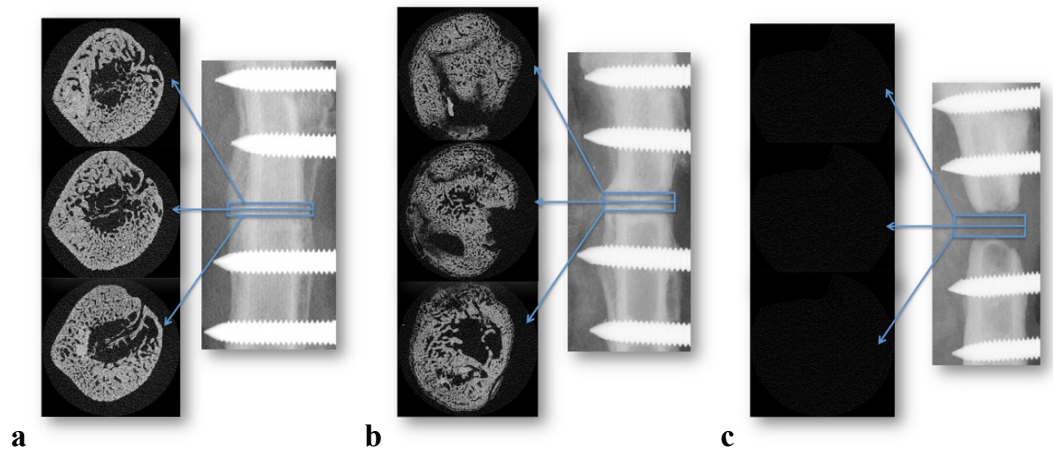

Figure 5.4: Radiographic and computed tomographic images showing microCT analysis of the 60% osteotomy gap window for a) 1.0mm osteotomy. b) 1.5mm osteotomy. c) 2.0mm osteotomy. A representative transverse slice is shown from the most proximal, mid and distal region of analysis.

Slices were filtered with a Gaussian blur (2d Space), square Kernel radius = 1 algorithm, then thresholded with a lower grey threshold of 100, upper grey threshold of 255. The callus was isolated using a 2D ROI shrink wrap stretching over holes <40 pixels, despeckled <150 voxels and then 3D analysis was performed (Campbell & Sophocleous 2014) with output into Excel (Microsoft, USA).

Histomorphometric analysis of callus

After microCT analysis the bones were decalcified in a solution of ethylenediaminetetraacetic acid (EDTA, Sigma Aldrich, UK), at 37°C, with constant gentle agitation for four weeks. Decalcification was confirmed radiographically and then specimens were sequentially dehydrated for 24 hours at the following alcohol concentrations: 50%, 70%, 90%, 100%, followed by de-fatting with chloroform for 48 hours and then embedded into wax, with the fixator pins orthogonal to the facing surface of the block (Figure 5.5a). Fixator blocks and pins were removed once the wax had set and a sledge microtome (ThermoFisher Scientific, UK) was used to make 5µm thick slices (Figure 5.5b). The alignment of the blocks within the microtome was altered as necessary to ensure a central sagittal slice through the femur. The position of a mid-sagittal section through the fracture gap was assessed using the fixator pin tract holes; at the mid position, the fixator pin tract holes for both the proximal and distal segment were in the centre of the femoral medullary cavity with a section of the cortical bone spaced equally from the pin holes.

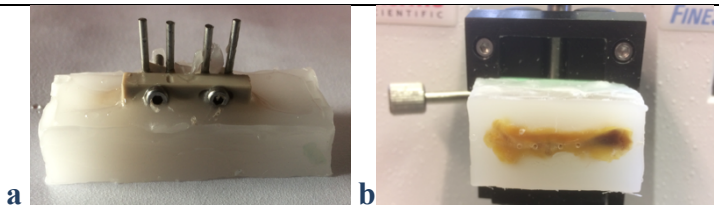

Figure 5.5: Photographs showing the post-mortem processing after limb removal at five weeks. a) Bone embedded ready for removal of fixator pins and blocks. b) Block being cut in the microtome.

Wax slices were mounted onto positively charged glass slides (X-tra, Leica biosystems, UK) and de-waxed twice in xylene, followed by two changes of 100% alcohol, prior to a hydration series of 90%, 70% and 50% alcohol. After hydration, samples were stained with haematoxylin nuclear stain for five minutes (Sigma-Aldrich, UK). Excess stain was removed by gentle washing with water for five minutes. Slides were counterstained in 1% eosin (Sigma-Aldrich, UK) for four minutes and then washed and dehydrated in increasing concentrations of alcohol. Slides were then cleaned in xylene and mounted under 40mm coverslips using Pertex Mounting Medium (CellPath plc, UK). Slides were observed under a

light microscope (KS-300 Zeiss, UK). All slides were imaged and saved as Tiff files. Histomorphometric analysis was performed on 1x and 2.5x magnified images (Figure 5.6). Four mid sagittal sections were made and the most central two were stained and the best was analysed.

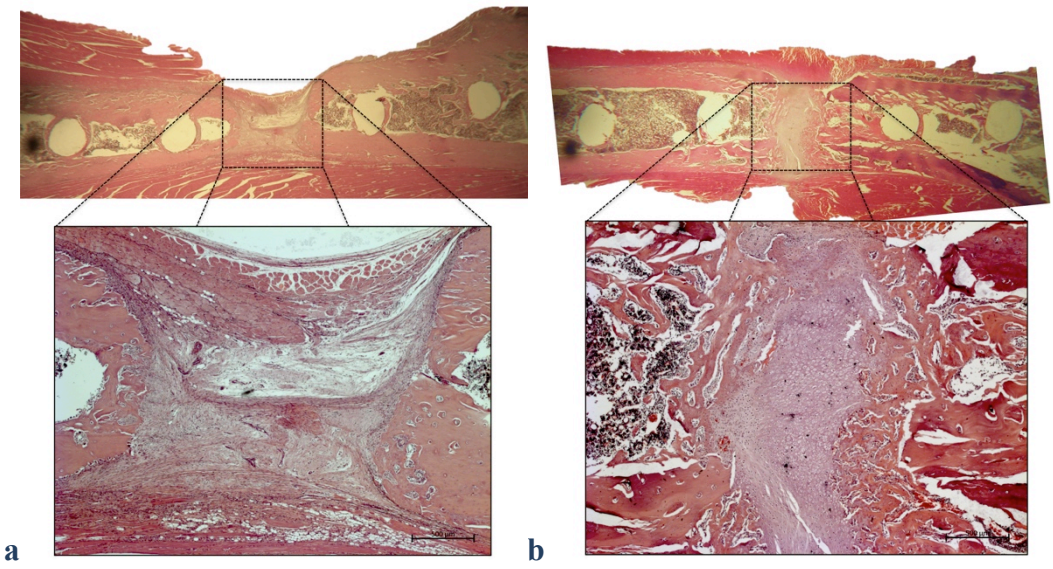

Figure 5.6: Histology images of the osteotomy gap. a) Shows a 1.5mm gap non-union. b) 1.5mm gap partial union. Both images are shown at x1 magnification with a central region for detailed histomorphometric analysis at x2.5.

As higher magnification images did not allow full visualisation of the callus, at 1x magnification, the total area between the two innermost pin tract holes and areas of fibrous or cartilaginous tissue were all measured using Image J (NIH, USA) (Figure 5.7a). On the digitised scaled images, the area of interest was delineated using the drawing tool. The measure function was then used to give an area measurement based on the square pixels present in the delineated region. This method was chosen as the image size and megapixels (3.0x10^6) were consistent in all x1 magnification images and it was not possible to have a scaled graticule incorporated into the images due to the equipment. The areas measured provided a useful comparison between samples in this study, but could not be used as an index to compare with other studies.

Histomorphometric analysis at 2.5x magnification was performed on the most central slice, using a line-intercept method with a grid scaled to the graticule and drawn using powerpoint (Microsoft, USA). The grid covered the entire visual field from top to bottom and was centered over the osteotomy; its width was equivalent to the original osteotomy (1.0, 1.5 or 2.0mm as appropriate). Grid ‘density’ was consistent between the different group osteotomy

sizes, such that the 1.0mm gap had 75 intersections, 1.5mm gap had 120 intersections and the 2.0mm gap had 165 intersections. Grid squares were 160um in both directions for all groups. Intersections were then scored as bone, cartilage, fibrous tissue, vascular (identified by red blood cells not within matrix) or void.

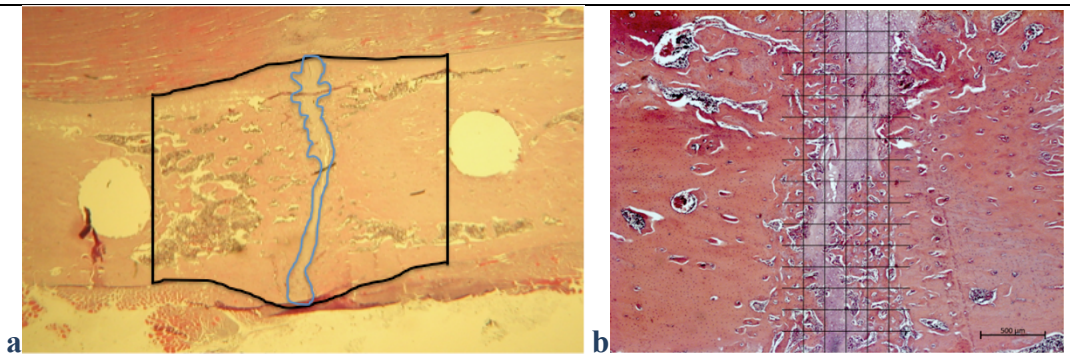

Figure 5.7: Histology images. a) Examples of 1x area analysis of a central sagittal slice. Total callus area was measured between the innermost margins of the fixator pin holes on all samples to provide a consistent landmark. This was possible as the surgical fixator guide gave a consistent distance between the two innermost pins and the edge of the osteotomy. The blue outline delineates a central region of cartilaginous tissue. b) 2.5x image, with a grid width equal to the original gap size, in this case 1mm. Intersection points were then scored for the tissue formed.

5.2.3 Statistical analysis

Due to the relatively small group sizes (n<9), non-parametric tests were performed to compare groups including Mann-Whitney U (MWU) and Kruskal-Wallis (KW) as appropriate. Significance was set at p<0.05 and tests were analysed with SPSS version 24 (IBM, Chicago, USA). Fisher exact test was performed to look for differences between radiographic fracture union (GraphPad Prism v6.00, USA).

5.3 RESULTS

5.3.1 Mechanical analysis

The mean±SD stiffness of the four femoral-ESF constructs for the 1.0, 1.5 and 2.0mm gaps were 32.6±5.4, 32.5±2.4, and 32.4±8.3 N/mm; the gap size over the ranges tested had no impact on the construct stiffness (p=0.779), however gap size did significantly reduce the IFS in the gap (p=0.013), with 1.0 gap having a significantly higher IFS than the 2.0mm gap (p=0.029). The mean±SD % IFS for the 1.0, 1.5 and 2.0mm gaps were 11.2±1.3, 8.4±1.5 and 6.1±1.2% respectively. The results for the individual femurs are summarized in table 5.2 and figure 5.8 and figure 5.9. The trends were consistent between femurs, however there were

differences in the absolute values, potentially relating to the position of the fixator or the size of the femur.

		Femur 1	Femur 2	Femur 3	Femur 4	Group mean±SD
1.0mm Gap	**Strain (%)**	12.9±0.3	11.4±0.7	9.7±0.5	10.9±0.1	11.2±1.2
	Stiffness (N/mm)	39.8±0.8	31.7±1.0	26.7±1.1	32.2±0.6	32.5±4.6
1.5mm Gap	**Strain (%)**	10.3±0.3	8.3±0.2	6.8±0.1	8.0±0.2	8.3±1.2
	Stiffness (N/mm)	29.4±2.7	34.9±0.9	33.7±0.1	31.8±0.2	32.5±2.4
2.0mm Gap	**Strain (%)**	7.9±0.1	5.7±0.4	5.5±0.1	5.3±0.3	6.0±1.1
	Stiffness (N/mm)	24.3±2.0	31.5±1.2	29.7±0.2	43.9±0.8	32.2±7.3

Table 5.2: Summary stiffness (N/mm) and strain (percentage change) of different femurs with different gap sizes. All values are the mean ± standard deviation

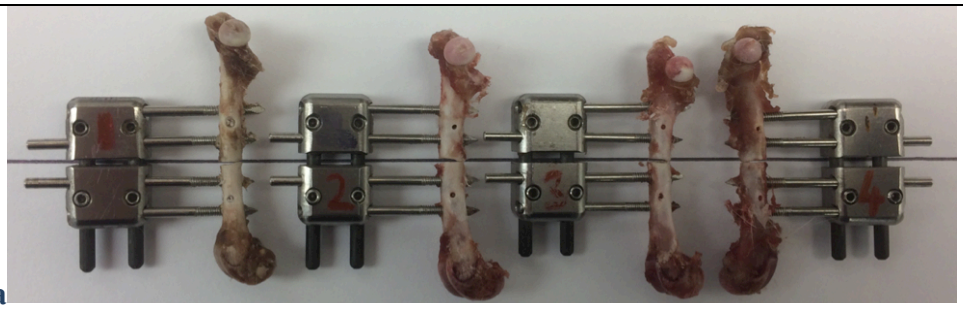

a

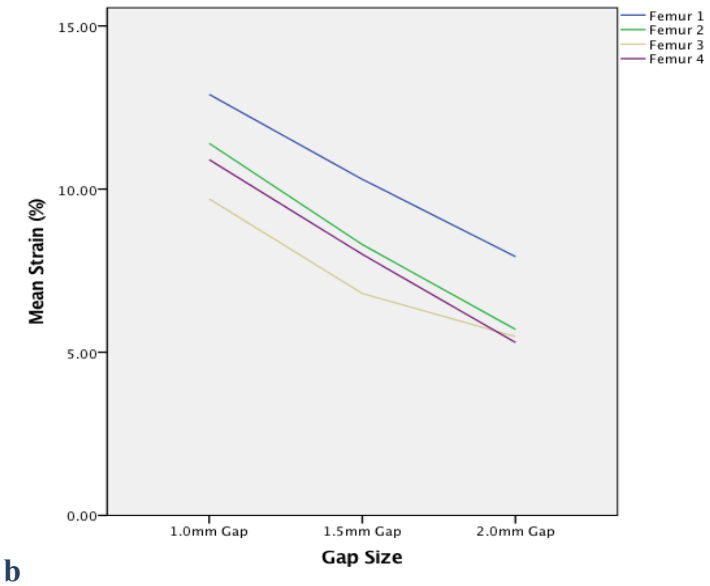

b

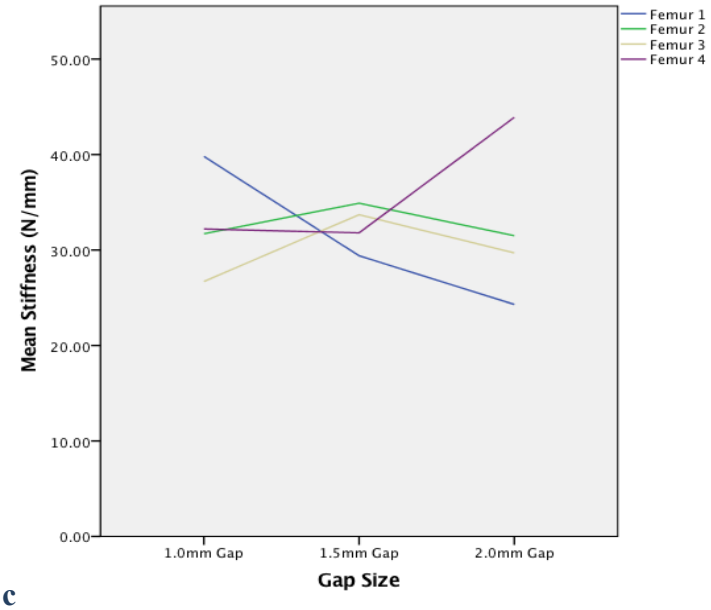

c

Figure 5.8: a) Photograph of the four femurs biomechanically tested showing the position of the fixator (numbered femur 1-4 from left to right). b) Line graph showing the mean IFS as the gap increased for each femur. c) Line graphs showing the mean stiffness (N/mm) as the gap size increased for each femur. Notably, all trends were consistent despite the variations in fixator position and femoral length, with the higher IFS being measured on femur 1 and lowest on femur 3. This could relate to individual bone variations, or the positioning of the fixator / osteotomy on the bone, from proximal to distal, potentially influencing the bending forces.

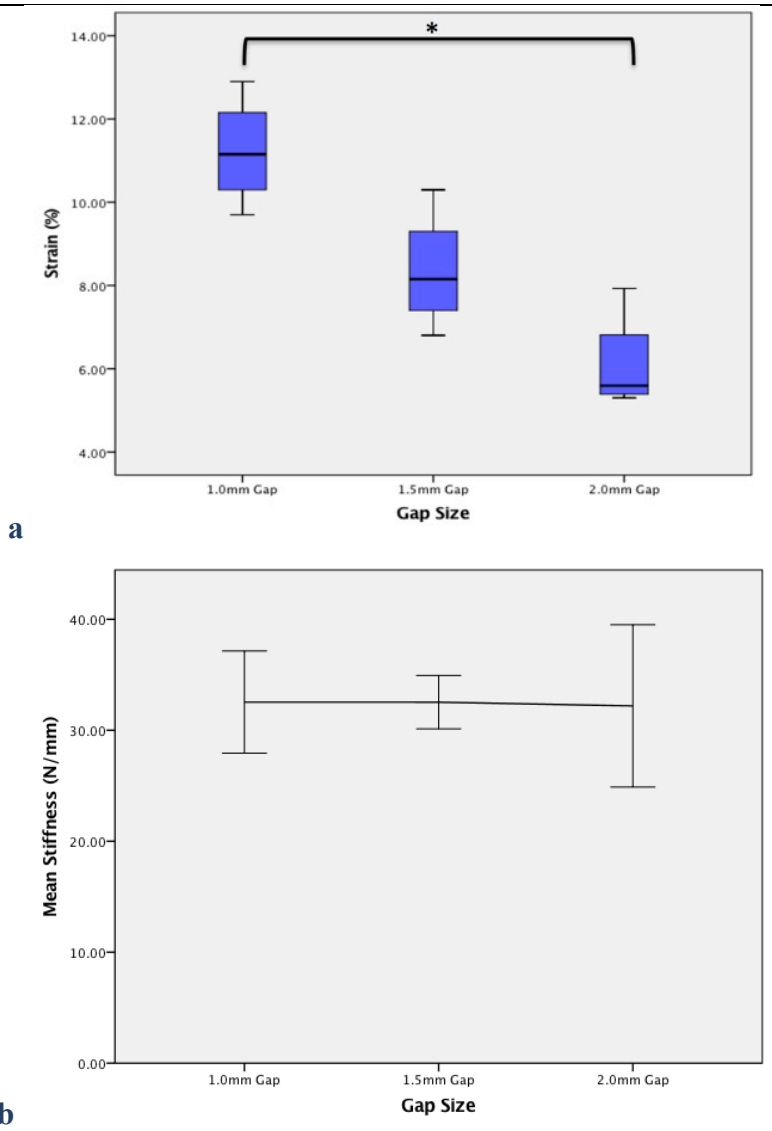

Figure 5.9: a) Boxplot plot showing the percentage IFS was significantly affected by gap size. (* p=0.029). b) Line graph of mean±SD construct stiffness (N/mm), which was unaffected by gap size (p=0.779).

5.3.2 Radiographic assessment

As the gap size increased there was an increase in non-union and partial-union development and a concomitant decrease in union rates, with the non-union rate more than doubling (Table 5.3). Fisher exact contingency tables comparison of union vs non-union combined with partial union did not show a significant effect of gap size (GraphPad Prism v6.00, USA). Some samples also appeared to have a tendency towards increased periosteal callus on the caudomedial aspect of the bone, i.e. on the opposite side to the fixator, which is probably the region experiencing the greatest compression and least tension.

Gap Size (mm)	Non-Union	Partial Union	Union
1.0	1/5 (20%)	1/5 (20%)	3/5 (60%)
1.5	3/7 (43%)	2/7 (29%)	2/7 (29%)
2.0	3/6 (50%)	2/6 (33%)	1/6 (17%)

Table 5.3: Radiographic assessment of degree of union from microCT scout image shown in absolute numbers and as a group percentage.

5.3.3 MicroCT analysis of osteotomy tissue formation

The 1.0mm gap size had approximately 50% greater callus volume per slice (0.069um^3) vs the 2mm gap (0.029um^3), and a higher bone volume per slice (0.035um^3 vs 0.026um^3) (Figure 5.10). Assessment of trabecular thickness was largely similar between groups, although the spacing between the regions of woven bone (trabecular spacing per splice) was greater in the smaller 1.0mm gap with its overall higher total bone volumes. The 1.5 and 2.0mm gaps had similar trabecular spacing, indicating the bone structure was similar but reduced in volume within the bigger gap. The measured trabecular thickness was significantly higher (p=0.048) in the smaller 1.0 gap than the larger 1.5mm gap (0.055±0.01um and 0.044±0.01um), however it increased again when the gap size increased to 2.0mm (0.057±0.02um). Tissue surface area per slice, giving a relative index of callus size, was also significantly higher (p=0.03) in the in the smallest 1.0mm gap (0.41±0.22um^2) than the largest 2.0mm (0.14±0.12um^2) (Figure 5.11a). Although bone volume per slice clearly showed a decreasing trend, significance was not shown (p=0.082) between the 1.0 and 2.0mm gaps. A post-hoc sample size calculation (power = 0.8 and p=0.05) indicated that 14 animals per group were needed to determine a significant difference in bone formation (microCT BV) between the smallest and the largest gap. Full microCT results are in table 5.4. The relationship between IFS and the microCT bone and tissue volumes formed within the callus is shown in figure 5.12.

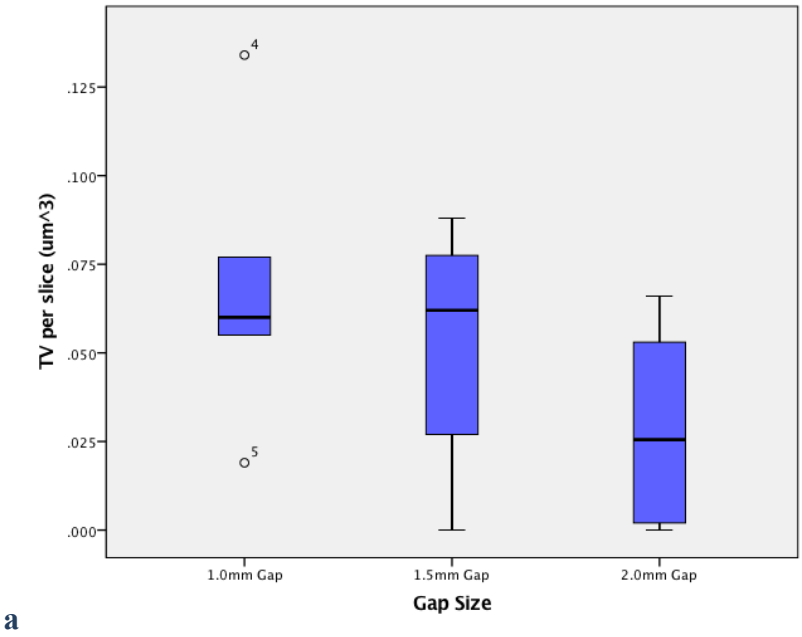

a

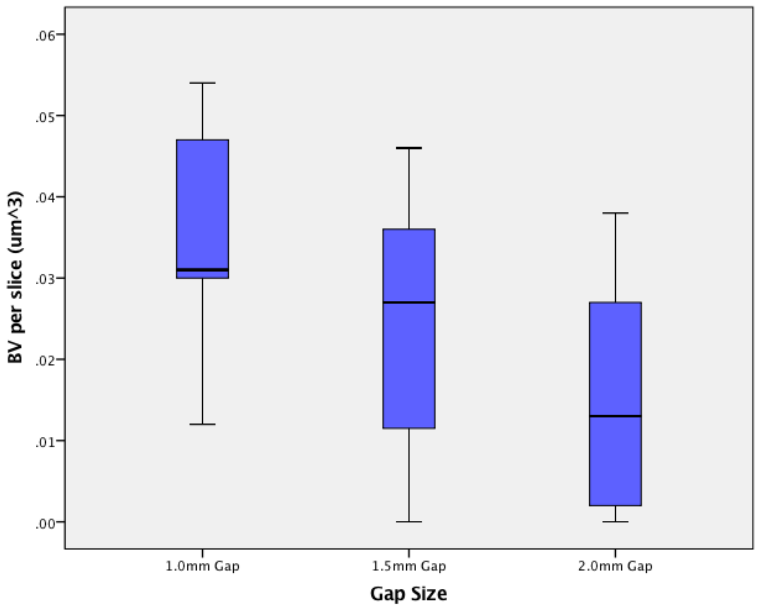

b

Figure 5.10: a) Boxplot showing a sequential reduction in overall callus size (TV per slice). b) Boxplot a reduction in mineralised callus (BV per slice) as the osteotomy gap increased in size.

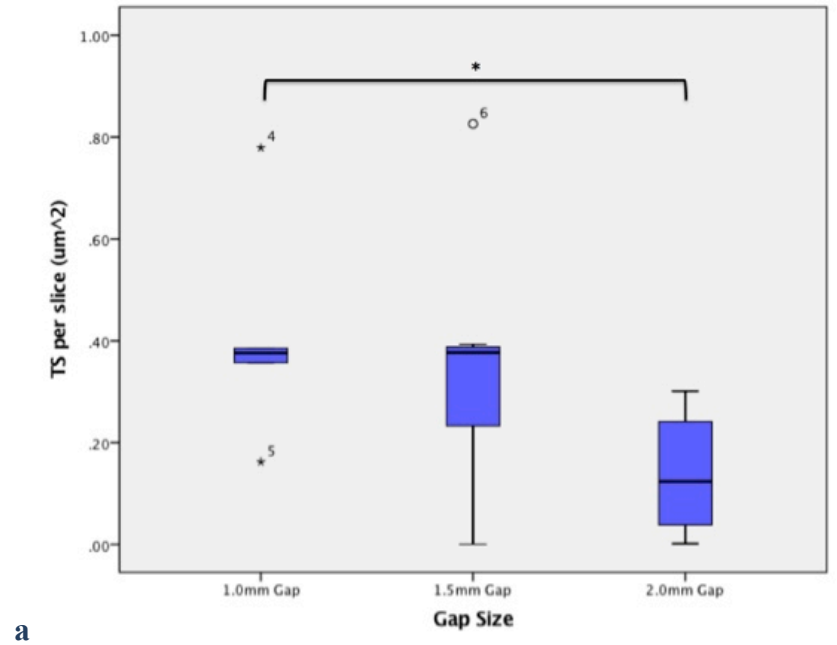

a

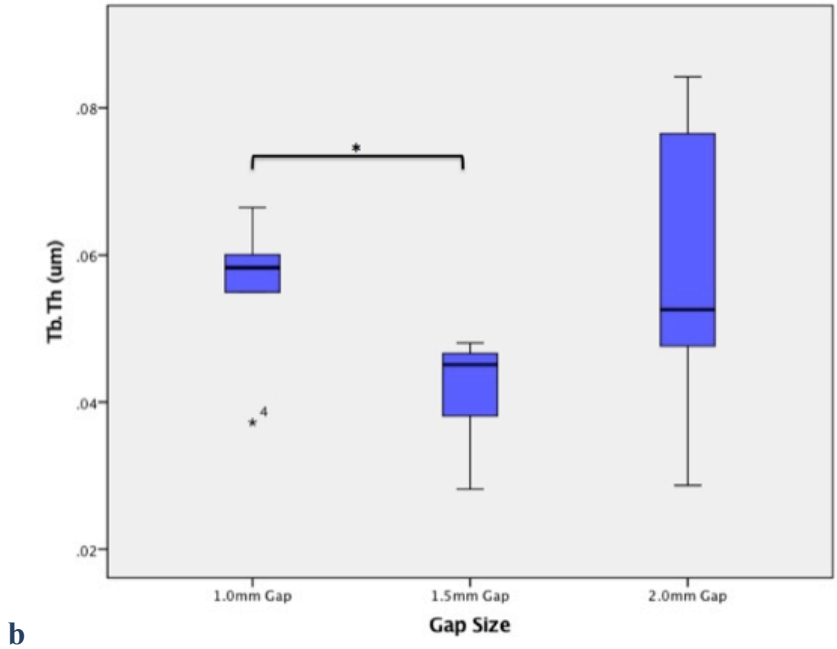

b

Figure 5.11: a) Boxplot showing a significant decrease in tissue surface area (TS) per slice, in the 2.0mm compared with the 1.0mm osteotomy. b) Boxplot showing a reduction in trabecular thickness between the 1.0 and 1.5mm osteotomies (* = $p<0.05$).

	1.0mm Gap	1.5mm Gap	2.0mm Gap
TV per slice (um^3)	0.07±0.04	0.05±0.03	0.03±0.03
BV per slice (um^3)	0.04±0.02	0.02±0.02	0.02±0.02
BV/TV (%)	54.25±9.38	53.79±20.82	66.39±15.37
TS per slice (um^2)	0.41±0.23	0.35±0.25	0.14±0.12
BS per slice (um^2)	2.09±1.62	1.81±1.22	0.90±0.94
Tb.Th (um)	0.06±0.01	0.04±0.01	0.06±0.02
Tb.Sp (um)	0.12±0.05	0.07±0.03	0.07±0.05
Tb.N (1/um)	9.88±0.87	14.10±9.32	13.42±8.26
Total porosity (%)	45.75±9.38	46.22±20.82	33.61±15.37

Table 5.4: Callus morphometry of the central 60% of the osteotomy gap obtained from microCT for the different gap sizes. All values are the mean±SD.

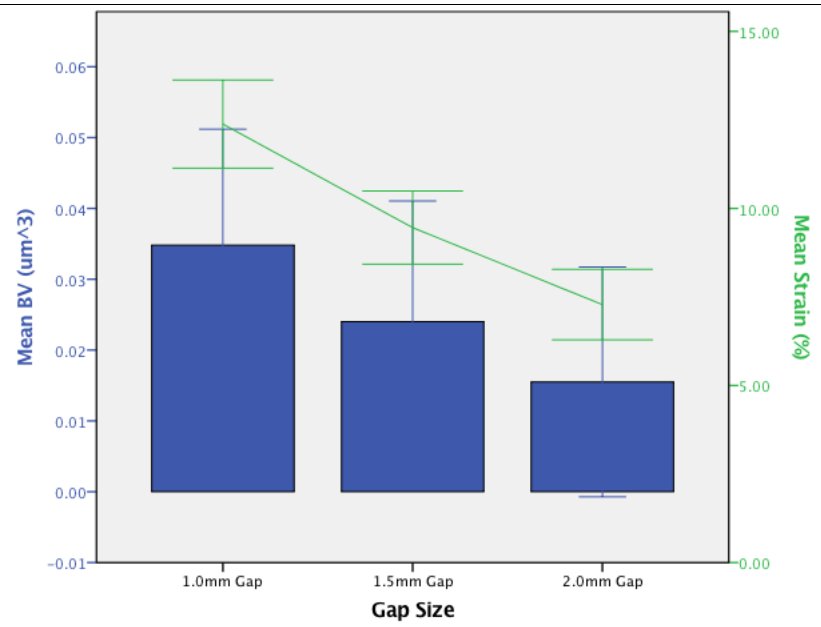

Figure 5.12: Bar chart showing bone volume per slice (BV um^3) overlaid with a line graph of IFS (%), vs gap size showing the relationship between the reducing IFS and reducing bone formation within the osteotomy gap. All values are the mean±SD.

5.3.4 Histomorphometric analysis of osteotomy healing

At the x1 magnification scale, there was a trend for the absolute overall callus area to be larger despite the smaller gap in the 1.0mm vs the 2.0mm gap (Table 5.5 and Figure 5.13). Only combined absolute fibrous-cartilage tissue area was significantly different between

groups (p=0.006), specifically being significantly higher in the 1.5mm group than the 1.0mm group (p=0.01) (Figure 5.13c).

TISSUE AREA	1.0mm Gap	1.5mm Gap	2.0mm Gap
Total callus	324682±99071	351681±89789	264502±88196
Bone	288311±111808	307513±98801	223095±100484
Cartilage	36371±30633	36839±28385	16621±15003
Fibrous	0±0	7329±19390	23786±29598
% TISSUE			
Bone	86.8±13.0	85.9±9.1	82.1±12.9
Cartilage & fibrous combined	13.1±13.0	14.1±9.1	17.9±12.9

Table 5.5: Histomorphometric characteristics of the tissue in between the two innermost fixator pin tract holes at x1 magnification. Absolute measurements are in square pixels. All values are the mean±SD.

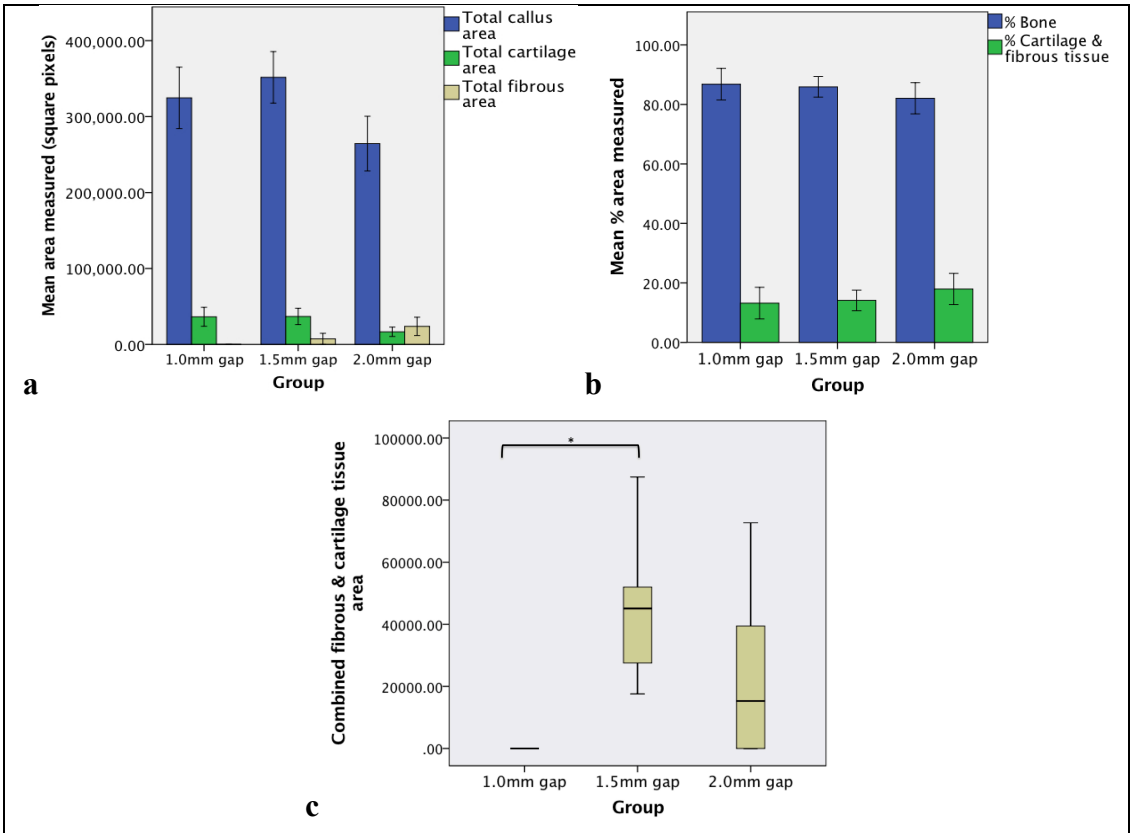

Figure 5.13: Shows the histomorphometric assessment of tissue formation between the two innermost pins at x1 magnification. a) Bar chart showing histomorphometric assessment of the actual area composition, measured in square pixels. Values are mean±SEM. b) Bar chart showing the calculated percentage area composition of the tissue in between the two innermost fixator pin tract holes. Values are the mean±SEM. c) Boxplot showing the area of combined fibrous and cartilage in the callus region as total area measured in square pixels at x1 magnification.

However, trends reflecting the microCT data were seen at the higher magnification of 2.5x. As the gap size increased the % bone within the callus decreased and fibrous tissue increased. Cartilage tissue was highest in the mid sized gap, which may have related to the degree of endochondral ossification present in that gap size; i.e. more cartilage as less bone has formed, however, fibrous tissue was still lower than the biggest gaps. None of these trends were statistically significant (Table 5.6 and Figure 5.14). Summary images of the healing are presented in Figures 5.15-5.18.

% TISSUE	1.0mm Gap	1.5mm Gap	2.0mm Gap
Bone	45.6±33.0	39.1±23.9	23.2±26.6
Cartilage	36.7±22.1	43.1±24.6	37.2±17.9
Fibrous	14.7±30.6	15.3±37.4	36.1±40.8
Vascular	3.0±1.9	2.4±2.0	3.5±3.4
Combined bone & cartilage	82.3±29.0	82.3±36.4	60.4±37.7

Table 5.6: Histomorphometric analysis of tissues formed within the osteotomy gap from line-intercept analysis at x2.5 magnification, expressed as the mean±SD percentage of total area.

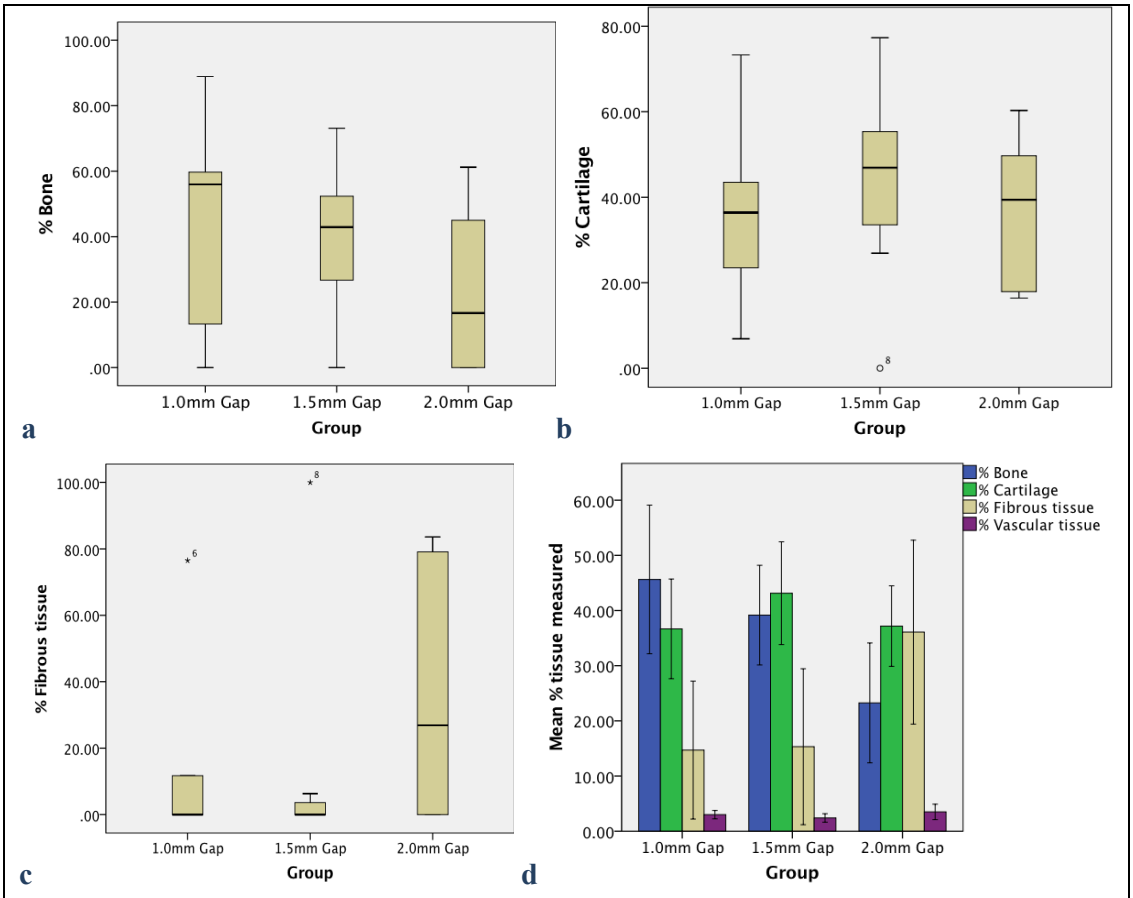

Figure 5.14: Histomorphometric analysis of tissues formed within the osteotomy gap from line-intercept analysis, at x2.5 magnification. a) Boxplot showing percentage bone formed within the osteotomy gaps. b) Boxplot showing percentage cartilage formed within the osteotomy gaps. c) Boxplot showing percentage fibrous tissue formed within the osteotomy gaps. d) Bar chart showing mean±SEM of all tissues formed within the different gap sizes. As the osteotomy gap increased in size, there was a reduction in bone. The percentage cartilage present remained similar, increasing slightly in the mid sized gap, however the increasing gap size was related to progressive increase in fibrous tissue.

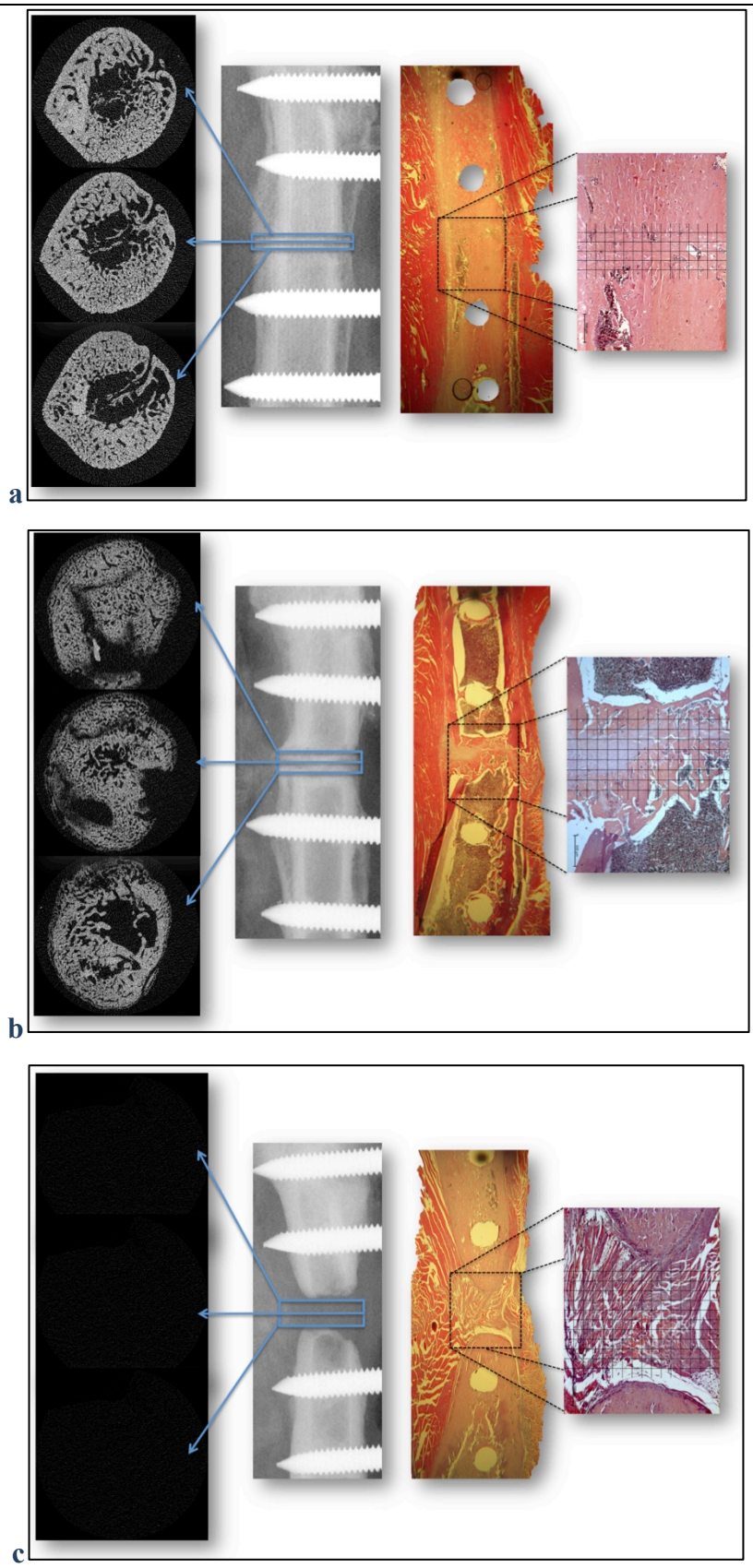

Figure 5.15: Representative imaging including microCT and histology. a) 1.0mm gap with complete union. b) 1.5mm gap with partial union. c) 2.0mm gap with non-union (atrophic).

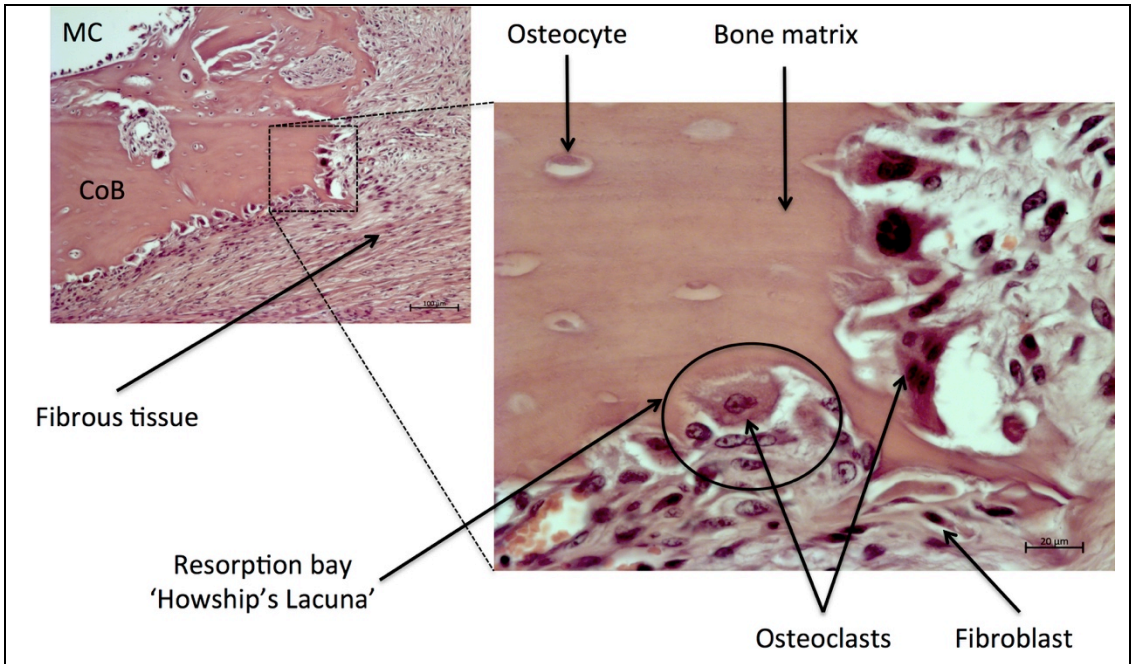

Figure 5.16: Histology images of an atrophic non-union seen in a 1.5mm osteotomy gap. Images are shown at x10 and x40 magnification. MC = marrow cavity, CoB = cortical bone.

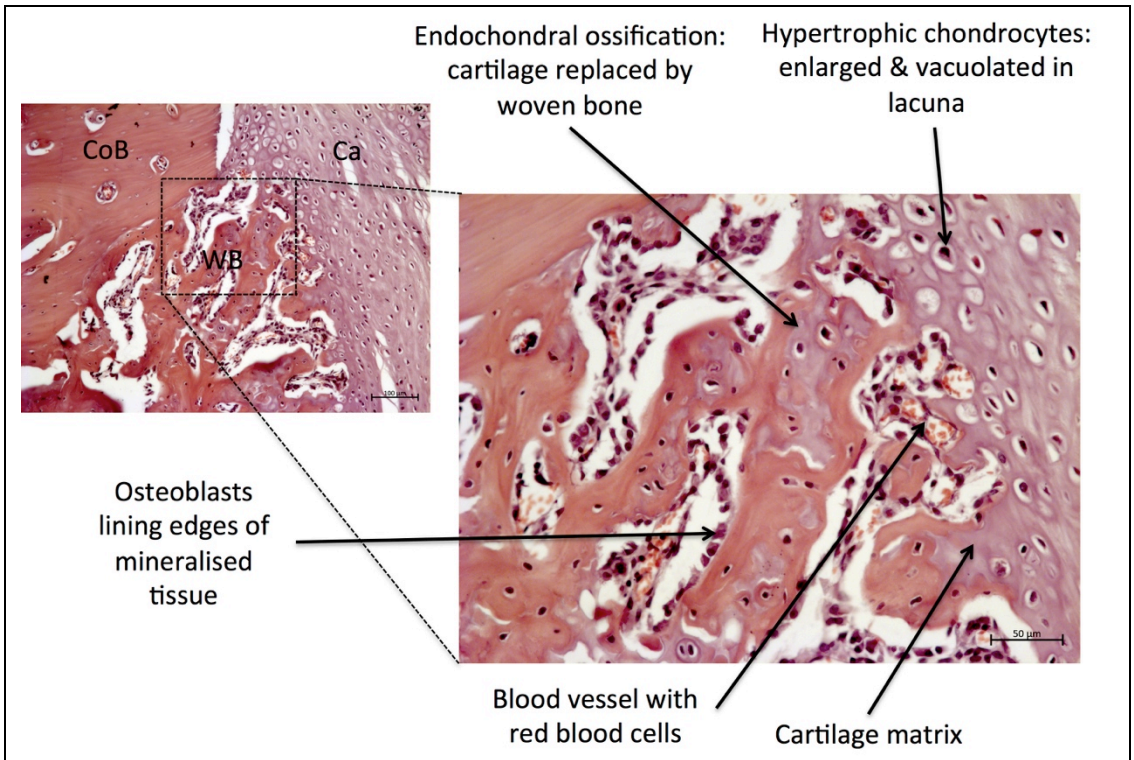

Figure 5.17: Histology images of delayed healing in a 1.5mm osteotomy gap. Images are shown at x10 and x20 magnification. CoB = cortical bone. WB = woven bone, Ca = cartilage.

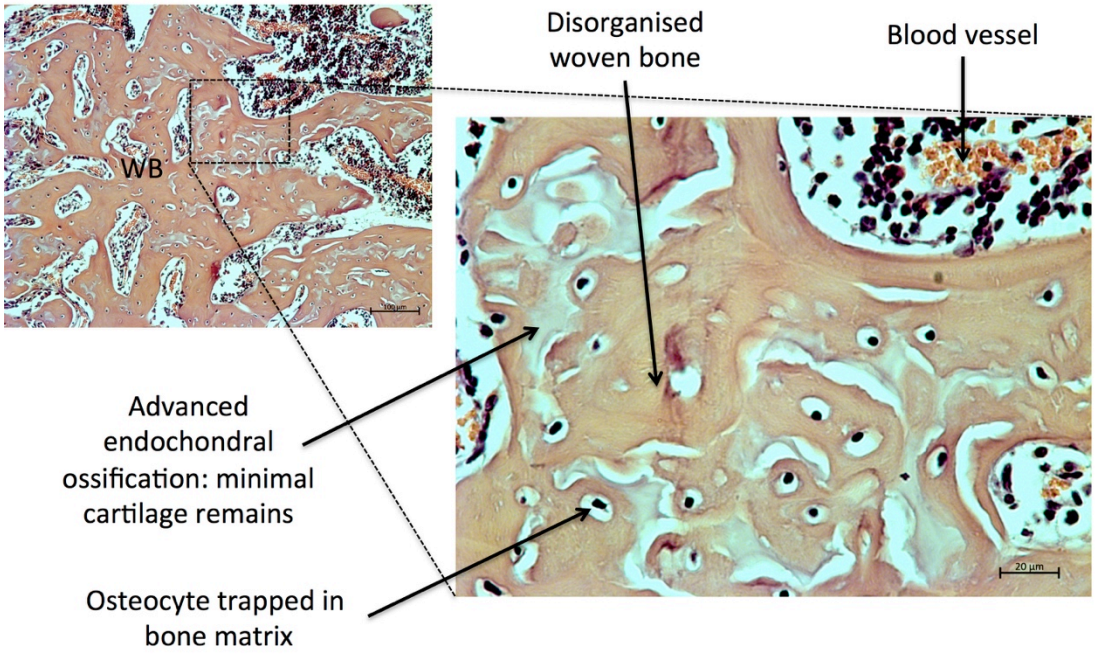

Figure 5.18: Histology images of healed 1.0mm osteotomy gap. Images are shown at x10 and x40 magnification. WB = woven bone.

5.4 DISCUSSION

5.4.1 Interfragmentary strain theory

Based on Stefan Perren's IFS theory (Perren 1979), my hypothesis for this chapter was that increasing the gap size, would decrease IFS and improve fracture healing. This hypothesis was not supported based on day 0 assessment of IFS.

Interfragmentary movement has been duplicitously described as both a stimulator and inhibitor of fracture healing. The IFS hypothesis predicts that the strain tolerance of a tissue is the maximum strain that the tissue can tolerate and continue to function. Above this threshold the tissue cannot function or indeed fails (Perren 1979). Perren went on to describe the strain range in context of healing fracture; for bone formation the IFS had to be below 2%. Cartilage can tolerate 2-10% IFS and hence endochondral ossification and secondary bone union should develop. Only granulation tissue can tolerate higher strains of up to 100%. However, I think it is far too simplistic to assume the IFS will be uniform throughout a fracture gap. Inevitably, there will be different 'micro-environments', which will permit different stages of bone healing relating to individual and regional IFS. This is corroborated in FE models which utilise homogenised tissue characteristics and have shown heterogeneity of strain within a uniform osteotomy (DiGioia et al. 1986). Therefore, the assessment of a global gap IFS may not elaborate the whole picture. A further confounder is the decreasing

gap size with ongoing healing, which predicts an increase in the IFS beyond the limits of bone formation (Elliott et al. 2016). Clearly this theoretical situation is surmounted, potentially by sequential tissue formation within the gap, widening of the bone diameter by periosteal callus formation and processes such as spiral osteoblast alignment (Claes et al. 1998). Claes et al. used an FE model to correlate histological data to mechanical strain, cell differentiation and hydrostatic pressure and determined that intramembranous ossification will develop with strains <5%, whereas endochondral ossification can develop in strains <15% (Claes et al. 1999); more in line with my experimental findings. Other large animal studies with known gap sizes and interfragmentary movements have also shown good bone healing with IFS >2-10% (Claes et al. 1995; Kenwright & Goodship 1989). Claes et al. showed that a high initial IFS, above the Perren 10% threshold, resulted in increased callus formation, however, a larger gap had less bone formation for the same initial strain (Claes et al 1997).

When a fracture occurs, a well established sequence of events follows (Elliott et al. 2016) with initial deposition of a strain toleratant tissue, such as granulation tissue, which does little to reduce strain. Most bone healing occurs in an environment of relative stability and therefore the initial IFS at day 0 after fracture will be higher than 2%. Perren suggests that the apparent osteonecrosis and bone lysis at the opposing fracture ends increases the gap and thus reduces the IFS. My study confirmed a reduction in IFS as the gap increased, however this did not appear to potentiate healing. Perhaps the bone loss described by Perren is a pathological process associated with de-vascularisation of the fracture ends and not intended as a 'strain-modifying' process to aid healing. Simultaneous to this increase in gap size, connective tissues, which are sequentially less strain tolerant, differentiate and form a wide tissue cuff or 'callus', stiffening the gap and further increasing fracture stability and reducing IFS (Perren 2015). When I looked at the bone surface (BS) and tissue surface (TS) measures on microCT, there was a trend for a smaller callus as the strain reduced, which could fit the idea of a bigger callus cuff being required when there is a higher IFS. Perren's theory has been expanded upon by Carter and Blenman who suggest that it is not only the amount of strain, but the way the strain is applied, be it in compression, tension, shear, and further that the degree of vascularisation has influence (Carter et al. 1988). Their finite element model also accounted for eccentric callus formation with an asymmetric cartilage deposition, which I noted in some of my samples. They suggested this was due to varying hydrostatic forces with a more 'compressive microenvironment' producing more cartilage and a 'tensile' environment resulting in more fibrous tissue deposition. This is consistent with the types of loading patterns that will be developed within the osteotomy of the rat femur, with its eccentric mechanical axis and the use of a unilateral external fixator. Some of my samples

also showed eccentricity of callus shape and structure. Prendergast suggested a further model with two biophysical stimuli; fluid velocity and shear strain components playing a role in the solid and liquid phases (Prendergast et al. 1997). However, despite the development of various models, they all only approximate *in vivo* findings in the extremes.

There is greater consensus with regards to rigid fracture fixation, that allows direct osteonal healing (McKibbin 1978). This is peculiar to a particular surgical method of fracture fixation, typically using plates and screws with fracture compression. This mechanical environment effectively creates an IFS <2% permitting physiological bone turnover, whereby osteonal remodeling occurs across the fracture line (contact healing), or where there are small gaps <1mm, woven bone is directly deposited and then later remodeled by lamellar bone (gap healing) (Marsell & Einhorn 2011).

5.4.2 Modulating interfragmentary strain - dynamisation

As an accessible mechanical device, the external fixator can be altered during fracture healing to influence its rigidity and the subsequent micro-movement and IFS experienced at the fracture site. Goodship et al. applied various loads to a fixator system at differing frequencies and phases of fracture healing and showed that application of increased micromotion early in fracture healing increased fracture stiffness and bone mineral density (Goodship et al. 1998). This phenomenon became known as active dynamisation, but this effect can also be achieved without motors, through the normal loads applied during weight bearing if the fixator rigidity is altered, termed passive dynamisation. In human fractures stabilised by a unilateral fixator, cyclic movements even occur with a locked unilateral fixator when walking (Richardson et al. 1995). In my model, dynamisation could be achieved by initially having a longer pin working length and subsequent sliding the connecting blocks closer to the limb to stiffen the construct, or by the use of a telescopic connecting bar to engineer the stain environment as the fracture heals.

5.4.3 Non-unions

It is orthopaedic dogma that non-unions are described as vascular or avascular based on their radiographic morphology. Hypertrophic non-unions for instance, are widely accepted to occur due to excessive fracture micromotion. The hypertrophy develops through florid intramembranous ossification, which originates from the periosteum of the fracture ends when there is a large interfragmentary motion (Harrison et al. 2003). The view that atrophic non-unions have reduced vascularisation is probably, at least in part mistaken, as human samples of clinical atrophic non-unions showed no difference in vascularisation than those that had healed (Reed et al. 2002). Interestingly, when evaluated in an experimental model,

there was a temporal difference in vascularisation, with vessels being seen later in non-unions, although the same total vascularisation was ultimately achieved in both groups (Reed et al. 2003). Perhaps the early lack of vascularisation is at a critical stage for cell migration, including stem cells, and thus ultimately prevents the correct cellular chain reaction for healing, despite a suitable IFS. It is worth considering that simply quantifying the numbers of blood vessels may not be sufficiently sophisticated to answer fully these questions and the actual oxygen tension readings may be more informative. Gender and possibly the associated impact of differing hormones may also have influence, as rat critical sized defects of the same size (5mm) gave delayed union in male rats and non-union in female rats (Mehta et al. 2010). However, it is also worth noting that the male bones were bigger and hence the proportional gap size was smaller.

My study showed over a doubling of non-union rates and halving of bone volume, with an increase in fibrous tissue within the osteotomy as IFS changed from 12% to 6%. The explanation is difficult, but these findings are recapitulated elsewhere with increasing gaps leading to reduced healing (Harrison et al. 2003; Mehta et al. 2010; Claes et al. 2003). Perren's theory predicts for a given interfragmentary movement, the bigger the gap, the better the predicted healing due to reduced IFS. However, large gaps and critical sized defects, even when fixed very rigidly, do not heal. This implies that if Perren's theory is in part correct, there must be thresholds or non mechanical factors that influence the outcome. The expectation from Perren's theory would be any fracture with an IFS under 10% should be able to undergo endochondral ossification and heal. This chapter showed that within the immediate fracture environment, were IFS ranged between 12-6%, the groups with the IFS >10% had improved healing than those <10%. This may also suggest that the purported die back phenomenon of bone to reduce IFS (Perren 2004; Perren 1979) may not be the reason, as reduced IFS from increased gap size appeared to negatively influence healing. My findings are corroborated elsewhere (Claes et al. 1997).

Perhaps critical sized defects do no heal due to the biological hurdles these large gaps create for fracture healing, or critical sized gap may have their own biomechanical rules for healing, which are distinct from the smaller gaps. Claes et al, showed that bigger gaps had reduced fracture healing in a sheep metatarsal model, however the stability of the fixation also influenced healing, with more rigid fixation producing less callus in small gaps, but this was not recapitulated in larger gaps (Claes et al. 1997). It is also possible that the fixation rigidity will affect the micromotion and hence the IFS seen. For the same fixation, a bigger gap will make the environment more mechanically elastic, or flexible due to the change in implant working length. Whether these defects require increased micromotion (Goodship et al. 1998), or a stiffer reduced IFS remains to be clearly determined.

5.4.4 Cellular responses to the mechanical environment

When considering a tissue's response to its mechanical environment, it is remiss not to acknowledge that the cell is at the heart of this response. *In vitro* experiments have demonstrated that different cells also have different strain tolerances. Fibroblasts respond to uniaxial stretching and the line of magnitude influences their alignment and response. Surprisingly, fibroblasts but not their synthesised tissues, appear less tolerant than osteoblasts to larger strains, whereas chondrocytes respond to a strain range of 1-3% (Jagodzinski & Krettek 2007). Osteoblasts in culture have also been shown to align along axes of strains, up to a maximum of 6% (Neidlinger-Wilke et al. 2001). When considering fracture healing and the recruitment of stem and progenitor cells to facilitate *de novo* tissue formation, the mechanical environment will exhibit its effects on stem cells, and that will in turn be part of the signaling for differentiation. Bone marrow mesenchymal stem cell differentiation is influenced by a combination of biological cues and the strain environment, with experiments showing chondrocyte (Angele et al. 2003) and osteoblast (Mauney et al. 2004) differentiation being influenced by strain. Undifferentiated stem cells plated on variably compliant polyacrylamide gels show sensitivity to their local matrix mechanical environment. Importantly, naïve MSCs with no lineage specific markers, are differently affected by the stiffness of the mechanical environment in which they inhabit, with stiffer environments driving osteogenic differentiation and softer environments favouring neuro or myogenic pathways. After several weeks of exposure to a particular mechanical environment, the mechanical influence becomes dominant over growth factor driven differentiation (Engler et al. 2006). The initial IFS therefore, and subsequent IFS over the duration of fracture healing will influence the tissue formation through its mechanical conditioning of the recruited stem cells. However, the exact interplay between mechanics at the micro and macro levels are not currently defined (Ghiasi et al. 2017). It is also possible that woven bone may behave differently to lamellar cortical bone, as cultured osteoblasts have a physiological strain range between 1-5% and cartilage callus forms when stains are 5-10%, and hence Perren's IFS theory may need to be further reconsidered in light of the tolerance of healing woven bone rather than remodeled bone (Elliott et al. 2016).

There are two arms to successful fracture healing; the mechanical and the biological. A purported key factor for the mechanical aspect is stability (presumed to be the correct IFS), and for the biological is blood supply (Rhinelander 1974). Ovine studies have shown that increased fracture gaps with the same IFS had reduced vascularisation and hence diminished ability to heal (Claes et al. 2003). However, other studies quantifying blood vessels have shown no difference between atrophic non-unions, hypertrophic non-unions and healing fractures (Reed et al. 2002), although blood vessels appear at a later stage and therefore early

vascularisation may be key (Reed et al. 2003). The histology from my study also showed a consistent level of vascularisation between different gap sizes and despite their subsequent healing fates. The histologic analysis was performed at five weeks and therefore it is conceivable with an increasing gap size, the time required for vascular development could be longer and perhaps critical blood vessel density was not reached at a sufficiently early time frame. This is speculation, however, this study either points to Perren's hypothesis of thresholds for tissue formation as incorrect if they are soley based on initial IFS at day 0, or there are other 'rules' or considerations at play, such as progressive changes in IFS as the fracture heals. Additionally, insufficient IFS has been reported to retard healing, with a postulated level of insufficient IFS of 1% (Elliott et al. 2016). Other complicating factors such as increasing animal age (Strube et al. 2008) or sex have influenced fracture healing in some studies, although the large difference in bodyweight between female and male rats was not controlled for (Mehta et al. 2010). My study had a tightly controlled age range and hence weight, and all were female Wistar rats.

5.4.5 Tissue formation

In terms of tissue formation analysis, this study made a direct comparison between the different gap sizes by analysing the same central proportion of the osteotomy. With consistent scan slice thickness of 5um, a universal measure of bone volume/slice was possible and allowed a direct comparison. It is acknowledged that this would not therefore analyse any intramembranous ossification that may have arisen directly adjacent to the periosteum at the cortical fracture ends (Harrison et al. 2003), but was focused on endochondral ossification of cartilage to woven bone within the osteotomy gap itself. This was intentional to ensure a consistent healing region within the osteotomy was analysed, such that there was no influence of 'capturing' the native ends of the osteotomy with their high bone volume distorting analysis. Histology on the other hand, covered a larger area for analysis and still corroborated the trends seen in the microCT. The histomorphometric analyses did not generally reach statistical significance, however, considering that histology represents analysis of the callus in only a single sagittal slice, it is not surprising that trends found with microCT volumetric analysis are harder to show histologically. Nonetheless, histology is an extremely useful partner to microCT data as it allows for soft-tissue distinction and cellular process evaluation as required.

My 1x analysis measured the gap plus the bone in between the two innermost pins. I would have therefore predicted an increasing overall area as the gap size increases, assuming all gaps healed in a similar manner. The increase from 1.0mm to 1.5mm did show an absolute increase, but then a decrease at 2.0mm indicating bone loss, consistent with the atrophic non-

union morphology seen in 50% of those samples. When appraising the 'non bone' within this region, specifically fibrous and cartilaginous tissue, the 1.5mm gap had significantly more, suggestive that the fracture gap enlargement from 1.0mm to 1.5mm is significantly filled by soft-callus type tissue; fibrocartilage. There is then, an absolute reduction in tissue in the 2.0mm gap simply because the callus is much smaller, as it tends towards atrophy.

The 2.5x images allowed assessment of tissue composition within the original osteotomy. The 1.0mm gap with its higher IFS of 12% had the most bone tissue, some cartilage and no fibrous tissue. As the gap size increased to 1.5mm and to 2.0mm, there was a sequential reduction in bone and an increase in cartilage and fibrous tissue. The 1.5mm gap with an 8% IFS, had greater cartilage than fibrous tissue, whereas 6% IFS 2.0mm gap had little bone and less cartilage than the 1.5mm gap, with the highest proportion of fibrous tissue. These changes should be considered in context of a callus, which is reducing in size as the gap enlarges. It is noteworthy that the trabecular thickness was unchanged across the groups although more spaced out in the 1.0mm gap compared with 1.5 and 2.0mm. This indicates the woven bone structure is the same and the changes are simply related to the amount present and potentially its arrangement.

5.4.6 Biomechanical testing

The second part of my hypothesis was that the stiffness would be affected by the gap size and I found that the construct stiffness was unaffected by the increasing gap size. Beyond the variable activity of individuals and any weight differences, there would have been no difference in the loading of the osteotomy and therefore the IFS was entirely varied by gap size alone. The uniform consistent stiffness is probably due to the double connecting bar making the construct relatively stiff, compared to any influence of increasing the working length of the bar between the connecting blocks as the gap size increased. To that end, this is an excellent model to evaluate the effect of gap and IFS alone as there is not a secondary influence of construct stiffness.

The test set-up was clinically relevant as loading was applied from the femoral head to the femoral condyles as it would be physiologically (Barak et al. 2008). The mechanical axis is therefore eccentric, creating an inherent bending force with compression on the medial aspect and tension on the lateral. The unilateral fixator is then at right angles to this being placed cranial to caudal and hence allows a second orthogonal bending moment. Although the exact type of loading, be it torsion, bending in one or other direction, or a composite, is difficult to determine, it should accurately mirror the *in vivo* situation and is therefore informative to the *in vivo* findings. Making use of a microstrain displacement sensor

positioned as close as possible to the proximal and distal ends of the osteotomy would significantly reduce artefactual whole construct displacement variation, which would have been present if determining such small displacements from the materials testing machine displacement sensor.

5.4.7 Conclusion

Despite the clear trends across the groups, and some showing statistical significance, I find it interesting that in every group there was a large variation in the individual's fracture healing potential, with non-union seen in 1.0mm gaps and union in 2.0mm gaps. The rats were out-bred strains and therefore genetic variation could have played a role. Otherwise they were all females of the same age, had identical procedures and treatment, and lived in the same environment. Do these variations relate to their inherent activity levels affecting osteotomy healing (Goodship & Kenwright 1985), or is this a biological innateness, or both? Mice have been shown to have significantly different levels of activity post external fixator surgery and the more mobile animals produced a bigger callus containing more cartilage (Connolly et al. 2006). Clinical findings also corroborate, with insufficient as well excessive activity both negatively influencing fracture healing (Gaston & Simpson 2007). It is also clear from in-bred mouse studies that there are genetic differences in skeletal stem cell regulation, influencing the temporal patterns of chondrogenic and osteogenic lineage development and this will affect the rate of fracture healing (Jepsen et al. 2008). Moving to in-bred rat strains may be sensible in future studies, however the variation in healing seen in my study is reflected in human fracture healing. In clinical fracture healing, comorbidities such as diabetes mellitus, thyroid disorders, malnutrition, age, prescribed medications such as NSAIDs, steroids, smoking and alcoholism can all influence healing (Gaston & Simpson 2007) and therefore the variation seen experimentally may have relevance to the clinical situation.

In conclusion, the construct stiffness was unaffected by the increasing gap size with the Stanmore micro external fixator, and increasing gap size resulted in decreased IFS as measured on day 0. On balance the most appropriate sized gap to use as an impaired fracture model for proceeding chapter was the 1.5mm gap.

CHAPTER 6: Modulation of Fracture Healing by Growth Factor & AMD3100 Administration

6.1 INTRODUCTION

Bone marrow stromal stem cells, subsequently termed MSCs, have both *in vitro* and *in vivo* potential to produce all tissues required to form a bone organ (Hankenson et al 2011; Owen & Friedenstein 1988; Bianco et al. 2013). Peripheral blood circulating cells that are plastic adherent and can form colonies with osteogenic potential, have been found in mice, rabbits, guinea pigs and humans in low numbers of around 1 in $10^{6\text{-}8}$ (Kuznetsov et al. 2001; Zvaifler et al. 2000).

Pitchford et al. showed significant mobilisation of EPCs in addition to MSCs, most notably when VEGF was combined with AMD3100 (Pitchford et al. 2009). The potential role of EPCs in fracture healing is logical as vascularisation is essential for bone formation and fracture healing (Keramaris et al. 2008; Hankenson et al 2011; Rhinelander 1968). EPCs have also been shown to be increased in the peripheral circulation after fracture in humans (Ma et al. 2012) and in models of distraction osteogenesis and fracture healing, with peaks early in the healing process (three days), although they remained elevated throughout (Lee et al. 2010). This has led to interest in isolating, culturing and transplanting EPCs to aid healing, in particular for cardiovascular disease (Chong et al. 2016; Ward et al. 2007). In fracture healing experiments, locally transplanted cultured EPCs have increased healing in a rat critical sized defect model, with significant increases in bone volume, trabecular number, trabecular thickness and trabecular spacing (Li et al. 2011). Isolated EPC populations have been shown to differentiate into endothelial cells and contribute to neovascularisation directly (Ward et al. 2007), however EPCs may also improve healing through provision of trophic stimulation to resident cells. Beyond the mobilisation work of Pitchford for EPCs, there is further evidence of a role of SDF1/CXCR4 with EPCs (Kawakami et al. 2015), where CXCR4 conditional knock-out sourced EPCs had reduced migration and colony forming ability *in vitro*, and the mice had reduced fracture healing *in vivo.*

The recruitment, migration and homing of cells to a fracture is essential for inflammation, blood vessel formation, chondrogensis, osteogenesis and therefore fracture healing. However, a significant number of bone defects and fractures do not heal (Rodriguez-Merchan et al. 2004), leading to delayed or non-union. Clinically we look for radiographic union, however, other higher resolution modalities such as histology or microCT are available in the research setting. In rodent studies, there is no clear definition for delayed or non-unions and a variety of different outcome points have been used, however, reduction in fracture movement, i.e. stability from healing is expected to reach 0% at around four weeks (Garcia et al. 2013). Experimental studies have looked towards a consensus definition and based on the somewhat arbitrary ratio of eight weeks for human long bone fractures to heal and a non-union

definition of six months, a three-fold time span was suggested. A rat non-union is hence defined as incomplete healing by 15 weeks, assuming five weeks for normal healing duration, and the same ratio gives a non-union definition of 12 weeks in mice (Garcia et al. 2013). However, there is known variation in the 'expected healing time' based upon numerous criteria including the individual, the fracture configuration/location, and the method of treatment. No gold-standard definition exists for human non-unions.

The NHS reports a non-union rate of 10% and treatment can be difficult with a cost of up to £80,000 per patient (Mills & Simpson 2013). Some of these failures are related to comorbidities (Gaston & Simpson 2007) such as diabetes mellitus, which has shown a direct influence on osteotomy healing in rats through reduced fracture SDF1 expression (Arakura et al. 2017). Another key group of fractures with impaired healing are the osteoporosis related fragility fractures, and again the SDF1-CXCR4 axis appears implicated with reductions of CXCR4 on T regulatory cells seen in ovariectomised mouse models (Fan et al. 2015). Delayed-unions, which are defined as "a fracture in which healing has not occurred in the expected time and where the outcome remains uncertain" (Harwood et al. 2010), are also problematic. Protracted healing and potential secondary interventions have an associated morbidity, with impact on full return to function for the patient.

Based on the most comprehensive evaluation of endogenous stem and progenitor mobilisation in mice (Pitchford et al. 2009), in chapter 3 I showed it was possible to increase the circulating levels of MSCs and EPCs in rats using AMD3100 combined with VEGF. This protocol was suggested to be the most effective combination of growth factor together with AMD3100 in order to mobilise MSCs and EPCs, however, despite significant increases in CFUs, the numbers of stem/progenitor cells isolated was still quite low; at 3/ml blood for PBMSCs and PBEPCs. This may have been an artefact of *in vitro* culture and the processing required to remove red blood cells, or perhaps associated with the older rats used. Further, this measure represented the circulating pool of cells at the predicted peak elution time point, one hour post administration of AMD3100 (Broxmeyer et al. 2005). When evaluating the potential of endogenous mobilisation for fracture healing *in vivo*, a single time point measurement may be misleading and the duration and character of the cell elution profile in the circulatory system may be more important. Cell culture based assessments also have their limitations, as the very act of *in vitro* cell culture induces cellular change, including their cell surface characteristics (Bara et al. 2014). Finally, it is impossible to determine the potential synergistic or otherwise interactions of different mobilised cells populations, including those not measured in chapter 3, in fracture healing. Therefore, the best means to assess whether there is a translational potential in this therapy is to conduct an *in vivo* fracture model study.

As MSCs and EPCs can both impact on fracture healing (Kawakami et al. 2015; Lee et al. 2010), the protocol described by Pitchford et al. where VEGF was used in combination with AMD3100 (Pitchford et al. 2009) to increase the circulating levels of EPCs and MSCs was of particular interest. However, although chapter 3 did show *in vitro* proof of concept with VEGF AMD3100 combination, all combinations tested in Pitchford's work (Pitchford et al. 2009) were evaluated in this *in vivo* fracture model chapter. In addition, two further treatment strategies that have been tested to improve fracture healing in mice were evaluated. One was an 'Einhorn style' intramedullary pin stabilised femoral fracture, with which they gave AMD3100 alone for three consecutive days and showed greater total callus volume at 21 days (Toupadakis et al. 2013). The other created a tibial fracture by 3-point bending, supported by a splint and treated with IGF1 with AMD3100 (Kumar & Ponnazhagan 2012), and showed significantly increased bone mineral density at eight weeks. It is important to note that both these models had a poorly controlled mechanical environment with which to evaluate a biological augmentation, and these fractures were not inherently compromised in their healing, and hence unlikely to develop a delayed or non-union. This therefore led me to my question and hypothesis:

Question: In a standardised biomechanical environment, could compromised fracture healing be improved through endogenous mobilisation of stem and progenitor cells?

Hypotheses: Administration of AMD3100 based mobilising protocols, which have been previously shown to increase the number of circulating MSCs and EPCs, will increase bone formation within the osteotomy and improve fracture union.

6.2 MATERIALS & METHODS

My work in chapter 5 confirmed impaired fracture healing with a 1.5mm osteotomy. In this chapter I evaluated bone formation within an osteotomy gap of 1.5mm when treated with different mobilisation strategies. The groups included:

- PBS + AMD3100 (n=5) (PBS-AMD)
- VEGF + AMD3100 (n=8) (VEGF-AMD)
- IGF1 + AMD3100 (n=6) (IGF1-AMD)
- GCSF + AMD3100 (n=5) (GCSF-AMD)
- (1.5mm gap control osteotomy with no treatment from chapter 5) (n=7)

6.2.1 Preparation of growth factors & AMD3100

Growth factors and AMD3100 were prepared as described in chapter 3 (3.2.2.1). The dose was 5mg/kg i.p. based on the peak mobilising concentration in mice (Broxmeyer et al. 2005). Rat Vascular Endothelial Growth Factor 165 (VEGF) (PeproTech, USA, 400-31) was prepared by dissolving the lyophilized product in sterile water to make a 0.1mg/ml stock solution. A working solution was prepared by adding 1ml of stock solution to 4mls of sterile PBS + 0.1% BSA (Sigma-Aldrich A9418), to achieve 100ug/ml injectable solution which was aliquoted and stored at -20°C until needed. Recombinant human Insulin-like Growth Factor-1 (IGF1) (PeproTech, USA, 100-11) and murine Granulocyte colony stimulating factor (GCSF) (PeproTech, USA 250-05) were prepared in the same manner. Finally, PBS + 0.1% BSA, 'sham growth factor', to determine the effects of AMD3100 alone was also prepared. The growth factor dose was 100ug/kg i.p. based on previous studies (Pitchford et al. 2009; Kumar & Ponnazhagan 2012; Toupadakis et al. 2013; Fu et al. 2012).

6.2.2 Surgery & mobilisation protocol

Surgery was performed as described in the previous chapter 4 (4.2.6). Twenty-four hours post surgery, rats were given a single i.p. injection of either VEGF, IGF1, GCSF, or PBS once daily for four days. On day five, they were given a single injection of AMD3100. All i.p. injections including AMD3100 and sham PBS were administered at a volume of 0.5mls/100g bodyweight based on the day 0 pre-surgical weight (Figure 6.1). All procedures were carried out at the Royal Veterinary College, North Mymms, in accordance with the Animals Scientific Procedures Act 1986. Home Office licences were held by those taking part in any surgical procedure.

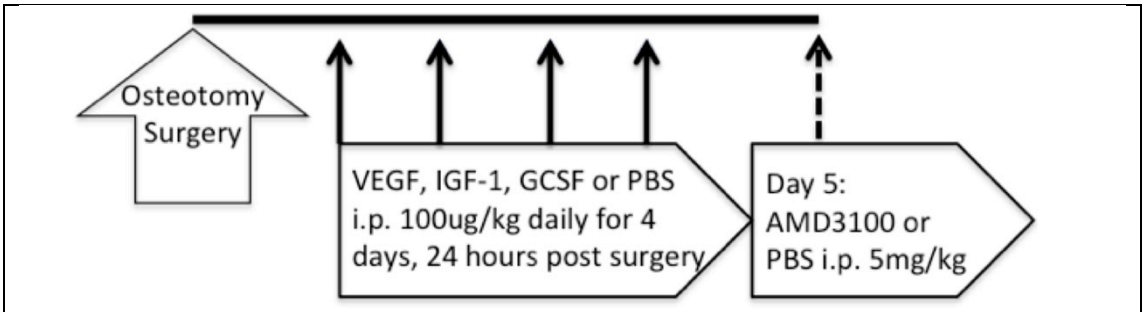

Figure 6.1: Diagram depicting the sequence of events for endogenous mobilisation of stem cells into the peripheral circulation after osteotomy surgery.

6.2.3 MicroCT & radiography

After five weeks, the rats were sacrificed and the left femur including the fixator was retrieved. Femurs were fixed (PBS-AMD n=5, VEGF-AMD n=8, IGF1-AMD n=6, GCSF-AMD n=5) and microCT scanned using the same settings and as described in previous chapter 5 (5.2.2.1). All groups had a 1.5mm osteotomy and the central 60% of the osteotomy gap was assessed (0.9mm = 180 slices at 5um thick). The reconstruction protocol and radiographic evaluation was performed as per chapter 5 (5.2.2.1).

6.2.4 Histomorphometric analysis of callus

Histology slides were prepared and analysed as described in chapter 5 (5.2.2.2), with four sections taken at the mid-sagittal region and the best two were stained, and one was evaluated. Briefly, histomorphometric analyses were performed at 1x and 2.5x magnification. The 1x images were analysed with imageJ (NIH, USA), to give an area measure of the different delineated tissue regions based on the square pixel number. At 2.5x magnification, tissues were semi-quantified with a 1.5mm scaled width line-intercept grid, with 120 intersections; grid squares were 160um in both directions. The grid was centered over the osteotomy and was scaled to be the same width as the original osteotomy (1.5mm). Intersections were then scored as percentage bone, cartilage, fibrous tissue, vascular (identified by red blood cells not present in matrix) or void.

6.2.5 Statistical analysis

Due to the relatively small group sizes ($n<9$), non-parametric tests were performed to compare groups including Mann-Whitney U (MWU) and Kruskal-Wallis (KW) as appropriate. Assessment of data spread was made with a Levene's test for equality of variance. Significance was set at $p<0.05$ and tests were analysed with SPSS version 24 (IBM, Chicago, USA). Fisher exact test was performed to look for difference between radiographic fracture union (GraphPad Prism v6.00, USA).

6.3 RESULTS

6.3.1 Surgical procedure

No adverse effects were seen with the growth factor or AMD3100 administration.

6.3.2 Radiographic evaluation

Group	Non-union	Partial-union	Union
1.5mm Control	3/7 (43%)	2/7 (29%)	2/7 (29%)
PBS AMD	1/5 (20%)	0/5 (0%)	4/5 (80%)
VEGF AMD	2/8 (25%)	2/8 (25%)	4/8 (50%)
GCSF AMD	3/5 (60%)	0/0 (0%)	2/5 (40%)
IGF1 AMD	2/6 (33%)	1/6 (17%)	3/6 (50%)

Table 6.1: Radiographic assessment of degree of union from microCT scout images, shown as absolute numbers and percentages.

There was a trend for an increase in union and reduction in non-union in the treated groups except for GCSF-AMD. The PBS-AMD group showed the largest positive effect (Table 6.1), however no significant differences from the control group were shown using Fisher's exact test.

6.3.3 MicroCT analysis of osteotomy tissue formation

MicroCT analysis PBS-AMD

Rats treated with PBS-AMD (n=5) had double the bone volume (BV) within the osteotomy (8.9±2.2 um^3, p=0.01), compared with the untreated control (4.3±3.1um^3) (Figure 6.2a). Not only was the BV increased, but the overall callus volume (TV) was greater than the controls (15.3±3.6 vs 9.2±6.1 um^3). The percentage bone volume was not significantly increased however, owing to a relative proportional increase in mineralised (BV) and non-mineralised callus tissue. Additionally, the bone structure was different to the controls with the PBS-AMD group having a significant increase in trabecular thickness (P=0.03); 0.061±0.002um compared with 0.042±0.003um (Figure 6.2b). There was also a trend for increasing tissue volume and trabecular number when compared with the empty gap control group. Notably, the data appeared less spread, however significance was not shown.

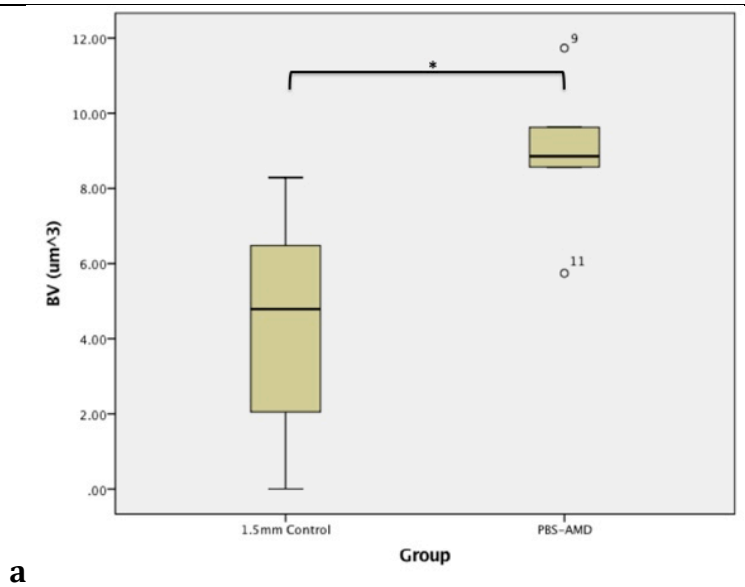

a

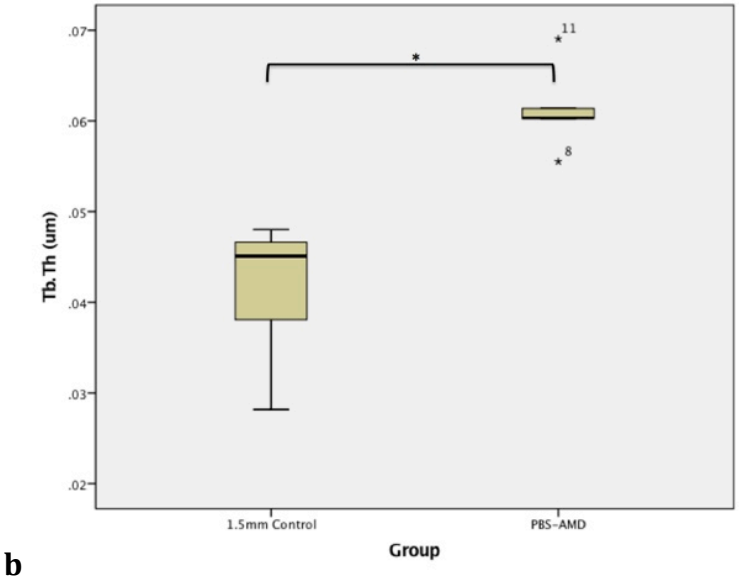

b

Fig 6.2: Boxplots comparing microCT measures of the control untreated group (1.5 Control) and the AMD3100 without additional growth factors (PBS-AMD). a) The bone volume (BV um^3) was significantly increased in the AMD3100 group (* p=0.01) b) Trabecular thickness was also significantly increased (Tb.Th um) (* p=0.003).

MicroCT analysis VEGF-AMD

The VEGF-AMD group (n=8) did not show any significant differences from the control group (n=7). The trends were consistent with the PBS-AMD group however, with mean bone volume for VEGF-AMD being higher than control (5.2±1.7um^3) (Figure 6.3a), as was trabecular thickness (0.05±0.01um) (Figure 6.3b). The overall data spread was significantly reduced in the VEGF-AMD3100 group when looking at tissue volume (TV um^3, p=0.036) and trabecular number (Tb.N, 1/um, p=0.048).

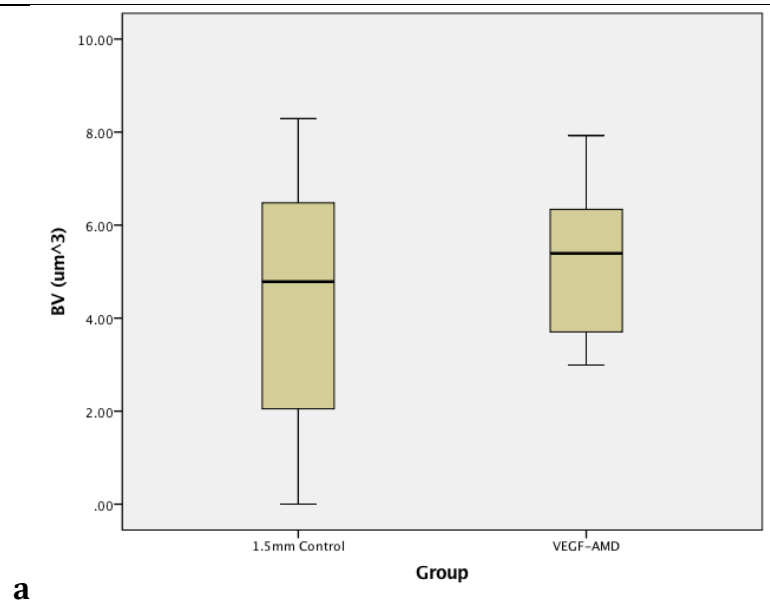

a

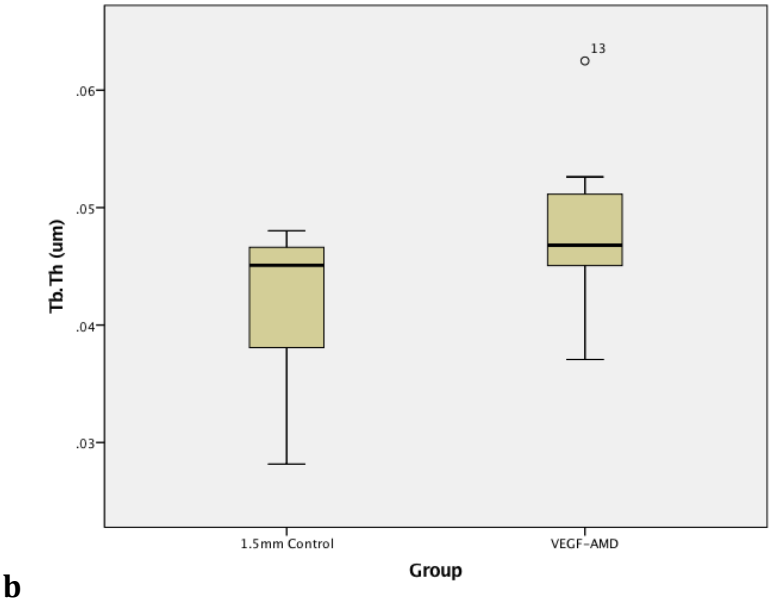

b

Fig 6.3. Boxplots comparing microCT measures of the control untreated group (1.5 Control) and the VEGF-AMD treated group. a) VEGF-AMD increased bone volume (BV um^3). b) Trabecular thickness (Tb.Th um) was also increased, but significance was not shown.

MicroCT analysis GCSF-AMD

Interestingly, treatment with GCSF-AMD resulted in a significant increase in percentage BV 63.1±7.3% vs 53.8±20.8% (p=0.048), however the actual volume of the callus (TV 4.3±4.7 vs 9.2±6.1um^3) and bone volume (BV, 2.5±2.6 vs 4.3±3.1um^3) was smaller compared with controls (Figure 6.4a). However, trabecular thickness was significantly higher 0.069±0.03 vs 0.042±0.008um (p=0.048) (Figure 6.4b) and total porosity was significantly lower 36.9±7.3% vs 46.2±20.8% (p=0.048) (Figure 6.4c). This suggests that although GCSF-AMD group had less overall total woven bone, the bone formed was less porous and the size of each bone forming region was greater than in controls. Only trabecular thickness (Tb.Th um) showed a significant reduction in data spread in the treatment group (p=0.041).

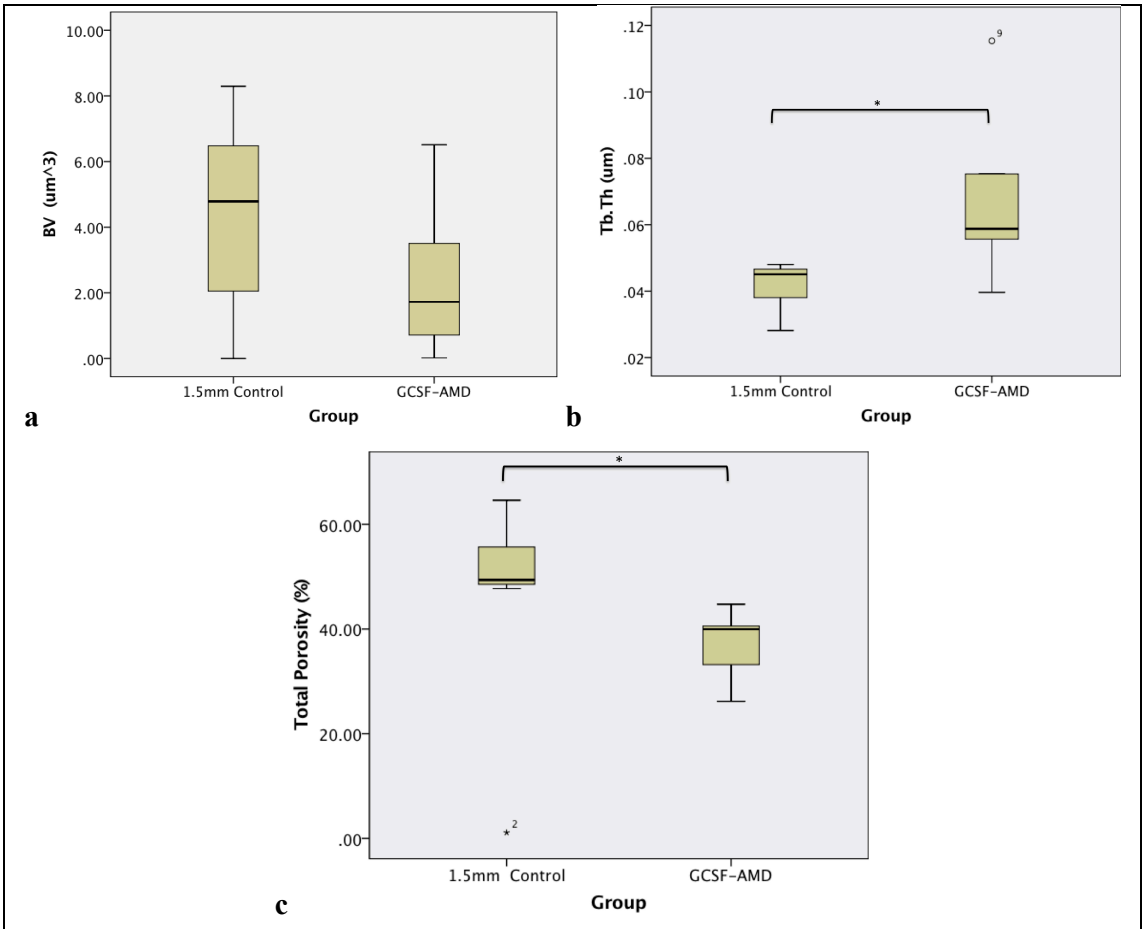

Figure 6.4. Boxplots comparing microCT measures of the control untreated group (1.5 Control) and the GCSF-AMD group. a) The bone volume (BV um^3) was reduced in the GCSF-AMD group. b) Trabecular thickness was increased (0.069±0.03um^3), as seen in other treatment groups (* p=0.048). c) Total porosity was significantly reduced to 36.9±7.3% (* p=0.048).

MicroCT analysis IGF1-AMD

Rats treated with IGF1-AMD (n=6) also had an increase in bone volume (5.1±4.2um^3), compared with controls (Figure 6.5a). Percentage bone volume was significantly increased (p=0.035), and the overall callus size was the same as controls (TV 9.1±7.6 vs controls 9.2±6.1um^3). There was also a significant increase in trabecular thickness 0.062±0.008um (p=0.01) (Figure 6.5b). Total porosity was significantly lower when treated with IGF1-AMD compared with controls; 40.8±5.6% vs 46.2±20.8% (p=0.035) (Figure 6.5c). There was also a trend for increased trabecular number when compared with the control group. The spread of data was not significantly different.

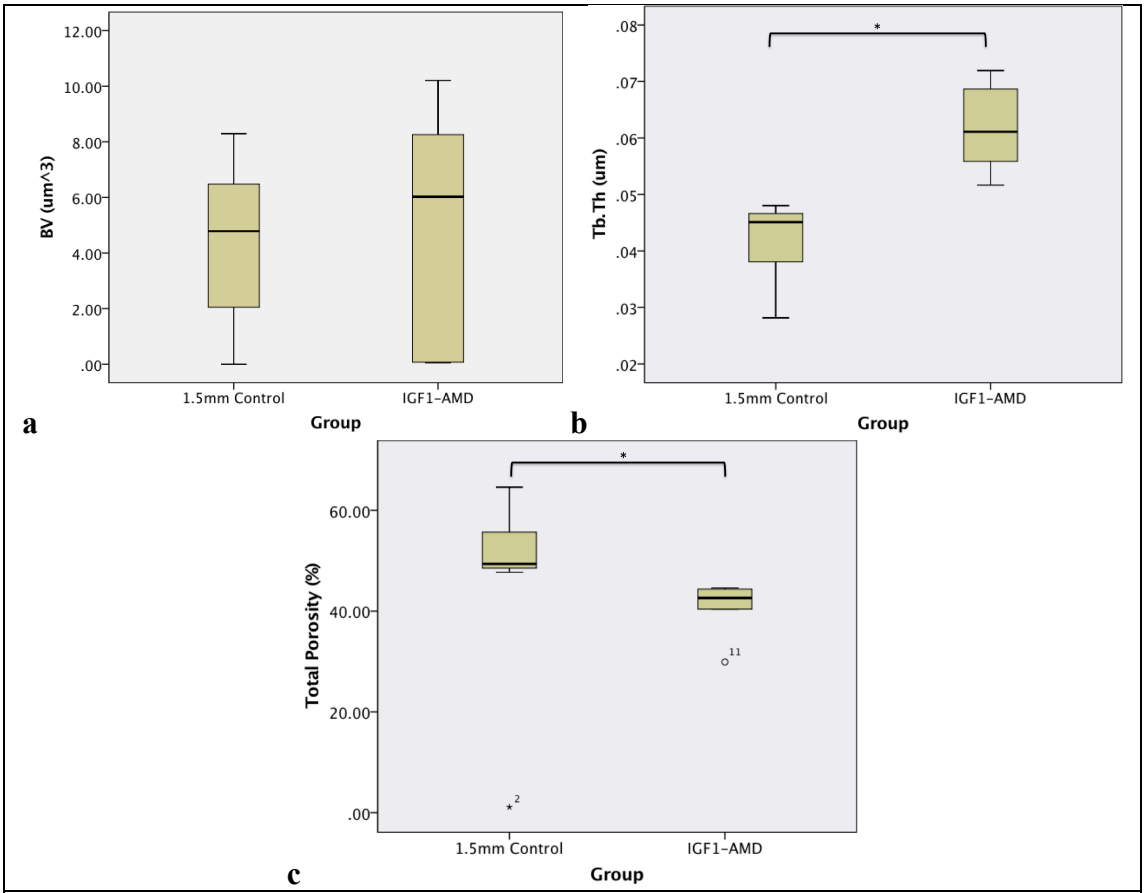

Figure 6.5: Boxplots comparing microCT measures of the control untreated group (1.5 Control) and the IGF1-AMD group. a) The bone volume (BV um^3) was increased in the AMD3100 group. b) Trabecular thickness was significantly increased (Tb.Th um) (* p=0.01). c) Total porosity (%) was significantly reduced (* p=0.035).

When comparing between all groups, there were significant differences in bone volume (BV) (p=0.033) (Figure 6.6), trabecular thickness (Tb.Th) (p=0.003) (Figure 6.7), total porosity (%) (p=0.043) (Figure 6.8), and percentage bone volume (TV/BV) (p=0.043) (Table 6.2). All treated groups had greater bone formation than control, other than GCSF-AMD, which had a

negative impact on healing. However only PBS-AMD reached statistical significance for increased overall bone volume (BV) (Figure 6.6), and IGF1-AMD for % bone (TV/BV) within the callus. All groups had significant increases in trabecular thickness other than VEGF-AMD.

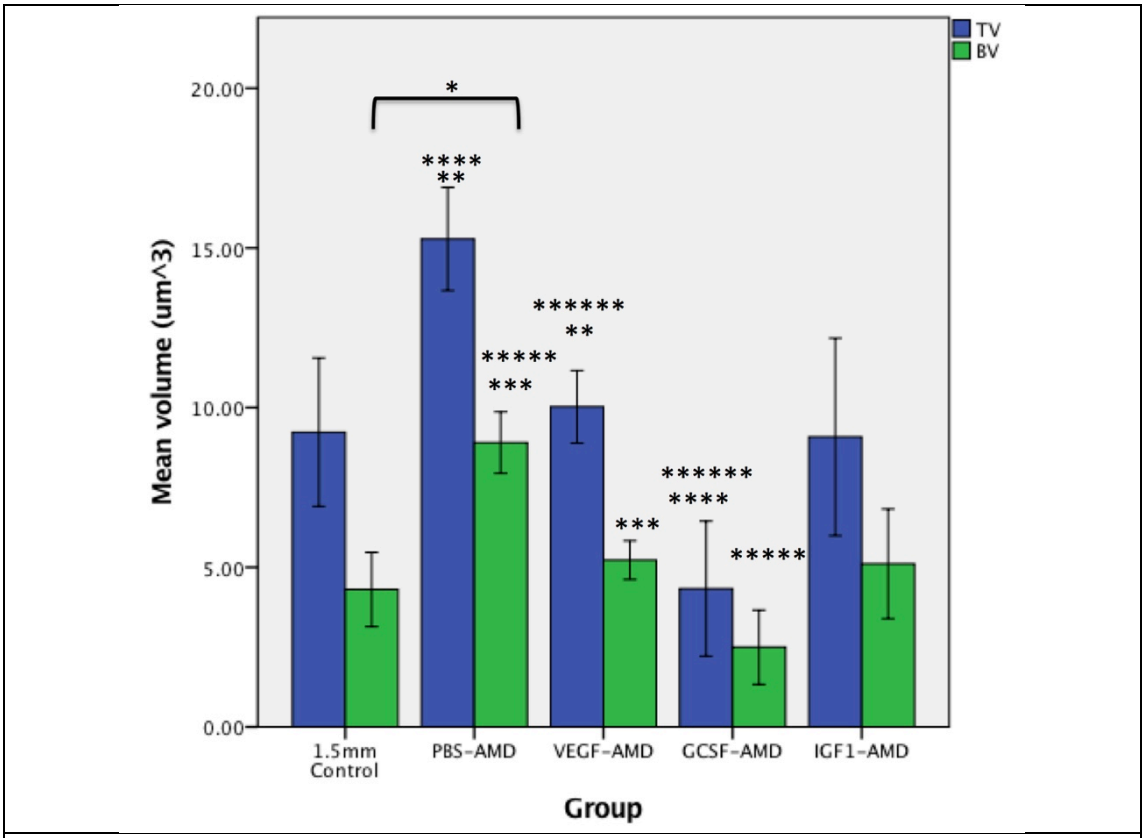

Figure 6.6: The mean±SEM tissue volume (TV) and bone volume (BV) within the osteotomy measured using microCT. * represents significant ($p<0.05$) differences compared with 1.5mm control. **,***,****,*****,****** indicate significant differences ($p<0.05$) between paired groups.

There were variations not only in the overall amount of new bone formed within the osteotomy, but also the bone structure. All treatment groups other than GCSF-AMD showed an increased trabecular separation of the woven bone (Figure 6.7), implying a different, more porous structure to the control group. All groups, including GCSF-AMD with its impaired overall bone formation, had increased trabecular thickness (Figure 6.7). Hence all treatment groups had a similarly increased thickness of the bone microstructure, despite variation in total bone formed.

Total porosity of the woven bone was reduced compared with control in GCSF-AMD, IGF1-AMD and GCSF-AMD (Figure 6.8). All groups had reduced trabecular number compared with control, although it was only significantly reduced when comparing between PBS-AMD and VEGF-AMD, consistent with the aforementioned trabecular separation findings.

Trabecular number showed a trend for being reduced compared with control, although non significant. Some groups showed a difference in mean surface area (Figure 6.9), with GCSF-AMD, having the lowest tissue (TS) and bone surface areas (BS) indicative of a smaller or more atrophic callus; BS was significantly reduced compared with PBS-AMD (p=0.016) and VEGF-AMD (p=0.019) treatment groups. Direct comparisons between all groups for microCT analyses are made in figures 6.6 through 6.9, and table 6.2. Representative 3D reconstructions of each group with a reveal to see through to the centre of the callus is shown in figure 6.10.

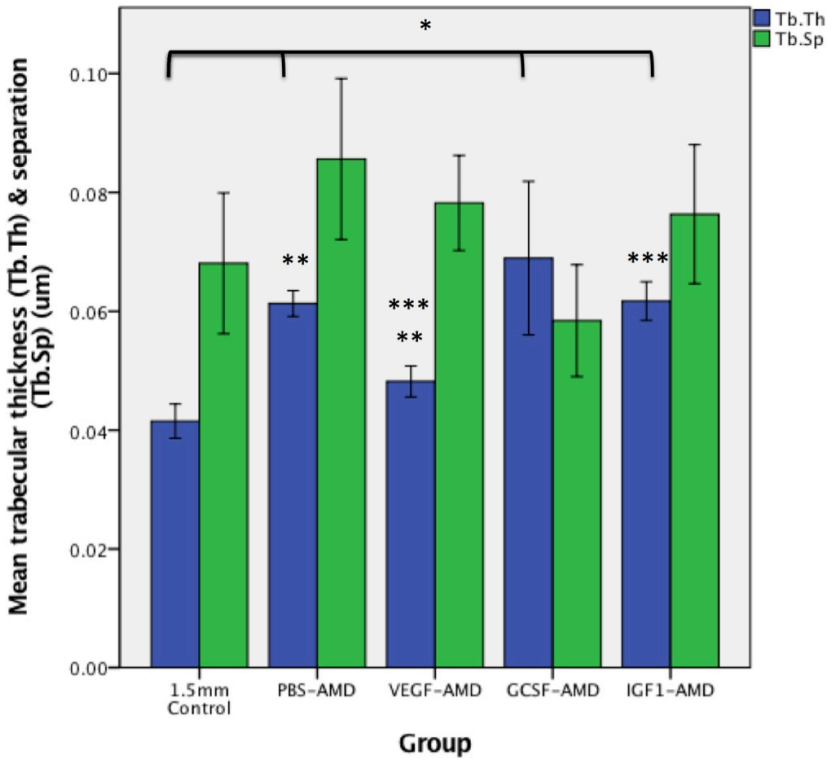

Figure 6.7: The mean±SEM trabecular thickness (Tb.Th) and separation distance (Tb.Sp) of bone formed within the osteotomy measured using microCT. * represents significant ($p<0.05$) differences compared with 1.5mm control. ** and *** indicate significant differences ($p<0.05$) between different groups.

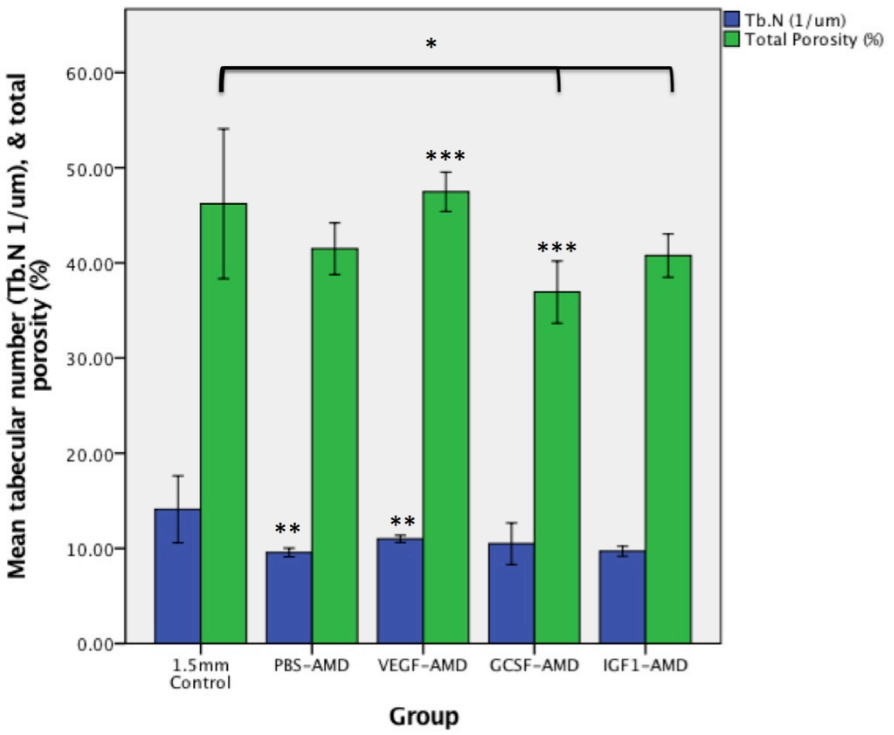

Figure 6.8: The mean±SEM trabecular number (Tb.N) and percentage total porosity of bone formed within the osteotomy measured using microCT. * represents significant ($p<0.05$) differences compared with 1.5mm control. ** and *** indicate significant differences ($p<0.05$) between different groups.

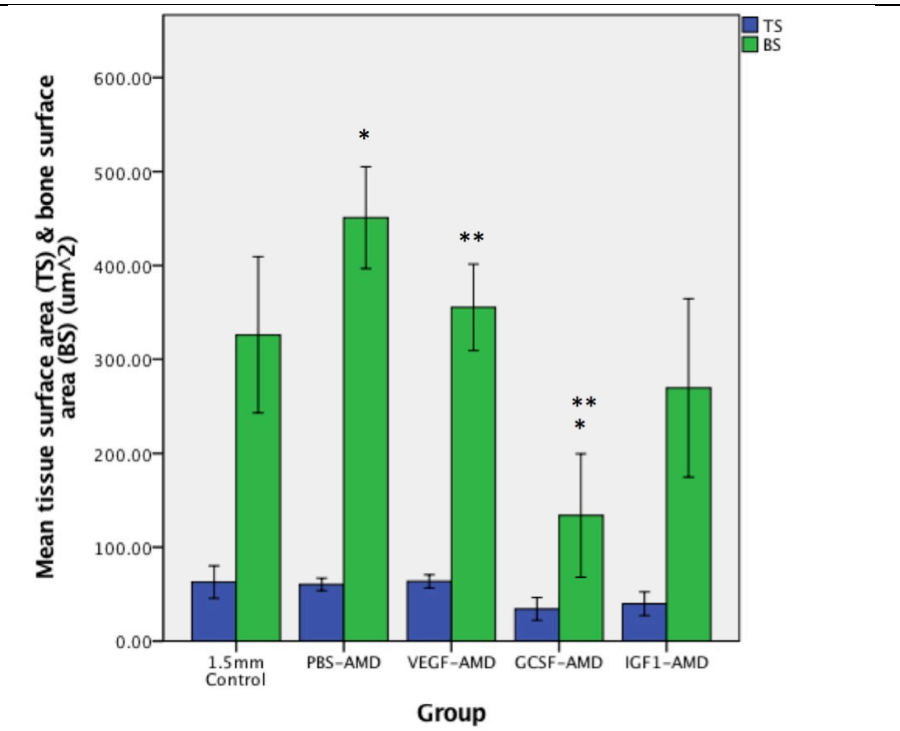

Figure 6.9: The mean±SEM tissue surface area (TS) and mean bone surface area (BS) of tissue formed within the osteotomy measured using microCT. * and ** indicate significant differences ($p<0.05$) between different groups.

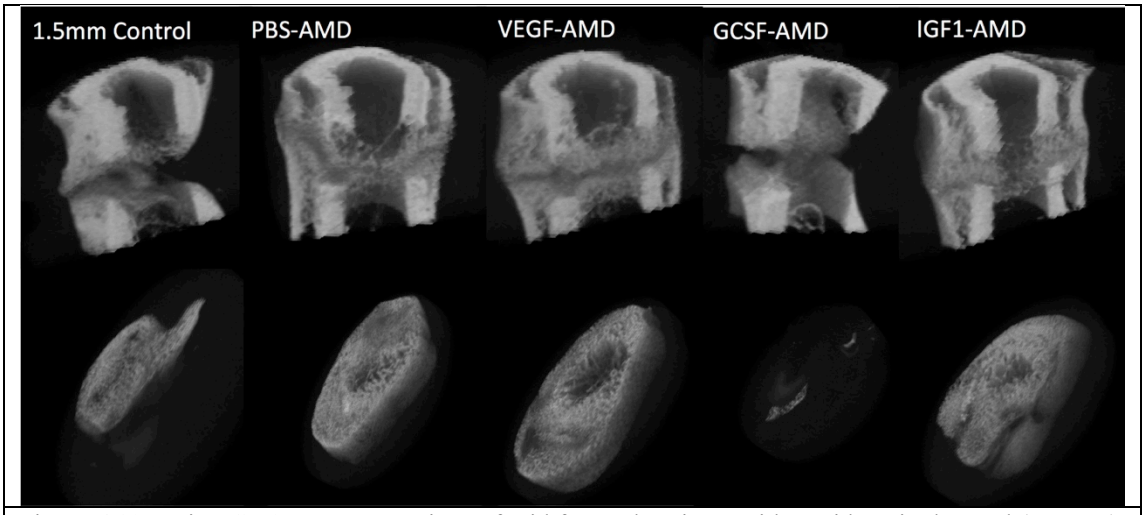

Figure 6.10: MicroCT 3D reconstructions of mid femoral regions, with a mid-sagittal reveal (top row). The bottom row shows a 3D reconstruction of the central 60% of the original osteotomy region (180 slices) within the osteotomy that was analysed for quantitative morphometry. All groups other than GCSF-AMD showed increased mineralised callus formation when compared with the untreated control osteotomy group.

	1.5mm Control	PBS-AMD	VEGF-AMD	GCSF-AMD	IGF1-AMD
TV (um^3)	9.23±6.14	15.28±3.61	10.03±3.22	4.33±4.72	9.08±7.57
BV (um^3)	4.31±3.08	8.91±2.16	5.22±1.71	2.50±2.60	5.11±4.21
TV/BV (%)	53.79±20.82	58.51±6.06	52.52±5.85	63.07±7.29	59.24±5.58
TS (um^2)	62.83±45.55	60.32±14.75	63.56±19.88	34.24±27.19	39.77±30.77
BS (um^2)	326.15±220.05	450.92±121.44	355.52±130.15	133.83±147.25	269.57±232.90
Tb.Th (um)	0.04±0.01	0.06±0.00	0.05±0.01	0.07±0.03	0.06±0.01
Tb.Sp (um)	0.07±0.03	0.09±0.03	0.08±0.02	0.06±0.02	0.08±0.03
Tb.N (1/um)	14.09±9.32	9.57±1.01	10.99±1.08	10.49±4.88	9.71±1.30
Total Porosity (%)	46.21±20.82	41.49±6.06	47.48±5.85	36.93±7.29	40.76±5.58

Table 6.2: Quantitative morphometry indices evaluated from the microCT analysis of bone formation within the central 60% volume of the osteotomies. All values are the mean±SD.

6.3.4 Histomorphometric analysis of osteotomy healing

At the x1 magnification scale, there was a trend for a smaller callus area at the mid-sagittal region, being significantly smaller for VEGF-AMD group only (p=0.029) (Figure 6.11), and overall tissue composition is shown in figure 6.12 and table 6.3.

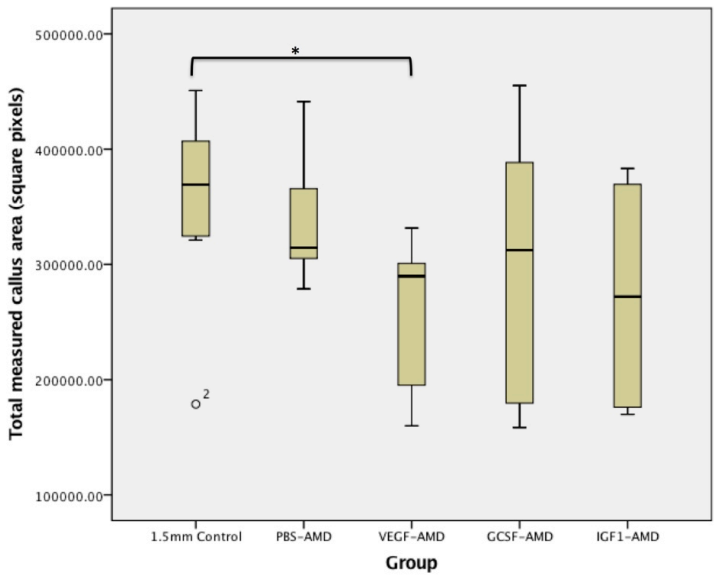

Figure 6.11: Boxplot showing the absolute measured area (square pixels) between the two innermost fixator pin tract holes, measured at 1x magnification. * represents significance p<0.05.

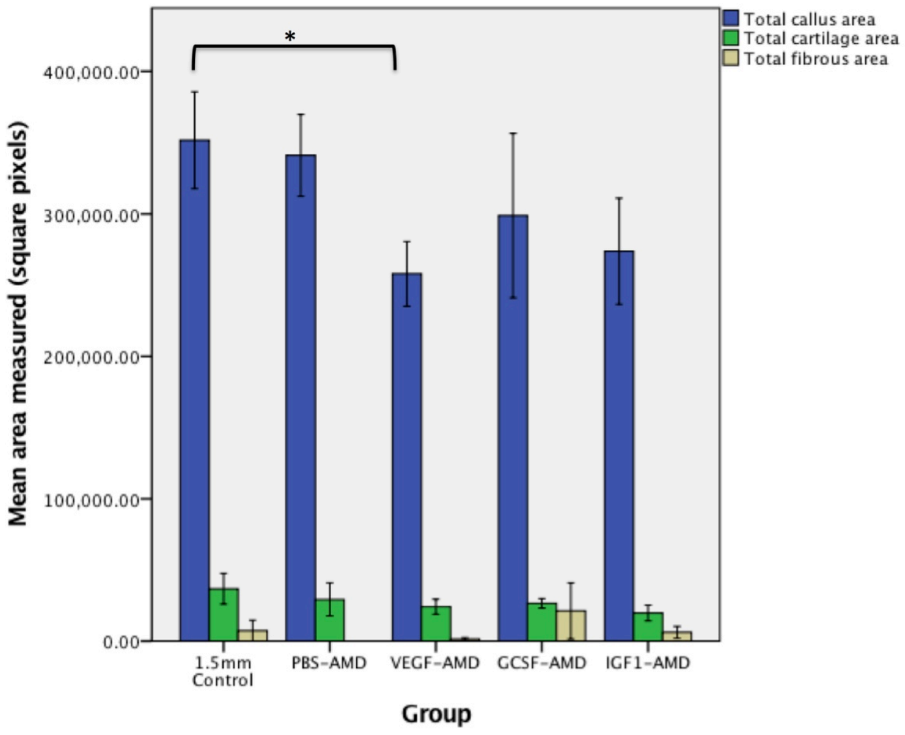

Figure 6.12: Mean±SEM absolute measured area (square pixels) of different tissue types between the two innermost fixator pin tract holes, measured at 1x magnification. * represents significance p<0.05.

TISSUE AREA (square pixels)	1.5mm Control	PBS-AMD	VEGF-AMD	GCSF-AMD	IGF1-AMD
Total callus	351681±89789	341085±64261	257928±64144	298808±128985	273779±91089
Bone	307513±98801	311770±46801	232199±59324	251017±113340	247786±102675
Cartilage	36839±28385	29315±26005	24226±14988	26596±7566	19796±13590
Fibrous	7329±19390	0±0	1504±2799	21195±44140	6198±10069
TISSUE AREA (%)					
Bone	85.9±90.9	91.9±5.5	90.0±4.3	89.5±4.1	90.4±8.8
Cartilage & fibrous combined	14.1±9.1	8.1±5.5	10.0±4.3	10.5±4.1	9.6±8.8

Table 6.3: Mean±SD tissue area measured (square pixels), showing histomorphometric characteristics of the tissue in between the two innermost fixator pin tract holes at x1 magnification.

The 2.5x histomorphologic analysis did not show any significant results, however clear trends were seen which corroborated the microCT data (Figures 6.13-6.17). The percentage cartilage (p=0.053) and percentage fibrous tissue (p=0.059) trended towards significance (KK test). Levene's test for equality of variances did not show a significantly reduced data spread between the control group and PBS-AMD, or GCSF-AMD or IGF1-AMD, however, there was a difference between control and VEGF-AMD for bone (p=0.032) and fibrous tissue (p=0.026), showing a reduction in variation.

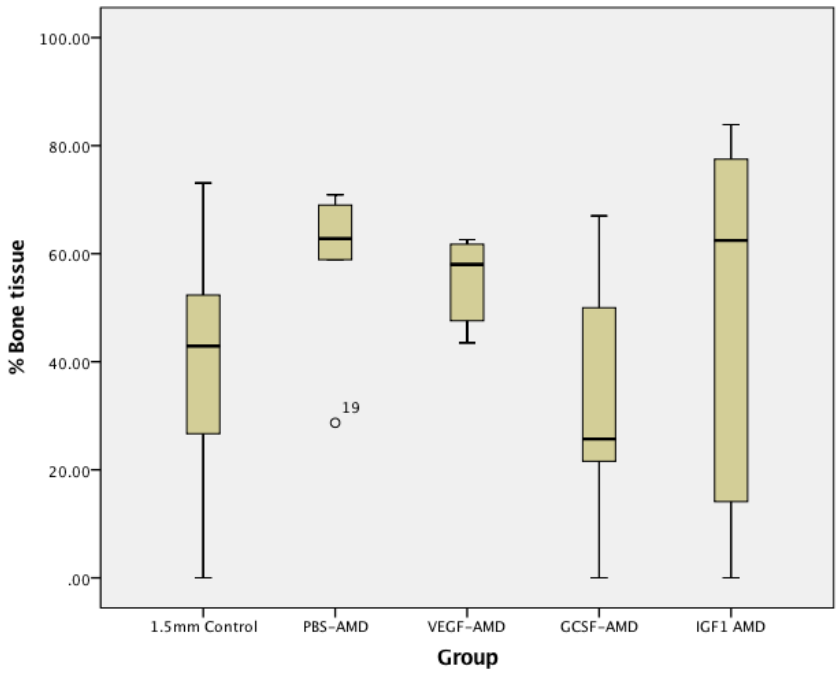

Fig 6.13: Boxplot showing the % bone formed within the osteotomy from 2.5x magnification histomorphometry.

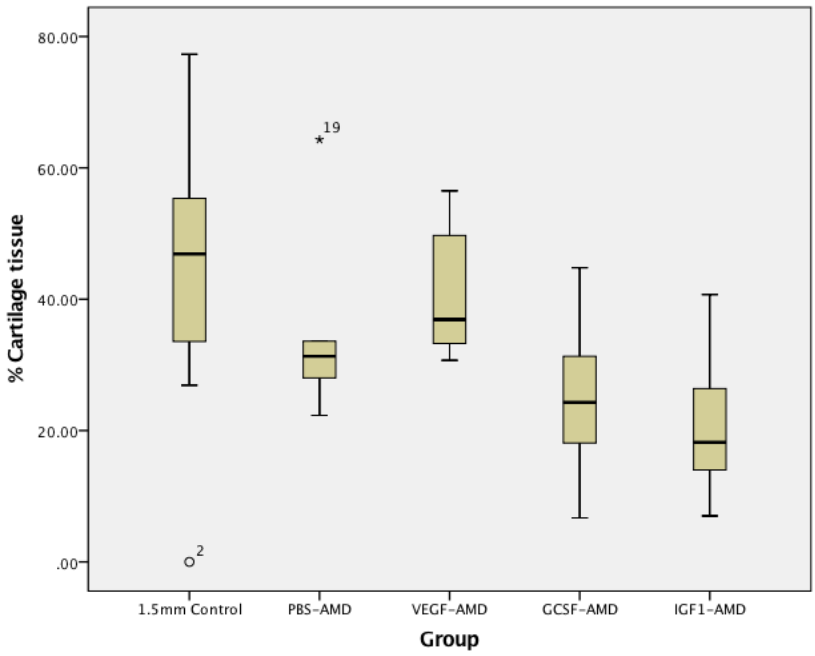

Figure 6.14: Boxplot showing the % cartilage formed within the osteotomy from 2.5x magnification histomorphometry.

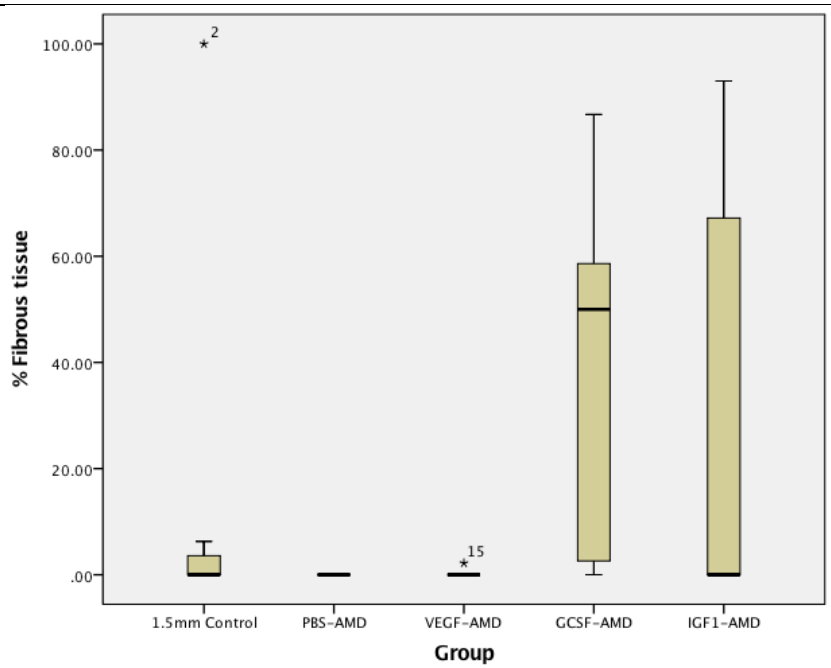

a

b

Figure 6.15: Boxplot showing the % fibrous tissue formed within the osteotomy from 2.5x magnification histomorphometry

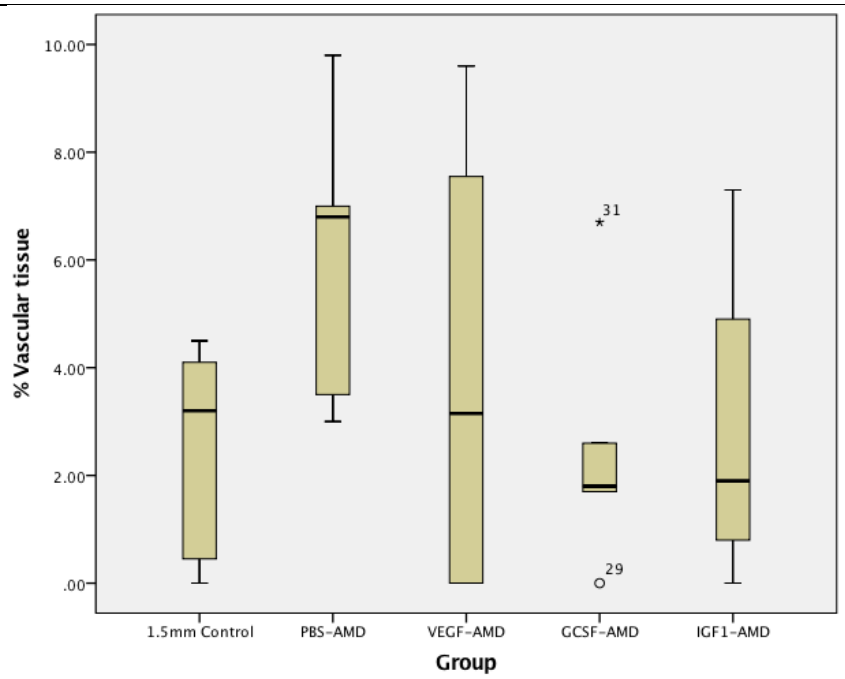

Figure 6.16: Boxplot, showing the % vascular tissue formed within the osteotomy from 2.5x magnification histomorphometry.

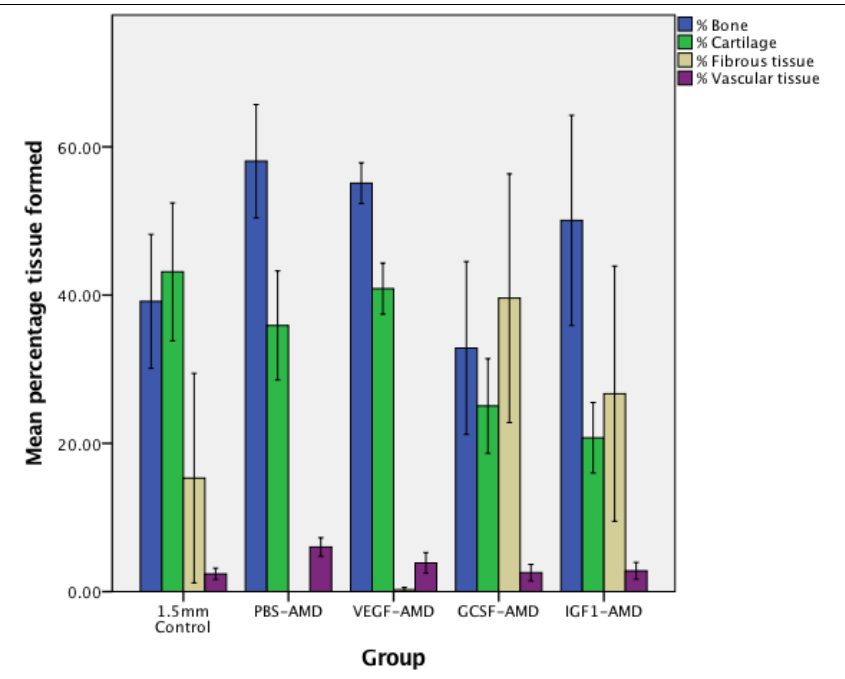

Figure 6.17: Mean±SEM percentage tissue formed within the osteotomy from 2.5x magnification histomorphometry.

Trends for increased bone formation were associated with decreased cartilage, whilst the worse performing groups had an increase in fibrous tissue with decreased bone and cartilage formation (Figure 6.17 and Table 6.4). The level of vascularisation of the tissues was not

significantly different, however, animals in the GCSF-AMD group had the lowest levels of vascularisation, whilst groups with more bone formation had higher levels of vascularisation (Figure 6.16). Notably, PBS-AMD, which had the highest levels of bone and vascular tissue, had reduced cartilage and no fibrous tissue (Figure 6.17). However, in other groups cartilage formation was increased, suggesting conversion to bone by endochondral ossification. The next highest bone formation was seen in VEGF-AMD, which also showed a low level of fibrous tissue and higher level of vascular tissue on histomorphometric analysis. Representative images of the histology are shown for 1.5mm control (Figure 6.18), PBS-AMD (Figure 6.19), VEGF-AMD (Figure 6.20), GCSF-AMD (Figure 6.21 and 6.22), and IGF1-AMD (Figure 6.23).

% Tissue	1.5mm Control	PBS-AMD	VEGF-AMD	GCSF-AMD	IGF1-AMD
Bone	39.1±23.9	58.1±17.1	55.1±7.8	32.8±26.1	50.0±34.7
Cartilage	43.1±24.6	35.9±16.5	40.9±9.8	25.0±14.3	20.7±11.6
Fibrous	15.3±37.4	0.0±0.0	0.3±0.8	39.6±37.5	26.7±42.2
Vascular	2.4±2.0	6.0±2.8	3.9±3.9	2.6±2.5	2.8±2.8
Combined bone & cartilage	82.3±36.4	94±2.8	96±3.7	57.9±38.8	70.8±40.3

Table 6.4: Histomorphometric percentage area of tissue formed within the original osteotomy gap as evaluated at x2.5 magnification. All data expressed as mean±SD.

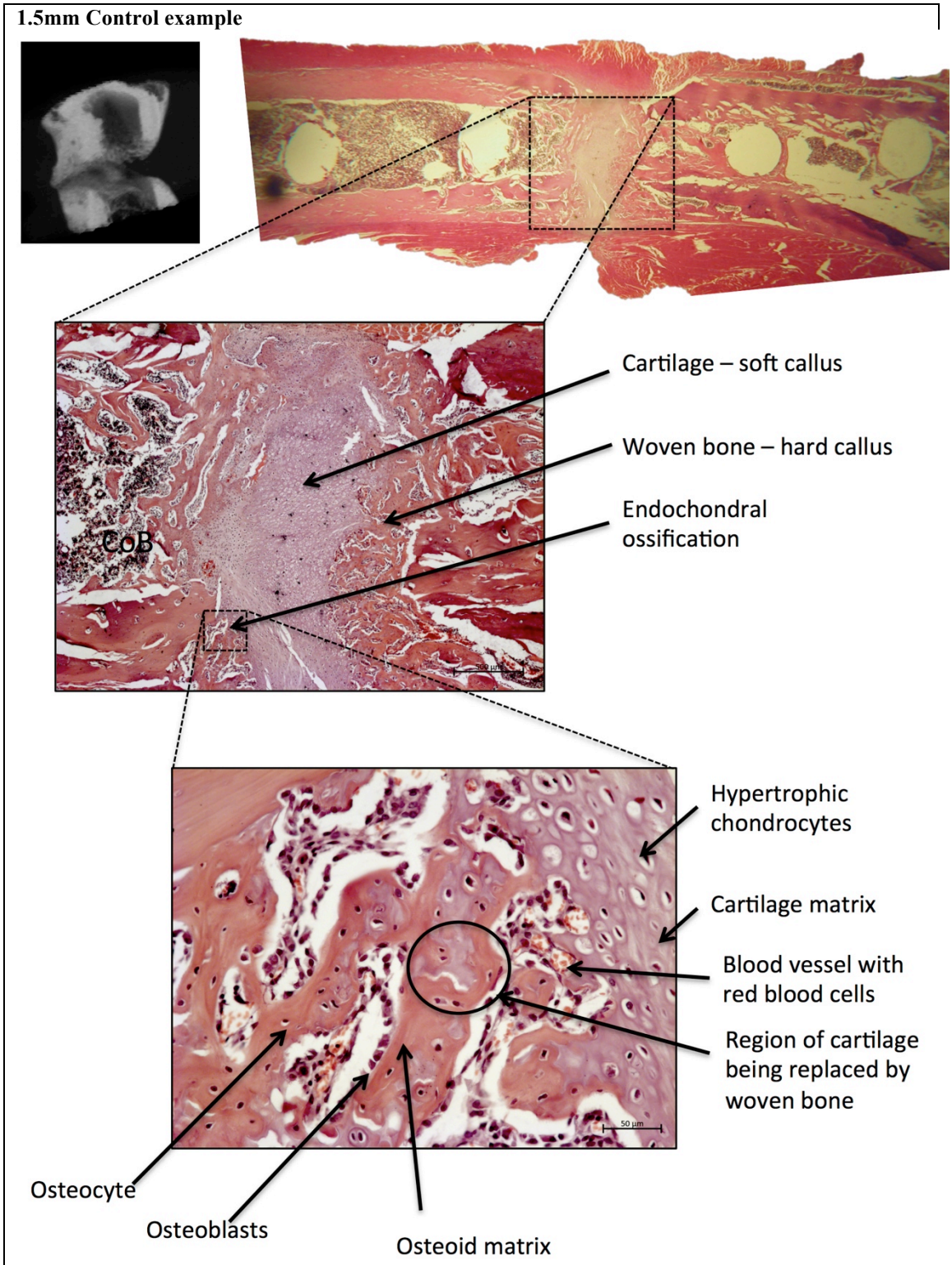

Figure 6.18: Histology images taken from a mid-sagittal 5um slice stained with H and E, from a 1.5 Control example, at x1, x2.5 and x20 magnification from top to bottom. A microCT reconstruction with a mid-sagittal reveal of the same sample is also shown. CoB = cortical bone.

PBS-AMD example

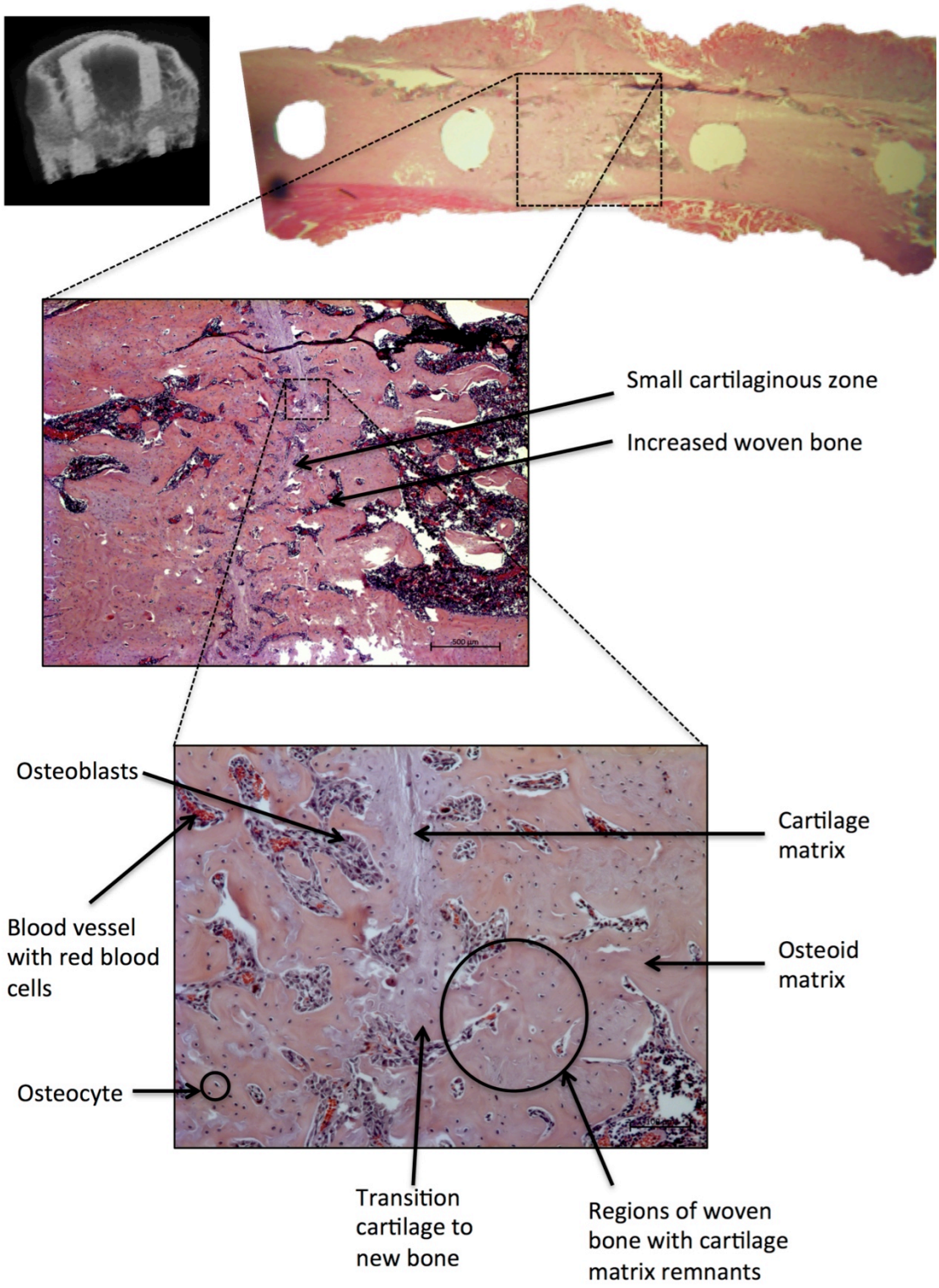

Figure 6.19: Histology images taken from a mid-sagittal 5um slice stained with H and E, from a PBS-AMD example, at x1, x2.5 and x10 magnification, from top to bottom. A microCT reconstruction with a mid-sagittal reveal of the same sample is also shown.

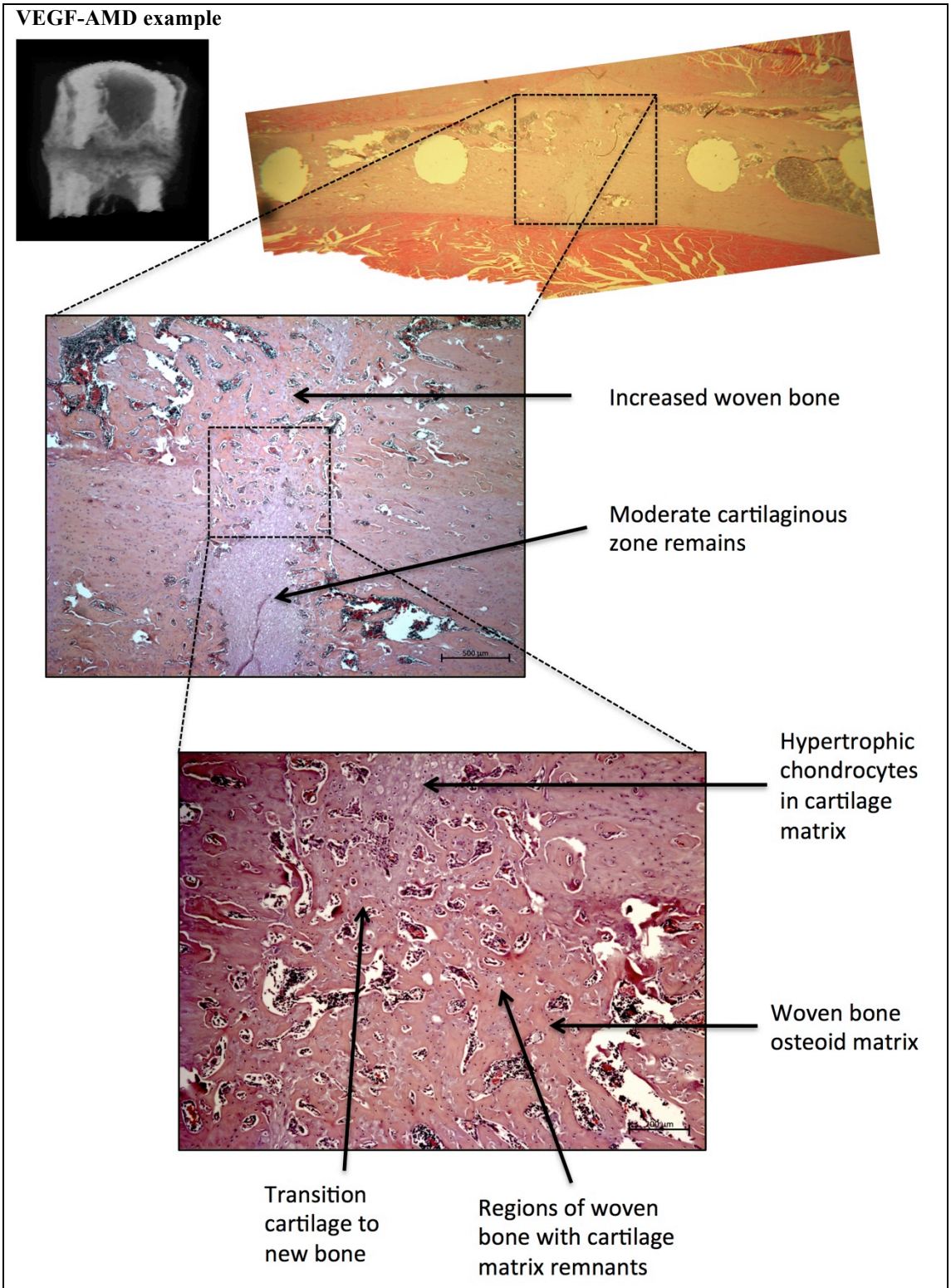

Figure 6.20: Histology images taken from a mid-sagittal 5um slice stained with H and E, from a VEGF-AMD example, at x1, x2.5 and x5 magnification, from top to bottom. A microCT reconstruction with a mid-sagittal reveal of the same sample is also shown.

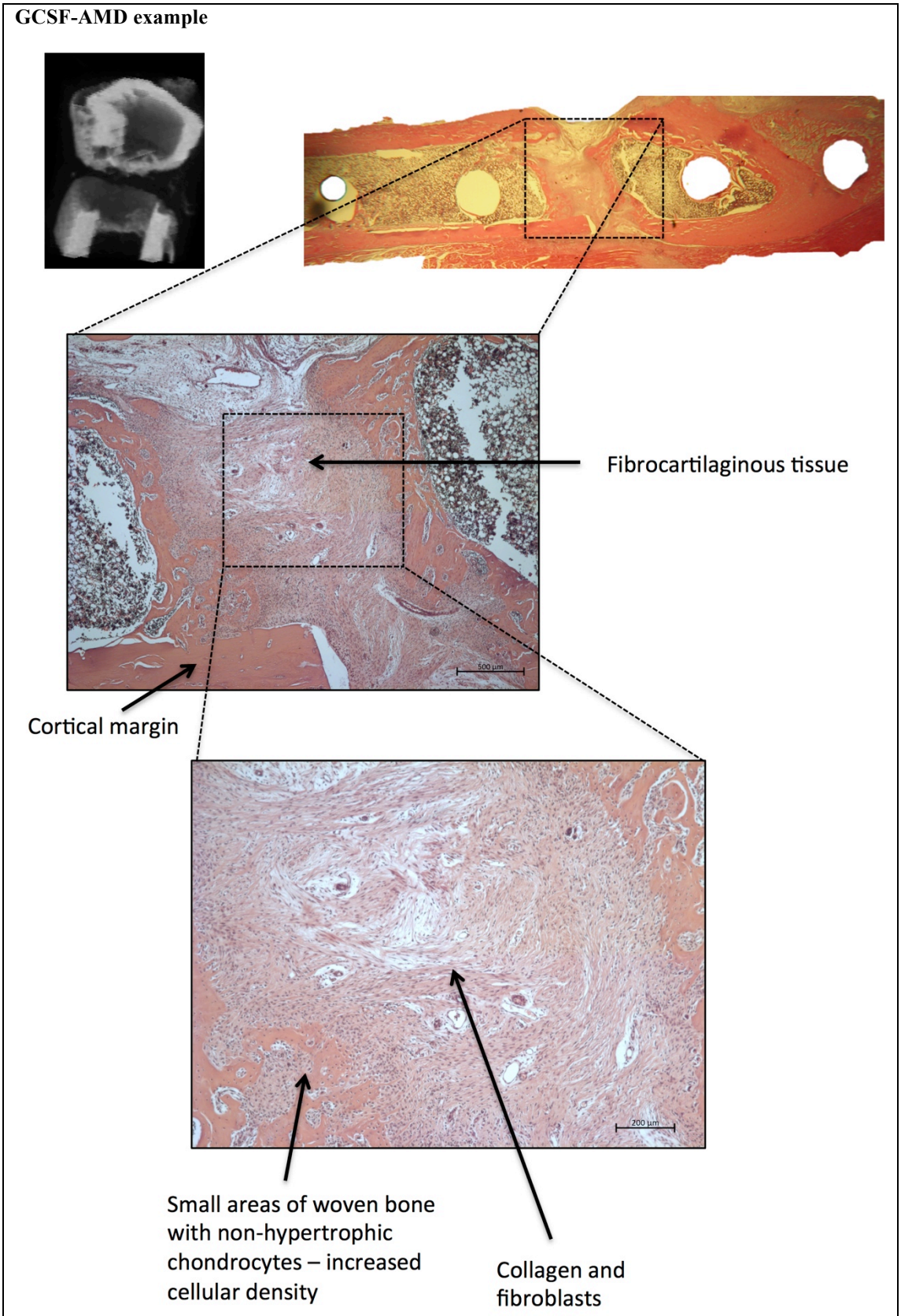

Figure 6.21: Histology images taken from a mid-sagittal 5um slice stained with H and E, from a GCSF-AMD example (GCSF-AMD 3), at x1, x2.5 and x5 magnification, from top to bottom. A microCT reconstruction with a mid-sagittal reveal of the same sample is also shown.

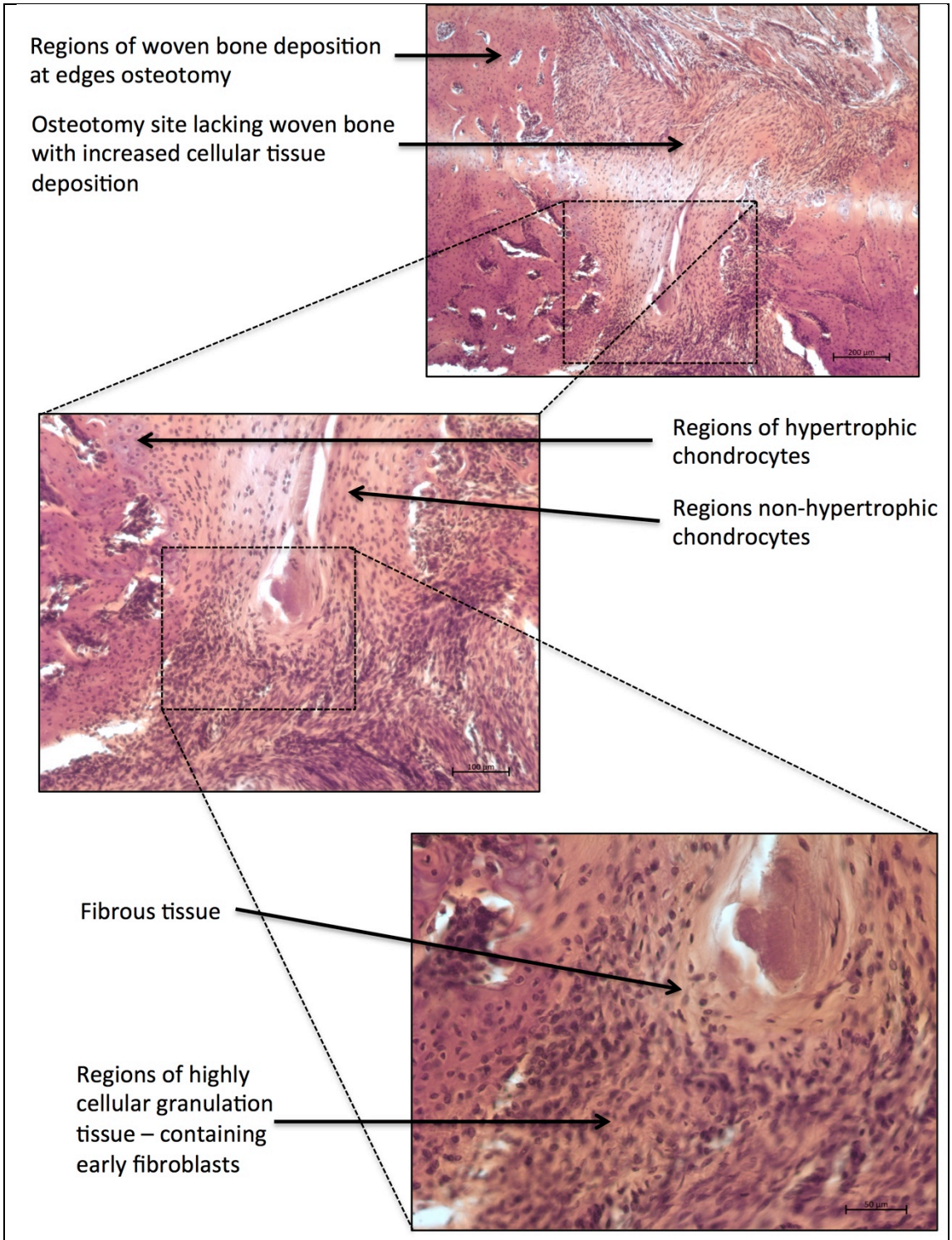

Figure 6.22: Histology images taken from a mid-sagittal 5um slice stained with H and E, from GCSF-AMD 5, at x5, x10 and x20 magnification from top to bottom, showing the marked cellularity and lack of hypertrophic chondrocytes.

IGF1-AMD example

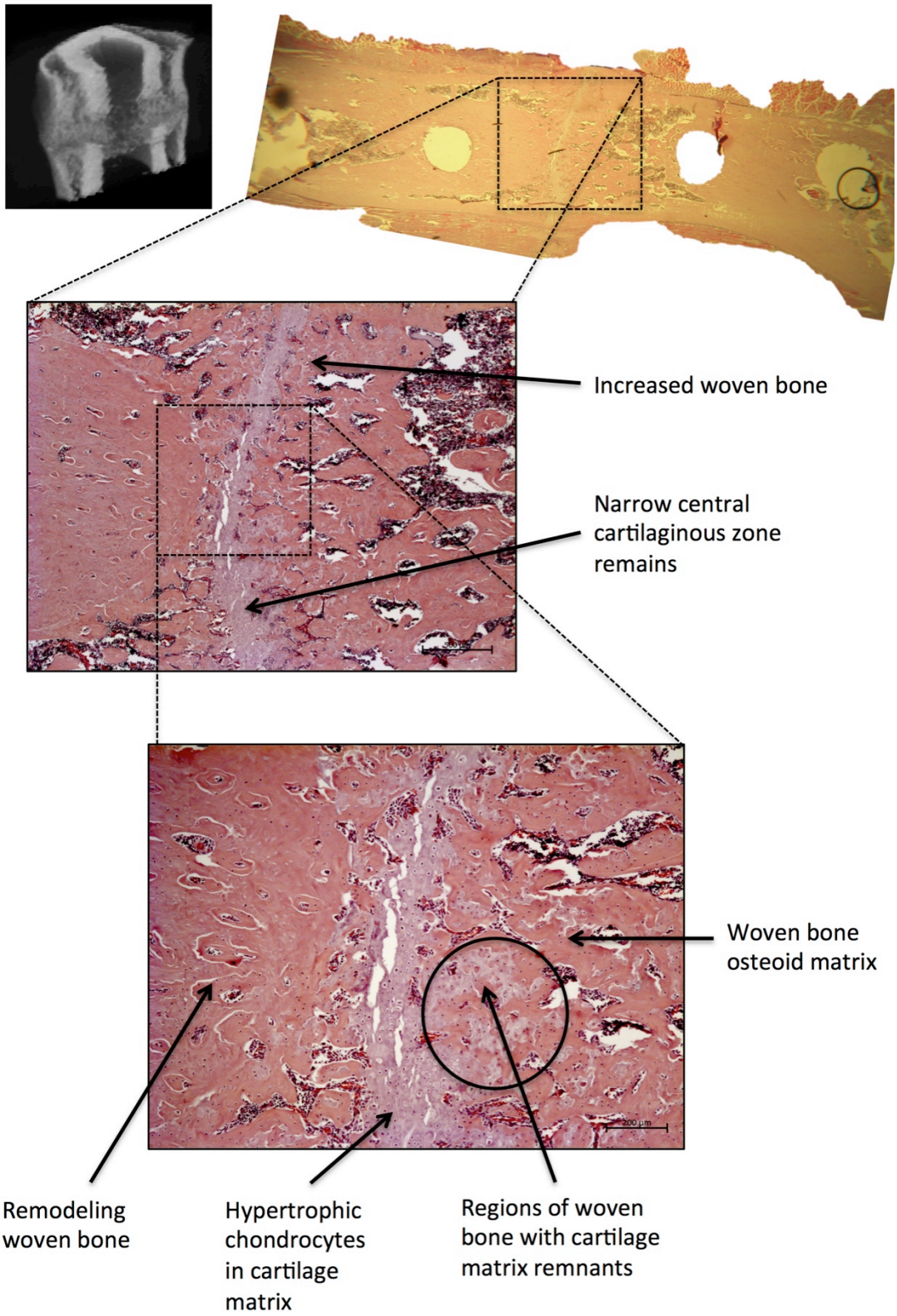

Figure 6.23: Histology images taken from a mid-sagittal 5um slice stained with H and E, from a IGF1-AMD example (IGF1-AMD 5), at x1, x2.5 and x10 magnification, from top to bottom. A microCT reconstruction with a mid-sagittal reveal of the same sample is also shown.

6.4 DISCUSSION

6.4.1 Overview of results

Blood circulating skeletal progenitors were first described by Paget in 1863 (Chesney & Bucala 1997) and have been evaluated in more detail since (Kuznetsov et al. 2001; Zvaifler et al. 2000). Patients with fractures have increased numbers of circulating osteoprogenitor stem cells (Alm et al. 2010) and EPCs (Ma et al. 2012) and parabiotic mouse studies support the mobilisation of progenitors to a fracture site (Kumagai et al. 2008). It is assumed that stem cells are mobilised from the bone marrow, however they could also be from other stem/progenitor niches, such as the periosteum or muscle (Knight & Hankenson 2013). The exact mechanism of contribution of the blood mobilised EPCs and MSCs to fracture healing is not clear however. They may have contributed to blood vessel or skeletal tissue formation directly or they may have provided immunomodulatory and trophic influence on tissue resident cells. In any case, it is clear that antagonising the SFD1-CXCR4 axis, which regulates stem/progenitor cell niches and facilitates mobilisation, was able to increase fracture healing and is worth further study.

There is evidence for the influence of SDF1-CXCR4 on fracture healing from a range of species. In human distraction osteogenesis procedures using Ilizarov fixators, circulating SFD1 levels were increased two to three days after initial osteotomy and remained elevated during the distraction period (Lee et al. 2010). A mouse ulna stress fracture model also demonstrated increases in fracture site SDF1 at four days (Kidd et al. 2010), suggesting an importance in early fracture healing, probably in recruitment of MSCs and EPCs. Increased SDF1 mRNA expression in the periosteum of healing bone indicates a likely role in early intramembranous bone formation, and fracture healing could be reduced with SDF1 blocking antibodies or by genetic reduction of SDF1 expression (Kitaori et al. 2009).

There is also evidence for a role of SDF1 in endochondral ossification, with increased SDF1 expression in pre-hypertrophic and hypertrophic chondrocytes of rib fractures. SDF1 double knock-out mice have shorter humeri, and in particular, a reduced hypertrophic zone (Murata et al. 2012) indicating a role of SDF1 in hypertrophic cartilage derived bone formation. Expression of SFD1 has been localised to the callus and in particular hypertrophic and immature cartilage near pre–existing cortical bone. Notably, SDF1 was expressed in areas where hydroxyprobe binding was high, indicating a role of hypoxia (Toupadakis et al. 2012). An upstream influence of hypoxia inducible factor 1alpha subunit (HIF1α) is suggested to drive SDF1 expression in fractures (Yellowley 2013). Under hypoxic conditions the breakdown of HIF1α is reduced (Hirota & Semenza 2006) and elevating concentrations of

HIF1α increases SDF1 expression and hence increases stem/progenitor recruitment (Ceradini et al. 2004). As fracture sites are known to be hypoxic (Heppenstall et al. 1975; Brighton & Krebs 1972), and reduced oxygen tension at endosteal surfaces is thought to increase SDF1 expression in the bone marrow (Eliasson & Jönsson 2010), it is plausible that the hypoxic fracture environment could be an instigator of raised SDF1 expression. The resultant SDF1 chemotaxis gradient is then surmised to drive trafficking and homing of stem and progenitors to the site of injury (Yellowley 2013).

Otsuru et al., using a bone marrow transplanted parabiotic mouse model with GFP labeled marrow, showed the role of CD45 negative osteoprogenitors being mobilised into the peripheral blood due to tissue injury, and under the influence of SDF1, the cells migrated to bone forming sites and became osteoblasts (Otsuru et al. 2008). Bioluminescence studies showed that MSCs expressing luciferase migrated to a tibial fracture site, and by sorting them for CXCR4, they showed its role in directed migration (Granero-Moltó et al. 2017). Not only did they show migration, they also demonstrated a positive effect of the trafficked MSCs with increased cartilage and bone content associated with callus morphology changes. The healing callus was typically bigger with increased cartilage in the treated group, however, this was at significantly earlier time points than in my study. Histologically, there were increased chondrocytes and notably increased hypertrophic chondrocytes, indicating increased endochondral ossification with MSC transplantation. Using Lac Z-tagged MSCs, the transplanted cells were seen along the margins of the woven bone as osteoblasts, but were not seen in the periosteal callus. A potential role for the MSCs in periosteal callus formation was suggested by their expression of BMP-2 driving paracrine bone formation.

My study was the first to evaluate the potential effects of CXCR4 antagonism on fracture healing in rats. Critically, my study evaluated the potential to rescue a compromised healing environment, rather than simply augmenting uncomplicated healing. *In answer to my question and hypothesis for this chapter; it was possible to improve compromised fracture healing using endogenous stem and progenitor mobilisation.* All strategies tested other than GCSF-AMD improved fracture healing, with an increase in radiographic union and decrease in non-union compared with controls. AMD3100 alone gave significant increases in bone formation as measured on microCT, with a bigger (proportionally mineralised) callus compared to controls. IGF1-AMD showed a relatively more mineralised callus with a significant increase in % bone, and VEGF-AMD showed a trend for increased bone formation over the control. Intriguingly, the intragroup spectrum of healing, from non-union to union, as seen in the controls, was also seen in the treated groups, with no strategies providing a homogenous result. If it is reasonable to conclude that individuals have variation in healing potential, as noted in the previous chapter, and mechanical loading from

individual activity will influence healing, it is not surprising that my work in this chapter showed a similar heterogeneity. It is feasible that increasing the pool of available stem cells for fracture healing is likely to be more beneficial in those with inherently better biological healing (Jepsen et al. 2008). In any case, the treatment does appear to benefit most individuals by moving them further along the healing scale. Ideally, a standardisation or even quantification of physical activity, and or inbred strains would be useful to clarify the causes of the heterogeneity.

In my study, microCT was the only modality to show significant increases in healing with certain mobilisation strategies. MicroCT also provides information on the hard callus microstructure and quantitative morphometry gives different indices of the microstructure, including trabecular thickness, separation and number, many of which are predictive of mechanical strength (Bouxsein et al. 2010). My scans were performed at 5um and currently <10um is recommended to achieve sufficient resolution to calculate these indices (Casanova et al. 2014). This high-resolution 3D imaging showed interesting variations not only in the overall amount of new bone formed but also in its structure. The trabecular thickness and the space between trabeculae (trabecular separation), provides commentary on the nature of the woven bone formed within the osteotomy. All treatment groups other than GCSF-AMD had increased trabecular separation with increased trabecular thickness, implying the woven bone formed was more porous, but the individual struts were thicker. Perhaps this represents a more advanced or more rapidly developed stage of endochondral ossification. In any case, AMD3100 alone had significantly more bone formed than control, and IGF1-AMD significantly increased the % bone content of the callus.

6.4.2 PBS-AMD group

The most effective treatment group was AMD3100 alone (PBS-AMD group). This group had the highest bone formation on microCT and histomorphometry. The efficacy of AMD3100 used alone has been shown previously in a mouse femoral fracture model, whereby AMD3100 was given for three days after fracture. At 24 days the callus was significantly larger, however by 84 days it was significantly smaller than controls (Toupadakis et al. 2013). A single injection of AMD3100 has also been shown to improve intramedullary trabecular bone regeneration after ablation at three weeks (McNulty et al. 2012). My work also showed structural change in the bone compared with control, with thicker trabeculae and increased trabecular spacing of the woven bone. This would likely correlate with increased mechanical strength. AMD3100 alone also had the highest percentage vascular tissue with the lowest fibrous and highest bone composition histologically, consistent with bone formation requiring vascular invasion to reduce the

hypoxia to a level necessary for bone to be synthesised (Einhorn & Gerstenfeld 2014; Stegen et al. 2015).

Toupadakis et al. showed using flow cytometry that AMD3100 alone was successful at mobilising haematopoietic stem cells, EPCs and MSCs (Toupadakis et al. 2013). Pitchford's work on the other hand, measured CFUs for EPCs, MSC and haematopoietic stem cells, and showed that VEGF combined with AMD3100 was more effective than AMD3100 alone in terms of mobilising MSCs and EPCs (Pitchford et al. 2009). Pitchford did not show MSC mobilisation with AMD3100 alone, whereas others have (Toupadakis et al. 2013; McNulty et al. 2012). Clearly there is some contradiction in the literature when cells are isolated in terms of isolation and culture techniques, surface markers evaluated, and hence these types of studies have limited merit when translating to a bone healing therapy. A critical limitation is that these studies only inform you about the populations you choose to look for and by the criteria you propose. As my study showed significantly increased bone formation with AMD3100, it seems whatever the combination and number of cells it mobilised, there was a beneficial effect.

6.4.3 Osteotomy influence – a role of endogenous growth factors?

When AMD3100 was used alone, exogenous growth factors were not co-administered precluding their direct humoral influence on bone formation, or their potential role as a bone marrow stem cell modulator. From the results seen with AMD3100 alone, this would imply that the exogenous growth factors are not necessary in an *in vivo* system of fracture healing. Again, the shortcomings of previous single time-point studies evaluating a selected population(s) (Pitchford et al. 2009; Kumar & Ponnazhagan 2012) shows that *in vivo* evaluation is necessary to evaluate a translational therapy.

A key difference between some *in vitro* mobilisation studies (Pitchford et al. 2009), the *in vitro* studies I completed in chapter 3, and the work in this chapter, is the presence and influence of the osteotomy. It is well know that fractures release increased levels of growth factors (Devescovi et al. 2008; Lieberman et al. 2002). *In vivo* work has demonstrated a range of growth factors associated with the fracture site (Simpson et al. 2006), including platelet derived growth factor, fibroblast growth factor, transforming growth factor, bone morphogenic proteins (BMP)s, and notably for my work, VEGF and IGF1. Clinically, VEGF is increased in human patients with long bone fractures within the first couple of weeks, lasting up to six months post trauma (Sarahrudi et al. 2009). Experimentally, VEGF mRNA transcripts are increased in a rat femoral drill hole model with temporal patterns of splice variants of VEGF. In this model, VEGF was detected from one day after fracture and remained high for 11 days before slowly declining. The timing between fracture and surgical

stabilisation with internal fixation also influences the levels of VEGF seen, with longer delays and more instability associated with higher levels of VEGF (Dong et al 2014).

When VEGF is exogenously administered in combination with AMD3100, the expectation is VEGF has a priming effect on the bone marrow. This effect is mediated not through up-regulation of MSCs or EPCs in the bone marrow, nor by altering CXCR4 expression, but by reducing the ability of haematopoietic stem cells to migrate to SDF1 by activating their cell cycling through VEGF receptor 1. It is then presumed that the reduced haematopoietic migration allows for increased MSC and EPC migration (Pitchford et al. 2009). As AMD3100 was given five days after osteotomy in my protocol, it is conceivable that endogenous VEGF was present and potentially priming the bone marrow niche in the AMD3100 only group.

IGF1 is produced by bone matrix, osteoblasts and chondrocytes (Lieberman et al. 2002), and IGF1 has been shown to be increased in both human and rodent fractures (Andrew et al. 1993; Edwall et al. 2009). In rodent studies, IGF1 was expressed by chondrocytes and osteoblasts, and was elevated by the initial measurement (day four) and had peaked at day eight (Edwall et al. 2009). Research from humans also showed no expression of IGF mRNA in the earliest stages of fracture haematoma. IGF1 was detected in some chondrocytes but only once osteoblasts appeared (Andrew et al. 1993). As IGF1 does not increase as early as VEGF, it is difficult to know if it was likely to have been present when the AMD3100 injection was given. It is possible that IGF1 would have been present to some extent, which may have further influenced the effect of AMD3100 on mobilisation and healing. Indeed, it may have been the proportions of different growth factors and their temporal relationships when combined with AMD3100 that facilitated the promotion of bone formation.

6.4.4 IGF1-AMD group

IGF1-AMD gave a significantly improved % bone formed as detected using microCT, with a callus volume similar to the controls. Kumar et al. showed IGF1-AMD mobilised slightly more CFU-f/ml than VEGF-AMD. However their study was quite limited as they only counted the CFU-Fs and looked at bi-differentiation from the IGF1-AMD group only (Kumar & Ponnazhagan 2012). Pitchford et al. did not evaluate IGF1 in combination with AMD3100, however their work comprehensively evaluated mobilisation of MSCs, EPCs and hematopoietic progenitor cells, and further they looked at cell surface markers for lineage assessment, in addition to differentiation testing (Pitchford et al. 2009). Kumar however, took the IGF1-AMD protocol further by evaluating its therapeutic potential to mobilise MSCs in a mouse fracture model. Using DXA, they showed a significant increase in fracture site bone mineral density, similar to my increased % bone formation, however, their results

showed IGF1 alone also gave a moderate improvement in bone density, whereas AMD3100 alone did not (Kumar & Ponnazhagan 2012).

IGF1 has a critical role in bone development and maintenance and hence can influence fracture healing. Growth hormone drives IGF1 synthesis from the liver and is essential for longitudinal bone growth at the physes with peaks at puberty (Spencer et al. 1991), and growth hormone has been shown to increase mechanical fracture strength in rats (Bak et al. 2009). IGF1 is thought to act through paracrine and autocrine mechanisms on bone cell differentiation (Hock et al. 1988; Mochizuki et al. 1992) and low levels of IGF1 are associated with reduced bone density. Osteoblast maturation and function is a complex process, but a role of IGF1 in promoting osteoblastogenesis and reducing bone cell apoptosis through β-catenin Wnt signaling is suggested (Kawai & Rosen 2012). IGF1 has also been shown to increase osteogenesis through regulation of marrow derived osteoblasts, and can also drive osteogenic differentiation of human MSCs (Levi et al. 2010).

Although it is difficult to distinguish the inherent effects of IGF1 on bone itself as apposed to the mobilising effects of IGF1 combined with AMD3100, Kumar et al. comprehensively demonstrated that although IGF1 did improve fracture healing, probably through humoral signaling mechanisms, the combination was by far more influential and stem cell mobilisation was thought to underlie the enhanced healing (Kumar & Ponnazhagan 2012). They determined that MSCs cultured in IGF1 had increased phospho-Akt, phospho-Erk1/2 and phospho-smad2/3 activity and hence upregulated bone forming pathways. To determine the effects of IGF1-AMD on stem cell function further, they isolated mononuclear cells from IGF1 with AMD3100 treated mice, and compared them to an AMD3100 treatment group. CFU formation, osteogenic and adipogenic differentiation were evaluated and there was increased staining indicative of increased differentiation potential in the IGF1 with AMD3100 group. They also showed increased proliferation and migration *in vitro*. They speculated that the increase in CFUs indicates the IGF1 had a priming effect on the bone marrow, increasing the number of available MSCs in the bone marrow to be mobilised, and hence the AMD3100 treatment combined with IGF1 was more efficacious at increasing a pool of more potent MSCs (Kumar & Ponnazhagan 2012). Although my study showed significant increases in % bone formation using microCT, the histomorphometry revealed relatively high levels of fibrous tissue within the callus. This outcome may be due to 2/5 animals in this group developing an atrophic non-union, whereas the other 3/5 had radiographic union.

6.4.5 GCSF-AMD group

GCSF was one of the first cytokines identified and was rapidly adopted into clinical medicine as a means to boost neutrophil populations in chemotherapy patients. Later, its ability to mobilise haematopoietic stem cells from the bone marrow into the peripheral circulation was exploited for stem cell transplantation (Bendall & Bradstock 2014). The mobilisation of stem cells by GCSF involves increased production of CD34+ cells within the bone marrow and proteolytic cleavage of VCAM-1 (Lapidot & Petit 2002), and SDF1 (Lévesque et al. 2003). In terms of mobilisation, Pitchford et al. showed GCSF combined with AMD3100 to be as effective as AMD3100 alone for mobilising MSCs, poorer than AMD3100 alone for EPCs and extremely potent at mobilising haematopoietic progenitor cells. The haematopoietic stem cells mobilised by GCSF were identified in the G0/G1 cell cycle phase, whereas bone marrow niche haematopoietic stem cells are actively cycling and probably unable to migrate (Pitchford et al. 2009). The question therefore, is whether it is a reduction in EPCs, or a flooding of HSCs that resulted in the impaired healing in my study? Pitchford et al. also showed that GCSF-AMD combinations gave maximal neutrophil mobilisation and this could potentially influence the inflammatory environment at the fracture site. A comparison of CD34+ cells to a total mononuclear cell fraction transplanted into a fracture gap showed the mononuclear mixed population had poorer healing, possibly due to increased inflammation (Fukui et al. 2015), and hence increased neutrophil migration and inflammation may have had a role. Additionally, if MSCs are important for bone regeneration, it would not be unexpected that their suppressed mobilisation with GCSF-AMD did not improve fracture healing.

Haematopoietic precursors mobilised preferentially by GCSF-AMD may have also provided precursors to osteoclasts (Fujikawa et al. 1996) and hence the reduction in bone volume and increased atrophic type non-unions (3/6) seen in this group. Histomorphometry showed a reduction in hypertrophic cartilage and bone formation, with a large increase in fibrous tissue. The GCSF-AMD samples also did not show as much chondrocyte hypertrophy as the other treated samples and as chondrocyte hypertrophy is a critical step to allow calcification, vascularisation and osteoblast differentiation (Babarina et al. 2001), it is therefore not surprising there was reduced bone formation. It is also possible that GCSF had direct humoral effects that were negative to bone healing, as GCSF has no beneficial effect on osteoblasts and only moderate effect on human endothelial cells (Liu et al. 2016). It is also known that long term clinical administration of GCSF results in osteopenia with associated vertebral fractures, and experimental evidence shows just five days of treatment reduces the number of osteoblasts present (Semerad 2005). Further evaluation of short-term treatment with GCSF in mice showed decreases in endosteal and trabecular osteoblasts, and osteoblast

turnover in the marrow was accelerated by inducing osteoblast apoptosis (Christopher & Link 2008). They also showed that osteoprotegerin was decreased and RANKL remained unchanged suggesting a possible mechanism for increased osteoclast activity from GCSF administration.

Studies using CD34+ cells in part contradict the work of this thesis (Kuroda et al. 2014). Human peripheral blood CD34+ cells have been systemically transplanted into non-healing femoral fractures of immunocompromised rats and fracture healing was significantly improved (Matsumoto et al. 2006). However, this and any similar studies are reliant upon transplantation rather than endogenous mobilisation and therefore only reflect a subset of the cells mobilised by GCSF-AMD. It should also be considered that CD34 is seen on both haematopoietic progenitors and some EPCs, and therefore the EPC fraction may be conferring the reported benefit seen (Atesok et al. 2010; Giles et al. 2017; Lee et al. 2008). Notably, when a mixed mononuclear population rather than a CD34+ selected population was transplanted into a fracture gap, the healing was reduced, associated with increased inflammation (Fukui et al. 2015).

6.4.6 VEGF-AMD group

Hypoxia and subsequent vascularisation of tissues within the fracture site plays a crucial role in progressive fracture healing and VEGF is a potent angiogenesis promoter, with a clear role in endochondral and intramembranous bone formation (Street et al. 2002; Gerber et al. 1999). Local delivery of VEGF in rabbit mandibular defects showed increased density of bone formation, but no difference in the quantity. Vascular development was sustained for longer periods and the consensus was VEGF will have a direct influence on healing, through improved vascularisation, particularly when it is compromised at the outset (Kleinheinz et al. 2005). Blocking VEGF with soluble receptors decreases angiogenesis, bone formation and callus mineralisation, whereas exogenous VEGF enhances vascularisation, ossification and callus formation in mouse femoral and rabbit radial defects (Street et al. 2002). Therefore, exogenous VEGF administration is likely to have both direct and indirect effects on bone formation. VEGF can act indirectly through its receptors on endothelial cells, influencing the development of a new vascular network, which then allows bone orientated stem and progenitors to migrate into the fracture callus and differentiate into osteoblasts (Stegen et al. 2015).

VEGF can also stimulate endothelial cells to produce cytokines that promote differentiation of progenitors down an osteoblastic lineage (Bouletreau et al. 2002). It has also been shown that osteoblasts not only synthesise VEGF but are activated by it, affecting differentiation, proliferation and migration (Street et al. 2002; Midy & Plouët 1994; Deckers et al. 2000;

Mayr-Wohlfart et al. 2002). Histomorphometric assessment of vascularisation was not the objective of this chapter, but notably the most efficacious group in terms of bone formation (PBS-AMD) also had the highest number of blood vessels, although, significant differences were not detected between groups. VEGF-AMD had the second highest percentage vascularised tissue, but the significance of that is difficult to know from this work. Immunohistochemistry analysis would be an option to quantify blood vessel formation in more detail by staining for endothelial markers.

The other question that remains is what was the contribution of mobilised EPCs? Pitchford et al. showed the highest mobilisation of EPCs when VEGF combined with AMD3100 (240 CFUs/ml), however even AMD3100 alone mobilised significant numbers (130 CFUs/ml) over and above no treatment (10 CFUs/ml), as did GCSF combined with AMD3100 (90 CFUs/ml) (Pitchford et al. 2009). This profiling does not explain the variations in healing between the groups, as VEGF-AMD was not the best performing group, however, how these cells may have contributed to the complex process of fracture healing may not be immediately represented by their number.

There is evidence that culturing and transplanting EPCs can improve fracture healing (Matsumoto et al. 2008), with rat models showing significantly increased torsional stiffness and bone formation (Li et al. 2011; Atesok et al. 2010), however, there are issues in the literature with the different culture techniques, criteria for definition and even cell types such as early vs late EPCs (Mund & Case 2011; Patel et al. 2016; Minami et al. 2015). Early EPCs have been shown to be more effective than late in one study for improving fracture healing (Giles et al. 2017). Despite this, CD31 positively expressing cells have been shown to be reduced in older fracture patients, and experimentally, CD31+ cells improved fracture healing in a rat model (Sass et al. 2017).

6.4.7 Conclusion

This chapter suggests a beneficial effect of CXCR4 antagonism using AMD3100, supporting the hypothesis. The exact interaction between AMD3100 alone and when combined with growth factors is less clear and indeed, as seen with GCSF, potentially negative.

The nature of the disturbance to the SDF1-CXCR4 axis is important. Short duration blockade may mobilise more stem and progenitor cells and hence increase the total pool available to the fracture site. However, the homing to the fracture site also relies upon the very interaction being antagonised. The short half-life of AMD3100 (De Clercq 2009) should be beneficial and hence the ‘pulse’ in the early inflammatory phase of fracture healing should have a greater mobilising effect at stem cell niches, rather than significantly

impairing the recruitment of cells to the fracture site, which occurs over days to weeks. However, longer term blockade throughout the period of fracture healing will significantly reduce callus cartilage, callus size and bone formation, with reduced expression of genes associated with endochondral ossification (Toupadakis et al. 2012). It is likely that continued antagonism of the CXCR4 receptor prevents migrating stem and progenitor cells from homing to the fracture site.

In this chapter, I have shown that AMD3100 treatment can influence fracture healing and pre-treatment with growth factors or not, also impacts on the outcome. GCSF-AMD had a negative effect and should be avoided, potentially due to increased inflammation and reduced endochondral ossification at the fracture site (Fukui et al. 2015). Notably, there was no panacea here, as all groups had at least one non-union, however, there were clear and significant improvements in fracture healing in a challenged healing environment. In contradiction to *in vitro* mobilisation studies, AMD3100 was highly effective on its own, which may be in part due to endogenous growth factors being physiologically present at the fracture site, or indeed the actions of the pharmacological antagonism provide sufficient mobilisation of the required cell populations. For clinical translation, this would be beneficial as it is already licensed for use in humans and it avoids the cost and potential risks of oncogenesis associated with some growth factors.

CHAPTER 7: Main Discussion

7.1 Hypothesis & aim

Failed fracture union remains a significant clinical issue. A regenerative medicine approach to improve fracture healing typically involves isolating a source of stem cells with delivery back to the body at a later stage. However, issues remain over the time, effectiveness, costs, disease transmission and donor site morbidity. An alternative is to increase circulating stem/progenitor cell populations endogenously through non-invasive mobilisation and thus increase the cells available to home to, and improve the healing of fractures. The aim of my thesis was to improve fracture healing through endogenous mobilisation of stem and progenitor cells. The main hypothesis was "***antagonism of the CXCR4-SDF1 axis will mobilise stem and progenitor cells into the circulation of rats, and by increasing the available pool of cells early in fracture healing, will improve fracture union"***. Over the course of my thesis I was able to prove my hypothesis.

7.2 Proof of concept: endogenous mobilisation

As MSCs and EPCs have critical roles in fracture healing and have improved fracture healing when transplanted (Kadiyala et al. 1997; Bruder et al. 1998; Ward et al. 2007; Kuroda et al. 2014), it was important to establish a mobilisation protocol that increased the availability of these cells. Pitchford et al. published the most comprehensive evaluation of peripheral mobilisation of different stem/progenitor populations. They established that VEGF combined with AMD3100 was the most effective protocol to mobilise MSC and EPCs into the peripheral circulation, compared with AMD3100 alone or when combined with GCSF. Their landmark study was in mice, whereas a rat model was my preferred test system due to their size; the larger rat allowed for a consistent and reproducible fracture that could be stabilised by an external fixator, to give a predictable mechanical environment for testing my hypothesis. At the time, AMD3100 and VEGF had not been evaluated in rats and therefore an initial proof of concept was required. Although SDF1 and CXCR4 expression had been confirmed in the rat and had also been associated with fractures, mobilisation data was only available in mice (Pitchford et al. 2009; Toupadakis et al. 2013; Kumar & Ponnazhagan 2012; McNulty et al. 2012). One rat mobilisation study had been published where Tacrolimus (an immunosuppressive drug) and AMD3100 were used and improved the healing of skin wounds. They associated this improvement with an increase in circulating "Lin-, c-Kit, CD34+, CD133+ cells and Lin- Triple positive" stem cells (Lin et al. 2014), but not MSCs.

Chapter 3 provided 'proof of concept' of endogenous mobilisation of stem and progenitor cells using VEGF combined with AMD3100 in a rat model. My hypothesis, based on the

work of Pitchford et al. was that VEGF combined with AMD3100 would significantly increase circulating MSCs and EPCs as measured by CFU-F and EPC CFUs in culture. Although I did show a significant increase in CFUs, the actual numbers of CFUs/ml were low with 3/ml for PBMSCs and PBEPCs, compared with Pitchford's work which had greater mobilisation of 15 MSC CFUs and 230 EPCs CFUs/ml (Pitchford et al. 2009). Although in chapter 2 the techniques to isolated and evaluate bone marrow MSCs worked well, the poorer yields for the PBMSCs may indicate a need for further studies where the dose, time and frequency of AMD3100 administration is optimised in order to release a higher number of stem cells. However, the low yields that I obtained may simply reflect a difference in the mobilisation potential in old rats compared with very young mice, which then lead to a low initial seeding density and slow growth (He et al. 2006). Perhaps rats mobilise differently compared to mice due to species variations in the CXCR4 receptor, although the receptor is generally well conserved, with 90% homology between mouse and human (Pawig et al 2015). Difficulty in isolating peripheral blood MSCs have however, been reported previously (Kassis et al. 2006). It also remains unknown at what time point these cells should be mobilised in the fracture healing process.

In chapter 2 I isolated rat bone marrow MSCs and evaluated their cell surface markers, and showed them to be CD34- CD45- CD90+ CD29+, in line with other studies on rats (Fafián-Labora et al. 2015; Fu et al. 2012; Dezawa et al. 2004). These cells could tri-differentiate and were used as my benchmark comparison for mobilised peripheral blood MSCs (PBMSCs). As a comparison for evaluating peripheral blood EPCs (PBEPCs), I looked to HUVECs, identified by their 'cobblestone' morphology, expression of CD31 and VEGFR2, and *in vitro* tube formation. Unexpectedly, the PBMSCs differed from bone marrow MSCs, with a comparatively reduced CD90/CD29 and increased CD45 expression. These cells had negligible adipogenic potential, but proved to be potent osteogenic progenitors and therefore may positively contribute to fracture healing. Unfortunately, due to the protracted culture times and low yields, it was not possible to evaluate chondrogenic potential, hence whether these cells were bi-potent or 'osteo-exclusive' remains unknown. Since I completed Chapters 2 and 3, another group has used AMD3100 in rats preconditioned with the hypoxia-mimicking agent, cobalt chloride. In line with my experience, they mobilised MSCs that were preferentially osteogenic, with reduced adipogenicity and equal chondrogenic potential to bone marrow MSCs. Interestingly, their highest levels of CFUs mobilised was similarly low at 3.8/ml (Liu et al. 2018). This suggests that mobilisation using AMD3100 may preferentially mobilise a subpopulation, or a later lineage population of MSCs. Although most literature cites MSCs as having tri-lineage potential, classical bone marrow stem cell work identified clonal populations frequently do not have full tri-differentiation, whilst

interestingly, the osteogenic lineage is always present (Pittenger et al. 1999). Others elaborated upon these findings showing a sequential loss of lineages for MSCs with osteogenic differentiation remaining (Muraglia et al. 2000). This affirms my suggestion that mobilised PBMSCs could be 'later' lineage determined cells. Future work could evaluate this lineage selection of mobilised compared with bone marrow isolated stem cells by looking at mRNA transcripts; 'stemness' could be evaluated using Rex1, Oct4, Sox2 and Nanog (Fafián-Labora et al. 2015), and lineage association by SOX9 (chondrogenic), Runx2, Osterix (osteogenic) and PPARγ (adipogenic) (Kubo et al. 2009). Should further work be undertaken to evaluate cell populations, I suggest evaluating mobilisation in young rats in case of improved yields, although in terms of translation, older rats are probably more appropriate. When considering other relevant test groups, as a potential translational therapy for fragility fractures, it would be worth evaluating the mobilisation response and impact on healing in an osteoporotic model, such as ovariectomised osteopenic rats.

The mobilised PBEPCs were morphologically distinct from the PBMSCs and similar looking to HUVECs, however, they did not fully match the HUVECs in terms of cell surface markers or tube formation. Again, I did achieve proof of concept that VEGF with AMD3100 mobilised several cell populations in rats, this time with adipogenic differentiation potential and no osteogenic potential. Exactly what they are and their potential contribution to fracture healing remains unclear and again was hampered by the extremely low yields and slow culture dynamics. It is arguable that rat endothelial cells, and potentially small vessel endothelial cells may have been a better comparator than HUVECs, however the vast majority of *in vitro* angiogenesis assays and gold standard endothelial cell characteristics are based on HUVECs (Staton et al. 2009). As endothelial cells vary by the location of isolation, vessel size, and whether from an artery or vein (Staton et al. 2009), future studies looking to evaluate EPC mobilisation in rats, may be better compared to a rat endothelial cell culture. In order to elucidate the mechanisms further in this model system, I would suggest moving to young rats. Ex-breeders were logically chosen at the outset as their increased size should give higher blood volumes and they better mimic a potential translational population. However younger animals are likely to have bigger niche populations and higher mobilisation levels (Fafián-Labora et al. 2015; Sethe et al. 2006; Kuznetsov et al. 2001), allowing further evaluation and potentially chondrogenic differentiation assessment. Another consideration is the influence of *in vitro* cell culture on the cells being isolated, in particular affecting their cell surface characteristics (Bara et al. 2014).

Finally, I noted that mobilisation appeared to be dependent on the individual. Some cultures did not mobilise, some had low levels and others had much higher levels of CFUs/ml. This could again relate to the varying ages of 'ex-breeders' or to different inherent biological

kinetics. To that end, I hypothesise that mobilisation may only induce a factorial increase of circulating stem/progenitors from the animal's inherent baseline. This was not possible to evaluate using the techniques employed in chapters 2 and 3, as sufficient blood volume was only achieved through terminal cardiac venipuncture. Sequential bleeds with the individual as its own control would be very informative, but the very act of taking blood could have impact on endogenous cell populations, through transient hypoxia or similar mechanisms. A large animal model whereby a larger volume, but a smaller proportion of the circulating blood volume could be isolated may be a route forward to answer that question.

Due to the difficulties associated with the *in vitro* stem/progenitor cultures, I did not evaluate other potential growth factor combinations with AMD3100 for circulating MSCs/EPCs. To some extent, the nature of the CFU analysis in chapter 3 is limited as there will be an elution profile and other cell populations and differing levels of stem/progenitors will be mobilised over a period of time (Broxmeyer et al. 2005). Other cell populations may also be important, or indeed, the particular combinations or temporal contributions could be critical to outcome. Other groups have evaluated IGF1 combined with AMD3100 in mice with a CFU-F count, but lacked an in-depth analysis of the cells mobilised (Kumar & Ponnazhagan 2012), with no account of EPCs or other cell types. They identified 26 CFU-F/ml, compared with 20 CFU/ml for VEGF with AMD3100, and 2.5CFU/ml for AMD3100 alone. However, in their published images, the colony looks very immature. I saw similar 'colonies', however, many didn't continue to grow and divide, bringing into question whether they should be classified as *bona fide* CFU-Fs; in my study, they were not. Critically, without any evaluation, it is impossible to know what those cells were. Quantification of stem cell mobilisation in another mouse study using AMD3100 alone reported significant increases in stem cells mobilised, but they actually just counted plastic adherent cells (Toupadakis et al. 2013). Contamination with fibroblasts and other cells would be possible and this does not fulfill the *in vitro* requirement of MSCs to be self-replicating/expandable (Dominici et al. 2006). Their evaluation of numbers of cells based on flow cytometry showing an increase was more convincing however (Toupadakis et al. 2013). To that end, with the limited scope of such studies in mind, but with some evidence of feasibility, it was sensible to evaluate these other two AMD3100/growth factor combinations in a fracture healing scenario. In chapter 6 I evaluated VEGF with AMD3100 in a fracture model, but also evaluated the other reported protocols to permit a direct comparison.

7.3 Fracture model

Chapters 4 and 5 were focused on improving the fidelity of the fracture model and determining the ideal test fracture gap to evaluate endogenous mobilisation. My aim was to

use a gap size together with a fixator that produced delayed healing. My rationale for this approach was that a full non-union model may be too aggressive to show any positive effects of mobilisation, and a model with a smaller gap size may not have been able to decipher the effects of mobilisation due to the fast healing rate. If my work is to be translated into clinical models then the main benefit would be to enhance bone formation in fractures which have a higher potential for delayed healing. As fracture healing is influence by both biological and mechanical factors (Betts & Müller 2014), I needed the mechanical test scenario to be reliable, repeatable and standardised, in order to evaluate a biological intervention such as endogenous mobilisation. Chapter 4 focused on redevelopment of an existing rat micro fixator system and the model was successfully improved by applying clinical principles of external fixator application and design. The modifications included development of a autoclave-stable drill and pin jig-guide, drilling at low speeds with irrigation, pin redevelopment to increase radial pre-load with a self-cutting thread design and altering the block profile to reduce soft-tissue interference.

Chapter 5 was designed to identify the ideal test situation for endogenous mobilisation and to understand the impact of changing the size of the gap on construct stiffness and interfragmentary strain (IFS). *The hypothesis was that "increasing gap size from 1.0 to 1.5mm to 2.0mm will decrease IFS, reduce construct stiffness and hence improve bone formation within the gap"*. The Stanmore micro fixator is a visibly rigid design compared with the commercially available AO rodent external fixator and has been shown to be significantly stiffer at 4.7 times the axial stiffness (Osagie-Clouard et al. 2018). Fitted with a double carbon-fiber connecting bar and using titanium connecting blocks with 1.4mm diameter pins, it was likely to provide a relatively rigid fixation. Interestingly, increasing the fracture gap, which increases the working length of the carbon-fiber bars did not have any effect on construct stiffness, indicative of the relatively rigid fixator design. Therefore, the increasing gap size in this test scenario only tested the influence of the gap size, as construct rigidity remained consistent. Based on Stefan Perren's theory of IFS (Perren 1979), my hypothesis for this chapter was that increasing the gap size, would decrease IFS and improve fracture healing. Based on the IFS at day 0, I could not support the hypothesis, with a doubling of non-union rates and halving of bone volume associated with a reciprocal increase in fibrous tissue, as IFS decreased from 12% to 6%. In contrast, IFS theory would predict a non-union in the 1mm group (12% IFS measured), and endochondral based healing in the 1.5 and 2.0mm group (Perren 1979), however the influence of subsequent tissue development within the gap on the IFS remain unclear. The trends for reduced healing was clear, with a significantly smaller surface area of callus in the 2mm vs 1mm gap, although statistical significance was not reached for bone volume. A post-hoc sample size calculation,

with a power of 0.8 and p=0.05, indicated that 14 animals per group would have been required. For future biomechanical studies using this fixator system, this sample size should be kept in mind. Others have also shown increasing gap size associated with decreased healing, however, I was able to corroborate that to the IFS using a micro-miniature differential variable reluctance transducer (accuracy 0.001mm). This made the measurements more accurate than those based on the materials testing machines displacement measures. The results of chapter 5 are important as despite the commonplace role of rodents in fracture healing research, most studies have evaluated the influence of IFS with large animal models *in vivo* (Claes et al. 1997; Claes et al. 1999; Claes et al. 2003) or using FE models only (Steiner et al. 2014; Wehner et al. 2014; Comiskey et al. 2010).

The work in chapter 5 lead to the selection of the 1.5mm osteotomy gap as a 'half-way house' in terms of a spectrum from healed to non-union, in a five week time frame, for the evaluation of mobilisation in chapter 6. Whether a bigger gap, such as 3mm with guaranteed non-union would have been able to show a benefit more clearly remains unknown; a smaller gap may equally have been unable to demonstrate enhancement. Ultimately, the 1.5mm gap was chosen as compromised healing is translationally appropriate, but without losing the opportunity to demonstrate an effect of endogenous mobilisation.

Osteotomy healing was evaluated with microCT and histology. MicroCT allowed 3D volumetric assessment of bone and soft-tissue, but without the ability to resolve cellular processes and different soft-tissue types. The two together were therefore synergistic, as the single histological section only provided information on the centre of the callus and wasn't truly global, but provided cellular detail. Due to time and cost considerations, a pragmatic decision was taken not to evaluate the mechanical stability of fracture healing in chapters 5 and 6. With the equipment I had available, it was not possible to perform accurate non-destructive mechanical testing, which would have rendered samples unavailable for microCT and histology. To a certain extent, the histology and microCT findings indicate the likely strength (Bouxsein et al. 2010), however smaller differences in bone formation may not be mechanically significant when tested. Should resources have permitted, mechanical testing would have been a useful addition.

7.3.1 Variation in healing

Despite a mechanically standardised fixator, repeatable surgical procedure, consistent age and strain of rats (albeit none were inbred), the results reported in chapters 5 and 6 showed a large variation in fracture healing, although the in-group incidence of complete healing and non-union fitted trends. Based on chapter 5's mechanical evaluation, this was unlikely to relate to an issue of the initial fracture stability provided by the fixator, and likewise the final imaging confirmed no pin tract lucency affecting stability. Potentially, the rats inherent activity levels may have affected osteotomy healing through variable passive dynamisation (Goodship & Kenwright 1985; Richardson et al. 1995). Mouse studies have shown significantly different levels of activity post external fixator surgery and this had an impact on callus size with more mobile animals producing a bigger callus (Connolly et al. 2006). It may be worth quantifying movement post surgery in the future and technology such as micro-pedometers could be considered. The rats I used were out-bred strains and therefore genetic variation could have also played a role. In-bred mouse studies have shown genetic differences in skeletal stem cell regulation affecting the rate of fracture healing (Jepsen et al. 2008). Moving to in-bred rat strains may be sensible in future studies, however, the variation in healing seen in my study is reflected in human fracture healing and therefore the experimental variation may mirror the clinical situation. If individuals have variation in their ability to heal *(Jepsen et al. 2008)*, and variable activity may have mechanically influenced healing, it was likely that chapter 6 also showed a similar heterogeneity. However, if there is individual variation in the biological potential to heal, it is feasible that mobilisation may be more effective in those with inherently better biological potential, as they may have a bigger or more responsive pool of stem cells.

7.3.2 Endogenous mobilisation in a fracture model

The hypothesis for chapter 6 was developed and based on the results of previous chapters. Chapter 6 was the first study that gave a comparison of different mobilisation strategies to improve fracture healing and notably they were tested in a compromised healing model. My hypothesis in chapter 6 was "*administration of mobilising protocols including AMD3100…would increase bone formation within the osteotomy and improve fracture union"*. In answer, *it was possible to improve compromised fracture healing using endogenous stem and progenitor mobilisation*. All strategies tested other than GCSF-AMD improved fracture healing, with an increase in radiographic union and decrease in non-union compared with controls. AMD3100 alone gave significant increases in bone formation as measured on microCT, and in fact, the entire callus was larger. This was similar to the findings of Toupadakis et al., who gave AMD3100 only, but a three-day dose, rather than a

single dose. They also showed a bigger callus at 21 days, but by 84 days (which is much longer in duration than my study), the AMD3100 treated group had a significantly more remodeled and smaller callus (Toupadakis et al. 2013). Whether or not my group would have progressed in the same manner remains unknown. This also highlights an unresolved question of timing of dosing and frequency; studies on the elution and pharmacokinetics of AMD3100 suggest that serial administration will induce a peak mobilisation at one hour post treatment to the same level each time, suggesting that there isn't a receptor/system desensitisation (Broxmeyer et al. 2005). Repeated dosing over several days may therefore increase the circulating pool several times and further potentiate its effects, however, consideration of the effect of CXCR4 blockade at the recipient fracture site needs thought as protracted treatment with AMD3100 throughout fracture healing or during distraction osteogenesis reduces healing (Toupadakis et al. 2012; Xu et al. 2017). For translation, the safety and patient tolerance is important. Animal safety trials showed AMD3100 caused sedation, spasms, and dyspnea in rats, and diarrhea or tachycardia in dogs (Hendrix et al 2000). In humans, therapeutic dosing of volunteers was well tolerated with only some transient gastrointestinal signs and headaches reported in 50%. However, repeat administration of AMD3100 at guideline doses in humans was not reported to cause significant side effects (Hendrix et al 2000; Broxmeyer 2005). It is reasonable to surmise that without a chemotactic gradient, cells such as haematopoietic stem cells will be mobilised but then return to their niche once the AMD3100 has been eliminated from the body.

Chapter 6 also showed a significant increase in bone within the osteotomy when treated with IGF1 and AMD3100, but the callus size was the same as the controls. This finding indicates enhanced bone formation, and Kumar et al. also showed increased bone mineral density when a mouse fracture was treated with IGF1 combined with AMD3100 (Kumar & Ponnazhagan 2012). In contrast, VEGF-AMD only showed a trend for increased bone formation over the control.

GCSF with AMD3100 inhibited bone formation

GSCF-AMD significantly reduced fracture healing, which has not been previously shown. Interestingly, the percentage bone was greater within the callus and the bone formed had increased trabecular thickness and reduced porosity. All treatment groups including GCSF-AMD had increased trabecular thickness indicating thicker woven bone formation. The callus formed however, was smaller with the GCSF-AMD group, but the bone that was present was more structurally dense. As I suggested in chapter 6, the reduced bone volume may relate to the less mature chondrocytes seen histologically, indicative of delayed endochondral ossification, which may in turn be due to excessive inflammation from

mobilised inflammatory cells, or indeed increased haematopoietic lineage osteoclast precursors, leading to bone reduction rather than deposition. Histologically, GCSF-AMD had the lowest level of bone, cartilage and vascular tissue, and the highest level of fibrous tissue, suggesting a pattern of reduced endochondral ossification, reduced blood supply and replacement with fibrous tissue instead.

Pitchford et al. (2009) showed that GCSF-AMD induced mild mobilisation of MSCs and EPCs, but was principally a very effective mobiliser of haematopoietic stem cells and neutrophils. It is possible that the increased influx of neutrophils may have affected the progression of early inflammation at the fracture site, which would normally move towards an environment of healing, but may have been protracted in this situation. CD34+ cells, which are a particularly well-represented population when mobilisation is performed with GSCF ± AMD3100, and was one of the criteria markers used by Pitchford et al. to define their haematopoietic stem cells, are considered a population enriched in endothelial progenitors and haematopoietic stem cells. Transplantation of these cells, which are typically isolated from humans and introduced into immunocompromised rodent fracture models, has shown improved healing in several studies (Kuroda et al. 2014; Matsumoto et al. 2008). However, this sub-selected CD34+ population although a significant part of the cells mobilised by GCSF-AMD3100, are a subset and this may explain the differences in healing seen when this subset is transplanted, compared with mobilised populations that include CD34+ cells. This has been somewhat borne out by studies showing a mixed GCSF mobilised mononuclear cell fraction being less efficacious than a sub-selected CD34+ population (Fukui et al. 2015), and excessive inflammation associated with the MNC population was suggested to be mediating the reduced fracture healing. Corroborating my experience with AMD3100 combined with GCSF, another group used this combination as an endogenous mobilising therapy in myocardial infarcts and showed no improvement (Rüder et al. 2014). One study however, has showed improved fracture healing with GCSF treatment alone, given on five consecutive days. Interestingly, their study lasted 200 days and significant differences were not seen until at least 20-30 days, with a reduction in the osteotomy gap distance. Bone volume was significantly increased from around 30 days, but all rats went on to non-union (Herrmann et al 2018). Their cell elution measures which were taken at several time points, showed significantly increased levels of mobilised CD34+ at day 1 through to day 11, which is in agreement with the effect of GCSF which does not induce a rapid peak mobilisation, unlike AMD3100 (Liles et al. 2005; Broxmeyer et al. 2005).

Timing

Pitchford et al. (2009) showed the influence of the growth factors on mobilisation was time dependent. When growth factor and AMD3100 are administered simultaneously, they did not have the same synergistic mobilising effect as when the growth factor was administered for several days prior to CXCR4 antagonism. This suggests that the growth factors are having bone marrow mediated effects that takes time to develop, which was demonstrated to have influence on cell cycle activation, preventing a cycling cell from being able to undergo chemotaxis. Although there is evidence of almost immediate stem cell migration to a fracture site (Dimitriou et al. 2005), and suggests that endogenous mobilisation was most likely to be effective in the early inflammatory phase, homing of parabiotic stem cells has been shown to peak at 7-14 days (Kumagai et al. 2008). Therefore, it may be worth considering later time frames for treatment as well. Studies have also shown that bone marrow has increased MSCs when a non-union develops (Tawonsawatruk et al. 2014) and hence there may be efficacy of mobilisation for atrophic non-union treatment, although re-initiating the early inflammatory cascade through surgical 'freshening' may be required.

7.4 AMD3100 alone

The improved bone formation associated with administration of AMD3100 alone was particularly interesting as this is a licensed drug, and without the need for growth factors, the route to translation is vastly simplified. AMD3100 alone had the highest bone formation within the gap out of all groups. Although AMD3100 was not been shown to be a good mobiliser of MSCs and EPCS when given alone (Pitchford et al. 2009; Kumar & Ponnazhagan 2012), it has shown *in vivo* bone formation efficacy; in a mouse femoral fracture model when given for three consecutive days (Toupadakis et al. 2013); after a single injection to improve intramedullary trabecular bone regeneration post ablation (McNulty et al. 2012); and in calvarial defect healing (Wang et al. 2011). Chapter 6 therefore corroborates their findings in a different species using a compromised diaphyseal fracture model. The mechanism of action may relate to the combination of the physiologically raised growth factors and cytokines at the fracture site (Devescovi et al. 2008; Lieberman et al. 2002) and migration of stem cells released from their niche. Other cell populations that were not cultured in my thesis may have been mobilised and may have had a positive influence, and the precise timing of their mobilisation using AMD3100 in relation to the fracture healing process warrants further work.

In my thesis, I did not investigate the *in vitro* cell mobilising effect of administration of AMD3100 alone. In chapter 6, I showed that AMD3100 had a positive and unexpected effect on fracture healing and so at the end of my PhD, I performed a small pilot to evaluate this

further; exbreeder rats (n=4) were treated with AMD3100 alone. Protocols were as chapter 3, with blood collection, preparation and culture for PBMSC and PBEPC CFUs. Out of four cultures, all had a high number of plastic adherent cells, which looked as though they were forming early CFUs (Figure 7.1a). However over the 20±2 days culture duration, no convincing mature PBMSC CFUs established in ¾ and one CFU formed in ¼ cultures (Figure 7.1b). This would suggest that PBMSC mobilisation, at least as measured at that time point, was not the underlying mechanism of improved healing. On the other hand, ¾ PBEPC cultures developed multiple 'late EPCs' (Figure 7.2a-c) with a mean of 14.6±7.0 CFUs/ml. This compares with the data from chapter 3 of 0.3±0.3 CFU/ml non-mobilised controls and 2.9±3.3 CFU/ml in the VEGF-AMD treated group (Figure 7.3). The increase was not statistically different between the controls (p=0.144) or between VEGF-AMD (p=0.414) and AMD3100 treated alone, most likely due to the small n-number and the wide data variation (Figure 7.3), generated by one individual not showing any cell mobilisation. Post hoc sample size calculation suggests n=8-10 was required.

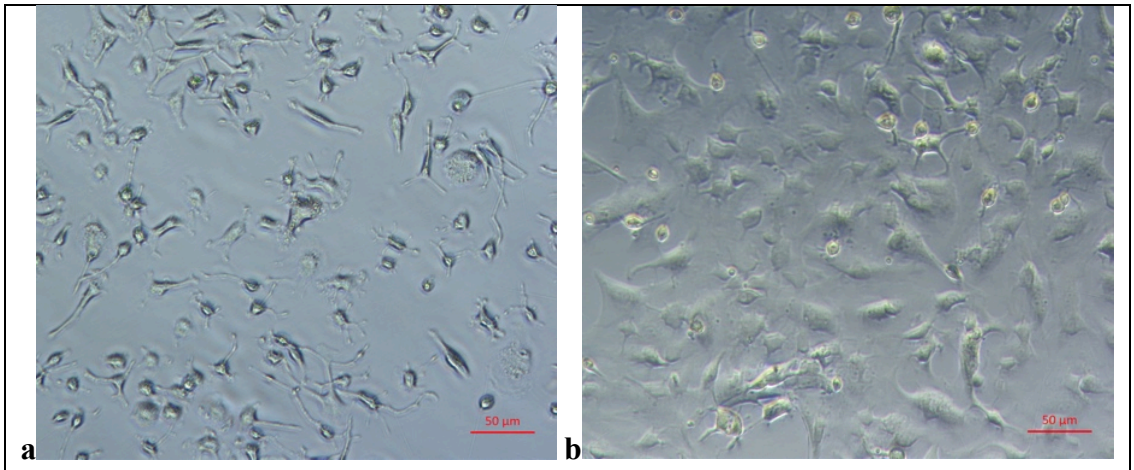

Figure 7.1: Light microscope images taken at x10 magnification of MSC culture of AMD3100 mobilised P0 cells at 20 days. a) Typical conformation of the high numbers of plastic adherent cells seen after culture of blood. These cells did not produce typical CFU-Fs in ¾ cultures. b) Only one culture developed a more typical CFU-F P0 MSC morphology.

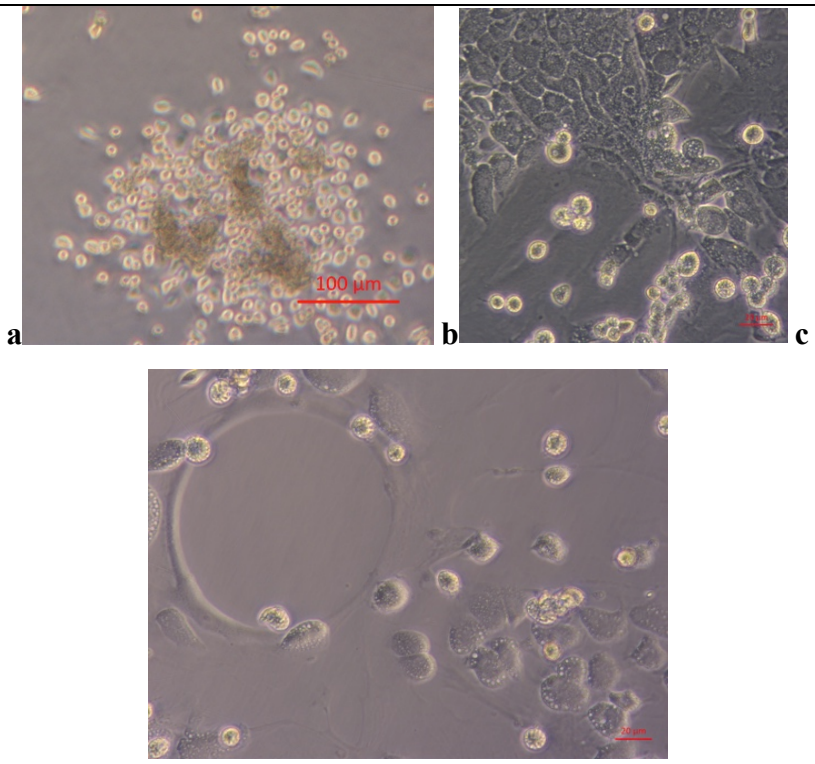

Figure 7.2: Light microscope images of PBEPC culture of AMD3100 mobilised P0 cells at 20 days. a) Circumscribed colony of cobblestone shaped cells, at x5 magnification. b) More advanced CFU at x20 magnification. c) PBEPCs forming luminal type structures at x20 magnification.

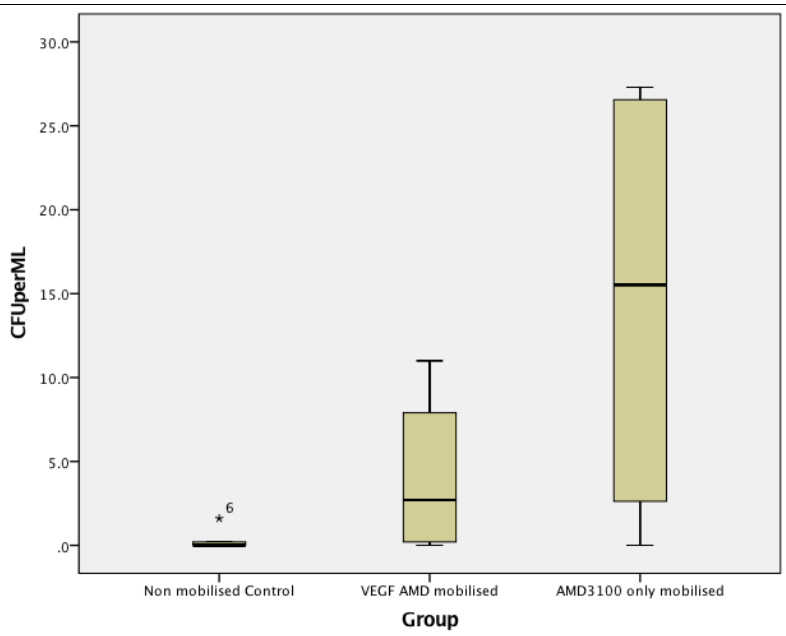

Figure 7.3: Boxplot showing the PBEPC CFUs/ml blood cultured, compared between rats that were not pre-treated with mobilising agents, those that had four days of VEGF followed by a single dose of AMD3100, and those that only had a single dose of AMD3100.

This small pilot suggested that the beneficial effects of AMD3100 alone might be from mobilisation of PBEPCs, which could feasibly improve vascularisation, potentiating MSC migration and osteoblast differentiation, facilitating healing. These cells were continued in primary cultured for 40 days and did not become uniformly confluent, although highly dense areas were seen.

7.5 Summary conclusions from my thesis:

- Mobilisation through antagonism of the SDF1-CXCR4 axis using VEGF with AMD3100 selectively mobilised a population of osteogenic precursor MSCs, and EPCs with adipogenic potential.
- In a rodent femoral osteotomy model, the IFS at day 0 did not predict the course of fracture healing. In contrast, a reduction in IFS as the gap size increased reduced bone healing, with an associated IFS reduction from 12 to 6%. Ultimately, the 1.5mm osteotomy gap stabilised by a relatively rigid linear Type Ia micro fixator was the preferred test scenario to evaluate endogenous mobilisation.
- Despite a uniform initial mechanical fracture environment, there was a wide variation in fracture healing progression at five weeks, however group trends were identified.
- CXCR4 antagonism using AMD3100 alone, or combined with VEGF or IGF1, improved fracture healing in a compromised healing environment. Whereas the haematopoietic stem cell preferentially mobilising treatment of GCSF combined with AMD3100 impaired fracture healing, associated with retarded endochondral ossification and increased fibrosis. AMD3100 alone had the biggest impact on fracture healing.
- AMD3100 appeared to be an effective mobiliser of PBEPCs rather than PBMSCs, however the biological influence of the presence of a fracture on cell mobilisation is unknown.

7.6 Summary limitations:

- Although VEGF-AMD mobilised stem and progenitors were comprehensively evaluated, the slow culture dynamics and low yields prevented further evaluation of other properties such as chondrogenicity, expanded panels of cell surface marker expression, or transcriptomic analysis of the populations mobilised.
- Cell identification was made on cultured cells and the act of cell culture can alter a cell's characteristics.

- PBEPCs were compared with HUVECs and a rat endothelial cell culture may have been more informative.
- Group sizes ranged from 5-8, which is usually sufficient for *in vivo* evaluation. There was however, a higher than expected variation in fracture healing, probably a result of activity, which was not controlled for.
- Although healing was radiographically and morphologically assessed with microCT and histology, no mechanical testing was performed. Although microCT can indicate likely mechanical strength, a mechanical test in itself may have given a different indication of functional healing.

7.7 Options for further work:

- As AMD3100 alone appears to have the most promising outcome for fracture healing translation, there would be merit in evaluating whether multiple dosing in the early phase of fracture healing could further boost mobilisation and healing.
- A large animal model to allow sequential longitudinal assessment of baseline and then mobilised cell population at different time points, would be able to determine whether the variation in mobilisation is proportionate to an individuals biological potential to mobilise. The volumes of blood available in a large animal model would better facilitate evaluation of elution characteristics of stem and progenitor populations longitudinally using flow cytometry on blood circulating cells, rather than cultured cells.
- Comparing mobilisation between young and old, with a view to evaluating the mechanisms of cell mobilisation in younger animals if yields are greater, facilitated by improved culture dynamics.
- To determine whether mobilisation (as measured by CFUs) is affected by the presence of fracture. This would have important ramifications as to whether this therapy can be used in a quiescent atrophic non-union, or whether it only has benefit in the early inflammatory/recruitment phase of healing.
- To evaluate the effects of AMD3100 alone in guaranteed healing and guaranteed non-union situations with serial evaluation of healing over a longer time frame. This would determine if this ‘boost’ could overcome a more profound inhibition of healing and whether it could also accelerate normal healing.
- To evaluate the potential of endogenous mobilisation using AMD3100 in other disease processes that may benefit from increasing homing of stem/progenitor cells such as osteoporosis and implant osseointegration.

7.8 Impact & clinical translation

This study was the first to mobilise a population of osteogenic precursors endogenously into the peripheral circulation of rats. This was also the first study to compare different mobilisation strategies directly and further to do this in compromised mechanically controlled fracture healing environment.

My thesis identified AMD3100 given without growth factors as the most promising option for translation. AMD3100 is already licensed for haematopoietic stem cell transplantation (usually in combination with GCSF), and therefore the route to translation is less complex, as toxicity and safety testing has already been completed. As there is a significant burden of non-union fractures and the cost of a dose of AMD3100 relatively low, this could make an excellent adjunct, or potential alternative to cancellous bone graft in atrophic non-union surgery. It could also be given as a prophylactic measure to patients in at risk fracture groups, such as fragility fractures, high energy comminuted fractures and open fractures. Finally, it may prove a non-invasive, low cost means to accelerate normal fracture healing, which could result in earlier implant removal such as for external fixator patients, reducing complications and facilitating faster return to full activity.

APPENDIX

Publications

VEGF with AMD3100 Endogenously Mobilizes Mesenchymal Stem Cells and Improves Fracture Healing. **Meeson R**, Sanghani-Keri A, Coathup M, Blunn GWB. *Journal of Orthopaedic Research. J Orthop Res. 2018 Oct 22. doi: 10.1002/jor.24164*

CXCR4 antagnism with AMD3100 is more effective at avoiding delayed union and increasing bone formation, than when combined with GCSF, VEGF or IGF1. Meeson R, Sanghani-Keri A, Coathup M, Blunn GWB. *Undergoing Minor Revisions*.

Conferences

Peripheral Blood Mesenchymal Stem Cells Mobilised Post Administration Of VEGF and AMD3100 Undergo Osteoblastic And Not Adipogenic Differentiation. **R L Meeson**, A Sanghani Kerai, M J Coathup, G W Blunn. *British Orthopaedic Research Society*, Conference September 2017. Imperial College London. Oral Podium.

Interfragmentary Strain Theory Does Not Predict Fracture Healing with Increasing Gap Size. **Meeson R**, Sanghani-Keri A, Coathup M, Blunn GWB, Moazen M. *8th World Congress of Biomechanics*. The CCD, Dublin. Poster Presentation.

Endogenous Mobilisation of Stem Cells with AMD3100 to Treat Non-Union **Meeson R,** Sanghani-Keri A, Coathup M, Blunn GWB. 26th Annual European *Orthopaedic Research Society Meeting*, Galway, Ireland, September 2018. Oral Presentation.

CXCR4 Antagonism Endogenously Mobilises Stem and Progenitor Cells and Rescues Non-union Development. **Meeson R,** Sanghani-Keri A, Coathup M, Blunn GWB. 2018 *TERMIS World Congress*, September 4-7, 2018, Kyoto International Conference Center, Kyoto, Japan. Oral Podium.

REFERENCES

Aerssens, J., Boonen, S., Lowet, G. and Dequeker, J. (1998) 'Interspecies differences in bone composition, density, and quality: potential implications for in vivo bone research.', Endocrinology, 139(2), pp. 663–670. doi: 10.1210/endo.139.2.5751.

Aguirre, A., Planell, J. A. and Engel, E. (2010) 'Dynamics of bone marrow-derived endothelial progenitor cell/mesenchymal stem cell interaction in co-culture and its implications in angiogenesis.', Biochemical and biophysical research communications, 400(2), pp. 284–291. doi: 10.1016/j.bbrc.2010.08.073.

Ahn, A. C. and Grodzinsky, A. J. (2009) 'Relevance of collagen piezoelectricity to "Wolff's Law": A critical review', Medical engineering & physics, 31(7), pp. 733–741. doi: 10.1016/j.medengphy.2009.02.006.

AI-Aql, Z. S., Alagl, A. S., Graves, D. T., Gerstenfeld, L. C. and Einhorn, T. A. (2008) 'Molecular Mechanisms Controlling Bone Formation during Fracture Healing and Distraction Osteogenesis', Journal of dental research. NIH Public Access, 87(2), pp. 107–118. doi: 10.1359/jbmr.2001.16.5.876.

Akiyama, H., Chaboissier, M.-C., Martin, J. F., Schedl, A. and de Crombrugghe, B. (2002) 'The transcription factor Sox9 has essential roles in successive steps of the chondrocyte differentiation pathway and is required for expression of Sox5 and Sox6.', Genes & development, 16(21), pp. 2813–2828. doi: 10.1101/gad.1017802.

Alev, C., Ii, M. and Asahara, T. (2011) 'Endothelial progenitor cells: a novel tool for the therapy of ischemic diseases.', Antioxidants & redox signaling, 15(4), pp. 949–965. doi: 10.1089/ars.2010.3872.

Alm, J. J., Koivu, H. M. A., Heino, T. J., Hentunen, T. A., Laitinen, S. and Aro, H. T. (2010) 'Circulating plastic adherent mesenchymal stem cells in aged hip fracture patients.', Journal of Orthopaedic Research, 28(12), pp. 1634–1642. doi: 10.1002/jor.21167.

Alsousou, J., Thompson, M., Hulley, P., Noble, A. and Willett, K. (2009) 'The biology of platelet-rich plasma and its application in trauma and orthopaedic surgery: a review of the literature.', The Journal of bone and joint surgery British volume, 91(8), pp. 987–996. doi: 10.1302/0301-620X.91B8.22546.

Amini, A. R., Laurencin, C. T. and Nukavarapu, S. P. (2012) 'Bone tissue engineering: recent advances and challenges.', Critical reviews in biomedical engineering, 40(5), pp. 363–408.

Andrew, J. G., Hoyland, J., Freemont, A. J. and Marsh, D. (1993b) 'Insulinlike growth factor gene expression in human fracture callus', Calcified Tissue International. Springer-Verlag, 53(2), pp. 97–102. doi: 10.1042/bj2600543.

Angele, P., Yoo, J. U., Smith, C., Mansour, J., Jepsen, K. J., Nerlich, M. and Johnstone, B. (2003) 'Cyclic hydrostatic pressure enhances the chondrogenic phenotype of human mesenchymal progenitor cells differentiated in vitro.', Journal of orthopaedic research : official publication of the Orthopaedic Research Society, 21(3), pp. 451–457. doi: 10.1016/S0736-0266(02)00230-9.

Arakura, M., Lee, S. Y., Takahara, S., Okumachi, E., Iwakura, T., Fukui, T., Nishida, K., Kurosaka, M., Kuroda, R. and Niikura, T. (2017) 'Altered expression of SDF-1 and CXCR4 during fracture healing in diabetes mellitus', International Orthopaedics, 41(6), pp. 1211–1217. doi: 10.1007/s00264-012-1751-y.

Asahara, T., Murohara, T., Sullivan, A., Silver, M., van der Zee, R., Li, T., Witzenbichler, B., Schatteman, G. and Isner, J. M. (1997) 'Isolation of putative progenitor endothelial cells for angiogenesis.', *Science (New York, NY)*, 275(5302), pp. 964–967.

Askari, A. T., Unzek, S., Popovic, Z. B., Goldman, C. K., Forudi, F., Kiedrowski, M., Rovner, A., Ellis, S. G., Thomas, J. D., DiCorleto, P. E., Topol, E. J. and Penn, M. S. (2003) 'Effect of stromal-cell-derived factor 1 on stem-cell homing and tissue regeneration in ischaemic cardiomyopathy.', *Lancet*, 362(9385), pp. 697–703. doi: 10.1016/S0140-6736(03)14232-8.

Atesok, K., Li, R., Stewart, D. J. and Schemitsch, E. H. (2010) 'Endothelial progenitor cells promote fracture healing in a segmental bone defect model', Journal of orthopaedic research : official publication of the Orthopaedic Research Society, pp. n/a–n/a. doi: 10.1002/jor.21083.

Augello, A., Kurth, T. B. and De Bari, C. (2010) 'Mesenchymal stem cells: a perspective from in vitro cultures to in vivo migration and niches.', European cells & materials, 20, pp. 121–133.

Augustin, G., Davila, S., Mihoci, K., Udiljak, T., Vedrina, D. S. and Antabak, A. (2007) 'Thermal osteonecrosis and bone drilling parameters revisited', Archives of Orthopaedic and Trauma Surgery, 128(1), pp. 71–77. doi: 10.1007/s00402-007-0427-3.

Babarina, A. V., Möllers, U., Bittner, K., Vischer, P. and Bruckner, P. (2001) 'Role of the subchondral vascular system in endochondral ossification: endothelial cell-derived proteinases derepress late cartilage differentiation in vitro.', Matrix biology : journal of the International Society for Matrix Biology, 20(3), pp. 205–213.

Bachus, K. N., Rondina, M. T. and Hutchinson, D. T. (2000) 'The effects of drilling force on cortical temperatures and their duration: an in vitro study.', Medical engineering & physics, 22(10), pp. 685–691.

Baggott, D. G., Goodship, A. E. and Lanyon, L. E. (1981) 'A quantitative assessment of compression plate fixation in vivo: an experimental study using the sheep radius.', Journal of biomechanics, 14(10), pp. 701–711.

Bak, B., Jørgensen, P. H. and Andreassen, T. T. (2009) 'Dose response of growth hormone on fracture healing in the rat', Acta orthopaedica Scandinavica, 61(1), pp. 54–57. doi: 10.1210/endo-98-3-562.

Bara, J. J., Richards, R. G., Alini, M. and Stoddart, M. J. (2014) 'Concise Review: Bone Marrow-Derived Mesenchymal Stem Cells Change Phenotype Following In Vitro Culture: Implications for Basic Research and the Clinic', Stem Cells, 32(7), pp. 1713–1723. doi: 10.1002/stem.1649.

Barak, M. M., Weiner, S. and Shahar, R. (2008) 'Importance of the integrity of trabecular bone to the relationship between load and deformation of rat femora: an optical metrology study', Journal of Materials Chemistry, 18(32), p. 3855. doi: 10.1016/j.tvjl.2007.1011.1022.

Barba, M., Cicione, C., Bernardini, C., Michetti, F. and Lattanzi, W. (2013) 'Adipose-derived mesenchymal cells for bone regereneration: state of the art.', BioMed research international, 2013, p. 416391. doi: 10.1155/2013/416391.

Barnes, G. L., Kostenuik, P. J., Gerstenfeld, L. C. and Einhorn, T. A. (1999) 'Growth factor regulation of fracture repair.', Journal of Bone and Mineral Research, 14(11), pp. 1805–1815. doi: 10.1359/jbmr.1999.14.11.1805.

Becker, A. J., Mcculloch, E. A. And Till, J. E. (1963) 'Cytological demonstration of the clonal nature of spleen colonies derived from transplanted mouse marrow cells.', Nature, 197, pp. 452–454.

Bendall, L. J. and Bradstock, K. F. (2014) 'G-CSF: From granulopoietic stimulant to bone marrow stem cell mobilizing agent', Cytokine & Growth Factor Reviews. doi: 10.1016/j.cytogfr.2014.07.011.

Berman, A. T., Reid, J. S., Yanicko, D. R., Sih, G. C. and Zimmerman, M. R. (1984) 'Thermally induced bone necrosis in rabbits. Relation to implant failure in humans.', Clinical orthopaedics and related research, (186), pp. 284–292.

Betts, D. C. and Müller, R. (2014) 'Mechanical regulation of bone regeneration: theories, models, and experiments.', Frontiers in endocrinology, 5, p. 211. doi: 10.3389/fendo.2014.00211.

Bianco, P., Cao, X., Frenette, P. S., Mao, J. J., Robey, P. G., Simmons, P. J. and Wang, C.-Y. (2013) 'The meaning, the sense and the significance: translating the science of mesenchymal stem cells into medicine', Nature Medicine, 19(1), pp. 35–42. doi: 10.1038/nm.3028.

Bianco, P., Robey, P. G. and Simmons, P. J. (2008) 'Mesenchymal Stem Cells: Revisiting History, Concepts, and Assays', Cell stem cell, 2(4), pp. 313–319. doi: 10.1016/j.stem.2008.03.002.

Bible, J. E. and Mir, H. R. (2015) 'External Fixation: Principles and Applications.', The Journal of the American Academy of Orthopaedic Surgeons, 23(11), pp. 683–690. doi: 10.5435/JAAOS-D-14-00281.

Bikfalvi, A., Cramer, E. M., Tenza, D. and Tobelem, G. (1991) 'Phenotypic modulations of human umbilical vein endothelial cells and human dermal fibroblasts using two angiogenic assays.', Biology of the cell, 72(3), pp. 275–278.

Biliouris, T. L., Schneider, E., A, R. B., Gasser, B. and Perren, S. M. (1989) 'The effect of radial preload on the implant-bone interface: a cadaveric study.', Journal of orthopaedic trauma, 3(4), pp. 323–332.

Bompais, H., Chagraoui, J., Canron, X., Crisan, M., Liu, X. H., Anjo, A., Tolla-Le Port, C., Leboeuf, M., Charbord, P., Bikfalvi, A. and Uzan, G. (2004) 'Human endothelial cells derived from circulating progenitors display specific functional properties compared with mature vessel wall endothelial cells.', Blood, 103(7), pp. 2577–2584. doi: 10.1182/blood-2003-08-2770.

Bongiovanni, D., Bassetti, B., Gambini, E., Gaipa, G., Frati, G., Achilli, F., Scacciatella, P., Carbucicchio, C. and Pompilio, G. (2014) 'The CD133 +Cell as Advanced Medicinal Product for Myocardial and Limb Ischemia', Stem cells and development, 23(20), pp. 2403–2421. doi: 10.1089/scd.2014.0111.

Bonnarens, F. and Einhorn, T. A. (1984) 'Production of a standard closed fracture in laboratory animal bone.', Journal of orthopaedic research : official publication of the Orthopaedic Research Society, 2(1), pp. 97–101. doi: 10.1002/jor.1100020115.

Bou Khzam, L., Bouchereau, O., Boulahya, R., Hachem, A., Zaid, Y., Abou-Saleh, H. and Merhi, Y. (2015) 'Early outgrowth cells versus endothelial colony forming cells functions in platelet aggregation.', Journal of translational medicine, 13, p. 353. doi: 10.1186/s12967-015-0723-6.

Bouletreau, P. J., Warren, S. M., Spector, J. A., Peled, Z. M., Gerrets, R. P., Greenwald, J. A. and Longaker, M. T. (2002) 'hypoxia and Vegf Up-regulate Bmp-2 mrna and Protein Expression in Microvascular Endothelial Cells: Implications for Fracture Healing', Plastic and reconstructive surgery. Plastic and Reconstructive Surgery, 109(7), pp. 2384–2397.

Bouvy, B. M., Markel, M. D., Chelikani, S., Egger, E. L., PIERMATTEI, D. L. and Vanderby, R. (1993) 'Ex vivo biomechanics of Kirschner-Ehmer external skeletal fixation applied to canine tibiae.', Veterinary surgery : VS, 22(3), pp. 194–207.

Bouxsein, M. L., Boyd, S. K., Christiansen, B. A., Guldberg, R. E., Jepsen, K. J. and Müller, R. (2010) 'Guidelines for assessment of bone microstructure in rodents using micro-computed tomography', Journal of Bone and Mineral Research, 25(7), pp. 1468–1486. doi: 10.1002/jbm.a.31142.

Boxall, S. A. and Jones, E. (2012) 'Markers for Characterization of Bone Marrow Multipotential Stromal Cells', Stem Cells International, 2012(5), pp. 1–12. doi: 10.1111/j.1432-0436.2006.00139.x.

Breur, G. J., VanEnkevort, B. A., Farnum, C. E. and Wilsman, N. J. (1991) 'Linear relationship between the volume of hypertrophic chondrocytes and the rate of longitudinal bone growth in growth plates.', Journal of orthopaedic research : official publication of the Orthopaedic Research Society, 9(3), pp. 348–359. doi: 10.1002/jor.1100090306.

Briggs, B. T. and Chao, E. Y. (1982) 'The mechanical performance of the standard Hoffmann-Vidal external fixation apparatus.', The Journal of bone and joint surgery. American volume, 64(4), pp. 566–573.

Brighton, C. T. and Hunt, R. M. (1991) 'Early histological and ultrastructural changes in medullary fracture callus.', The Journal of bone and joint surgery. American volume, 73(6), pp. 832–847.

Brighton, C. T. and Krebs, A. G. (1972) 'Oxygen tension of healing fractures in the rabbit.', The Journal of bone and joint surgery. American volume, 54(2), pp. 323–332.

Brighton, C. T., Black, J., Friedenberg, Z. B., Esterhai, J. L., Day, L. J. and Connolly, J. F. (1981) 'A multicenter study of the treatment of non-union with constant direct current.', The Journal of bone and joint surgery. American volume, 63(1), pp. 2–13.

Broxmeyer, H. E., Orschell, C. M., Clapp, D. W., Hangoc, G., Cooper, S., Plett, P. A., Liles, W. C., Li, X., Graham-Evans, B., Campbell, T. B., Calandra, G., Bridger, G., Dale, D. C. and Srour, E. F. (2005) 'Rapid mobilization of murine and human hematopoietic stem and progenitor cells with AMD3100, a CXCR4 antagonist.', The Journal of experimental medicine, 201(8), pp. 1307–1318. doi: 10.1084/jem.20041385.

Bruder, S. P., Kurth, A. A., Shea, M., Hayes, W. C., Jaiswal, N. and Kadiyala, S. (1998) 'Bone regeneration by implantation of purified, culture-expanded human mesenchymal stem cells.', Journal of orthopaedic research : official publication of the Orthopaedic Research Society, 16(2), pp. 155–162. doi: 10.1002/jor.1100160202.

Buckwalter, J. A., Glimcher, M. J., Cooper, R. R. and Recker, R. (1996) 'Bone biology. I: Structure, blood supply, cells, matrix, and mineralization.', Instructional course lectures, 45, pp. 371–386.

Busse, J. W., Kaur, J., Mollon, B., Bhandari, M., Tornetta, P., Schünemann, H. J. and Guyatt, G. H. (2009) 'Low intensity pulsed ultrasonography for fractures: systematic review of randomised controlled trials.', BMJ, 338, p. b351.

Calandra, G., McCarty, J., McGuirk, J., Tricot, G., Crocker, S.-A., Badel, K., Grove, B., Dye, A. and Bridger, G. (2008) 'AMD3100 plus G-CSF can successfully mobilize CD34+ cells from non-Hodgkin"s lymphoma, Hodgkin"s disease and multiple myeloma patients previously failing mobilization with chemotherapy and/or cytokine treatment: compassionate use data.', Bone marrow transplantation, 41(4), pp. 331–338. doi: 10.1038/sj.bmt.1705908.

Campbell, G. M. and Sophocleous, A. (2014) 'Quantitative analysis of bone and soft tissue by micro-computed tomography: applications to ex vivo and in vivo studies', BoneKEy reports. Nature Publishing Group, 3, pp. 1–12. doi: 10.1038/bonekey.2014.59.

Cano, E., Gebala, V. and Gerhardt, H. (2017) 'Pericytes or Mesenchymal Stem Cells: Is That the Question?', Cell stem cell, 20(3), pp. 296–297. doi: 10.1016/j.stem.2017.02.005.

Caplan, A. I. (1991) ‘Mesenchymal stem cells.’, Journal of orthopaedic research : official publication of the Orthopaedic Research Society, 9(5), pp. 641–650. doi: 10.1002/jor.1100090504.

Carter, D. R., Beaupré, G. S., Giori, N. J. and Helms, J. A. (1998) ‘Mechanobiology of Skeletal Regeneration.’, *Clinical Orthopaedics and Related Research (1976-2007) KW* -, 355, p. S41.

Carter, D. R., Blenman, P. R. and Beaupré, G. S. (1988) ‘Correlations between mechanical stress history and tissue differentiation in initial fracture healing.’, Journal of orthopaedic research : official publication of the Orthopaedic Research Society, 6(5), pp. 736–748. doi: 10.1002/jor.1100060517.

Casanova, M., Schindeler, A., Little, D., ller, R. M. U. and Schneider, P. (2014) ‘Quantitative phenotyping of bone fracture repair: a review’, BoneKEy reports. Nature Publishing Group, 3, pp. 1–8. doi: 10.1038/bonekey.2014.45.

Case, J., Mead, L. E., Bessler, W. K., Prater, D., White, H. A., Saadatzadeh, M. R., Bhavsar, J. R., Yoder, M. C., Haneline, L. S. and Ingram, D. A. (2007) ‘Human CD34+AC133+VEGFR-2+ cells are not endothelial progenitor cells but distinct, primitive hematopoietic progenitors.’, Experimental Hematology, 35(7), pp. 1109–1118. doi: 10.1016/j.exphem.2007.04.002.

Ceradini, D. J., Kulkarni, A. R., Callaghan, M. J., Tepper, O. M., Bastidas, N., Kleinman, M. E., Capla, J. M., Galiano, R. D., Levine, J. P. and Gurtner, G. C. (2004) ‘Progenitor cell trafficking is regulated by hypoxic gradients through HIF-1 induction of SDF-1.’, Nature Medicine, 10(8), pp. 858–864. doi: 10.1038/nm1075.

Chen, D., Xia, Y., Zuo, K., Wang, Y., Zhang, S., Kuang, D., Duan, Y., Zhao, X. and Wang, G. (2015) ‘Crosstalk between SDF-1/CXCR4 and SDF-1/CXCR7 in cardiac stem cell migration.’, Scientific reports, 5, p. 16813. doi: 10.1038/srep16813.

Chen, J. L., Hunt, P., McElvain, M., Black, T., Kaufman, S. and Choi, E. S. (1997) ‘Osteoblast precursor cells are found in CD34+ cells from human bone marrow.’, Stem Cells, 15(5), pp. 368–377. doi: 10.1002/stem.150368.

Chen, Y. and Alman, B. A. (2009) ‘Wnt pathway, an essential role in bone regeneration’, Journal of cellular biochemistry, 106(3), pp. 353–362. doi: 10.1111/j.1469-7580.2005.00473.x.

Cheng, C.-C., Chang, S.-J., Chueh, Y.-N., Huang, T.-S., Huang, P.-H., Cheng, S.-M., Tsai, T.-N., Chen, J.-W. and Wang, H.-W. (2013) ‘Distinct angiogenesis roles and surface markers of early and late endothelial progenitor cells revealed by functional group analyses.’, BMC genomics, 14, p. 182. doi: 10.1186/1471-2164-14-182.

Cheng, H., Jiang, W., Phillips, F. M., Haydon, R. C., Peng, Y., Zhou, L., Luu, H. H., An, N., Breyer, B., Vanichakarn, P., Szatkowski, J. P., Park, J. Y. and He, T.-C. (2003) ‘Osteogenic activity of the fourteen types of human bone morphogenetic proteins (BMPs).’, The Journal of bone and joint surgery. American volume, 85-A(8), pp. 1544–1552.

Chesney, J. and Bucala, R. (1997) ‘Peripheral blood fibrocytes: novel fibroblast-like cells that present antigen and mediate tissue repair.’, Biochemical Society Transactions, 25(2), pp. 520–524.

Cho, T.-J., Gerstenfeld, L. C. and Einhorn, T. A. (2002) ‘Differential temporal expression of members of the transforming growth factor beta superfamily during murine fracture healing.’, Journal of Bone and Mineral Research, 17(3), pp. 513–520. doi: 10.1359/jbmr.2002.17.3.513.

Chong, M. S. K., Ng, W. K. and Chan, J. K. Y. (2016) ‘Concise Review: Endothelial Progenitor Cells in Regenerative Medicine: Applications and Challenges.’, Stem cells translational medicine, 5(4), pp. 530–538. doi: 10.5966/sctm.2015-0227.

Christopher, M. J. and Link, D. C. (2008) ‘Granulocyte colony-stimulating factor induces osteoblast apoptosis and inhibits osteoblast differentiation.’, Journal of Bone and Mineral Research, 23(11), pp. 1765–1774. doi: 10.1359/jbmr.080612.

Claes, L. E. and Heigele, C. A. (1999) ‘Magnitudes of local stress and strain along bony surfaces predict the course and type of fracture healing.’, Journal of biomechanics, 32(3), pp. 255–266.

Claes, L. E., Heigele, C. A., Neidlinger-Wilke, C., Kaspar, D., Seidl, W., Margevicius, K. J. and Augat, P. (1998) ‘Effects of mechanical factors on the fracture healing process.’, *Clinical orthopaedics and related research*, (355 Suppl), pp. S132–47.

Claes, L. E., Wilke, H. J., Augat, P., Rübenacker, S. and Margevicius, K. J. (1995) ‘Effect of dynamization on gap healing of diaphyseal fractures under external fixation.’, Clinical biomechanics (Bristol, Avon), 10(5), pp. 227–234.

Claes, L., Augat, P., Suger, G. and Wilke, H. J. (1997) ‘Influence of size and stability of the osteotomy gap on the success of fracture healing.’, Journal of orthopaedic research : official publication of the Orthopaedic Research Society, 15(4), pp. 577–584. doi: 10.1002/jor.1100150414.

Claes, L., Eckert-Hubner, K. and Augat, P. (2003) ‘The fracture gap size influences the local vascularization and tissue differentiation in callus healing’, Langenbeck's Archives of Surgery, 388(5), pp. 316–322. doi: 10.1007/s00423-003-0396-0.

Clary, E. M. and Roe, S. C. (1996) ‘In vitro biomechanical and histological assessment of pilot hole diameter for positive-profile external skeletal fixation pins in canine tibiae.’, Veterinary surgery : VS, 25(6), pp. 453–462.

Colnot, C. (2009) ‘Skeletal Cell Fate Decisions Within Periosteum and Bone Marrow During Bone Regeneration’, Journal of Bone and Mineral Research, 24(2), pp. 274–282. doi: 10.1359/jbmr.081003.

Comiskey, D. P., MacDonald, B. J., McCartney, W. T., Synnott, K. and Byrne, J. O. (2010) ‘The role of interfragmentary strain on the rate of bone healing—A new interpretation and mathematical model’, Journal of biomechanics. Elsevier, 43(14), pp. 2830–2834. doi: 10.1016/j.jbiomech.2010.06.016.

Connolly, C. K., Li, G., Bunn, J. R., Mushipe, M., Dickson, G. R. and Marsh, D. R. (2006) 'A reliable externally fixated murine femoral fracture model that accounts for variation in movement between animals', Journal of Orthopaedic Research, 21(5), pp. 843–849. doi: 10.2106/00004623-195537050-00013.

Connolly, J. O., Simpson, N., Hewlett, L. and Hall, A. (2002) 'Rac regulates endothelial morphogenesis and capillary assembly.', Molecular Biology of the Cell, 13(7), pp. 2474–2485. doi: 10.1091/mbc.E02-01-0006.

da Silva Meirelles, L., Chagastelles, P. C. and Nardi, N. B. (2006) 'Mesenchymal stem cells reside in virtually all post-natal organs and tissues.', Journal of Cell Science, 119(Pt 11), pp. 2204–2213. doi: 10.1242/jcs.02932.

Davies, O. G., Cooper, P. R., Shelton, R. M., Smith, A. J. and Scheven, B. A. (2015) 'Isolation of adipose and bone marrow mesenchymal stem cells using CD29 and CD90 modifies their capacity for osteogenic and adipogenic differentiation', Journal of Tissue Engineering, 6(0). doi: 10.1177/2041731415592356.

De Clercq, E. (2009) 'The AMD3100 story: The path to the discovery of a stem cell mobilizer (Mozobil)', Biochemical Pharmacology, 77(11), pp. 1655–1664. doi: 10.1016/j.bcp.2008.12.014.

De Lucas, B., Pérez, L. M. and Gálvez, B. G. (2017) 'Importance and regulation of adult stem cell migration', Journal of Cellular and Molecular Medicine, 7, p. 656. doi: 10.1016/j.ceb.2008.01.005.

DeCicco-Skinner, K. L., Henry, G. H., Cataisson, C., Tabib, T., Gwilliam, J. C., Watson, N. J., Bullwinkle, E. M., Falkenburg, L., O'Neill, R. C., Morin, A. and Wiest, J. S. (2014) 'Endothelial Cell Tube Formation Assay for the In Vitro Study of Angiogenesis', Journal of Visualized Experiments, (91). doi: 10.3791/51312.

Deckers, M. M. L., Karperien, M., van der Bent, C., Yamashita, T., Papapoulos, S. E. and Löwik, C. W. G. M. (2000) 'Expression of Vascular Endothelial Growth Factors and Their Receptors during Osteoblast Differentiation', Endocrinology. Oxford University Press, 141(5), pp. 1667–1674. doi: 10.1210/endo.141.5.7458.

DeLisser, H. M., Newman, P. J. and Albelda, S. M. (1994) 'Molecular and functional aspects of PECAM-1/CD31.', Immunology today, 15(10), pp. 490–495. doi: 10.1016/0167-5699(94)90195-3.

Devescovi, V., Leonardi, E., Ciapetti, G. and Cenni, E. (2008) 'Growth factors in bone repair', La Chirurgia degli Organi di Movimento. Springer Milan, 92(3), pp. 161–168. doi: 10.1007/s12306-008-0064-1.

Dezawa, M., Kanno, H., Hoshino, M., Cho, H., Matsumoto, N., Itokazu, Y., Tajima, N., Yamada, H., Sawada, H., Ishikawa, H., Mimura, T., Kitada, M., Suzuki, Y. and Ide, C. (2004) 'Specific induction of neuronal cells from bone marrow stromal cells and application for autologous transplantation.', The Journal of clinical investigation, 113(12), pp. 1701–1710. doi: 10.1172/JCI20935.

DiGioia, A. M., Cheal, E. J. and Hayes, W. C. (1986) 'Three-dimensional strain fields in a uniform osteotomy gap.', Journal of biomechanical engineering, 108(3), pp. 273–280.

Dimitriou, R., Tsiridis, E. and Giannoudis, P. V. (2005) 'Current concepts of molecular aspects of bone healing.', Injury, 36(12), pp. 1392–1404. doi: 10.1016/j.injury.2005.07.019.

Dominici, M., Le Blanc, K., Mueller, I., Slaper-Cortenbach, I., Marini, F., Krause, D., Deans, R., Keating, A., Prockop, D. and Horwitz, E. (2006) 'Minimal criteria for defining multipotent mesenchymal stromal cells. The International Society for Cellular Therapy position statement.', Journal of Cytotherapy, 8(4), pp. 315–317. doi: 10.1080/14653240600855905.

Dong, L.-Q., Yin, H., Wang, C.-X. and Hu, W.-F. (2014) 'Effect of the timing of surgery on the fracture healing process and the expression levels of vascular endothelial growth factor and bone morphogenetic protein-2.', Experimental and Therapeutic Medicine, 8(2), pp. 595–599. doi: 10.3892/etm.2014.1735.

Donovan, D., Brown, N. J., Bishop, E. T. and Lewis, C. E. (2001) 'Comparison of three in vitro human "angiogenesis" assays with capillaries formed in vivo.', Angiogenesis, 4(2), pp. 113–121.

Ducy, P., Zhang, R., Geoffroy, V., Ridall, A. L. and Karsenty, G. (1997) 'Osf2/Cbfa1: a transcriptional activator of osteoblast differentiation.', Cell , 89(5), pp. 747–754.

Edwall, D., Prisell, P. T., Levinovitz, A., Jennische, E. and Norstedt, G. (2009) 'Expression of insulin-like growth factor I messenger ribonucleic acid in regenerating bone after fracture: Influence of indomethacin', Journal of Bone and Mineral Research. John Wiley and Sons and The American Society for Bone and Mineral Research (ASBMR), 7(2), pp. 207–213. doi: 10.1002/jbmr.5650070212.

Egger, E. L. (1992) 'Instrumentation for external fixation.', The Veterinary clinics of North America. Small animal practice, 22(1), pp. 19–43.

Einhorn, T. A. and Gerstenfeld, L. C. (2014) 'Fracture healing: mechanisms and interventions', Nature Publishing Group. Nature Publishing Group, 11(1), pp. 45–54. doi: 10.1038/nrrheum.2014.164.

Eliasson, P. and Jönsson, J.-I. (2010) 'The hematopoietic stem cell niche: low in oxygen but a nice place to be.', Journal of Cellular Physiology, 222(1), pp. 17–22. doi: 10.1002/jcp.21908.

Elliott, D. S., Newman, K. J. H., Forward, D. P., Hahn, D. M., Ollivere, B., Kojima, K., Handley, R., Rossiter, N. D., Wixted, J. J., Smith, R. M. and Moran, C. G. (2016) 'A unified theory of bone healing and nonunion: BHN theory.', The bone & joint journal, 98-B(7), pp. 884–891. doi: 10.1302/0301-620X.98B7.36061.

Engler, A. J., Sen, S., Sweeney, H. L. and Discher, D. E. (2006) 'Matrix elasticity directs stem cell lineage specification.', Cell , 126(4), pp. 677–689. doi: 10.1016/j.cell.2006.06.044.

Eriksson, R. A., Albrektsson, T. and Magnusson, B. (1984) 'Assessment of bone viability after heat trauma. A histological, histochemical and vital microscopic study in the rabbit.', Scandinavian journal of plastic and reconstructive surgery, 18(3), pp. 261–268.

Eslaminejad, M. B., Fani, N. and Shahhoseini, M. (2013) 'Epigenetic regulation of osteogenic and chondrogenic differentiation of mesenchymal stem cells in culture.', Cell journal, 15(1), pp. 1–10.

Evans, C. H. (2012) 'Gene delivery to bone.', Advanced drug delivery reviews, 64(12), pp. 1331–1340. doi: 10.1016/j.addr.2012.03.013.

Fafián-Labora, J., Fernández-Pernas, P., Fuentes, I., De Toro, J., Oreiro, N., Sangiao-Alvarellos, S., Mateos, J. and Arufe, M. C. (2015) 'Influence of age on rat bone-marrow mesenchymal stem cellspotential', Nature Publishing Group. Nature Publishing Group, pp. 1–20. doi: 10.1038/srep16765.

Fan, X.-L., Duan, X.-B., Chen, Z.-H., Li, M., Xu, J.-S. and Ding, G.-M. (2015) 'Lack of estrogen down-regulates CXCR4 expression on Treg cells and reduces Treg cell population in bone marrow in OVX mice.', Cellular and molecular biology (Noisy-le-Grand, France), 61(2), pp. 13–17.

Faulkner, A., Purcell, R., Hibbert, A., Latham, S., Thomson, S., Hall, W. L., Wheeler-Jones, C. and Bishop-Bailey, D. (2014) 'A thin layer angiogenesis assay: a modified basement matrix assay for assessment of endothelial cell differentiation', pp. 1–9. doi: 10.1186/s12860-014-0041-5.

Ferrara, N., Gerber, H.-P. and LeCouter, J. (2003) 'The biology of VEGF and its receptors', Nature Medicine, 9(6), pp. 669–676. doi: 10.1038/nm0603-669.

Fortier, L. A. (2005) 'Stem Cells: Classifications, Controversies, and Clinical Applications', Veterinary surgery : VS, 34(5), pp. 415–423. doi: 10.1111/j.1532-950X.2005.00063.x.

Frenette, P. S., Subbarao, S., Mazo, I. B., Andrian, von, U. H. and Wagner, D. D. (1998) 'Endothelial selectins and vascular cell adhesion molecule-1 promote hematopoietic progenitor homing to bone marrow.', Proceedings of the National Academy of Sciences of the United States of America, 95(24), pp. 14423–14428.

Friedenstein, A. J., Chailakhjan, R. K. and Lalykina, K. S. (1970) 'The development of fibroblast colonies in monolayer cultures of guinea-pig bone marrow and spleen cells.', Cell and tissue kinetics, 3(4), pp. 393–403.

Friedenstein, A. J., Chailakhyan, R. K., Latsinik, N. V., Panasyuk, A. F. and Keiliss-Borok, I. V. (1974) 'Stromal cells responsible for transferring the microenvironment of the hemopoietic tissues. Cloning in vitro and retransplantation in vivo.', Transplantation, 17(4), pp. 331–340.

Friedenstein, A. J., Petrakova, K. V., Kurolesova, A. I. and Frolova, G. P. (1968) 'Heterotopic of bone marrow. Analysis of precursor cells for osteogenic and hematopoietic tissues.', Transplantation, 6(2), pp. 230–247.

Friedman, M. S., Long, M. W. and Hankenson, K. D. (2006) 'Osteogenic differentiation of human mesenchymal stem cells is regulated by bone morphogenetic protein-6.', Journal of cellular biochemistry, 98(3), pp. 538–554. doi: 10.1002/jcb.20719.

Fu, W. L., Zhou, C. Y. and Yu, J. K. (2014) 'A New Source of Mesenchymal Stem Cells for Articular Cartilage Repair: MSCs Derived From Mobilized Peripheral Blood Share Similar Biological Characteristics In Vitro and Chondrogenesis In Vivo as MSCs From Bone Marrow in a Rabbit Model', The American Journal of Sports Medicine, 42(3), pp. 592–601. doi: 10.1177/0363546513512778.

Fu, W.-L., Li, J., Chen, G., Li, Q., Tang, X. and Zhang, C.-H. (2015) 'Mesenchymal Stem Cells Derived from Peripheral Blood Retain Their Pluripotency, but Undergo Senescence During Long-Term Culture.', Tissue engineering. Part C, Methods, 21(10), pp. 1088–1097. doi: 10.1089/ten.TEC.2014.0595.

Fu, W.-L., Zhang, J.-Y., Fu, X., Duan, X.-N., Leung, K. K. M., Jia, Z.-Q., Wang, W.-P., Zhou, C.-Y. and Yu, J.-K. (2012) 'Comparative study of the biological characteristics of mesenchymal stem cells from bone marrow and peripheral blood of rats.', Tissue engineering. Part A, 18(17-18), pp. 1793–1803. doi: 10.1089/ten.TEA.2011.0530.

Fujikawa, Y., Quinn, J. M., Sabokbar, A., McGee, J. O. and Athanasou, N. A. (1996) 'The human osteoclast precursor circulates in the monocyte fraction.', Endocrinology, 137(9), pp. 4058–4060. doi: 10.1210/endo.137.9.8756585.

Fukui, T., Mifune, Y., Matsumoto, T., Shoji, T., Kawakami, Y., Kawamoto, A., Ii, M., Akimaru, H., Kuroda, T., Horii, M., Yokoyama, A., Alev, C., Kuroda, R., Kurosaka, M. and Asahara, T. (2015) 'Superior Potential of CD34-Positive Cells Compared to Total Mononuclear Cells for Healing of Nonunion Following Bone Fracture.', Cell Transplantation, 24(7), pp. 1379–1393. doi: 10.3727/096368914X681586.

Garcia, P., Histing, T., Holstein, J. H., Klein, M., Laschke, M. W., Matthys, R., Ignatius, A., Wildemann, B., Lienau, J., Peters, A., Willie, B., DUDA, G., Claes, L., Pohlemann, T. and Menger, M. D. (2013) 'Rodent animal models of delayed bone healing and non-union formation: a comprehensive review.', European cells & materials, 26, pp. 1–12– discussion 12–4. doi: 10.22203/eCM.v026a01.

Gaston, M. S. and Simpson, A. H. R. W. (2007) 'Inhibition of fracture healing.', The Journal of bone and joint surgery British volume, 89(12), pp. 1553–1560. doi: 10.1302/0301-620X.89B12.19671.

Gerber, H. P., Vu, T. H., Ryan, A. M., Kowalski, J., Werb, Z. and Ferrara, N. (1999) 'VEGF couples hypertrophic cartilage remodeling, ossification and angiogenesis during endochondral bone formation.', Nature Medicine, 5(6), pp. 623–628. doi: 10.1038/9467.

Gerlach, L.-O., Skerlj, R. T., Bridger, G. J. and Schwartz, T. W. (2001) 'Molecular Interactions of Cyclam and Bicyclam Non-peptide Antagonists with the CXCR4 Chemokine Receptor', Journal of Biological Chemistry, 276(17), pp. 14153–14160. doi: 10.2165/00126839-199902050-00010.

Gerstenfeld, L. C., Cullinane, D. M., Barnes, G. L., Graves, D. T. and Einhorn, T. A. (2003) 'Fracture healing as a post-natal developmental process: molecular, spatial, and temporal aspects of its regulation.', Journal of cellular biochemistry, 88(5), pp. 873–884. doi: 10.1002/jcb.10435.

Ghiasi, M. S., Chen, J., Vaziri, A., Rodriguez, E. K. and Nazarian, A. (2017) 'Bone fracture healing in mechanobiological modeling: A review of principles and methods.', Bone Reports, 6, pp. 87–100. doi: 10.1016/j.bonr.2017.03.002.

Giannoudis, P. V., Einhorn, T. A. and Marsh, D. (2007) 'Fracture healing: the diamond concept.', Injury, 38 Suppl 4, pp. S3–6.

Giles, E. M., Godbout, C., Chi, W., Glick, M. A., Lin, T., Li, R., Schemitsch, E. H. and Nauth, A. (2017) 'Subtypes of endothelial progenitor cells affect healing of segmental bone defects differently.', International Orthopaedics, 41(11), pp. 2337–2343. doi: 10.1007/s00264-017-3613-0.

Giuliani, N., Lisignoli, G., Magnani, M., Racano, C., Bolzoni, M., Dalla Palma, B., Spolzino, A., Manferdini, C., Abati, C., Toscani, D., Facchini, A. and Aversa, F. (2013) 'New Insights into Osteogenic and Chondrogenic Differentiation of Human Bone Marrow Mesenchymal Stem Cells and Their Potential Clinical Applications for Bone Regeneration in Pediatric Orthopaedics', Stem Cells International. Hindawi, 2013(5), pp. 1–11. doi: 10.1016/j.diff.2009.08.001.

Goodship, A. E. and Kenwright, J. (1985) 'The influence of induced micromovement upon the healing of experimental tibial fractures.', The Journal of bone and joint surgery British volume, 67(4), pp. 650–655.

Goodship, A. E., Cunningham, J. L. and Kenwright, J. (1998) 'Strain rate and timing of stimulation in mechanical modulation of fracture healing.', Clinical orthopaedics and related research, (355 Suppl), pp. S105–15.

Gothard, D., Greenhough, J., Ralph, E. and Oreffo, R. O. (2014) 'Prospective isolation of human bone marrow stromal cell subsets: A comparative study between Stro-1-, CD146- and CD105-enriched populations', Journal of Tissue Engineering. SAGE Publications, 5(0). doi: 10.1177/2041731414551763.

Granero-Moltó, F., Weis, J. A., Miga, M. I., Landis, B., Myers, T. J., O'Rear, L., Longobardi, L., Jansen, E. D., Mortlock, D. P. and Spagnoli, A. (2017) 'Effect of SDF-1/Cxcr4 Signaling Antagonist AMD3100 on Bone Mineralization in Distraction Osteogenesis', Stem Cells, 250(8), pp. 1887–1898. doi: 10.1002/stem.103.

Gruber, R., Koch, H., Doll, B. A., Tegtmeier, F., Einhorn, T. A. and Hollinger, J. O. (2006) 'Fracture healing in the elderly patient.', Experimental gerontology, 41(11), pp. 1080–1093. doi: 10.1016/j.exger.2006.09.008.

Guo, M. Z., Xia, Z. S. and Lin, L. B. (1991) 'The mechanical and biological properties of demineralised cortical bone allografts in animals.', The Journal of bone and joint surgery British volume, 73(5), pp. 791–794.

Hadjiargyrou, M. and O'Keefe, R. J. (2014) 'The convergence of fracture repair and stem cells: interplay of genes, aging, environmental factors and disease.', Journal of Bone and Mineral Research, 29(11), pp. 2307–2322. doi: 10.1002/jbmr.2373.

Hankenson, K. D., Dishowitz, M., Gray, C. and Schenker, M. (2011) 'Angiogenesis in bone regeneration.', Injury, 42(6), pp. 556–561. doi: 10.1016/j.injury.2011.03.035.

Harrison, L. J., Cunningham, J. L., Strömberg, L. and Goodship, A. E. (2003) 'Controlled induction of a pseudarthrosis: a study using a rodent model.', Journal of orthopaedic trauma, 17(1), pp. 11–21.

Harwood, P. J., Newman, J. B. and Michael, A. L. (2010) '(ii) An update on fracture healing and non-union', Orthopaedics and Trauma. Elsevier Ltd, 24(1), pp. 9–23. doi: 10.1016/j.mporth.2009.12.004.

Hausman, M. R., Schaffler, M. B. and Majeska, R. J. (2001) 'Prevention of fracture healing in rats by an inhibitor of angiogenesis.', Bone, 29(6), pp. 560–564. doi: 10.1016/S8756-3282(01)00608-1.

Hayashi, O., Katsube, Y., Hirose, M., Ohgushi, H. and Ito, H. (2008) 'Comparison of osteogenic ability of rat mesenchymal stem cells from bone marrow, periosteum, and adipose tissue.', Calcified Tissue International, 82(3), pp. 238–247. doi: 10.1007/s00223-008-9112-y.

Hayashi, T., Misawa, H., Nakahara, H., Noguchi, H., Yoshida, A., Kobayashi, N., Tanaka, M. and Ozaki, T. (2012) 'Transplantation of osteogenically differentiated mouse iPS cells for bone repair.', Cell Transplantation, 21(2-3), pp. 591–600. doi: 10.3727/096368911X605529.

He, Q., Wan, C. and Li, G. (2006) 'Concise Review: Multipotent Mesenchymal Stromal Cells in Blood', Stem Cells, 25(1), pp. 69–77. doi: 10.1634/stemcells.2006-0335.

Hendrix, C. W., Flexner, C., MacFarland, R. T., Giandomenico, C., Fuchs, E. J., Redpath, E., Bridger, G. and Henson, G. W. (2000) 'Pharmacokinetics and safety of AMD-3100, a novel antagonist of the CXCR-4 chemokine receptor, in human volunteers.', Antimicrobial agents and chemotherapy, 44(6), pp. 1667–1673.

Heppenstall, R. B., Brighton, C. T., Esterhai, J. L., Katz, M. and Schumacher, R. (1987) 'Synovial pseudarthrosis: a clinical, roentgenographic-scintigraphic, and pathologic study.', The Journal of trauma, 27(5), pp. 463–470.

Heppenstall, R. B., Grislis, G. and Hunt, T. K. (1975) 'Tissue gas tensions and oxygen consumption in healing bone defects.', Clinical orthopaedics and related research, (106), pp. 357–365.

Hernigou, P. (2016) 'History of external fixation for treatment of fractures', International Orthopaedics. Springer Berlin Heidelberg, 41(4), pp. 845–853. doi: 10.1097/00007611-193907000-00010.

Hernigou, P., Poignard, A., Beaujean, F. and Rouard, H. (2005) 'Percutaneous autologous bone-marrow grafting for nonunions. Influence of the number and concentration of progenitor cells.', The Journal of bone and joint surgery. American volume, 87(7), pp. 1430–1437. doi: 10.2106/JBJS.D.02215.

Herrmann, M., Zeiter, S., Eberli, U., Hildebrand, M., Camenisch, K., Menzel, U., Alini, M., Verrier, S. and Stadelmann, V. A. (2018) 'Five Days Granulocyte Colony-Stimulating Factor Treatment Increases Bone Formation and Reduces Gap Size of a Rat Segmental Bone Defect: A Pilot Study.', Frontiers in Bioengineering and Biotechnology, 6, p. 5. doi: 10.3389/fbioe.2018.00005.

Hillier, M. L. and Bell, L. S. (2007) 'Differentiating Human Bone from Animal Bone: A Review of Histological Methods', Journal of Forensic Sciences, 52(2), pp. 249–263. doi: 10.1111/j.1556-4029.2006.00368.x.

Hippocrates (1939) The genuine works of Hippocrates, trans. Francis Adams. Williams and Wilkins, Baltimore

Hirota, K. and Semenza, G. L. (2006) 'Regulation of angiogenesis by hypoxia-inducible factor 1.', Critical reviews in oncology/hematology, 59(1), pp. 15–26. doi: 10.1016/j.critrevonc.2005.12.003.

Ho, C.-Y., Sanghani, A., Hua, J., Coathup, M. J., PhD, Kalia, P. and Blunn, G. (2014) 'Mesenchymal stem cells with increased SDF-1 expression enhanced fracture healing.', Tissue engineering. Part A, p. 140924064904001. doi: 10.1089/ten.TEA.2013.0762.

Hock, J. M., Centrella, M. and Canalis, E. (1988) 'Insulin-like growth factor I has independent effects on bone matrix formation and cell replication.', Endocrinology, 122(1), pp. 254–260. doi: 10.1210/endo-122-1-254.

Hristov, M., Erl, W. and Weber, P. C. (2003) 'Endothelial progenitor cells: mobilization, differentiation, and homing.', Arteriosclerosis, thrombosis, and vascular biology, 23(7), pp. 1185–1189. doi: 10.1161/01.ATV.0000073832.49290.B5.

Huber, T. L., Kouskoff, V., Fehling, H. J., Palis, J. and Keller, G. (2004) 'Haemangioblast commitment is initiated in the primitive streak of the mouse embryo.', Nature, 432(7017), pp. 625–630. doi: 10.1038/nature03122.

Huiskes, R. and Chao, E. Y. (1986) ‘Guidelines for external fixation frame rigidity and stresses.’, Journal of orthopaedic research : official publication of the Orthopaedic Research Society, 4(1), pp. 68–75. doi: 10.1002/jor.1100040108.

Huiskes, R., Chao, E. Y. and Crippen, T. E. (1985) ‘Parametric analyses of pin-bone stresses in external fracture fixation devices.’, Journal of orthopaedic research : official publication of the Orthopaedic Research Society, 3(3), pp. 341–349. doi: 10.1002/jor.1100030311.

Hur, J., Yoon, C.-H., Kim, H.-S., Choi, J.-H., Kang, H.-J., Hwang, K.-K., Oh, B.-H., Lee, M.-M. and Park, Y.-B. (2004) ‘Characterization of two types of endothelial progenitor cells and their different contributions to neovasculogenesis.’, Arteriosclerosis, thrombosis, and vascular biology, 24(2), pp. 288–293. doi: 10.1161/01.ATV.0000114236.77009.06.

Ikeda, T., Kamekura, S., Mabuchi, A., Kou, I., Seki, S., Takato, T., Nakamura, K., Kawaguchi, H., Ikegawa, S. and Chung, U.-I. (2004) ‘The combination of SOX5, SOX6, and SOX9 (the SOX trio) provides signals sufficient for induction of permanent cartilage.’, Arthritis and rheumatism, 50(11), pp. 3561–3573. doi: 10.1002/art.20611.

Ilizarov GA (1990) ‘Clinical application of the tension-stress effect for limb lengthening’. Clin Orthop 250:8–26

Im, G.-I. and Shin, K.-J. (2015) ‘Epigenetic approaches to regeneration of bone and cartilage from stem cells’, Expert opinion on biological therapy, 15(2), pp. 181–193. doi: 10.1517/14712598.2015.960838.

Imitola, J., Raddassi, K., Park, K. I., Mueller, F.-J., Nieto, M., Teng, Y. D., Frenkel, D., Li, J., Sidman, R. L., Walsh, C. A., Snyder, E. Y. and Khoury, S. J. (2004) ‘Directed migration of neural stem cells to sites of CNS injury by the stromal cell-derived factor 1alpha/CXC chemokine receptor 4 pathway.’, Proceedings of the National Academy of Sciences of the United States of America, 101(52), pp. 18117–18122. doi: 10.1073/pnas.0408258102.

Innes, J. F. and Myint, P. (2010) ‘Demineralised bone matrix in veterinary orthopaedics: A review’, Veterinary and comparative orthopaedics and traumatology : V.C.O.T, 23(6), pp. 393–399. doi: 10.3415/VCOT-10-02-0022.

Iyer, S., Weiss, C. and Mehta, A. (1997) ‘Effects of drill speed on heat production and the rate and quality of bone formation in dental implant osteotomies. Part I: Relationship between drill speed and heat production.’, The International journal of prosthodontics, 10(5), pp. 411–414.

Jaffe, E. A., Nachman, R. L., Becker, C. G. and Minick, C. R. (1973) ‘Culture of Human Endothelial Cells Derived from Umbilical Veins. Identification By Morphologic And Immunologic Criteria’, The Journal of clinical investigation, 52(11), pp. 2745–2756. doi: 10.1172/JCI107470.

Jäger, M., Degistirici, Ö., Knipper, A., Fischer, J., Sager, M. and Krauspe, R. (2007) ‘Bone Healing and Migration of Cord Blood-Derived Stem Cells Into a Critical Size Femoral Defect After

Xenotransplantation', Journal of Bone and Mineral Research, 22(8), pp. 1224–1233. doi: 10.1097/01.blo.0000143819.82510.0d.

Jagodzinski, M. and Krettek, C. (2007) 'Effect of mechanical stability on fracture healing — an update', Injury, 38(1), pp. S3–S10. doi: 10.1016/j.injury.2007.02.005.

Janeczek Portalska, K., Leferink, A., Groen, N., Fernandes, H., Moroni, L., van Blitterswijk, C. and de Boer, J. (2012) 'Endothelial Differentiation of Mesenchymal Stromal Cells', PloS one. Edited by I. Kerkis, 7(10), p. e46842. doi: 10.1371/journal.pone.0046842.t001.

Janssens, R., Struyf, S. and Proost, P. (2017) 'The unique structural and functional features of CXCL12', Nature Publishing Group. Nature Publishing Group, pp. 1–13. doi: 10.1038/cmi.2017.107.

Jepsen, K. J., Price, C., Silkman, L. J., Nicholls, F. H., Nasser, P., Hu, B., Hadi, N., Alapatt, M., Stapleton, S. N., Kakar, S., Einhorn, T. A. and Gerstenfeld, L. C. (2008) 'Genetic Variation in the Patterns of Skeletal Progenitor Cell Differentiation and Progression During Endochondral Bone Formation Affects the Rate of Fracture Healing', Journal of Bone and Mineral Research, 23(8), pp. 1204–1216. doi: 10.1016/0034-5288(94)90196-1.

Frith, J., and Genever, P. (2008) 'Transcriptional Control of Mesenchymal Stem Cell Differentiation', Transfusion Medicine and Hemotherapy. Karger Publishers, 35(3), p. 216. doi: 10.1159/000127448s.

Jones, H. H., Priest, J. D., Hayes, W. C., Tichenor, C. C. and Nagel, D. A. (1977) 'Humeral hypertrophy in response to exercise.', The Journal of bone and joint surgery. American volume, 59(2), pp. 204–208.

Jukes, J. M., Both, S. K., Leusink, A., Sterk, L. M. T., van Blitterswijk, C. A. and de Boer, J. (2008) 'Endochondral bone tissue engineering using embryonic stem cells.', Proceedings of the National Academy of Sciences, 105(19), pp. 6840–6845. doi: 10.1073/pnas.0711662105.

Kadiyala, S., Young, R. G., Thiede, M. A. and Bruder, S. P. (1997) 'Culture expanded canine mesenchymal stem cells possess osteochondrogenic potential in vivo and in vitro.', Cell Transplantation, 6(2), pp. 125–134.

Kamal, A., Iskandriati, D., Dilogo, I., Siregar, N., Hutagalung, E., Yusuf, A., Mariya, S. and Husodo, K. (2014) 'Comparison of cultured mesenchymal stem cells derived from bone marrow or peripheral blood of rats', Journal of Experimental and Integrative Medicine, 4(1), p. 17. doi: 10.5455/jeim.180913.or.091.

Kanczler, J. M. and Oreffo, R. O. C. (2008) 'Osteogenesis and angiogenesis: the potential for engineering bone.', European cells & materials, 15, pp. 100–114.

Kassis, I., Zangi, L., Rivkin, R., Levdansky, L., Samuel, S., Marx, G. and Gorodetsky, R. (2006) 'Isolation of mesenchymal stem cells from G-CSF-mobilized human peripheral blood using fibrin microbeads.', Bone marrow transplantation, 37(10), pp. 967–976. doi: 10.1038/sj.bmt.1705358.

Kawai, M. and Rosen, C. J. (2012) 'The insulin-like growth factor system in bone: basic and clinical implications.', Endocrinology and metabolism clinics of North America, 41(2), pp. 323–33– vi. doi: 10.1016/j.ecl.2012.04.013.

Kawakami, Y., Ii, M., Matsumoto, T., Kuroda, R., Kuroda, T., Kwon, S.-M., Kawamoto, A., Akimaru, H., Mifune, Y., Shoji, T., Fukui, T., Kurosaka, M. and Asahara, T. (2015) 'SDF-1/CXCR4 axis in Tie2-lineage cells including endothelial progenitor cells contributes to bone fracture healing.', Journal of Bone and Mineral Research, 30(1), pp. 95–105. doi: 10.1002/jbmr.2318.

Kazmers, N. H., Fragomen, A. T. and Rozbruch, S. R. (2016) 'Prevention of pin site infection in external fixation: a review of the literature', Strategies in Trauma and Limb Reconstruction. Springer Milan, 11(2), pp. 75–85. doi: 10.1007/s11751-016-0256-4.

Kenwright, J. and Goodship, A. E. (1989) 'Controlled mechanical stimulation in the treatment of tibial fractures.', Clinical orthopaedics and related research, (241), pp. 36–47.

Keramaris, N. C., Calori, G. M., Nikolaou, V. S., Schemitsch, E. H. and Giannoudis, P. V. (2008) 'Fracture vascularity and bone healing: a systematic review of the role of VEGF.', Injury, 39 Suppl 2, pp. S45–57. doi: 10.1016/S0020-1383(08)70015-9.

Ketenjian, A. Y. and Arsenis, C. (1975) 'Morphological and biochemical studies during differentiation and calcification of fracture callus cartilage.', Clinical orthopaedics and related research, (107), pp. 266–273.

Key, J. A. (1934) 'The effect of a local calcium depot on osteogenesis and healing of fractures.', J Bone Joint Surg 16:176–184.

Khan, S. N., Cammisa, F. P., Sandhu, H. S., Diwan, A. D., Girardi, F. P. and Lane, J. M. (2005) 'The biology of bone grafting.', Journal of the American Academy of Orthopaedic Surgeons, 13(1), pp. 77–86.

Khosla, S. and Eghbali-Fatourechi, G. Z. (2006) 'Circulating cells with osteogenic potential.', Annals of the New York Academy of Sciences, 1068, pp. 489–497. doi: 10.1196/annals.1346.022.

Kidd, L. J., Stephens, A. S., Kuliwaba, J. S., Fazzalari, N. L., Wu, A. C. K. and Forwood, M. R. (2010) 'Temporal pattern of gene expression and histology of stress fracture healing', Bone. Elsevier Inc., 46(2), pp. 369–378. doi: 10.1016/j.bone.2009.10.009.

Kim, S., Kim, S.-S., Lee, S.-H., Eun Ahn, S., Gwak, S.-J., Song, J.-H., Kim, B.-S. and Chung, H.-M. (2008) 'In vivo bone formation from human embryonic stem cell-derived osteogenic cells in poly(d,l-lactic-co-glycolic acid)/hydroxyapatite composite scaffolds', Biomaterials, 29(8), pp. 1043–1053. doi: 10.1016/j.biomaterials.2007.11.005.

Kitaori, T., Ito, H., Schwarz, E. M., Tsutsumi, R., Yoshitomi, H., Oishi, S., Nakano, M., Fujii, N., Nagasawa, T. and Nakamura, T. (2009) 'Stromal cell–derived factor 1/CXCR4 signaling is critical for the recruitment of mesenchymal stem cells to the fracture site during skeletal repair in a mouse model', Arthritis and rheumatism. Wiley Online Library, 60(3), pp. 813–823.

Klein-Nulend, J., Bacabac, R. G. and Bakker, A. D. (2012) 'Mechanical loading and how it affects bone cells: the role of the osteocyte cytoskeleton in maintaining our skeleton.', European cells & materials, 24, pp. 278–291.

Klein, P., Schell, H., Streitparth, F., Heller, M., Kassi, J.-P., Kandziora, F., Bragulla, H., Haas, N. P. and Duda, G. N. (2003) 'The initial phase of fracture healing is specifically sensitive to mechanical conditions.', Journal of orthopaedic research : official publication of the Orthopaedic Research Society, 21(4), pp. 662–669. doi: 10.1016/S0736-0266(02)00259-0.

Kleinheinz, J., Stratmann, U., Joos, U. and Wiesmann, H.-P. (2005) 'VEGF-Activated Angiogenesis During Bone Regeneration', Journal of Oral and Maxillofacial Surgery, 63(9), pp. 1310–1316. doi: 10.1016/j.joms.2005.05.303.

Knight, M. N. and Hankenson, K. D. (2013) 'Mesenchymal Stem Cells in Bone Regeneration', Advances in Wound Care, 2(6), pp. 306–316. doi: 10.1089/wound.2012.0420.

Kriston-Pál, É., Czibula, Á., Gyuris, Z., Balka, G., Seregi, A., Sükösd, F., Süth, M., Kiss-Tóth, E., Haracska, L., Uher, F. and Monostori, É. (2017) 'Characterization and therapeutic application of canine adipose mesenchymal stem cells to treat elbow osteoarthritis.', Canadian journal of veterinary research = Revue canadienne de recherche vétérinaire, 81(1), pp. 73–78.

Krølner, B. and Toft, B. (1983) 'Vertebral bone loss: an unheeded side effect of therapeutic bed rest.', Clinical science (London, England : 1979), 64(5), pp. 537–540.

Kubo, H., Shimizu, M., Taya, Y., Kawamoto, T., Michida, M., Kaneko, E., Igarashi, A., Nishimura, M., Segoshi, K., Shimazu, Y., Tsuji, K., Aoba, T. and Kato, Y. (2009) 'Identification of mesenchymal stem cell (MSC)-transcription factors by microarray and knockdown analyses, and signature molecule-marked MSC in bone marrow by immunohistochemistry.', Genes to cells : devoted to molecular & cellular mechanisms, 14(3), pp. 407–424. doi: 10.1111/j.1365-2443.2009.01281.x.

Kuhn, A., Mc Iff, T., JJ, C., Baumgart, F. W. and A, R. B. (1995) 'Bone deformation by thread-cutting and thread-forming cortex screws', Injury, 26, pp. 12–20.

Kumagai, K., Vasanji, A., Drazba, J. A., Butler, R. S. and Muschler, G. F. (2008) 'Circulating cells with osteogenic potential are physiologically mobilized into the fracture healing site in the parabiotic mice model.', Journal of Orthopaedic Research, 26(2), pp. 165–175. doi: 10.1002/jor.20477.

Kumar, S. and Ponnazhagan, S. (2012) 'Mobilization of bone marrow mesenchymal stem cells in vivo augments bone healing in a mouse model of segmental bone defect.', Bone, 50(4), pp. 1012–1018. doi: 10.1016/j.bone.2012.01.027.

Kumar, S., Wan, C., Ramaswamy, G., Clemens, T. L. and Ponnazhagan, S. (2010) 'Mesenchymal stem cells expressing osteogenic and angiogenic factors synergistically enhance bone formation in a mouse model of segmental bone defect.', Molecular therapy : the journal of the American Society of Gene Therapy, 18(5), pp. 1026–1034. doi: 10.1038/mt.2009.315.

Kuroda, R., Matsumoto, T., Kawakami, Y., Fukui, T., Mifune, Y. and Kurosaka, M. (2014) 'Clinical Impact of Circulating CD34-Positive Cells on Bone Regeneration and Healing', Tissue engineering. Part B, Reviews, 20(3), pp. 190–199. doi: 10.1089/ten.teb.2013.0511.

Kusuma, G. D., Menicanin, D., Gronthos, S., Manuelpillai, U., Abumaree, M. H., Pertile, M. D., Brennecke, S. P. and Kalionis, B. (2015) 'Ectopic Bone Formation by Mesenchymal Stem Cells Derived from Human Term Placenta and the Decidua.', PloS one, 10(10), p. e0141246. doi: 10.1371/journal.pone.0141246.

Kuznetsov, S. A., Mankani, M. H., Gronthos, S., Satomura, K., Bianco, P. and Robey, P. G. (2001) 'Circulating Skeletal Stem Cells', The Journal of Cell Biology, 153(5), pp. 1133–1140. doi: 10.1002/1097-4644(20000901)78:3<391::AID-JCB5>3.0.CO;2-E.

Lambotte, A. (1913) Chirurgie operatoire des fractures. Masson, Paris

Lanyon, L. E. (1984) 'Functional strain as a determinant for bone remodeling', Calcified Tissue International, 36(S1), pp. S56–S61. doi: 10.1007/BF02406134.

Lanyon, L. E., Paul, I. L., Rubin, C. T., Thrasher, E. L., DeLaura, R., Rose, R. M. and Radin, E. L. (1981) 'In vivo strain measurements from bone and prosthesis following total hip replacement. An experimental study in sheep.', The Journal of bone and joint surgery. American volume, 63(6), pp. 989–1001.

Lapidot, T. and Petit, I. (2002) 'Current understanding of stem cell mobilization: the roles of chemokines, proteolytic enzymes, adhesion molecules, cytokines, and stromal cells.', Experimental Hematology, 30(9), pp. 973–981.

Lee, D. V., Bertram, J. E. and Todhunter, R. J. (1999) 'Acceleration and balance in trotting dogs.', The Journal of experimental biology, 202(Pt 24), pp. 3565–3573.

Lee, D. Y., Cho, T.-J., Kim, J. A., Lee, H. R., Yoo, W. J., Chung, C. Y. and Choi, I. H. (2008) 'Mobilization of endothelial progenitor cells in fracture healing and distraction osteogenesis.', Bone, 42(5), pp. 932–941. doi: 10.1016/j.bone.2008.01.007.

Lee, D. Y., Cho, T.-J., Lee, H. R., Park, M. S., Yoo, W. J., Chung, C. Y. and Choi, I. H. (2010) 'Distraction osteogenesis induces endothelial progenitor cell mobilization without inflammatory response in man.', Bone, 46(3), pp. 673–679. doi: 10.1016/j.bone.2009.10.018.

Lethaby, A., Temple, J. and Santy-Tomlinson, J. (1996) Pin site care for preventing infections associated with external bone fixators and pins. Edited by A. Lethaby. Chichester, UK: John Wiley & Sons, Ltd. doi: 10.1002/14651858.CD004551.pub3.

Lévesque, J.-P., Hendy, J., Takamatsu, Y., Simmons, P. J. and Bendall, L. J. (2003) 'Disruption of the CXCR4/CXCL12 chemotactic interaction during hematopoietic stem cell mobilization induced by GCSF or cyclophosphamide.', The Journal of clinical investigation, 111(2), pp. 187–196. doi: 10.1172/JCI15994.

Lévesque, J.-P., Winkler, I. G., Larsen, S. R. and Rasko, J. E. J. (2007) 'Mobilization of bone marrow-derived progenitors.', Handbook of experimental pharmacology, (180), pp. 3–36. doi: 10.1007/978-3-540-68976-8_1.

Levi, B., James, A. W., Wan, D. C., Glotzbach, J. P., Commons, G. W. and Longaker, M. T. (2010) 'Regulation of human adipose-derived stromal cell osteogenic differentiation by insulin-like growth factor-1 and platelet-derived growth factor-alpha.', Plastic and reconstructive surgery, 126(1), pp. 41–52. doi: 10.1097/PRS.0b013e3181da8858.

Lewellis, S. W. and Knaut, H. (2012) 'Attractive guidance: How the chemokine SDF1/CXCL12 guides different cells to different locations', Seminars in cell & developmental biology, 23(3), pp. 333–340. doi: 10.1016/j.semcdb.2012.03.009.

Lewis, D. D., Cross, A. R., Carmichael, S. and Anderson, M. A. (2001) 'Recent advances in external skeletal fixation.', The Journal of small animal practice, 42(3), pp. 103–112.

Li, R., Atesok, K., Nauth, A., Wright, D., Qamirani, E., Whyne, C. M. and Schemitsch, E. H. (2011) 'Endothelial progenitor cells for fracture healing: a microcomputed tomography and biomechanical analysis.', Journal of orthopaedic trauma, 25(8), pp. 467–471. doi: 10.1097/BOT.0b013e31821ad4ec.

Lieberman, J. R., Daluiski, A. and Einhorn, T. A. (2002) 'The role of growth factors in the repair of bone. Biology and clinical applications.', The Journal of bone and joint surgery. American volume, 84-A(6), pp. 1032–1044.

Liles, W. C., Broxmeyer, H. E., Rodger, E., Wood, B., Hübel, K., Cooper, S., Hangoc, G., Bridger, G. J., Henson, G. W., Calandra, G. and Dale, D. C. (2003) 'Mobilization of hematopoietic progenitor cells in healthy volunteers by AMD3100, a CXCR4 antagonist.', Blood, 102(8), pp. 2728–2730. doi: 10.1182/blood-2003-02-0663.

Liles, W. C., Rodger, E., Broxmeyer, H. E., Dehner, C., Badel, K., Calandra, G., Christensen, J., Wood, B., Price, T. H. and Dale, D. C. (2005) 'Augmented mobilization and collection of CD34+ hematopoietic cells from normal human volunteers stimulated with granulocyte-colony-stimulating factor by single-dose administration of AMD3100, a CXCR4 antagonist.', Transfusion, 45(3), pp. 295–300. doi: 10.1111/j.1537-2995.2005.04222.x.

Lin, C.-S., Ning, H., Lin, G. and Lue, T. F. (2012) 'Is CD34 truly a negative marker for mesenchymal stromal cells?', Cytotherapy, 14(10), pp. 1159–1163. doi: 10.3109/14653249.2012.729817.

Lin, C.-S., Xin, Z.-C., Dai, J. and Lue, T. F. (2013) 'Commonly used mesenchymal stem cell markers and tracking labels: Limitations and challenges.', Histology and histopathology, 28(9), pp. 1109–1116. doi: 10.14670/HH-28.1109.

Lin, Q., Lin, Q., Wesson, R. N., Wesson, R. N., Maeda, H., Maeda, H., Wang, Y., Wang, Y., Cui, Z., Cui, Z., Liu, J. O., Liu, J. O., Cameron, A. M., Cameron, A. M., Gao, B., Gao, B., Montgomery, R. A., Montgomery, R. A., Williams, G. M., Williams, G. M., Sun, Z. and Sun, Z. (2014) 'Pharmacological Mobilization of Endogenous Stem Cells Significantly Promotes Skin Regeneration after Full-Thickness Excision: The Synergistic Activity of AMD3100 and Tacrolimus', Journal of Investigative Dermatology. Nature Publishing Group, 134(9), pp. 2458–2468. doi: 10.1038/jid.2014.162.

Lindaman, L. M. (2001) 'Bone healing in children.', Clinics in podiatric medicine and surgery, 18(1), pp. 97–108.

Little, M.T. and Storb, R. (2002) 'History of haematopoietic stem-cell transplantation.', Nature reviews. Cancer, 2(3), pp. 231–238. doi: 10.1038/nrc748.

Liu, J. W., Dunoyer-Geindre, S., Serre-Beinier, V., Mai, G., Lambert, J.-F., Fish, R. J., Pernod, G., Buehler, L., Bounameaux, H. and Kruithof, E. K. O. (2007) 'Characterization of endothelial-like cells derived from human mesenchymal stem cells.', Journal of thrombosis and haemostasis : JTH, 5(4), pp. 826–834. doi: 10.1111/j.1538-7836.2007.02381.x.

Liu, L., Yu, Q., Fu, S., Wang, B., Hu, K., Wang, L., Hu, Y., Xu, Y., Yu, X. and Huang, H. (2018) 'CXCR4 Antagonist AMD3100 Promotes Mesenchymal Stem Cell Mobilization in Rats Preconditioned with the Hypoxia-Mimicking Agent Cobalt Chloride', Stem cells and development, 27(7), pp. 466–478. doi: 10.1089/scd.2017.0191.

Liu, X. L., Hu, X., Cai, W. X., Lu, W. W. and Zheng, L. W. (2016) 'Effect of Granulocyte-Colony Stimulating Factor on Endothelial Cells and Osteoblasts.', BioMed research international, 2016, p. 8485721. doi: 10.1155/2016/8485721.

Loboa, E. G., Beaupré, G. S. and Carter, D. R. (2001) 'Mechanobiology of initial pseudarthrosis formation with oblique fractures.', Journal of orthopaedic research : official publication of the Orthopaedic Research Society, 19(6), pp. 1067–1072. doi: 10.1016/S0736-0266(01)00028-6.

Ma, X.-L., Sun, X.-L., Wan, C.-Y., Ma, J.-X. and Tian, P. (2012) 'Significance of circulating endothelial progenitor cells in patients with fracture healing process', Journal of orthopaedic research : official publication of the Orthopaedic Research Society, 30(11), pp. 1860–1866. doi: 10.1002/jor.22134.

Magyar, G., Toksvig-Larsen, S. and Moroni, A. (1997) 'Hydroxyapatite coating of threaded pins enhances fixation.', The Journal of bone and joint surgery British volume, 79(3), pp. 487–489.

Malgaigne, J. F. (1847) Traité des fractures et des luxations. J. B. Baillière, Paris, pp 771–772

Mansilla, E., Marín, G. H., Drago, H., Sturla, F., Salas, E., Gardiner, C., Bossi, S., Lamonega, R., Guzmán, A., Nuñez, A., Gil, M. A., Piccinelli, G., Ibar, R. and Soratti, C. (2006) 'Bloodstream cells phenotypically identical to human mesenchymal bone marrow stem cells circulate in large amounts under the influence of acute large skin damage: new evidence for their use in regenerative medicine.', Transplantation proceedings, 38(3), pp. 967–969. doi: 10.1016/j.transproceed.2006.02.053.

Mareschi, K., Rustichelli, D., Calabrese, R., Gunetti, M., Sanavio, F., Castiglia, S., Risso, A., Ferrero, I., Tarella, C. and Fagioli, F. (2012) 'Multipotent Mesenchymal Stromal Stem Cell Expansion by Plating Whole Bone Marrow at a Low Cellular Density: A More Advantageous Method for Clinical Use', Stem Cells International, 2012(2), pp. 1–10. doi: 10.1016/j.arcmed.2003.09.006.

Marsell, R. and Einhorn, T. A. (2009) 'The role of endogenous bone morphogenetic proteins in normal skeletal repair.', Injury, 40 Suppl 3, pp. S4–7. doi: 10.1016/S0020-1383(09)70003-8.

Marsell, R. and Einhorn, T. A. (2011) 'The biology of fracture healing', Injury, 42(6), pp. 551–555. doi: 10.1016/j.injury.2011.03.031.

Martin, C., Bridger, G. J. and Rankin, S. M. (2006) 'Structural analogues of AMD3100 mobilise haematopoietic progenitor cells from bone marrow in vivo according to their ability to inhibit CXCL12 binding to CXCR4 in vitro.', British journal of haematology, 134(3), pp. 326–329. doi: 10.1111/j.1365-2141.2006.06181.x.

Martin, R. B. and Burr, D. B. (1989) Structure, function, and adaptation of compact bone. Raven Pr.

Martinez de Albornoz, P., Khanna, A., Longo, U. G., Forriol, F. and Maffulli, N. (2011) 'The evidence of low-intensity pulsed ultrasound for in vitro, animal and human fracture healing', British medical bulletin, 100(1), pp. 39–57. doi: 10.1016/j.ultrasmedbio.2005.07.012.

Matsumoto, T., Kawamoto, A., Kuroda, R., Ishikawa, M., Mifune, Y., Iwasaki, H., Miwa, M., Horii, M., Hayashi, S., Oyamada, A., Nishimura, H., Murasawa, S., Doita, M., Kurosaka, M. and Asahara, T. (2006) 'Therapeutic potential of vasculogenesis and osteogenesis promoted by peripheral blood CD34-positive cells for functional bone healing.', The American journal of pathology, 169(4), pp. 1440–1457. doi: 10.2353/ajpath.2006.060064.

Matsumoto, T., Kuroda, R., Mifune, Y., Kawamoto, A., Shoji, T., Miwa, M., Asahara, T. and Kurosaka, M. (2008) 'Circulating endothelial/skeletal progenitor cells for bone regeneration and healing.', Bone, 43(3), pp. 434–439. doi: 10.1016/j.bone.2008.05.001.

Matthews, L. S. and Hirsch, C. (1972) 'Temperatures measured in human cortical bone when drilling.', The Journal of bone and joint surgery. American volume, 54(2), pp. 297–308.

Matthews, L. S., Green, C. A. and Goldstein, S. A. (1984) 'The thermal effects of skeletal fixation-pin insertion in bone.', The Journal of bone and joint surgery. American volume, 66(7), pp. 1077–1083.

Mauney, J. R., Sjostorm, S., Blumberg, J., Horan, R., O'Leary, J. P., Vunjak-Novakovic, G., Volloch, V. and Kaplan, D. L. (2004) 'Mechanical stimulation promotes osteogenic differentiation of human bone marrow stromal cells on 3-D partially demineralized bone scaffolds in vitro.', Calcified Tissue International, 74(5), pp. 458–468. doi: 10.1007/s00223-003-0104-7.

Mayr-Wohlfart, U., Waltenberger, J., Hausser, H., Kessler, S., Günther, K.-P., Dehio, C., Puhl, W. and Brenner, R. E. (2002) 'Vascular endothelial growth factor stimulates chemotactic migration of primary human osteoblasts.', Bone, 30(3), pp. 472–477. doi: 10.1016/S8756-3282(01)00690-1.

McKibbin, B. (1978) 'The biology of fracture healing in long bones.', The Journal of bone and joint surgery British volume, 60-B(2), pp. 150–162.

McNulty, M. A., Virdi, A. S., Christopherson, K. W., Sena, K., Frank, R. R. and Sumner, D. R. (2012) 'Adult stem cell mobilization enhances intramembranous bone regeneration: a pilot study.', Clinical orthopaedics and related research, 470(9), pp. 2503–2512. doi: 10.1007/s11999-012-2357-9.

Medina, R. J., O'Neill, C. L., Sweeney, M., Guduric-Fuchs, J., Gardiner, T. A., Simpson, D. A. and Stitt, A. W. (2010) 'Molecular analysis of endothelial progenitor cell (EPC) subtypes reveals two distinct cell populations with different identities.', BMC medical genomics, 3, p. 18. doi: 10.1186/1755-8794-3-18.

Mehta, M., Schell, H., Schwarz, C., Peters, A., Schmidt-Bleek, K., Ellinghaus, A., Bail, H. J., Duda, G. N. and Lienau, J. (2010) 'A 5-mm femoral defect in female but not in male rats leads to a reproducible atrophic non-union', Archives of Orthopaedic and Trauma Surgery, 131(1), pp. 121–129. doi: 10.1007/s00402-010-1155-7.

Midy, V. and Plouët, J. (1994) 'Vasculotropin/vascular endothelial growth factor induces differentiation in cultured osteoblasts.', Biochemical and biophysical research communications, 199(1), pp. 380–386. doi: 10.1006/bbrc.1994.1240.

Mills, L. A. and Simpson, A. (2012) 'In vivo models of bone repair', Journal of Bone & Joint Surgery, British Volume. British Editorial Society of Bone and Joint Surgery, 94(7), pp. 865–874. doi: 10.1302/0301-620X.94B7.

Mills, L. A. and Simpson, A. H. R. W. (2013) 'The relative incidence of fracture non-union in the Scottish population (5.17 million): a 5-year epidemiological study', BMJ Open, 3(2), pp. e002276–e002276. doi: 10.1136/bmjopen-2012-002276.

Minami, Y., Nakajima, T., Ikutomi, M., Morita, T., Komuro, I., Sata, M. and Sahara, M. (2015) 'Angiogenic potential of early and late outgrowth endothelial progenitor cells is dependent on the time of emergence.', International journal of cardiology, 186, pp. 305–314. doi: 10.1016/j.ijcard.2015.03.166.

Mochizuki, H., Hakeda, Y., Wakatsuki, N., Usui, N., Akashi, S., Sato, T., Tanaka, K. and Kumegawa, M. (1992) 'Insulin-like growth factor-I supports formation and activation of osteoclasts.', Endocrinology, 131(3), pp. 1075–1080. doi: 10.1210/endo.131.3.1505451.

Moerman, E. J., Teng, K., Lipschitz, D. A. and Lecka-Czernik, B. (2004) 'Aging activates adipogenic and suppresses osteogenic programs in mesenchymal marrow stroma/stem cells: the role of PPAR-γ2 transcription factor and TGF-β/BMP signaling pathways', Aging Cell. NIH Public Access, 3(6), pp. 379–389. doi: 10.1074/jbc.R100034200.

Mollon, B., da Silva, V., Busse, J. W., Einhorn, T. A. and Bhandari, M. (2008) 'Electrical stimulation for long-bone fracture-healing: a meta-analysis of randomized controlled trials.', The Journal of bone and joint surgery. American volume, 90(11), pp. 2322–2330. doi: 10.2106/JBJS.H.00111.

Moraes, D. A., Sibov, T. T., Pavon, L. F., Alvim, P. Q., Bonadio, R. S., Da Silva, J. R., Pic-Taylor, A., Toledo, O. A., Marti, L. C., Azevedo, R. B. and Oliveira, D. M. (2016) 'A reduction in CD90 (THY-1) expression results in increased differentiation of mesenchymal stromal cells.', Stem cell research & therapy, 7(1), p. 97. doi: 10.1186/s13287-016-0359-3.

Moss, D. P. and Tejwani, N. C. (2007) 'Biomechanics of external fixation: a review of the literature.', Bulletin of the NYU hospital for joint diseases, 65(4), pp. 294–299.

Mountziaris, P. M. and Mikos, A. G. (2008) 'Modulation of the Inflammatory Response for Enhanced Bone Tissue Regeneration', Tissue engineering. Part B, Reviews, 14(2), pp. 179–186. doi: 10.1089/ten.teb.2008.0038.

Muir, P., Johnson, K.A. & Markel, M.D., (1995) 'Area Moment of Inertia for Comparison of Implant Cross-Sectional Geometry and Bending Stiffness', VCOT 8, 146–152.

Mund, J. A. and Case, J. (2011) 'The ontogeny of endothelial progenitor cells through flow cytometry', Current Opinion in Hematology, 18(3), pp. 166–170. doi: 10.1097/MOH.0b013e328345a16a.

Muraglia, A., Cancedda, R. and Quarto, R. (2000) 'Clonal mesenchymal progenitors from human bone marrow differentiate in vitro according to a hierarchical model.', Journal of Cell Science, 113 (Pt 7), pp. 1161–1166.

Murata, K., Kitaori, T., Oishi, S., Watanabe, N., Yoshitomi, H., Tanida, S., Ishikawa, M., Kasahara, T., Shibuya, H., Fujii, N., Nagasawa, T., Nakamura, T. and Ito, H. (2012) 'Stromal cell-derived factor 1 regulates the actin organization of chondrocytes and chondrocyte hypertrophy.', PloS one, 7(5), p. e37163. doi: 10.1371/journal.pone.0037163.

Muscari, C., Gamberini, C., Basile, I., Bonafé, F., Valgimigli, S., Capitani, O., Guarnieri, C. and Marcello Caldarera, C. (2010) 'Comparison between Culture Conditions Improving Growth and Differentiation of Blood and Bone Marrow Cells Committed to the Endothelial Cell Lineage', Biological Procedures Online, 12(1), pp. 89–106. doi: 10.1007/s12575-009-9023-y.

Nagasawa, T., Kikutani, H. and Kishimoto, T. (1994) 'Molecular cloning and structure of a pre-B-cell growth-stimulating factor.', Proceedings of the National Academy of Sciences of the United States of America, 91(6), pp. 2305–2309.

Namba, R. S., Kabo, J. M. and Meals, R. A. (1987) 'Biomechanical effects of point configuration in Kirschner-wire fixation.', Clinical orthopaedics and related research, (214), pp. 19–22.

Nandra, R., Grover, L. and Porter, K. (2015) 'Fracture non-union epidemiology and treatment', Trauma. 7 edn, 18(1), pp. 3–11. doi: 10.1007/s00402-014-2014-8.

Neidlinger-Wilke, C., Grood, E. S., Wang JH-C, Brand, R. A. and Claes, L. (2001) 'Cell alignment is induced by cyclic changes in cell length: studies of cells grown in cyclically stretched substrates.', Journal of orthopaedic research : official publication of the Orthopaedic Research Society, 19(2), pp. 286–293. doi: 10.1016/S0736-0266(00)00029-2.

Netelenbos, T., van den Born, J., Kessler, F. L., Zweegman, S., Merle, P. A., van Oostveen, J. W., Zwaginga, J. J., Huijgens, P. C. and Dräger, A. M. (2003) 'Proteoglycans on bone marrow endothelial cells bind and present SDF-1 towards hematopoietic progenitor cells', Leukemia, 17(1), pp. 175–184. doi: 10.1002/(SICI)1521-4141(199902)29:02<700::AID-IMMU700>3.0.CO;2-1.

Newman, E., Turner, A. S. and Wark, J. D. (1995) 'The potential of sheep for the study of osteopenia: current status and comparison with other animal models.', Bone, 16(4 Suppl), pp. 277S–284S.

Nguyen, V. D., London, J. and 3rd, R. C. (1986) 'Ring sequestrum: radiographic characteristics of skeletal fixation pin-tract osteomyelitis.', Radiology.

Nicholls, F., Janic, K., Filomeno, P., Willett, T., Grynpas, M. and Ferguson, P. (2013) 'Effects of radiation and surgery on healing of femoral fractures in a rat model', Journal of orthopaedic research : official publication of the Orthopaedic Research Society, 31(8), pp. 1323–1331. doi: 10.1007/s00330-005-0010-7.

Nilsson, L. T., Johansson, A. and Strömqvist, B. (1993) 'Factors predicting healing complications in femoral neck fractures. 138 patients followed for 2 years.', Acta orthopaedica Scandinavica, 64(2), pp. 175–177.

Nitzsche, F., Müller, C., Lukomska, B., Jolkkonen, J., Deten, A. and Boltze, J. (2017) 'Concise Review: MSC Adhesion Cascade-Insights into Homing and Transendothelial Migration', Stem Cells, 35(6), pp. 1446–1460. doi: 10.1016/j.jcyt.2016.10.006.

Nöth, U., Rackwitz, L., Steinert, A. F. and Tuan, R. S. (2010) 'Cell delivery therapeutics for musculoskeletal regeneration.', Advanced drug delivery reviews, 62(7-8), pp. 765–783. doi: 10.1016/j.addr.2010.04.004.

Oliphant, B. W., Kim, H., Osgood, G. M., Golden, R. D., Hawks, M. A., Hsieh, A. H. and O'Toole, R. V. (2013) 'Predrilling does not improve the pullout strength of external fixator pins: a biomechanical study.', Journal of orthopaedic trauma, 27(2), pp. e25–30. doi: 10.1097/BOT.0b013e3182511ed7.

Oreffo, R. O., Driessens, F. C., Planell, J. A. and Triffitt, J. T. (1998) 'Growth and differentiation of human bone marrow osteoprogenitors on novel calcium phosphate cements.', Biomaterials, 19(20), pp. 1845–1854. doi: 10.1016/S0142-9612(98)00084-2.

Ormiston, M. L., Toshner, M. R., Kiskin, F. N., Huang, C. J. Z., Groves, E., Morrell, N. W. and Rana, A. A. (2015) 'Generation and Culture of Blood Outgrowth Endothelial Cells from Human Peripheral Blood', Journal of Visualized Experiments, (106). doi: 10.3791/53384.

Osagie-Clouard, L., Kaufmann, J., Blunn, G., Coathup, M., Pendegrass, C., Meeson, R., Briggs, T. and Moazen, M. (2018) 'Biomechanics of Two External Fixator Devices Used in Rat Femoral Fractures.', Journal of Orthopaedic Research. doi: 10.1002/jor.24034.

Oswald, J., Boxberger, S., Jørgensen, B., Feldmann, S., Ehninger, G., Bornhäuser, M. and Werner, C. (2004) 'Mesenchymal stem cells can be differentiated into endothelial cells in vitro.', Stem Cells, 22(3), pp. 377–384. doi: 10.1634/stemcells.22-3-377.

Otsuru, S., Tamai, K., Yamazaki, T., Yoshikawa, H. and Kaneda, Y. (2008) 'Circulating Bone Marrow-Derived Osteoblast Progenitor Cells Are Recruited to the Bone-Forming Site by the CXCR4/Stromal Cell-Derived Factor-1 Pathway', Stem Cells. John Wiley & Sons, Ltd., 26(1), pp. 223–234. doi: 10.1634/stemcells.2007-0515.

Owen, M. and Friedenstein, A. J. (1988) 'Stromal stem cells: marrow-derived osteogenic precursors.', Ciba Foundation symposium, 136, pp. 42–60.

Ozaki, A., Tsunoda, M., Kinoshita, S. and Saura, R. (2000) 'Role of fracture hematoma and periosteum during fracture healing in rats: interaction of fracture hematoma and the periosteum in the initial step of the healing process.', Journal of orthopaedic science : official journal of the Japanese Orthopaedic Association, 5(1), pp. 64–70.

Palmer, R. H., Hulse, D. A., Hyman, W. A. and Palmer, D. R. (1992) 'Principles of bone healing and biomechanics of external skeletal fixation.', The Veterinary clinics of North America. Small animal practice, 22(1), pp. 45–68.

Pandey, R. K. and Panda, S. S. (2013) 'Drilling of bone: A comprehensive review', Journal of Clinical Orthopaedics and Trauma. Elsevier Ltd, 4(1), pp. 15–30. doi: 10.1016/j.jcot.2013.01.002.

Parkhill C (1897) 'A new apparatus for the fixation of bones after resection and in fractures with a tendency to displacement'. Trans Am Surg Assoc 15:251–256.

Patel, J., Donovan, P. and Khosrotehrani, K. (2016) ‘Concise Review: Functional Definition of Endothelial Progenitor Cells: A Molecular Perspective’, Stem cells translational medicine, 5(10), pp. 1302–1306. doi: 10.1093/emboj/18.8.2196.

Pawig, L., Klasen, C., Weber, C., Bernhagen, J. and Noels, H. (2015) ‘Diversity and Inter-Connections in the CXCR4 Chemokine Receptor/Ligand Family: Molecular Perspectives.’, Frontiers in immunology, 6, p. 429. doi: 10.3389/fimmu.2015.00429.

Peichev, M., Naiyer, A. J., Pereira, D., Zhu, Z., Lane, W. J., Williams, M., Oz, M. C., Hicklin, D. J., Witte, L., Moore, M. A. and Rafii, S. (2000) ‘Expression of VEGFR-2 and AC133 by circulating human CD34(+) cells identifies a population of functional endothelial precursors.’, Blood, 95(3), pp. 952–958.

Peled, A. (1999) ‘Dependence of Human Stem Cell Engraftment and Repopulation of NOD/SCID Mice on CXCR4’, Science (New York, NY). American Association for the Advancement of Science, 283(5403), pp. 845–848. doi: 10.1126/science.283.5403.845.

Perren, S. M. (1979) ‘Physical and biological aspects of fracture healing with special reference to internal fixation.’, Clinical orthopaedics and related research, (138), pp. 175–196.

Perren, S. M. (2004) ‘Evolution of the internal fixation of long bone fractures. The scientific basis of biological internal fixation: choosing a new balance between stability and Biology.’, The Bone & Joint Journal, pp. 1–18.

Perren, S. M. (2015) ‘Fracture healing: fracture healing understood as the result of a fascinating cascade of physical and biological interactions. Part II.’, Acta chirurgiae orthopaedicae et traumatologiae Cechoslovaca, 82(1), pp. 13–21.

Pettit, G. D. (1992) ‘History of external skeletal fixation.’, The Veterinary clinics of North America. Small animal practice, 22(1), pp. 1–10.

Pitchford, S. C., Furze, R. C., Jones, C. P., Wengner, A. M. and Rankin, S. M. (2009) ‘Differential mobilization of subsets of progenitor cells from the bone marrow.’, Cell stem cell, 4(1), pp. 62–72. doi: 10.1016/j.stem.2008.10.017.

Pitchford, S. C., Hahnel, M. J., Jones, C. P. and Rankin, S. M. (2010) ‘Troubleshooting: Quantification of mobilization of progenitor cell subsets from bone marrow in vivo.’, Journal of pharmacological and toxicological methods, 61(2), pp. 113–121. doi: 10.1016/j.vascn.2010.01.013.

Pittenger, M. F., Mackay, A. M., Beck, S. C., Jaiswal, R. K., Douglas, R., Mosca, J. D., Moorman, M. A., Simonetti, D. W., Craig, S. and Marshak, D. R. (1999) ‘Multilineage potential of adult human mesenchymal stem cells.’, Science (New York, NY), 284(5411), pp. 143–147.

Prendergast, P. J., Huiskes, R. and Søballe, K. (1997) 'ESB Research Award 1996. Biophysical stimuli on cells during tissue differentiation at implant interfaces.', Journal of biomechanics, 30(6), pp. 539–548.

Puchert, M. and Engele, J. (2014) 'The peculiarities of the SDF-1/CXCL12 system: in some cells, CXCR4 and CXCR7 sing solos, in others, they sing duets.', Cell and tissue research, 355(2), pp. 239–253. doi: 10.1007/s00441-013-1747-y.

Rahn, A., Gallinaro, P., Baltensperger, A. and Perren, S. M. (1971) 'Primary bone healing. An experimental study in the rabbit.', The Journal of bone and joint surgery. American volume, 53(4), pp. 783–786.

Reed, A. A. C., Joyner, C. J., Brownlow, H. C. and Simpson, A. H. R. W. (2002) 'Human atrophic fracture non-unions are not avascular.', Journal of orthopaedic research : official publication of the Orthopaedic Research Society, 20(3), pp. 593–599. doi: 10.1016/S0736-0266(01)00142-5.

Reed, A. A. C., Joyner, C. J., Isefuku, S., Brownlow, H. C. and Simpson, A. H. R. W. (2003) 'Vascularity in a new model of atrophic nonunion.', The Journal of bone and joint surgery British volume, 85(4), pp. 604–610.

Rehman, J., Li, J., Orschell, C. M. and March, K. L. (2003) 'Peripheral blood "endothelial progenitor cells" are derived from monocyte/macrophages and secrete angiogenic growth factors.', Circulation, 107(8), pp. 1164–1169.

Rhinelander, F. W. (1968) 'The normal microcirculation of diaphyseal cortex and its response to fracture.', The Journal of bone and joint surgery. American volume, 50(4), pp. 784–800.

Rhinelander, F. W. (1974) 'Tibial blood supply in relation to fracture healing.', Clinical orthopaedics and related research, (105), pp. 34–81.

Richardson, J. B., Gardner, T. N., Hardy, J. R., Evans, M., Kuiper, J. H. and Kenwright, J. (1995) 'Dynamisation of tibial fractures.', The Journal of bone and joint surgery British volume, 77(3), pp. 412–416.

Rodan, G. A. (1992) 'Introduction to bone biology.', Bone, 13 Suppl 1, pp. S3–6.

Rodriguez-Merchan, E. C., Rodriguez-Merchan, E. C., Gomez-Castresana, F. and Gomez-Castresana, F. (2004) 'Internal Fixation of Nonunions.', Clinical orthopaedics and related research, 419, p. 13.

Rosen, E. D., Hsu, C.-H., Wang, X., Sakai, S., Freeman, M. W., Gonzalez, F. J. and Spiegelman, B. M. (2002) 'C/EBPalpha induces adipogenesis through PPARgamma: a unified pathway.', Genes & development, 16(1), pp. 22–26. doi: 10.1101/gad.948702.

Rosenkilde, M. M., Gerlach, L.-O., Jakobsen, J. S., Skerlj, R. T., Bridger, G. J. and Schwartz, T. W. (2004) 'Molecular Mechanism of AMD3100 Antagonism in the CXCR4 Receptor', Journal of Biological Chemistry, 279(4), pp. 3033–3041. doi: 10.1126/science.289.5480.739.

Rubin, H. (2002) 'The disparity between human cell senescence in vitro and lifelong replication in vivo.', Nature biotechnology, 20(7), pp. 675–681. doi: 10.1038/nbt0702-675.

Rüder, C., Haase, T., Krost, A., Langwieser, N., Peter, J., Kamann, S. and Zohlnhöfer, D. (2014) 'Combinatorial G-CSF/AMD3100 treatment in cardiac repair after myocardial infarction.', PloS one, 9(8), p. e104644. doi: 10.1371/journal.pone.0104644.

Rüster, B., Göttig, S., Ludwig, R. J., Bistrian, R., Müller, S., Seifried, E., Gille, J. and Henschler, R. (2006) 'Mesenchymal stem cells display coordinated rolling and adhesion behavior on endothelial cells.', Blood, 108(12), pp. 3938–3944. doi: 10.1182/blood-2006-05-025098.

Saag, K. G., Shane, E., Boonen, S., Marín, F., Donley, D. W., Taylor, K. A., Dalsky, G. P. and Marcus, R. (2007) 'Teriparatide or alendronate in glucocorticoid-induced osteoporosis.', New England Journal of Medicine, 357(20), pp. 2028–2039. doi: 10.1056/NEJMoa071408.

Saithna, A. (2010) 'The influence of hydroxyapatite coating of external fixator pins on pin loosening and pin track infection: A systematic review', Injury, 41(2), pp. 128–132. doi: 10.1016/j.injury.2009.01.001.

Sanghani-Kerai, A., Coathup, M., Samazideh, S., Kalia, P., Silvio, L. D., Idowu, B. and Blunn, G. (2017) 'Osteoporosis and ageing affects the migration of stem cells and this is ameliorated by transfection with CXCR4.', Bone and Joint Research, 6(6), pp. 358–365. doi: 10.1302/2046-3758.66.BJR-2016-0259.R1.

Sarahrudi, K., Thomas, A., Braunsteiner, T., Wolf, H., Vécsei, V. and Aharinejad, S. (2009) 'VEGF serum concentrations in patients with long bone fractures: A comparison between impaired and normal fracture healing', Journal of orthopaedic research : official publication of the Orthopaedic Research Society, 27(10), pp. 1293–1297. doi: 10.1002/jor.20906.

Sass, F. A., Schmidt-Bleek, K., Ellinghaus, A., Filter, S., Rose, A., Preininger, B., Reinke, S., Geissler, S., Volk, H.-D., Duda, G. N. and Dienelt, A. (2017) 'CD31+ Cells From Peripheral Blood Facilitate Bone Regeneration in Biologically Impaired Conditions Through Combined Effects on Immunomodulation and Angiogenesis', Journal of Bone and Mineral Research, 32(5), pp. 902–912. doi: 10.1172/JCI5928.

Savaridas, T., Wallace, R. J., Muir, A. Y., Salter, D. M. and Simpson, A. H. R. W. (2012) 'The development of a novel model of direct fracture healing in the rat.', Bone and Joint Research, 1(11), pp. 289–296. doi: 10.1302/2046-3758.111.2000087.

Schell, H., Epari, D. R., Kassi, J. P., Bragulla, H., Bail, H. J. and Duda, G. N. (2005) 'The course of bone healing is influenced by the initial shear fixation stability.', Journal of orthopaedic research : official publication of the Orthopaedic Research Society, 23(5), pp. 1022–1028. doi: 10.1016/j.orthres.2005.03.005.

Schemitsch, E. and Kuzyk, P. (2009) 'The science of electrical stimulation therapy for fracture healing', Indian Journal of Orthopaedics, 43(2), p. 127. doi: 10.4103/0019-5413.50846.

Schmitz, J. P. and Hollinger, J. O. (1986) 'The critical size defect as an experimental model for craniomandibulofacial nonunions.', Clinical orthopaedics and related research, (205), pp. 299–308.

Semerad, C. L. (2005) 'G-CSF potently inhibits osteoblast activity and CXCL12 mRNA expression in the bone marrow', Blood. American Society of Hematology, 106(9), pp. 3020–3027. doi: 10.1182/blood-2004-01-0272.

Sen, M. K. and Miclau, T. (2007) 'Autologous iliac crest bone graft: should it still be the gold standard for treating nonunions?', Injury, 38 Suppl 1, pp. S75–80. doi: 10.1016/j.injury.2007.02.012.

Sener, B. C., Dergin, G., Gursoy, B., Kelesoglu, E. and Slih, I. (2009) 'Effects of irrigation temperature on heat control in vitroat different drilling depths', Clinical Oral Implants Research, 20(3), pp. 294–298. doi: 10.1111/j.1600-0501.2008.01643.x.

Sethe, S., Scutt, A. and Stolzing, A. (2006) 'Aging of mesenchymal stem cells.', Ageing research reviews, 5(1), pp. 91–116. doi: 10.1016/j.arr.2005.10.001.

Shapiro, F. (1988) 'Cortical bone repair. The relationship of the lacunar-canalicular system and intercellular gap junctions to the repair process.', The Journal of bone and joint surgery. American volume, 70(7), pp. 1067–1081.

Sharawy, M., Misch, C. E., Weller, N. and Tehemar, S. (2002) 'Heat generation during implant drilling: the significance of motor speed.', Journal of oral and maxillofacial surgery : official journal of the American Association of Oral and Maxillofacial Surgeons, 60(10), pp. 1160–1169.

Sheng, G. (2015) 'The developmental basis of mesenchymal stem/stromal cells (MSCs)', BMC Developmental Biology. BioMed Central, 15. doi: 10.1186/s12861-015-0094-5.

Shi, Q., Rafii, S., Wu, M. H., Wijelath, E. S., Yu, C., Ishida, A., Fujita, Y., Kothari, S., Mohle, R., Sauvage, L. R., Moore, M. A., Storb, R. F. and Hammond, W. P. (1998) 'Evidence for circulating bone marrow-derived endothelial cells.', Blood, 92(2), pp. 362–367.

Shi, S. & Gronothos, S. (2003) 'Perivascular niche of postnatal mesenchymal stem cells in human bone marrow and dental pulp'. Journal of bone and mineral research, 18, 696- 704.

Shrivats, A. R., McDermott, M. C. and Hollinger, J. O. (2014) 'Bone tissue engineering: state of the union', Drug Discovery Today. Elsevier Ltd, 19(6), pp. 781–786. doi: 10.1016/j.drudis.2014.04.010.

Si, J.-W. (2015) ‘Perinatal stem cells: A promising cell resource for tissue engineering of craniofacial bone’, World journal of stem cells, 7(1), p. 149. doi: 10.4252/wjsc.v7.i1.149.

Sidney, L. E., Branch, M. J., Dunphy, S. E., Dua, H. S. and Hopkinson, A. (2014) ‘Concise Review: Evidence for CD34 as a Common Marker for Diverse Progenitors’, Stem Cells, 32(6), pp. 1380–1389. doi: 10.1002/stem.1661.

Simpson, A. H. R. W., Mills, L. and Noble, B. (2006) ‘The role of growth factors and related agents in accelerating fracture healing.’, The Journal of bone and joint surgery British volume, 88(6), pp. 701–705. doi: 10.1302/0301-620X.88B6.17524.

Slukvin, I. I. and Vodyanik, M. (2011) ‘Endothelial origin of mesenchymal stem cells.’, Cell cycle (Georgetown, Tex.), 10(9), pp. 1370–1373. doi: 10.4161/cc.10.9.15345.

Smith, R. K., Garvican, E. R. and Fortier, L. A. (2014) ‘The current “state of play” of regenerative medicine in horses: what the horse can tell the human’, Regenerative Medicine, 9(5), pp. 673–685. doi: 10.1016/j.cveq.2011.06.005.

Smitham, P., Crossfield, L., Hughes, G., Goodship, A., Blunn, G. and Chenu, C. (2014) ‘Low dose of propranolol does not affect rat osteotomy healing and callus strength.’, Journal of Orthopaedic Research, 32(7), pp. 887–893. doi: 10.1002/jor.22619.

Sohni, A. and Verfaillie, C. M. (2013) ‘Mesenchymal Stem Cells Migration Homing and Tracking’, Stem Cells International. Hindawi Publishing Corporation. Hindawi Publishing Corporation, 2013(4), pp. 1–8. doi: 10.1161/CIRCULATIONAHA.105.537480.

Spencer, E. M., Liu, C. C., Si, E. C. and Howard, G. A. (1991) ‘In vivo actions of insulin-like growth factor-I (IGF-I) on bone formation and resorption in rats.’, Bone, 12(1), pp. 21–26.

Spencer, N. D., Gimble, J. M. and Lopez, M. J. (2011) ‘Mesenchymal Stromal Cells: Past, Present, and Future’, Veterinary Surgery, 40(2), pp. 129–139. doi: 10.1111/j.1532-950X.2010.00776.x.

Staton, C. A., Reed, M. W. R. and Brown, N. J. (2009) ‘A critical analysis of current in vitro and in vivo angiogenesis assays’, International Journal of Experimental Pathology, 90(3), pp. 195–221. doi: 10.1111/j.1365-2613.2008.00633.x.

Stegen, S., van Gastel, N. and Carmeliet, G. (2015) ‘Bringing new life to damaged bone: the importance of angiogenesis in bone repair and regeneration.’, Bone, 70, pp. 19–27. doi: 10.1016/j.bone.2014.09.017.

Steiner, M., Claes, L., Ignatius, A., Simon, U. and Wehner, T. (2014) ‘Numerical Simulation of Callus Healing for Optimization of Fracture Fixation Stiffness’, PloS one. Edited by J. Costa-Rodrigues, 9(7), p. e101370. doi: 10.1371/journal.pone.0101370.t003.

Street, J., Bao, M., deGuzman, L., Bunting, S., Peale, F. V., Ferrara, N., Steinmetz, H., Hoeffel, J., Cleland, J. L., Daugherty, A., van Bruggen, N., Redmond, H. P., Carano, R. A. D. and Filvaroff, E. H. (2002) 'Vascular endothelial growth factor stimulates bone repair by promoting angiogenesis and bone turnover.', Proceedings of the National Academy of Sciences of the United States of America, 99(15), pp. 9656–9661. doi: 10.1073/pnas.152324099.

Strube, P., Sentuerk, U., Riha, T., Kaspar, K., Mueller, M., Kasper, G., Matziolis, G., Duda, G. N. and Perka, C. (2008) 'Influence of age and mechanical stability on bone defect healing: Age reverses mechanical effects', Bone, 42(4), pp. 758–764. doi: 10.1016/j.bone.2007.12.223.

Stump, M. M., Jordan, G. L., Debakey, M. E. And Halpert, B. (1963) 'Endothelium Grown From Circulating Blood On Isolated Intravascular Dacron Hub.', The American journal of pathology, 43, pp. 361–367.

Stupakov, G. P., Kazeĭkin, V. S., Kozlovskiĭ, A. P. and Korolev, V. V. (1984) '[Evaluation of the changes in the bone structures of the human axial skeleton in prolonged space flight].', Kosmicheskaia biologiia i aviakosmicheskaia meditsina, 18(2), pp. 33–37.

Sugiyama, T., Kohara, H., Noda, M. and Nagasawa, T. (2006) 'Maintenance of the hematopoietic stem cell pool by CXCL12-CXCR4 chemokine signaling in bone marrow stromal cell niches.', Immunity, 25(6), pp. 977–988. doi: 10.1016/j.immuni.2006.10.016.

Taguchi, K., Ogawa, R., Migita, M., Hanawa, H., Ito, H. and Orimo, H. (2005) 'The role of bone marrow-derived cells in bone fracture repair in a green fluorescent protein chimeric mouse model.', Biochemical and biophysical research communications, 331(1), pp. 31–36. doi: 10.1016/j.bbrc.2005.03.119.

Takahashi, K. and Yamanaka, S. (2006) 'Induction of pluripotent stem cells from mouse embryonic and adult fibroblast cultures by defined factors.', Cell, 126(4), pp. 663–676. doi: 10.1016/j.cell.2006.07.024.

Takahashi, K., Tanabe, K., Ohnuki, M., Narita, M., Ichisaka, T., Tomoda, K. and Yamanaka, S. (2007) 'Induction of pluripotent stem cells from adult human fibroblasts by defined factors.', Cell, 131(5), pp. 861–872. doi: 10.1016/j.cell.2007.11.019.

Tavassoli, M. and Crosby, W. H. (1968) 'Transplantation of Marrow to Extramedullary Sites', Science (New York, NY), 161(3836), pp. 54–56. doi: 10.1126/science.161.3836.54.

Tawonsawatruk, T., Kelly, M. and Simpson, H. (2014) 'Evaluation of native mesenchymal stem cells from bone marrow and local tissue in an atrophic nonunion model.', Tissue engineering. Part C, Methods, 20(6), pp. 524–532. doi: 10.1089/ten.TEC.2013.0465.

Tawonsawatruk, T., Spadaccino, A., Murray, I. R., Péault, B. and Simpson, H. A. H. R. W. S. (2012) 'Growth kinetics of rat mesenchymal stem cells from 3 potential sources: bone marrow, periosteum and adipose tissue.', Journal of the Medical Association of Thailand = Chotmaihet thangphaet, 95 Suppl 10, pp. S189–97.

Teixidó, J., Martínez-Moreno, M., Díaz-Martínez, M. and Sevilla-Movilla, S. (2018) 'The good and bad faces of the CXCR4 chemokine receptor.', The International Journal of Biochemistry & Cell Biology, 95, pp. 121–131. doi: 10.1016/j.biocel.2017.12.018.

Thompson, H. C. (1958) 'Effect of drilling into bone.', Journal of oral surgery, 16(1), pp. 22–30.

Tian, X. F., Heng, B. C., Ge, Z., Lu, K., Rufaihah, A. J., Fan, V. T. W., Yeo, J. F. and Cao, T. (2009) 'Comparison of osteogenesis of human embryonic stem cells within 2D and 3D culture systems', Scandinavian journal of clinical and laboratory investigation, 68(1), pp. 58–67. doi: 10.1089/ten.2006.0141.

Till, J. E. And Mcculloch, E. A. (1961) 'A direct measurement of the radiation sensitivity of normal mouse bone marrow cells.', Radiation research, 14, pp. 213–222.

Tögel, F., Isaac, J., Hu, Z., Weiss, K. and Westenfelder, C. (2005) 'Renal SDF-1 signals mobilization and homing of CXCR4-positive cells to the kidney after ischemic injury.', Kidney international, 67(5), pp. 1772–1784. doi: 10.1111/j.1523-1755.2005.00275.x.

Toksoy, A., Müller, V., Gillitzer, R. and Goebeler, M. (2007) 'Biphasic expression of stromal cell-derived factor-1 during human wound healing.', The British journal of dermatology, 157(6), pp. 1148–1154. doi: 10.1111/j.1365-2133.2007.08240.x.

Toombs, J. P., Wallace, L. J., Bjorling, D. E. and Rowland, G. N. (1985) 'Evaluation of Key's hypothesis in the feline tibia: an experimental model for augmented bone healing studies.', American journal of veterinary research, 46(2), pp. 513–518.

Toupadakis, C. A., Granick, J. L., Sagy, M., Wong, A., Ghassemi, E., Chung, D.-J., Borjesson, D. L. and Yellowley, C. E. (2013) 'Mobilization of endogenous stem cell populations enhances fracture healing in a murine femoral fracture model.', *Cytotherapy*, 15(9), pp. 1136–1147. doi: 10.1016/j.jcyt.2013.05.004.

Toupadakis, C. A., Wong, A., Genetos, D. C., Chung, D.-J., Murugesh, D., Anderson, M. J., Loots, G. G., Christiansen, B. A., Kapatkin, A. S. and Yellowley, C. E. (2012) 'Long-term administration of AMD3100, an antagonist of SDF-1/CXCR4 signaling, alters fracture repair.', *Journal of Orthopaedic Research*, 30(11), pp. 1853–1859. doi: 10.1002/jor.22145.

Urist, M. R. (1965) 'Bone: Formation by Autoinduction', Science (New York, NY), 150(3698), pp. 893–899. doi: 10.1126/science.150.3698.893.

Vas, W. J., Shah, M., Blacker, T. S., Duchen, M. R., Sibbons, P. and Roberts, S. J. (2018) 'Decellularized Cartilage Directs Chondrogenic Differentiation: Creation of a Fracture Callus Mimetic', Tissue engineering. Part A, p. ten.tea.2017.0450. doi: 10.1089/ten.tea.2017.0450.

Vodyanik, M. A., Yu, J., Zhang, X., Tian, S., Stewart, R., Thomson, J. A. and Slukvin, I. I. (2010) 'A Mesoderm-Derived Precursor for Mesenchymal Stem and Endothelial Cells', Cell stem cell, 7(6), pp. 718–729. doi: 10.1016/j.stem.2010.11.011.

Voyta, J. C., Via, D. P., Butterfield, C. E. and Zetter, B. R. (1984) 'Identification and isolation of endothelial cells based on their increased uptake of acetylated-low density lipoprotein.', The Journal of Cell Biology, 99(6), pp. 2034–2040.

Wan, Y. (2013) 'Bone marrow mesenchymal stem cells: Fat on and blast off by FGF21', International Journal of Biochemistry and Cell Biology. Elsevier Ltd, 45(3), pp. 546–549. doi: 10.1016/j.biocel.2012.12.014.

Wang, Q., Huang, C., Zeng, F., Xue, M. and Zhang, X. (2010) 'Activation of the Hh pathway in periosteum-derived mesenchymal stem cells induces bone formation in vivo: implication for postnatal bone repair.', The American journal of pathology, 177(6), pp. 3100–3111. doi: 10.2353/ajpath.2010.100060.

Wang, X. X., Allen, R. J., Tutela, J. P., Sailon, A., Allori, A. C., Davidson, E. H., Paek, G. K., Saadeh, P. B., McCarthy, J. G. and Warren, S. M. (2011) 'Progenitor cell mobilization enhances bone healing by means of improved neovascularization and osteogenesis.', *Plastic and reconstructive surgery*, 128(2), pp. 395–405. doi: 10.1097/PRS.0b013e31821e6e10.

Wang, Y., Johnsen, H. E., Mortensen, S., Bindslev, L., Ripa, R. S., Haack-Sørensen, M., Jørgensen, E., Fang, W. and Kastrup, J. (2006) 'Changes in circulating mesenchymal stem cells, stem cell homing factor, and vascular growth factors in patients with acute ST elevation myocardial infarction treated with primary percutaneous coronary intervention.', *Heart (British Cardiac Society)*, 92(6), pp. 768–774. doi: 10.1136/hrt.2005.069799.

Ward, M. R., Stewart, D. J. and Kutryk, M. J. B. (2007) 'Endothelial progenitor cell therapy for the treatment of coronary disease, acute MI, and pulmonary arterial hypertension: current perspectives.', Catheterization and cardiovascular interventions : official journal of the Society for Cardiac Angiography & Interventions, 70(7), pp. 983–998. doi: 10.1002/ccd.21302.

Weber BG, Cech O. (1976) 'Pseudoarthrosis: Pathology, Biomechanics, Therapy, Results.' Hans Huber Medical Publishing Stuttgart, Berne, Switzerland. ISBN 10: 3456801955

Wehner, T., Steiner, M., Ignatius, A. and Claes, L. (2014) 'Prediction of the Time Course of Callus Stiffness as a Function of Mechanical Parameters in Experimental Rat Fracture Healing Studies - A Numerical Study', PloS one. Edited by C. M. Aegerter, 9(12), p. e115695. doi: 10.1371/journal.pone.0115695.s003.

Whitman, S. C., Daugherty, A. and Post, S. R. (2000) 'Regulation of acetylated low density lipoprotein uptake in macrophages by pertussis toxin-sensitive G proteins.', Journal of lipid research, 41(5), pp. 807–813.

Wilson, A. and Trumpp, A. (2006) 'Bone-marrow haematopoietic-stem-cell niches.', Nature reviews. Immunology, 6(2), pp. 93–106. doi: 10.1038/nri1779.

Wobus, A. M. and Boheler, K. R. (2005) 'Embryonic stem cells: prospects for developmental biology and cell therapy.', Physiological reviews, 85(2), pp. 635–678. doi: 10.1152/physrev.00054.2003.

Wolff J. (1892) 'Das Gesetz der Transformation der Knochen'. Berlin, Germany: Verlag von August Hirschwald.

Wright, D. E., Wagers, A. J., Gulati, A. P., Johnson, F. L. and Weissman, I. L. (2001) 'Physiological migration of hematopoietic stem and progenitor cells.', *Science (New York, NY)*, 294(5548), pp. 1933–1936. doi: 10.1126/science.1064081.

Wu, M., Zhang, R., Zou, Q., Chen, Y., Zhou, M., Li, X., Ran, R. and Chen, Q. (2018) 'Comparison of the Biological Characteristics of Mesenchymal Stem Cells Derived from the Human Placenta and Umbilical Cord', Scientific reports. Springer US, pp. 1–9. doi: 10.1038/s41598-018-23396-1.

Wu, T., Yu, S., Chen, D. and Wang, Y. (2017) 'Bionic Design, Materials and Performance of Bone Tissue Scaffolds', Materials, 10(10), p. 1187. doi: 10.1016/j.bone.2012.07.003.

Xu, J., Chen, Y., Liu, Y., Zhang, J., Kang, Q., Ho, K., Chai, Y. and Li, G. (2017) 'Effect of SDF-1/Cxcr4 Signaling Antagonist AMD3100 on Bone Mineralization in Distraction Osteogenesis.', Calcified Tissue International, 100(6), pp. 641–652. doi: 10.1007/s00223-017-0249-4.

Yeh, S.-P., Chang, J.-G., Lo, W.-J., Liaw, Y.-C., Lin, C.-L., Lee, C.-C. and Chiu, C.-F. (2006) 'Induction of CD45 expression on bone marrow-derived mesenchymal stem cells', Leukemia, 20(5), pp. 894–896. doi: 10.1038/sj.leu.2404181.

Yellowley, C. (2013) 'CXCL12/CXCR4 signaling and other recruitment and homing pathways in fracture repair.', BoneKEy reports, 2, p. 300. doi: 10.1038/bonekey.2013.34.

Zuk, P. A., Zhu, M., Mizuno, H., Huang, J., Futrell, J. W., Katz, A. J., Benhaim, P., Lorenz, H. P. and Hedrick, M. H. (2001) 'Multilineage cells from human adipose tissue: implications for cell-based therapies.', Tissue engineering, 7(2), pp. 211–228. doi: 10.1089/107632701300062859.

Zvaifler, N. J., Marinova-Mutafchieva, L., Adams, G., Edwards, C. J., Moss, J., Burger, J. A. and Maini, R. N. (2000) 'Mesenchymal precursor cells in the blood of normal individuals.', Arthritis research, 2(6), pp. 477–488. doi: 10.1186/ar130.